Mechanisms underlying perioperative myocardial injury

A thesis submitted in partial fulfilment of the

requirements of the degree of Doctor of

Philosophy

Shaun May

William Harvey Research Institute

Barts and the London School of Medicine and Dentistry

Queen Mary University of London

Declaration of Originality

I, Shaun May, confirm that the research included within this thesis is my own work, or that where it has been carried out in collaboration with, or supported by others, that this is duly acknowledged below, and my contribution indicated. Previously published material is also acknowledged below.

I attest that I have exercised reasonable care to ensure that the work is original and does not to the best of my knowledge break any UK law, infringe any third party's copyright or other Intellectual Property Right, or contain any confidential material.

I accept that the College has the right to use plagiarism detection software to check the electronic version of the thesis.

I confirm that this thesis has not been previously submitted for the award of a degree by this or any other university.

Signature:

Date: 4th December 2022

Abstract

Troponin is a biomarker for myocardial injury: it is associated with poor outcomes after noncardiac surgery, but the underlying mechanisms remain unclear. Circulating microRNAs are small non-coding RNAs which regulate post-translational gene expression and are released or secreted after cardiac injury. I examined whether perioperative myocardial injury and acute coronary syndrome share common microRNA signatures by comparing cardiac injury-specific serum microRNAs between matched patients with and without raised postoperative troponin within three days of surgery. MicroRNA expression was quantified using real-time polymerase chain reaction before and after surgery, blinded to troponin status. Cardiac-specific microRNAs showed increased expression after surgery, independent of troponin rise. Bioinformatic analyses identified pathways associated with cellular stress involving adrenergic signalling in the cardiomyocyte, and proteins regulating cardiomyocyte calcium homeostasis.

Because pre-existing vagal dysfunction is associated with troponin rise after noncardiac surgery, I hypothesised that an acquired loss of cardiac vagal protective signalling promotes troponin elevation after noncardiac surgery. Serial cardiac autonomic measurements were made in patients before and after noncardiac surgery. Using 5-minute electrocardiogram recordings, cardiac autonomic modulation was quantified by heart rate (HR) variability and HR recovery after a standardised orthostatic manoeuvre. The primary outcome was myocardial injury (high-sensitivity troponin T$\geq$15ng.L^{-1}) within 48h of surgery, and the exposure of interest was cardiac vagal activity (high-frequency power spectrum [HFLn]) and HR recovery from peak HR after an orthostatic manoeuvre. HFLn was reduced after 24 hours after surgery in patients who developed myocardial injury and orthostatic HR recovery was slower in patients with myocardial injury, compared with patients who remained free of myocardial injury.

Elevations in perioperative troponin may occur due to a lack of cardioprotective vagal mechanisms against adrenergic stress. The data highlight the need for a more considered approach to the interpretation of raised circulating troponin, which is frequently ascribed to an ischaemic aetiology.

Table of contents

List of figures

List of tables

Abbreviations

ABP	Arterial blood pressure
Ach	Acetylcholine
ACS	Acute coronary syndrome
ANOVA	Analysis of variance
AP-1	Activating protein-1
ATP	Adenosine triphosphate
AVN	Atrioventricular node
Bcl-2	B-cell lymphoma 2
BRR	Baroreceptor reflex
C	Celsius
Ca^{2+}	Calcium
cAMP	Cyclic adenosine monophosphate
cGMP	Cyclic guanosine monophosphate
CHD	Coronary heart disease
cMyC	Cardiac myosin heavy chain
CPET	Cardiopulmonary exercise testing
Cq	Quantification cycle
cTn	Cardiac troponin
CVLM	Caudal ventrolateral medulla
DAG	Diacyl glycerol
DNA	Deoxyribonucleic acids
DVC	Dorsal vagal complex
DVMN	Dorsal vagal motor nucleus
ECG	Electrocardiogram
ELISA	Enzyme linked immunosorbent assays
ENIGMA	Evaluation of Nitrous oxide in Gas Mixture of Anaesthesia-II study
ERK	Extracellular regulated kinases
FC	Fold change
FDR	False discovery rate
GABA	Gamma-aminobutyric acid
GDP	Guanosine diphosphate
GTP	Guanosine triphosphate
h_20_2	Hydrogen peroxide
HF	High frequency
HR	Heart rate
HRR	Heart rate recovery
HRV	Heart rate variability
hsa	Homo sapiens
HsTnT	High Sensitivity Troponin T
IL	Interleukin
IML	Intermediolateral cell column

IP_3	Inositol trisphosphate
IPC	Internal plate calibrator
IQR	Interquartile range
KEGG	Known Encyclopaedia of Genes and Genomes
LF	Low frequency
Ln	Natural logarithm
mAchR	Muscarinic acetylcholine receptor
MAPK	Mitogen-activated protein kinases
METS	**M**easurement of **E**xercise **T**olerance before **S**urgery
MI	Myocardial infarction
MINS	Myocardial injury after noncardiac surgery
MIQE	Minimum Information for Publication of Quantitative Real-Time PCR Experiments
miTG	miRNA targeted genes
MRE	MicroRNA recognition elements
mRNA	Messenger ribonucleic acids
NA	Nucleus ambiguus
nAchR	Nicotinic acetylcholine receptors
NCX	Sodium (Na+)/Calcium (Ca2+) exchange protein
NGS	Next generation sequencing
NLR	Neutrophil to lymphocyte ratio
NTS	Nucleus tractus solitarius
PINK-1	PTEN-induced putative kinase 1
PKA	Protein kinase A
PMI	Perioperative myocardial injury
PNS	Parasympathetic nervous system
POISE	Perioperative Ischaemic Evaluation study
POMS	Postoperative morbidity survey
PP2A	Protein phosphatase 2A
qPCR	Quantitive polymerase chain reaction
RISC	RNA-induced silencing complex
RMSSD	Root mean square of the standard deviation
RNA	Ribonucleic acids
RSA	Respiratory sinus arrythmia
RT-qPCR	Reverse transcription quantitative polymerase chain reaction
RyR	Ryanodine receptors
SAN	Sinoatrial node
SBP	Systolic blood pressure
SDNN	Standard deviations of the RR interval
SNS	Sympathetic nervous system
SOD	Superoxide dismutase
STROBE	Strengthening and Reporting of observational Studies in Epidemiology
Tm	Melting temperature
TnC	Troponin C

TNF-α	Tumour necrosis factor-alpha
TnI	Troponin I
TnT	Troponin T
TRBP	Transactivation-response RNA binding proteins
UDMI	Universal Definition of Myocardial Infarction
UTR	Untranslated region
VLF	Very low frequency
XMINS	Vagus (**X**)- **M**yocardial **I**njury in **N**on-cardiac **S**urgery

Units

µL	Microlitre
bpm	Beat per minute
h	Hours
Hz	Hertz
L	Litre
ml	Millilitre
min	Minute
ng	Nanograms
rpm	Revolutions per minute

Acknowledgements

My supervisor: Professor Gareth Ackland, for guidance, inspiration and imparting his relentless enthusiasm for perioperative research. I am grateful for his support during a PhD completed during a global pandemic which entailed great personal and professional challenges for us all.

Dr Ana Gutierrez Del Arroyo for her patience and friendship, and for teaching me the laboratory techniques and presentation skills required for the work in this thesis.

Professor Rupert Pearse and the Critical Care and Perioperative Research Group for their invaluable support and guidance throughout my PhD studies.

My colleagues at the William Harvey Research Group: Sophie, Jennie, Tim, Eric and Julie for their friendship, support and help in the laboratory.

The perioperative research team at University College London Hospital: the research nurses Ann Reyes and Gladys Martir, and Dr Robert Stephens, without whom I would not have been able to conduct and complete the XMINS study.

I would like to thank Joseph Reynolds, whom I helped supervise for his MSc at Queen Mary University London. Data for chapter 5 was extracted and processed with Joe's assistance.

I would also like to acknowledge the King Edward VII's Hospital for funding towards laboratory consumables and my salary during my PhD studies.

I would like to thank my family: Mom, Booba, Carli and Dan: for their unfailing support in all my endeavours. In particular, I am grateful to Dylan, our newest addition, for believing in me as his best uncle-saurus.

Finally, I would like to thank Michelle for her critical eye, attention to detail and her love and friendship over the last 6 years.

Publications and presentations arising from work in thesis

Journal publications

May S.M., Abbott T.E.F., Del Arroyo A.G., Reyes A., Martir G., Brealey D., Stephens R., Cuthbertson B.H., Wijesundera D., Pearse R.M., Ackland G. *microRNA signatures of perioperative myocardial injury after elective non-cardiac surgery: prospective observational mechanistic cohort study*. British Journal of Anaesthesia. 2020 Vol. 125. Issue 5 P661-671

Written by May with editorial advice from Ackland. Data and samples collected by METS study group. MicroRNA experiment designs, isolation and analysis by May. Methodology, results and discussion are included in this thesis.

May S.M., Reyes A., Martir G., Brealey D., Stephens R., Ackland G. *Acquired loss of cardiac vagal activity is associated with myocardial injury in patients undergoing non-cardiac surgery: prospective observational mechanistic cohort study*. British Journal of Anaesthesia. 2019 Vol. 123 Issue 6 P758-767

Written by May with editorial advice from Ackland. May was lead investigator for the study. Methodology, results and discussion are included in this thesis.

Conference Abstracts

May S.M., Del Arroyo A.G., Reyes A., Martir G., Stephens R.C., Brealey D., Ackland G.L. *Plasma MicroRNA signatures for perioperative myocardial injury*. Abstract presented as an oral presentation at the Abstract group discussion Experimental Circulation Session, at the American Society of Anaesthesiology annual meeting, Orlando 2019

May S.M., Abbott T.E.F., Del Arroyo A.G., Cuthbertson B.H., Wijeysundera D.N., Pearse R.M., Ackland G.L. *Serum microRNAs and perioperative myocardial injury*. British Journal of Anaesthesia. Volume 122, Issue 3, 2019 e45. Abstract presented as an oral presentation at the Anaesthetic Research Society winter meeting. Dundee, 2018

May S., Karmali S., Reyes A., Gallego Paredes L., Martir G., Stephens R., Brealey D., Ackland, G.L. *Serial holter recordings in non-cardiac surgery patients reveal postoperative autonomic impairment within 48 hours*. British Journal of Anaesthesia. Volume 120, Issue 5, 2018, Pages e16-e17. Abstract presented as an oral presentation at the Anaesthetic Research Society winter meeting, Leicester, 2017

National oral presentations and prizes

Unravelling the enigma of elevated troponin after non-cardiac surgery. National Institute of Academic Anaesthesia (NIAA) Research award winner, presented at the Anaesthesia Research Virtual Meeting, 2021.

Chapter 1
General Introduction

There are an estimated 312 million surgical operations performed worldwide each year [1] with a reported morbidity of up to 16.8%.[2] One of the most significant fatal complications after noncardiac surgery is myocardial injury, defined as an elevation in troponin after surgery.[3] Therefore, a fundamental understanding of the mechanisms underlying its aetiology is vital to the development of screening programmes to detect patients at risk of developing myocardial injury, and ultimately implementing effective therapies to prevent and treat myocardial injury.

In this chapter, I will give an outline of the relevant anatomy and physiology. It is not exhaustive in detail, but aims to place the thesis hypotheses in context and to facilitate the discussion of results. I then discuss the incidence and significance of perioperative myocardial injury to demonstrate the clinical importance of understanding the underlying pathological mechanisms and its aetiology. Potential mechanisms will be outlined: in particular, microRNA and the potential involvement of the parasympathetic nervous system. Finally, I outline the main aims and hypotheses for my thesis.

1.1 Cardiac anatomy and physiology

1.1.1 Cardiac anatomy

The heart consists of four chambers: two contractile reservoirs called atria, and two muscular pumps called ventricles. The main function of the heart is to pump oxygenated blood to tissues and return waste products and carbon dioxide to the lungs. Cardiomyocytes form the main component of cardiac muscle. The contraction (systole) and relaxation (diastole) of cardiomyocytes within the atria and ventricle is co-ordinated by a system of adapted cardiomyocytes fibres known as the electrical conduction system. Contractions are initiated by pacemaker cells located in the sinoatrial node (SAN), which is located in the posterior right atrium. Action potentials travel along adjacent cardiomyocytes within the atria and are delayed from entering the ventricle by the atrioventricular node (AVN), located in the posterior region of the atrial septum. Electrical impulses are then conveyed to the ventricles via the bundle of His and its bundle branches, and subsequently by Purkinje fibres. The propagation of the action potential, and the depolarisation of cardiomyocytes initiating contraction, are controlled by a complex network of cardiomyocyte ion membrane channels, cellular proteins and intracellular messengers.[4]

1.1.2 Cardiomyocyte

Cardiomyocytes contain contractile bundles called myofibrils. Each myofibril contains contractile units called sarcomeres, composed of thick myosin filaments interposed between thin actin filaments. Shortening of the sarcomere generates contraction within an individual cardiomyocyte. Myosin molecules contain a head that can bind to a groove within the thin

actin filament. The groove of the actin molecules contains a protein called tropomyosin that is attached to a regulatory complex of troponins (Troponin T, Troponin C, Troponin I) to form the tropomyosin-troponin complex. The troponin components are named based on their function related to the crossbridge cycle.[5] Troponin T binds the tropomyosin-troponin complex together. Troponin I inhibits actin-myosin interaction in the absence of calcium (Ca^{2+}). A rise in intracellular calcium from the sarcoplasmic reticulum facilitates calcium binding to Troponin C. This causes the tropomyosin-troponin complex to shift, exposing the myosin binding site on the myosin, allowing crossbridge formations between myosin and actin.

1.1.3 Excitation-contraction coupling

Intracellular calcium regulation is vital to the control of electrical excitation-contraction coupling within the cardiomyocyte. During systole, action potentials migrate along the cardiomyocyte and t-tubule, triggering calcium influx via voltage gated L-type Ca^{2+} channels. Ryanodine receptors (RyR) on the junctional sarcoplasmic reticulum release calcium in response to the rise in intracellular calcium concentration: this is called calcium induced calcium release. Calcium initiates shortening of the sarcomere by exposing the myosin binding sites on actin. The force and movement of contraction is related to the change in angle of the myosin head. The magnitude of contraction is proportional to the number of crossbridges that are formed, which in turn depends on the calcium concentration.[4]

During diastole, calcium is removed by 2 mechanisms: firstly, calcium ATPase pumps (SERCA2A) on the sarcoplasmic reticulum (SR) are activated by the rise of intracellular calcium and reconstitute the calcium back into the SR; secondly, Na^{+}-Ca^{2+} exchangers (NCX) pump calcium out of the cell.

Excitation-contraction coupling is modulated by intracellular secondary messengers, such as cyclic adenosine monophosphate (cAMP) and inositol trisphosphate (IP_3), through adrenergic and muscarinic G-protein coupled receptor activation. Both adrenergic and muscarinic receptors belong to the group of G-protein linked receptors. The G-protein consists of three subunits: alpha, beta and gamma: and exists as a trimer. Activation of the receptors by an agonist (i.e. noradrenaline or adrenaline) catalyses the conversion of guanosine triphosphate (GTP) to guanosine diphosphate (GDP), causing the G-protein to dissociate into its alpha subunit and beta/gamma subunit. These active forms of the G-protein then inhibit (Gi) or activate (Gs) signalling cascades within cells.[6]

1.1.4 Heart rate

The sinoatrial node located in the posterior right atria consists of specialised cardiomyocytes called pacemaker cells. The intrinsic rate at which action potentials propagate along the conduction system is determined by the rate of spontaneous membrane potential decay of these cells. An action potential is generated in a cardiomyocyte when the membrane potential exceeds a threshold. Cardiomyocytes have stable membrane potentials that are altered by a propagation of external action potentials. The pacemaker cell membrane potential decays spontaneously and is controlled by multiple ionic currents via ion channels. These include the inward Na^+ current ("funny current") via hyperpolarisation activated cyclic nucleotide-gated channels (HCN), NCX and inward calcium current via L and T-type calcium channels. The interval between heart beats is determined by the rate of decay also known as the "slope".[4]

The ionic currents, and thereby the slope of decay and interval between heart beats, can be modulated by the parasympathetic and sympathetic system via activation of the G-protein linked muscarinic and adrenoreceptors located on the membrane of the SAN. (Introduction Section 1.2.2)

1.2 Autonomic nervous system: anatomy and physiology

The autonomic nervous system consists of two divisions: the parasympathetic nervous system (PNS) and the sympathetic nervous system (SNS). These integrate to control visceral function and body homeostasis in response to internal and external challenges.[7] The efferent pathways of both divisions consist of preganglionic neurons, ganglia and postganglionic neurons.

The PNS preganglionic neurons have a cranial and sacral component that innervate peripheral ganglia. The cranial component consists of the cranial nerves oculomotor (CN III), trochlear (CN VI), glossopharyngeal (CN IX), vagus (CN X) and the sacral component, which consists of the 2nd to 4th sacral level of the spinal cord. The ganglia are located close to or within the target tissue or organ.

The SNS preganglionic neurons originate in the lateral horn of the T1-L2 segments of the spinal cord. They synapse with postganglionic neurons that reside in paravertebral ganglia forming the spinal cord chain along the vertebral bodies. The postganglionic neurons terminate on target organs.

Sensory afferent inputs that integrate with both divisions of the autonomic nervous system play an important role in homeostatic responses such as the baroreflex.

Individual descriptions of the autonomic nervous system innervation for all body systems are beyond the scope of this thesis. In this section I will focus on the autonomic innervation of the heart and its role in homeostatic responses such as the baroreflex and orthostatic control. I will

pay particular attention to the efferent and afferent components of the vagus nerve to contextualise my hypotheses and discussion of results.

1.2.1 Vagus nerve

The vagus nerve originates from the medulla oblongata within the brainstem. It enters the lateral aspect of the medulla oblongata containing three main components: preganglionic parasympathetic neurons; axons of the skeletal motor neurons; and central processes of the sensory neurons of the sensory nodusum.[8, 9] Together these form the afferent (20%) and efferent (80%) components of the vagus nerve and are the main parasympathetic innervation of the thoracic and abdominopelvic viscera.

1.2.1.1 Vagal sensory input pathways

Neuronal tracing studies have shown that vagal nuclei receive sensory inputs from the aortic arch, epicardium, myocardium and endocardium, lower airways and lung, thymus, pancreas, liver, portal vein and bile ducts, gastrointestinal tract, uterus, and brain.[10] Tracing studies having shown these neurons terminate within the dorsal vagal complex of the medulla oblongata. The dorsal vagal complex (DVC) consists of the nucleus tractus solitarius (NTS), the dorsal vagal motor nucleus (DVMN) and the area postrema (AP).[10]

1.2.1.2 Vagal efferent pathways

Neural tracing studies have located vagal preganglionic neurons in in the dorsal vagal motor nucleus (DVMN), nucleus ambiguus (NA), nucleus retroambiguus (NRA), nucleus

dorsomedialis (NDM) and the spinal nucleus of the accessory nerve (NSPA).[11] These preganglionic neurons synapse with the postganglionic neurons in the ganglia close to the viscera they innervate. The NA can be classified into subregions based on the projection of the axons. The ventral division of the NA has nuclei from the preganglionic neurons and the dorsal division nuclei from motor neurons of the pharynx and thoracic viscera.[12] The cardiac vagal preganglionic neurons originate from the nucleus ambiguous and the dorsal vagal motor neuron.[13] The DVMN is organised into a coloumn of cells where each trophic level has outflow to the different viscera.[14] The DVMN receives a large number of modulatory inputs from vagal afferents (i.e. from the gastrointestinal tract) that integrate within the NTS.[15]

1.2.2 Cardiac autonomic innervation of the heart

The heart is innervated by both divisions of the autonomic nervous system which is discussed below.[16]

1.2.2.1 Cardiac vagal innervation of the heart

Efferent pathways

The role of the vagus nerve is the control of negative chronotropy (rate), inotropy (contraction), lusitropy (relaxation) and dromotropy (conduction) of the heart. Vagal preganglionic neurons leave the brainstem and synapse on ganglionic sites located in the atria, ventricles and interventricular septum.[17] Postganglionic neurons from the ganglionic sites innervate SAN, AVN and conducting tissue.[17] By synapsing on SAN and AVN pacemaker cells, the vagus nerve is able to modulate heart rate and conduction;[18] by synapsing on atria and ventricle

cardiomyocyte cells, the vagus nerve is able to influence contractility and excitability.[19, 20] Cardiac preganglionic vagal motor neurons arise from two nuclei located in the brainstem: the nucleus ambiguus (NA) and the dorsal motor neuron nucleus (DVMN).[13]

The vagal preganglionic nerves arising from the NA modulate heart rate and are tonically active, as demonstrated by decreasing the intrinsic heart rate of the SAN.[4] Neural discharge from the NA, and therefore control of heart rate, is under the influence of inputs from the arterial baroreflex, chemoreflexes, and pulmonary afferents via the NTS and the central respiratory rhythm.[21]

The heart rate changes in response to the different stages of the respiratory cycle. This is known as respiratory sinus arrythmia (RSA) where the heart rate increases in expiration and decreases in inspiration.[22] This is mediated by changes in cardiac vagal motor neuron tone.[23] The magnitude of RSA is therefore a function of the excitability of the preganglionic vagal motor neurons.[24] The mechanisms influencing intrinsic vagal tone are not fully understood. However, it has been shown experimentally that tonal influences originate from the brain stem by using decerebrate unanaesthetised rat models in which baroreceptor, chemoreceptor and stretch reflexes are removed.[25] The co-ordinated discharge is thought to ensure that heart rate (and therefore cardiac output) is matched to changes in the peripheral circulation and respiratory minute volume [26] and therefore ensures cardio-respiratory efficiency.[27]

Vagal preganglionic motor neurons from the DVMN are unaffected by inputs from the baroreceptor, chemoreceptor and central respiratory drive.[13] As described above, the DVMN receives input via vagal afferents to the NTS.[15] Projections from the DVMN to the left ventricle

decrease contractility,[28] have a tonic restraining effect of contractility in the presence of sympathetic stimulation,[20] and control ventricle excitability.[19]

Neurotransmitters and receptors

The main neurotransmitter is acetylcholine (Ach), and the main postganglionic receptors are nicotinic acetylcholine receptors (nAchR). Postganglionic neurons project to target tissues on the SAN, AVN, atria and the ventricles. The main neurotransmitter and target tissue receptors are Ach and the muscarinic acetylcholine receptor (mAchR), respectively.[6]

The vagus nerve modulates heart rate and contraction of atria and ventricles via activation of muscarinic receptors located on the cardiomyocyte membrane. Muscarinic receptors are G-protein linked receptors. There are 5 subtypes (M_{1-5}): M_{1-3} are found in the heart. Gi muscarinic receptors mediate their response via the inhibitory alpha subunit that inhibits adenylate cyclase, and therefore cAMP production. Gs muscarinic receptors mediate their response by producing diacyl glycerol (DAG) and IP_3, which activate protein kinase C. Muscarinic M_2 is the main muscarinic receptor subtype found in the heart and is a Gi receptor. M_1 and M_3 muscarinic receptors are also found in the heart and are Gs receptors.[29]

Heart rate is decreased by reducing the slope of pacemaker cells. The downstream signalling effect of cAMP inhibition reduces the sodium and calcium inward currents, thus delaying the cell reaching the threshold potential. Cardiomyocyte hyperpolarisation is mediated by the beta/gamma subunit which activates an inward potassium channel.

1.2.2.2 Sympathetic nervous system:

Efferent pathways

The role of the sympathetic nervous system (SNS) is positive chronotropy, inotropy, lusitropy and dromotropy. Preganglionic cell bodies are located at the level of T1-T4 in the thoracic spinal cord. The preganglionic neurons leave the spinal cord by the ventral roots to join the sympathetic chain, where they synapse with post ganglionic neurons to form the stellate ganglion. Postganglionic sympathetic neurons innervate the cardiomyocytes in the atria and ventricles together with the SAN and AVN to modulate chronotropy, inotropy, lusitropy and dromotropy.[30]

Neurotransmitters and receptors

The main neurotransmitters and receptors at the target tissue are noradrenaline and adrenaline which bind to adrenergic receptors. The adrenergic receptors also belong to the group of G-protein linked receptors. The myocardium has both alpha (α) and beta (β) receptors. The β receptor has 3 subtypes: β_1, β_2 and β_3. β_1 is the predominant subtype found in the human myocardium (~80%) (β_2 (~15%), β_3 (~5%)).[6] There are 2 types of alpha receptor, each of which has 3 subtypes: α1 (α_{1A}, α_{1B}, α_{1D}); and α2 (α_{2A}, α_{2B}, α_{2C}).[31, 32] The human myocardium primarily expresses α_{1A} and α_{1B}.[33] Activation of β1 receptor in the cardiomyocyte triggers a G-protein signalling cascade. The alpha subunit activates the enzyme adenylate cyclase which catalyses the conversion of adenosine triphosphate ATP to adenosine 3′,5′-monophosphate or cAMP. cAMP then activates protein kinase A (PKA). α receptor-linked proteins activate phospholipase C-β which generates secondary messengers: IP_3 and DAG. The chronotropic

effects of the adrenergic stimulation are modulated by the secondary messengers. cAMP opens sodium inward pacemaker currents, thereby increasing the rate of membrane potential decay and increasing heart rate. PKA phosphorylates L-type calcium channels which also accelerates decay and thereby heart rate. The inotropic effect is due to the increased intracellular calcium through cAMP cascade signalling and via IP_3 binding to the SR inducing more calcium store release. The increase in calcium allows more cross-bridge formation and thus increasing force of contraction during systole.[4]

1.2.2.3 Reciprocal vagal control with sympathetic innervation on the myocardium

The ability of the vagal nerve to decrease ventricular contractility [28] appears to be increased in the presence of sympathetic activity;[34] this may in part be related to acetylcholine activation increasing cyclic guanosine monophosphate (cGMP) levels.[35] This in turn decreases cAMP levels generated by sympathetic stimulation, thus decreasing myocyte contractility.[36]

1.2.3 Autonomic reflexes relevant to this thesis

The vagus nerve with its multiple afferent inputs and efferent projections plays an important role in bodily homeostatic processes. These include cardiovascular processes such as the baroreflex and orthostatic control,[4] oxygen concentration via the chemoreflex,[37] gastrointestinal motility, pancreatic endocrine and exocrine function, hepatic glucose production,[38] and neuroimmunomodulation.[39] Below, I discuss the reflexes that are relevant to this thesis: the baroreceptor reflex (including orthostatic control) and the cholinergic inflammatory reflex.

1.2.3.1 Baroreflex/orthostatic control

The baroreceptor reflex (BRR) is a short term negative feedback mechanism for regulating arterial blood pressure (ABP). Arterial pressure is sensed by stretch receptors located in the aortic arch and carotid sinuses. Afferent fibres from the receptors run within the glossopharyngeal and vagus nerves and terminate within the NTS in the dorsomedial medulla oblongata. Second order neurons then project to the cardiac vagal motor neurons in the NA or to interneurons in the caudal ventrolateral medulla (CVLM). Interneurons from the CVLM are inhibitory gamma-aminobutyric acid (GABA)ergic neurons which project and inhibit sympathetic premotor neurons within the rostral ventral lateral medulla (RVLM). These neurons then project and synapse in the intermediolateral cell column (IML). Sympathetic neurons from the IML then synapse with postganglionic neurons to innervate atrial pacemaker cells and smooth muscle cells with the wall of arterioles.[40] (Figure 1.1)

Orthostatic (upright posture) manoeuvres can be used to illustrate the BRR and the homeostatic interplay of sympathetic and vagal influence on heart rate.[41] When going from the lying to the standing/sitting position, venous blood redistributes to the lower extremities due to gravity. As a result, there is a lowering of ABP, and therefore a decrease in firing from the stretch receptors in the aortic arch and carotid sinuses. Consequently, there is an increase in sympathetic vasomotor activity that increases total vascular resistance and sympathetic cardiac activity. Combined with a decrease in cardiac vagal activity, this increases heart rate and cardiac contractility to increase cardiac output.[37] The increase in total vascular resistance and heart rate restores ABP. During static exercise, which can be considered as an orthostatic manoeuvre, the ratio of contribution to the reflex response is 20% heart rate and 80% vasomotor

tone.[41, 42] Cardiac output is restored prior to achieving peak heart rate.[43] The restoration of heart to baseline is mediated by increased cardiac vagal activity.[44] (Figure 1.1)

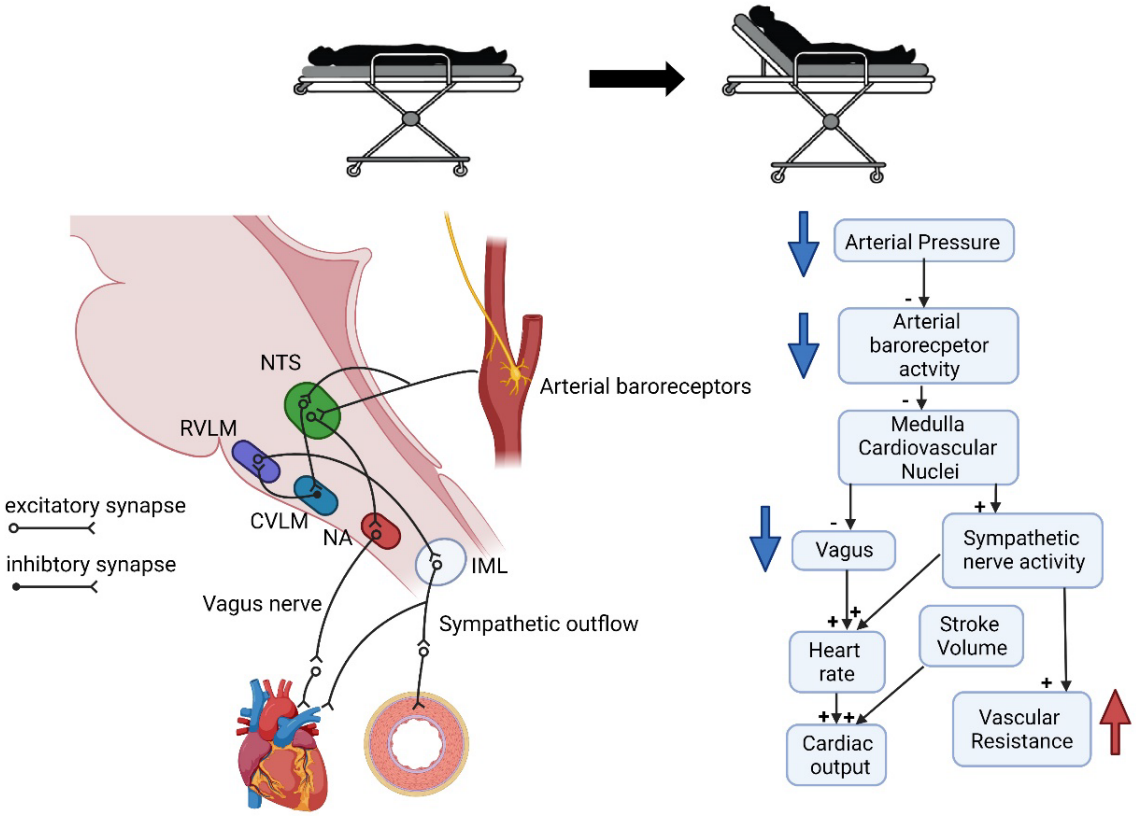

Figure 1.1 Baroreceptor reflex control after an orthostatic manoeuvre

The diagram above shows a simplified diagram of neuronal pathways within the lower brainstem involved in the baroreceptor reflex. NTS; nucleus tractus solitarius. NA; nucleus ambiguus. RVLM; rostral ventrolateral medulla. CVLM; caudal ventrolateral medulla. IML intermediolateral cell coloumn

Adapted from Rowell et al.[45] and Dampney et al.[37]

1.2.3.2 Vagal inflammatory reflex

The vagus nerve plays an integral role in neuromodulation of the immune response to inflammation.[39, 46, 47] Following tissue injury there is activation of the innate immune response at the site of injury. This leads to activation and recruitment of macrophages, neutrophils, dendritic cells, and natural killer cells. The response is further mediated by pro- and anti-inflammatory mediators such as cytokines: interleukins, interferons and tumour necrosis factor.[48] These mediators facilitate migration of cells to the site, amplify the response by activating other cells, and act on the endothelial cells to increase vasodilation and vascular permeability.[49] Afferent sensory nerve fibres are stimulated by the local cytokines such as interleukin-1 (IL-1)[50, 51] and relayed to the NTS in the DVC.[52] Vagal efferent fibres from the DMN synapse in the coeliac plexus and activate the splenic projecting cholinergic fibres.[53] Secreted noradrenaline within the spleen then triggers nearby T-cells that contain acetylcholinesterase to produce acetylcholine.[54] Acetylcholine then acts on macrophage surface α7nAchRs suppressing further release of cytokines and thereby inflammation.[55] This cholinergic anti-inflammatory pathway[56] acts to reduce excessive inflammation in the heart, lung, liver, pancreas and gastrointestinal tract and at the local site of injury or infection.[46, 57]

1.3 Perioperative myocardial injury

1.3.1 Definition of myocardial injury

The definition of myocardial injury in the perioperative setting is unclear in the literature and there is currently no consensus for its definition.[58, 59] Clinically the term myocardial injury covers the spectrum of myocardial stress states ranging from no permanent injury to necrosis of the cardiomyocyte. The fourth Universal Definition of Myocardial Infarction (UDMI) expert consensus document defines myocardial injury clinically as the "detection of an elevated cardiac troponin (cTn) value above the 99th percentile upper reference range for a given cTn assay. The injury is considered acute if there is a rise and/or fall of cTn values".[60] The UDMI crucially makes no assumption about the aetiology of the myocardial injury.[61]

Myocardial death due to prolonged ischaemia, i.e. myocardial infarction, is clinically defined as the "detection of a rise and/or fall of cTn values with at least one value above the 99th percentile for the reference range of the immunoassay test, and in the setting of evidence of acute myocardial ischaemia". The evidence includes clinical symptoms of myocardial ischaemia, new ischaemic electrocardiogram (ECG) changes, development of pathological Q waves, evidence on imaging of new loss of viable myocardium or new regional wall motion abnormality in a pattern consistent with an ischaemic aetiology, and identification of a coronary thrombus by angiography or autopsy. The incidence of myocardial infarction following noncardiac surgery is approximately 5%.[62] There are two further classifications of myocardial infarction relevant to noncardiac surgery: Type 1 myocardial infarction occurs when the precipitating event is plaque rupture; Type 2 myocardial infarction occurs when there is a mismatch between oxygen demand and supply.[60]

1.3.2 Myocardial injury after noncardiac surgery (MINS)

The extant literature on perioperative myocardial injury (PMI) is biased towards an assumption that PMI is ischaemic in nature. This has led to some intrinsic contradiction in the definition and the diagnostic terms used to describe the phenomenon. The term MINS (myocardial injury after noncardiac surgery) was coined by Botto et al.[63] This defines myocardial injury as a rise in cTn with or without ischaemic signs and symptoms within 30 days of noncardiac surgery. However, the definition excludes patients with non-ischaemic cardiac causes of elevated post-surgery troponin such as tachyarrhythmias, trauma, pericarditis, and extra-cardiac causes (pulmonary embolism, chronic kidney disease and sepsis). Although ischaemic signs and symptoms are not required for the diagnosis, the prima facie assumption is that the (predominant) aetiology of a troponin rise after surgery is ischaemia. The 2017 VISION (**V**ascular events **I**n noncardiac **S**urgery patients c**O**hort evaluatio**N**) study[64] further refined the definition of MINS with respect to the troponin assay levels: MINS was defined as a rise in troponin after noncardiac surgery, where the high sensitivity troponin assay was recorded after surgery as either between 20 $ng.L^{-1}$ to <65 $ng.L^{-1}$ with an absolute change ≥5 $ng.L^{-1}$ from before surgery, or an absolute troponin value ≥65 $ng.L^{-1}$. However, a prospective study by Puelacher et al.,[65] that assessed the incidence of myocardial injury after noncardiac surgery and its association with mortality, defined myocardial injury as an absolute increase in HsTnT ≥14$ng.L^{-1}$, without excluding secondary causes of HsTnT elevation. This definition is more in line with the UDMI definition, and again does not make assumptions regarding the cause of troponin rise after surgery.

1.3.3 Troponin elevation is common and mostly asymptomatic after surgery

Two large multicentre prospective cohort studies by the VISION study group have evaluated the link between post-operative troponin assays and morbidity and mortality. The first of these studies, published in 2012,[66] used the Roche 4th-generation Elecsys Troponin T assay to measure troponin. 11.6% of the 15133 patients followed up had TnT assays levels above normal threshold values ($\geq$0.03 ng.ml^{-1}). The study was repeated in 2017 using the more widely clinically utilised Roche 5th Generation High sensitivity Troponin T (HsTnT) assay.[64] 35.2% of the 21819 patients followed up had a peak troponin level after surgery above the threshold value ($\geq$14ng.L^{-1}). In addition to the VISION studies, a planned sub-analysis on the patient cohort from the Evaluation of Nitrous oxide in Gas Mixture of Anaesthesia-II (ENIGMA) trial showed that 18.5% (1296 out of 6992 patients) had a raised troponin within 72 hours after surgery.[67] A meta-analysis of observational studies reporting MINS with cardiac biomarkers estimated the incidence to be 19.6% (95%CI 17.8-21.4%).[68] However, the authors note in the review that the heterogeneity of the definition of MINS, and the range of cardiac markers utilised, makes confirming overall estimates challenging.

It was observed that many patients with an elevated troponin after surgery did not demonstrate clinical features of myocardial ischaemia. 78% of the patients in the 2017 VISION study with an elevated HsTnT after surgery did not have any clinical ischaemic features. These features had been defined as ischaemic symptoms (i.e. chest pain), ischaemic electrocardiographic changes or new regional wall abnormality on echocardiogram.[64] Similarly, in the Perioperative Ischaemic Evaluation (POISE) study where 5% of patients were diagnosed with myocardial infarction after surgery, only 65.3% experienced ischaemic symptoms.[62]

1.3.4 Elevated troponin and its association with morbidity and mortality

Despite the lack of a definitive and precise definition, what is undisputed is that a rise in troponin detected after noncardiac surgery is associated with significant morbidity and mortality. Meta-analysis of data from 25 studies looking at short- and long-term outcomes after surgery in the presence of MINS showed an association with increased risk of overall in-hospital mortality, 30 day mortality and 1 year mortality.[68] The first VISION study showed that patients with peak troponin levels ($\geq$0.03ng.ml^{-1}) after noncardiac surgery were associated with higher 30 day mortality compared to patients with peak levels $\leq$0.01 ng.ml^{-1} (adjusted hazard ratio, 10.48; 95% CI, 6.25-16.62).[66] In addition, Botto et al. 2014 showed that an asymptomatic rise in troponin was associated with an increased risk of non-fatal cardiac arrest, congestive heart failure and stroke after surgery.[63] The follow up VISION study supported the association with 30 day mortality when ischaemic features were not present (adjusted HR, 3.20; 95% CI, 2.37-4.32).[64] A sub-analysis of the ENIGMA study demonstrated that an isolated rise in troponin after surgery (i.e. not associated with myocardial infarction) is associated with long term (1 year) mortality of 10.6% vs 4.6%.[69]

The emphasis on an acute rise in troponin relative to baseline, as emphasised by the VISION study investigators, may not be significant in the perioperative setting: it has been shown that a raised troponin above the 99th percentile is associated with worse outcomes, irrespective of pre-surgery troponin levels.[65] However, what may be important is the *timing* of the rise after surgery, as it has been shown that early elevation of HsTnT, within 24 hours after surgery, is associated with increased morbidity.[70]

1.3.5 Pathophysiology for perioperative myocardial injury

The aetiologies for an elevated troponin after surgery can be categorised into cardiac causes (coronary and noncoronary), and noncardiac causes (perioperative and pre-existing).[71] However, the pathophysiology for an elevated troponin after surgery remains poorly understood.

Cardiac causes related to coronary artery pathophysiology are conventionally explained using the universal clinical definitions and diagnostic criteria for myocardial injury and myocardial infarction (MI):[60] plaque rupture, erosion or fissuring with acute thrombosis formation (Type 1 MI); or myocardial oxygen supply-demand mismatch (Type 2 MI), both leading to myocardial ischaemia.[72] The causes of Type 2 MI in noncardiac surgery are multifactorial and may include the toxic effects of increased endogenous catecholamines, coronary vasospasm, endothelial dysfunction,[73] intraoperative tachycardia,[74] and intraoperative hypotension.[74] Other noncoronary cardiac causes for a raised troponin include myocarditis, valvular disease, cardiomyopathy and cardiac contusion.[71] Noncardiac causes of elevated troponin can be divided into pre-existing disease states such as renal failure and chronic inflammation, and perioperative factors such as pulmonary embolus, sepsis, hypertension and anaemia.[71]

The observational studies applying the unchallenged definition of MINS have attributed an asymptomatic elevation of troponin to an ischaemic aetiology.[63] However, an elevation of troponin in the absence of myocardial infarction represents myocardial injury of unknown origin, and therefore troponin should be viewed as “organ specific not disease specific”.[75] There is now growing evidence that the pathophysiological mechanism for elevated troponin after surgery in the absence of noncardiac causes is not solely ischaemic in origin.

A study assessing preoperative coronary anatomy using computer tomography angiograms in patients who experienced elevated troponin after noncardiac surgery showed that 29% of patients who had a troponin rise had coronary arteries classified as normal or non-obstructive.[76] Histological examination of the coronary arteries of patients who had fatal myocardial infarctions after noncardiac surgery showed that only 46% contained plaque rupture.[77] Pharmacological agents such as aspirin that are protective in acute coronary syndrome have been shown to provide only limited protection against myocardial injury after surgery.[78] It should also be noted that in the VISION studies, 78% of patients who had a raised troponin had no defining perioperative ischaemic symptoms or electrocardiographic ischaemic features.[64]

In summary, an elevation of cardiac troponin after noncardiac surgery is common, predominantly asymptomatic, and associated with significant morbidity and mortality. Investigation into potential aetiologies beyond the accepted dogma of cardiac ischaemia is crucial to the development of future prognostication and therapies.

1.3.6 Adrenergic surgical stress and perioperative myocardial injury

Adrenergic stress is mediated by the stimulation of adrenergic receptors by catecholamines and their downstream pathway effects.[79] Surgery can activate the adrenergic stress response via the hypothalamus activating the SNS. This leads to an increase in catecholamines released from the adrenal medulla, and noradrenaline from presynaptic terminals.[80] The downstream pathway effects of adrenoreceptor (alpha and beta) stimulation on the heart have been described above: in summary, there is a positive chronotropic, inotropic, and dromotropic effect on the heart.[4] This physiological response to surgery is beneficial in preserving oxygen supply to tissues during the increased metabolic demand of the surgical insult.

The intended benefits of increased heart rate and cardiac contractility, as part of the physiological adrenergic stress response, may be limited by the adverse effects of adrenergic stimulation of the heart. These adverse features may contribute to the pathophysiology of PMI.

Tachycardia increases the potential risk of mismatch between oxygen supply and demand in the myocardium, thus increasing the risk of myocardial ischaemia.[72, 81] Tachyarrhythmias can also be triggered by β adrenoreceptor overstimulation.[82] The overstimulation of the β adrenoreceptor leads to calcium overload, which then drives the sodium-calcium exchanger, depolarising the cardiomyocyte towards its action potential threshold, and making the cell more arrhythmogenic.[83]

Stimulation of the cardiac adrenoreceptors can also induce direct myocardial injury and necrosis.[84] Experimental studies have shown that acute β-adrenergic stimulation with isoprenaline causes cardiomyocyte necrosis and apoptosis. The damage is mediated by an increase in sarcolemmal calcium in the cardiomyocyte though β-adrenergic cascade

signalling.[85] However, there is also is also experimental evidence that in certain conditions such as ischaemia/reperfusion injury, myocardial ischaemia and chronic heart failure, that beta-adrenergic agonist stimulation can be cardioprotective through the activation of anti-apoptotic pathways.[86, 87]

Elevated troponin after surgery may also be detected as a result of increased permeability of the cardiomyocytes following β-adrenergic-induced increased contractility and myocardial stretch.[88] The adrenergic stress response contributing to PMI may theoretically be augmented by the delivery of routine adrenoreceptor agonist pharmacological agents such as metaraminol, noradrenaline, phenylephrine or adrenaline during the perioperative period.

1.3.7 Cardiac troponin as a biomarker perioperative myocardial injury

The cardiac troponin (cTn) products that are released into the blood stream from the cardiomyocyte consist of both intact troponin complex and its degraded products.[89] cTnT appears in blood as its free form or as part of its original I:C:T complex, whereas cTnI appears mainly as the I:C complex.[90] The different components of the troponin complex and the release kinetics of the fragments may potentially provide an opportunity to differentiate the mechanism of its release. However, there is currently no consensus on what forms of cTn are present in blood for different causes of myocardial injury.[91]

Troponin release from the structural component of the myofibril requires both a leaky plasma membrane, and degradation and/or dissociation from the myofibril complex.[88, 92] Release of troponin from the myofibrils is due to proteolytic degradation in the myocardium by enzymes: calpain, caspase and matrix metalloproteinase.[75] However, a proportion of cTn and its components are found in the cytosol, and therefore the release does not always require structural degradation. The cellular mechanisms leading to troponin release are thought to include cellular necrosis, cell apoptosis, leakage through cell wounds, or the release of membranous blebs.[75]

Cardiomyocytes are vulnerable to cellular necrosis triggered by ischaemia, calcium overload, direct trauma, inflammation or toxins.[93] During ischaemia, ATP reserves are consumed, and as a consequence the actin-myosin crossbridge formation remains fixed, as the excitation-coupling process is ATP dependent.[94] The fixed crossbridge state or contracture results in increased cardiomyocyte fragility, ultimately resulting in myofibril band necrosis.[95] The prolonged ischaemia also results in reverse mode sodium-calcium exchange (NCX), leading to

increased cytosolic calcium, which causes increased contraction after reperfusion and further necrosis.[96] Apoptosis can be triggered by stretch of the cardiomyocytes[97] and by brief periods of ischaemia that do not cause infarction.[98] Experimental studies have shown that the release of proteins such as cTn from cardiomyocytes in the absence of cell death can be mediated though transient increases in cell membrane permeability referred to as "cell wounds".[88]

Troponin found in cardiac muscle has a distinct protein structure, and therefore a different amino acid sequence, from skeletal muscle troponin.[99] This has allowed for the development of antibody assays that are highly specific [100] for cardiac troponin found in the blood stream. Quantitative assays developed for cTnI and cTnT use non-competitive enzyme linked immunosorbent assays (ELISA) utilising antibodies that are highly specific to cTn epitopes. The antibodies are linked to a signal generating system to allow for quantification.

To determine what level constitutes a "positive" troponin, and hence myocardial infarction/injury, the manufacturers of the assays have determined a reference value from a healthy population. The reference value is set at the 99th percentile for the healthy population and assay. The high sensitivity assays are able to detect troponin levels at very low concentrations, and therefore the thresholds to detect myocardial injury/infarction will identify patients with elevated troponins attributable to other causes.[101] Moreover, a study investigating cardiac troponin thresholds and kinetics for patients presenting with symptoms of acute coronary syndrome showed that cardiac troponin concentrations at presentation, and their subsequent kinetics, are not sufficient to distinguish Type 1 MI from other causes of myocardial injury.[102] The cardiac troponin assay tests are useful for identifying patients who meet the UDMI definition of myocardial injury and could be used to risk stratify patients in perioperative screening programmes.[103] However, as the troponin assay cannot distinguish the

aetiology for myocardial injury, patients may be inadvertently, and incorrectly, treated for a presumed ischaemic aetiology; therefore alternative biomarkers that offer better mechanistic insights into pathophysiology should be explored to elucidate the mechanisms underlying PMI.

1.4 MicroRNA

The human genome represents a complete set of deoxyribonucleic acids (DNA) that contains genetic instructions for the organism. Nucleotides form sequences, known as genes, that code for proteins. To create proteins from the genetic sequence, the DNA needs to be transcribed into ribonucleic acids (RNA). The RNA transcripts are collectively known as the transcriptome and consist of protein coding RNA (messenger RNA; mRNA) and non-coding RNA which includes microRNA, long coding RNA and ribosomal microRNA. MicroRNA were first described in the nematode Caenorhabditis elegans,[104] and are the most extensively investigated non-coding RNA over the last decade.[105] They have a crucial function in the regulation of post-transcriptional gene expression[106] and biological signalling processes.[107] Loss of function studies have demonstrated the importance of microRNA in organ development, demonstrating that they have a key role in tissue identity.[108] They are released by tissues and can be readily detected in plasma and serum,[109] thus making them accessible for measurement by real-time quantitative polymerase chain reaction techniques.

It is beyond the scope of this thesis to produce a detailed account of microRNA-mediated gene silencing. I will summarise microRNA biogenesis and its role and regulation in gene expression, before going on to outline the role of microRNA in biological and cellular functions, specifically with reference to cardiovascular physiology and pathophysiology. I conclude by describing the characteristics of specific microRNA which will be investigated in this thesis for their potential as tools to determine the mechanisms underlying elevated troponin after noncardiac surgery.

1.4.1 MicroRNA biogenesis

MicroRNA are small (18-22 nucleotides) endogenous non-coding RNA molecules synthesised in the nucleus of cells. MicroRNA genes are transcribed within the nucleus by RNAse polymerase II to form a long primary microRNA (Pri-miRNA) hairpin structure.

The Pri-microRNA genes lie within both intron and exon regions for non-coding and coding transcripts. The Pri-microRNA hairpin structure contains a terminal stem loop, 3-33 base pairs, and 2 single stranded RNA segments with 5' and 3' ends.[110] The microRNA sequence is embedded within the Pri-microRNA. Within the nucleus, a microprocessor complex consisting of the protein DGCR8 and ribonuclease III Drosha enzyme, cleaves the stem loop of the Pri-microRNA to form a smaller hairpin structure called pre-microRNA.[111] Pre-microRNA is then exported into the cytoplasm by forming a complex with protein exportin 5.[112] The pre-microRNA terminal loop is cleaved by the Dicer RNase III type endonuclease to form a mature microRNA duplex.[113] Dicer Rnase III is dependent on forming complexes with ds-RNA binding proteins such as transactivation-response RNA binding proteins (TRBP).[114] TRBP is itself stabilised through phosphorylation by mitogen-activated protein kinases (MAPK) and extracellular regulated kinases (ERK).[115] The mature strand of the microRNA duplex is then loaded onto an Argonaute protein to form an RNA-induced silencing complex (RISC) in a process called RISC loading it exerts its gene silencing function. The other microRNA strand is degraded (Figure 1.2).

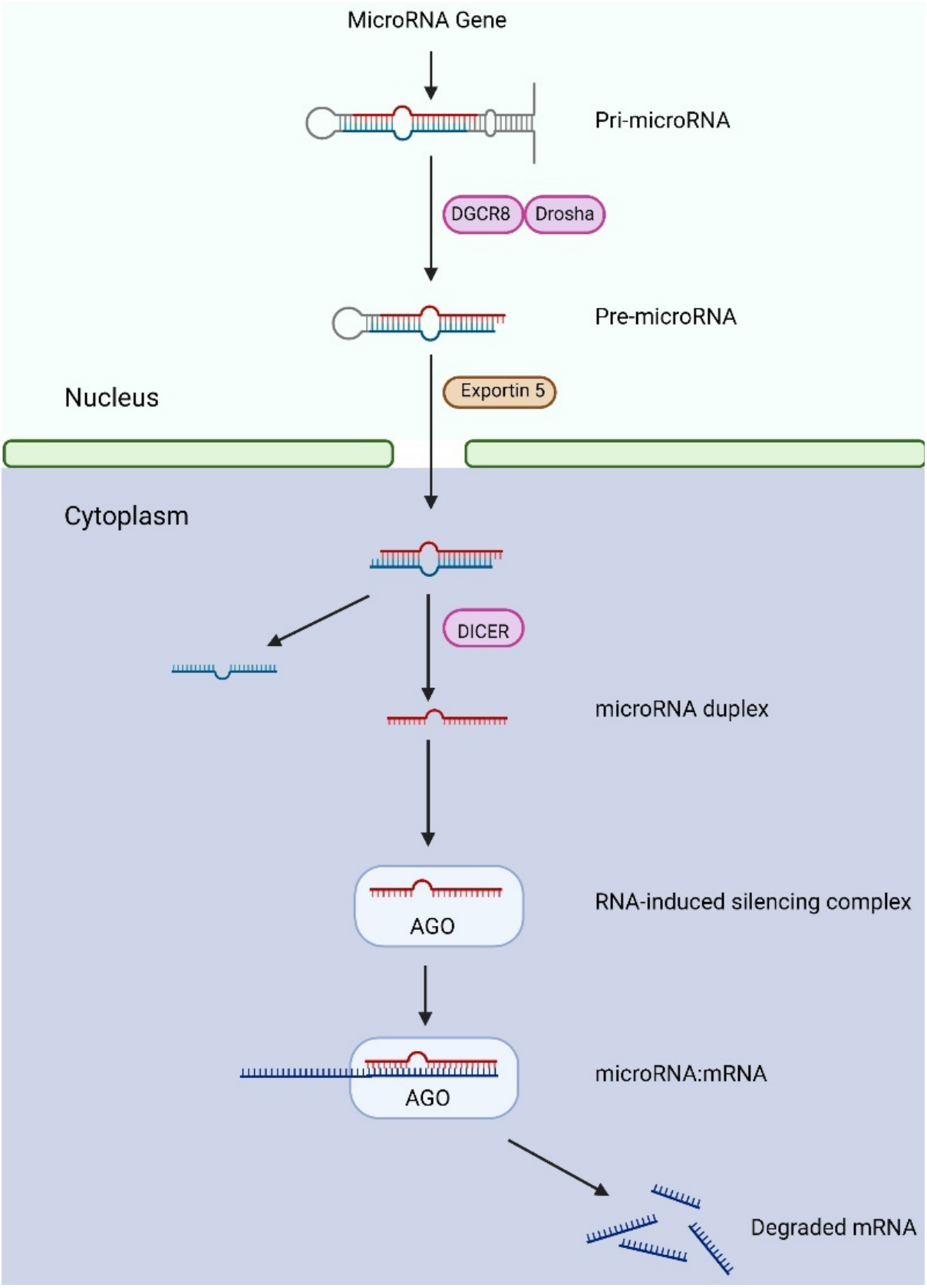
MicroRNA Gene
Pri-microRNA
DGCR8
Drosha
Pre-microRNA
Nucleus
Exportin 5
Cytoplasm
DICER
microRNA duplex
AGO
RNA-induced silencing complex
AGO
microRNA:mRNA
Degraded mRNA

Figure 1.2 MicroRNA biogenesis and function

The schematic diagram is adapted from Bartel 2018.[108] MicroRNA are transcribed to Pri-microRNA within the nucleus. A complex of protein DGCR8 and ribonuclease III Drosha enzyme cleaves the stem loop of the Pri-microRNA to form a smaller hairpin structure called Pre-microRNA. Protein exportin 5 then exports the Pre-microRNA into the cytoplasm. The Pre-microRNA terminal loop is cleaved by the Dicer RNase III type endonuclease to form a mature microRNA duplex. The mature strand of the microRNA duplex is then loaded onto an Argonaute protein (AGO) to form an RNA-induced silencing complex (RISC). The other microRNA strand is degraded. After the formation of a microRNA:mRNA interaction, the RISC recruits a glycine-tryptophan protein (GW182 protein) to mediate deadenylation of the messenger RNA,[116] thereby silencing gene function. AGO; Argonaute protein. Figure created with biorender.com

1.4.2 Nomenclature for microRNA

As described above, microRNA are short RNA molecules consisting of 18-22 nucleotides. MiRbase is a comprehensive searchable database of microRNA sequences and their nomenclature.[117] For this thesis, Ver. 22 (2018) was used to annotate microRNA sequences.[117] The miRBase repository contains sequences for 48860 mature microRNA products from 271 species. The first three letters denote the species: "hsa" denotes homo sapiens (human) and "mmu" denotes mus musculus (mouse). The miR refers to the mature microRNA whereas mir refers to the microRNA gene sequence. The numbering of the microRNA is sequential depending on when the microRNA was first identified. The 3p or 5p suffix refers to the 5' or 3' arm of the pre-microRNA duplex (Figure 1.3).

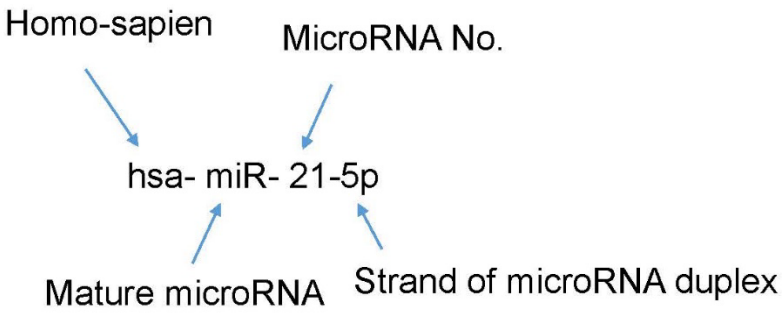

Figure 1.3 Explanation of microRNA nomenclature

hsa-miR-21-5p is used as an example to illustrate the nomenclature

1.4.3 Functions of microRNA

MicroRNA are described as the "sculptors of the transcriptome"[108] because of their ability to silence gene expression. This is regulated by the microRNA-RISC complex through mRNA decay or translation inhibition.[118] MicroRNA targets mRNA by base-pairing their "seed"

nucleotides with the nucleotides on the 3' untranslated region (UTR) of mRNA.[119] After the formation of a microRNA:mRNA interaction, the RISC recruits a glycine-tryptophan protein (GW182 protein) to mediate deadenylation of the messenger RNA,[116] thereby silencing gene function (Figure 1.2). Each of the more than 30000 microRNA now identified can interact with multiple mRNA 3'UTR target sites. This illustrates the complex regulation of microRNA and gene function[108] in many cell types such as endothelial cells, monocytes, macrophages, cardiomyocytes, vascular smooth muscle cells and platelets.[120]

1.4.4 Regulation of microRNA function

The regulation of microRNA function, and thereby gene expression, lies in the regulation of their biogenesis: gene transcription, microRNA processing and RISC loading. Intracellular and extracellular stimuli can alter the different steps of biogenesis.[121] Cellular oxidative stress pathways may also regulate microRNA function through the regulation of Drosha interaction with DGCR8. Drosha has been shown to be phosphorylated by oxidative stress-induced MAPK phosphorylation pathways.[122] This causes Drosha to reduce its interaction with DGCR8 and increase Drosha degradation and cell death.[123] In hypoxic conditions, epidermal growth factor signalling phosphorylates Argonaute protein, which impairs its interaction with Dicer during RISC loading,[124] thus decreasing microRNA:mRNA interaction.

1.4.5 microRNA in cardiovascular physiology and pathophysiology

MicroRNA have been demonstrated to be enriched in the myocardium.[125-130] Sequencing and profiling experiments have shown microRNA to be involved in normal myocardium physiology and pathophysiological states. They play a role in cardiomyocyte cell

differentiation and survival,[131] cardiomyocyte calcium regulation,[132-134] cardiac myocyte apoptosis,[135-139] cardiac conduction,[140] cardiac inflammation[141 142, 143] and cardiomyocyte death.[144] Their function is not only restricted to the intracellular environment but may also be involved in cell to cell communication: they have been suggested to act as paracrine mediators[145] by the modification of gene expression within the target cell.[146] Despite low yields, microRNA have been shown to be remarkably stable in plasma and serum. Their stability outside of the cell is a result of binding to Argonaute-containing protein complexes or by being packaged within extracellular vesicle structures such as exosomes.[147] This stability and tissue-specificity has led to microRNA being hailed as a "liquid biopsy" for biological functions and disease states.[109] MicroRNA can be utilised to better understand the mechanisms of gene regulation for specific diseases, and therefore the pathophysiology. MicroRNA profiling has been used to explore pathological processes in cardiovascular disease.[148] Both circulating plasma and serum microRNA have been identified in cardiovascular disease states such as cardiac ageing,[149] cardiac hypertrophy, heart failure,[150] coronary artery disease[151, 152] and acute coronary syndrome.[129, 148, 151, 153-156]

1.4.6 Cardiac microRNA of interest selected for this thesis

MicroRNA have not been previously profiled in patients who develop PMI after noncardiac surgery. For this thesis, microRNA -1, 21, 146, 133, 208 and 499 were selected to elucidate the potential mechanisms for PMI. The selected microRNA are all expressed in myocardial tissue.[125-130] Good correlation between HsTnT troponin levels and microRNA expression in coronary circulation has been demonstrated in patients with ACS. This suggests that these microRNA are indeed released into the coronary circulation and therefore detectable in serum and plasma after myocardial injury.[157] These microRNA have been shown experimentally to

be involved with cardiomyocyte function and have a potential role in its pathophysiology.[130] Figure 1.4 summarises the physiological and pathophysiological states with which they are associated; each microRNA is discussed in turn below.

MicroRNA-1

Experimental studies with knockout mice have demonstrated the importance of the expression of microRNA-1 in myocyte differentiation and proliferation.[158, 159] It has a potential role in the regulation of conduction: microRNA-1 targets genes of the subunits for the L-type Ca^{2+} channel and K^{+} voltage channels involved in repolarisation and depolarisation.[160] Rat experimental models have shown that over-expression of microRNA-1 enhances cardiac excitation of contraction coupling by enhancing the phosphorylation of L-type and RyrR2 channels[161] via targeting protein phosphatase 2A (PP2A). In normal physiological conditions, the sodium/calcium co-transporter (NCX) plays an important role in removing calcium from the cardiomyocyte during excitation-contraction coupling.[162] NCX expression is regulated by microRNA-1 expression through the serum-response factor (SRF)-miR-1 Axis.[132]

MicroRNA-21

MicroRNA-21 is expressed in cardiomyocytes.[163] Through loss of function and gain of function experiments, its role in cardiomyocytes has been shown to be mediated by its target genes: programmed cell death 4 (PDCD4) and Sprouty RTK Signaling Antagonist 1 (SPRY1).[164] MicroRNA-21 has been shown to be protective against ischaemia-induced cell apoptosis in cultured cardiomyocytes by targeting PDCD4 and the activator protein pathway.[165, 166]

MicroRNA-133

Similar to microRNA-1, microRNA-133 is crucial to cardiomyocyte development and differentiation from smooth muscle cells.[167] PP2A is a target of microRNA-133 and therefore it has a role, via the dephosphorylation of RyR2, in maintaining calcium homeostasis.[133] MicroRNA-133 also targets voltage gated K+ channels[168] and therefore contributes to the pacemaker current slope.

MicroRNA-146

MicroRNA-146 has been shown to be upregulated in cultured human cardiac cells and rat cardiomyocytes when treated with tumour necrosis factor-alpha (TNF-α), a pro-inflammatory cytokine.[143] In the same experiment, Fos expression was downregulated when microRNA-146 was overexpressed. This corresponded to a decrease in Activating protein-1 (AP-1) DNA binding activity and matrix metalloproteinase activity. AP-1 is a heterodimeric transcription factor composed of transcription factors Jun, Fos and activating transcription factor, that regulates gene expression in response to external stimuli. By targeting Fos, a component of AP-1, microRNA-146 may exercise a protective role by attenuating AP-1 activity and modulating inflammation by reducing interleukin-6 (IL-6) and matrix metalloproteinase 9 expression.[143]

MicroRNA-208

MicroRNA-208 is abundantly expressed in cardiac tissue[130] and has two isomers: microRNA-208a and microRNA-208b. Both are involved in the later stages of cardiac development, and

microRNA-208a regulates cardiac myosin heavy chain (MyC7) expression.[169] Overexpression of microRNA-208a in mice leads to cardiomyocyte hypertrophy; gain and loss of function experiments both induce arrythmia, thus indicating a role in cardiomyocyte conduction.[170]

MicroRNA-499

MicroRNA-499 is highly enriched in ventricular cardiomyocytes[125, 126] and is important to the late differentiation stages of cardiomyocytes.[163] Overexpression of microRNA-499 in transgenic mice leads to cardiac contractile dysfunction in response to cardiac stress (aortic banding).[125] However, microRNA-499 has also been shown to be potentially protective against hydrogen peroxide (H_2O_2) apoptosis by inhibiting PDCD4 expression, a key pro-apoptotic protein in the mitochondrial apoptosis pathway.[136]

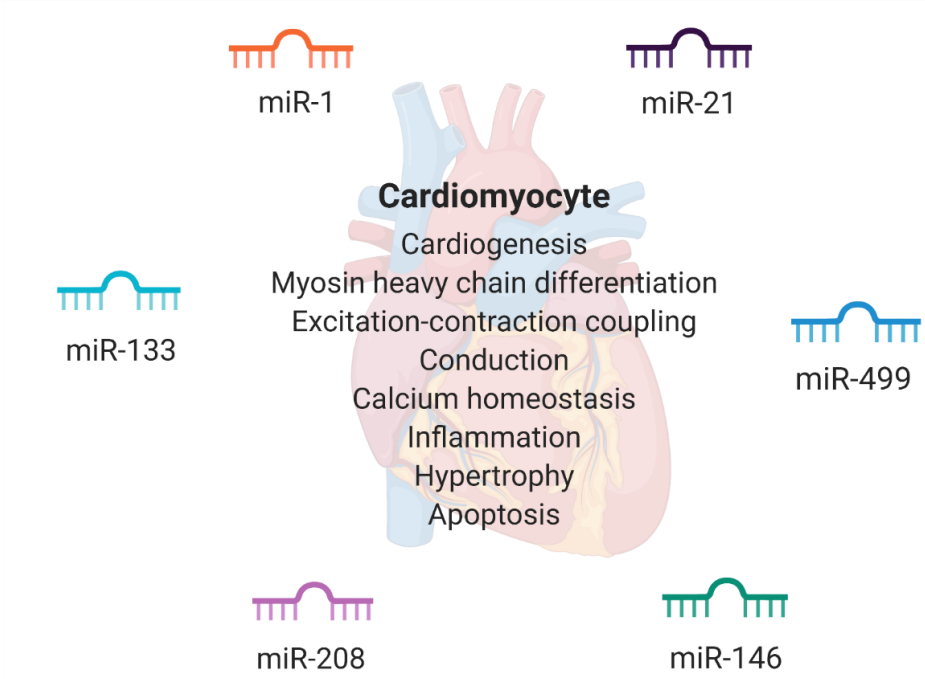

Figure 1.4 Selected microRNA and summary of their cardiac physiology and pathophysiological functions

1.4.7 Selected microRNA and cardiovascular disease

The selected microRNA have been detected in circulating plasma and serum for different cardiovascular disease states including acute coronary syndrome (ACS). [148] [171, 172] ACS is an umbrella term that refers to a group of clinical symptoms compatible with myocardial ischaemia.[173] The underlying aetiology may be secondary to atherosclerotic plaque disruption leading to reduced blood flow to the heart, or a mismatch of oxygen supply to myocardial demand.[174] Regardless, the pertinent point is that acute coronary syndrome has an *ischaemic* aetiology. As part of a systematic review, Kaur et al.[172] analysed studies comparing microRNA expression in patients who developed ACS versus controls, where controls were defined as patients having no angiographic evidence of coronary artery disease. In 118 studies, microRNA 1, 21, 133, 208 and 499 were among the microRNA most upregulated in patients who developed ACS.[172] These cardiac-related microRNA may therefore provide a mechanistic insight into the pathophysiological mechanisms associated with cardiac injury in acute coronary syndrome.

Table 1.1 (below) highlights some of the clinical studies in which the selected microRNA were upregulated in patients with ACS as compared to a control group. From Table 1.1, it is apparent that one of the limitations when comparing these studies is that there is variation in the definition of the control group, which can account for differences in microRNA expression. The control group for ACS microRNA expression comparison was defined based on the aim of each individual study. For example, if the study was investigating a more sensitive biomarker for ACS, patients with non-CHD confirmed with angiography were used.[129, 175] However, if the aim was to explore microRNA to detect myocardial injury, then samples from healthy volunteers were taken.[176] It also noted in the systematic review by Kaur et al. 2019[172]

that there is significant heterogeneity in the methodologies to analyse microRNA expression. These are discussed and addressed in the General Methods Section 2.6.

Table 1.1 Clinical studies investigating microRNA in patients with acute coronary syndrome.

Non-ACS conditions include stable angina, rhythm disorders, heart failure, pericarditis, "other cardiac diagnosis", and noncardiac chest pain. AMI: acute myocardial infarction. Non-CHD (coronary heart disease): chest pain but no coronary heart disease, as confirmed by angiography. STEMI: ST elevation myocardial infarction. Healthy volunteers: separate cohort. Control: chest pain with no cardiac disease.

Study	Sample Type	Comparator groups	MicroRNA upregulated
Oerlemans et al., 2012 [175]	serum	ACS versus non-ACS	miR-1 miR-21 miR-133 miR-146 miR-499
Wang et al., 2010 [129]	plasma	AMI versus non-CHD AMI versus healthy volunteers	miR-1 miR-133 miR-208 miR-499
D'Alessandra et al., 2010[177]	plasma	STEMI versus healthy volunteers	miR-1 miR-133 miR-499
Corsten et al., 2010 [176]	plasma	AMI versus control	miR-208 miR-499

In summary, these specific microRNA were selected because they are cardiac specific, implicated in cardiomyocyte function, and can be detected in circulating human plasma and serum samples. Moreover, they are predictive for diagnosing cardiac injury in ACS. The microRNA have not previously been investigated in a cohort of patients with PMI after noncardiac surgery. To investigate whether a rise in troponin after surgery represents an occult ischaemic episode, this thesis will explore whether these microRNA which are common and specific for ACS can be detected, thus lending credence to an ischaemic aetiology for PMI.

1.5 Measurement of cardiac vagal activity and its association with morbidity and mortality

The non-invasive measurement of efferent cardiac vagal activity in perioperative settings employs measures that assess parasympathetic influences on the heart rate.[178] The two techniques utilised in this thesis are heart rate variability and heart rate recovery after a postural manoeuvre. A general overview of the techniques and their association with morbidity and mortality is given below with technical details given in General Methods Section 2.7**.**

1.5.1 Heart rate variability

Heart rate (HR) fluctuates on a beat-to-beat basis. These fluctuations represent the shifting sympathovagal outflow in response to naturally occurring physiological events.[179] For example, the blood pressure oscillates with ventilation due to changes in intrathoracic pressure. These changes are detected by baroreceptors and alter autonomic outflow to the myocardium and modulate heart rate.[180] Therefore heart rate variability (HRV) reflects the physiological changes to cardiovascular homeostasis. The variation is controlled by a complex interaction between parasympathetic, sympathetic and mechanical (e.g. Bainbridge reflex) factors acting on the pacemaker cells of the heart.[181]

There are two commonly used methods to analyse HRV that can provide indices of cardiac autonomic activity: time domain and frequency domain analysis.[182] These are outlined with standard values in the Task Force of the European Society of Cardiology and the North American Society of Pacing and Electrophysiology 1996.[182]

1.5.1.1 Time domain analysis

Time domain analyses are statistical analyses that are derived directly from R-R intervals or from the differences in the R-R intervals between QRS complexes on an electrocardiogram (ECG).[182] The mean RR interval can be calculated together with mean HR. The standard deviations of the RR interval (conventionally referred to as SDNN) can be calculated as indices for overall HRV and therefore combined autonomic regulation.[182] SDNN has previously been shown to be a predictor of mortality in chronic heart failure patients[183, 184] and for patients post-myocardial infarction.[185] The root mean square of the standard deviation (RMSSD) and the number of RR intervals less than 50ms (nn50) are measures of short term variation and correlate with parasympathetic modulation.[182]

1.5.1.2 Frequency domain analysis

The R-R signal can be decomposed into frequency components by a power spectral analysis. The power spectral density of each of these frequencies can then be quantified for analysis of HRV. The types of power spectral density analysis can be classified as non-parametric (Fast Fourier Transform) and parametric (autoregressive spectral estimation).

The common frequency bandwidths analysed in short recordings (<5 minutes) are: very low frequency (VLF) <0.04 Hz; low frequency (LF) 0.04-0.15Hz; and high frequency (HF) 0.15-0.4Hz.

Using a series of pharmacological blockade in-vivo experiments, the frequency bandwidths have been shown to reflect autonomic modulation of heart rate variability.[179] Power spectral

density of HF is strongly associated with parasympathetic modulation of the heart.[179, 182] However it would be an oversimplification to assume that consequently LF represents cardiac sympathetic activity.[186] Denervation of the vagus nerve to the SAN in canine models resulted in a decrease in both peak HF and LF.[187] LF peak was shown to further decrease with β-adrenoreceptor antagonists, suggesting that peak low frequency reflects both divisions of the autonomic nervous system.[187] LF power spectral density has been shown to better correspond with baroreceptor function rather than solely sympathetic function.[188, 189] Therefore LF most likely represents a combination of both parasympathetic and sympathetic modulation.[181]

The ratio between LF and HF (LF:HF) is frequently reported as a measure of the sympathovagal balance.[190] However, it is based on the assumptions that sympathetic and parasympathetic activity are solely responsible for LF and HF respectively; that physiological challenges to the autonomic system have reciprocal changes on each component; and that the relationship between sympathetic and parasympathetic modulation of HRV are linear.[191] Apart from HF and its association with parasympathetic activity, a critical review of the LF:HF has shown that these assumptions are an oversimplification, and therefore not an accurate quantification of sympathovagal balance.[186]

1.5.2 HRV and heart rate

It has been controversially suggested that heart rate variability is not a measure of cardiac autonomic tone, but is primarily affected by intrinsic cardiac heart rate.[192] Using a mathematical model for the sinoatrial node action potential, Monfredi et al demonstrated that there is an exponential decay-like relationship between HRV (measured as SDNN) and heart rate.[193] More significantly, this relationship has been supported by measuring HRV and HR in

humans, living animals, isolated Langendorff-perfused hearts, and single sinoatrial nodal cells (Figure 1.5).[193] It is recommended by Monfredi et al that studies evaluating HRV need to be adjusted for HR in their measurements, to account for the possibility that it is intrinsic cardiac activity affecting the HRV.

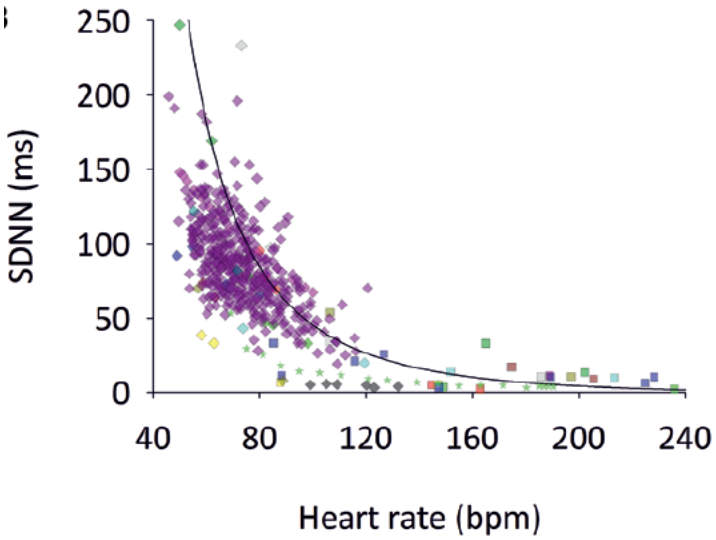

Figure 1.5 Relationship between SDNN and heart rate

Figure from Monfredi et al 2014. Each point represents an experimental data point and the solid line represents the mathematical model for sinoatrial node.

However, it is well established that the autonomic nervous system does control SAN periodicity.[194] Furthermore, it has been shown that autonomic blockage of the parasympathetic nervous system in canine models abolishes the HF component of HRV (Figure 1.6).[179] It would therefore be too simplistic to make the assumption that HRV is simply a surrogate for HR as argued by Monfredi et al. In addition, computational modelling for correcting the HRV for HR have been shown to reduce overall variability of the HRV metrics.[195]

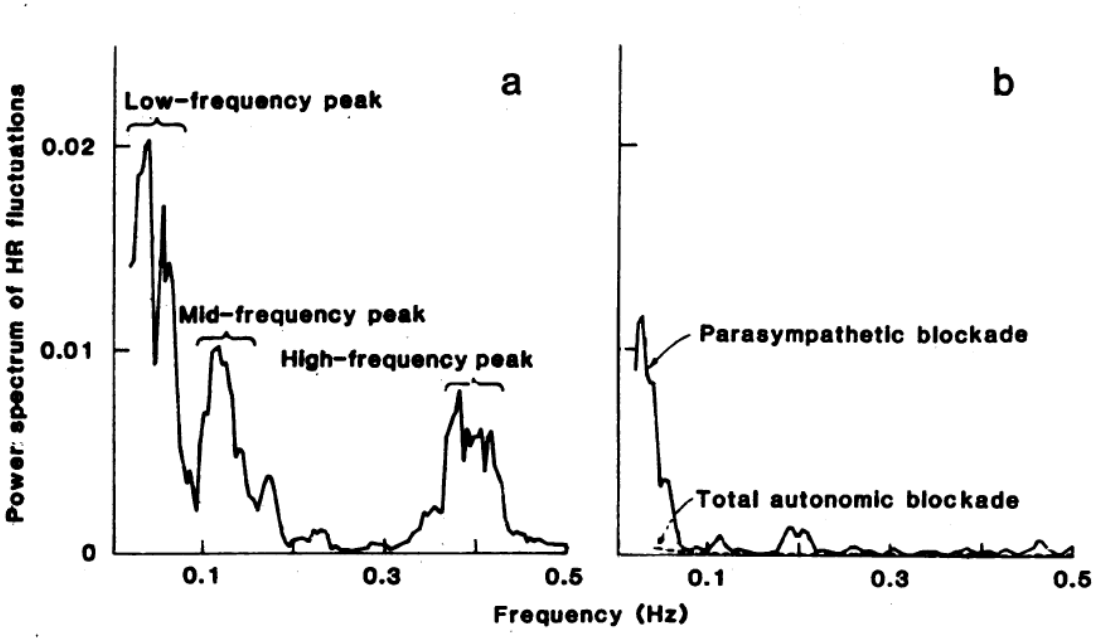

Figure 1.6 Power Spectrum of heart rate in adult conscious canines

Figure is from Akselrod et al 1981. Graph A shows power spectrum of HR in adult canines. Graph B shows the power spectrum of HR with parasympathetic blockage and loss of high frequency peak, suggesting that parasympathetic nervous system modulates the amplitude of the power spectrum.

To avoid a loss of significant variance in HRV analysis by HR correction, a more pragmatic approach is recommended by reporting HR with HRV metrics which has been adopted for this thesis.[195]

1.5.3 HRV and cardiovascular morbidity and mortality

Low HRV values are associated with an increased risk of cardiovascular events in the absence of known cardiovascular risk factors.[196] A similar trend is shown in a sub-study of the Framingham heart study, where low HRV values were associated with an increased risk of

overall mortality.[197] Both time domain and frequency domain measures are associated with an increased mortality following myocardial infarction.[198-200]

1.5.4 HRV: anaesthesia and noncardiac surgery

Intravenous (propofol) and inhalation (isoflurane) anaesthesia has been shown to reduce high and low frequency components, suggesting that both agents may decrease both cardiac vagal and sympathetic components of the autonomic nervous system.[201, 202] In animal studies, it is established that anaesthetic agents inhibit central vagal nerve activity;[203] it remains unclear if central inhibition takes place in human studies.

Studies investigating longitudinal HRV measures before and after noncardiac surgery are limited. The apparent trend is that high frequency and low frequency components are reduced after surgery, and that this persists for at least 72 hours after surgery. In patients undergoing abdominal and thoracic surgery (n=28) low and high frequency components of HRV were reduced after surgery, and this persisted for 72 hours after surgery.[204] In a separate cohort of patients undergoing elective hip arthroplasty (n=14), a similar pattern of persistent attenuated high and low frequency components was observed for 4 days after the initial surgery.[205] In a randomised control trial investigating whether chewing gum would preserve vagal neural activity after elective orthopaedic surgery, patients from both arms of the trial showed a decrease in time and frequency domain components 3 days after surgery.[206]

HRV measures have been shown to be associated with poor surgical outcomes.[207] Decreased HRV components before surgery are associated with increased 1 year mortality after high risk noncardiac surgery.[208] Patients undergoing elective abdominal surgery who had reduced HF

and LF components after surgery were found to be associated with an increased length of stay.[209]

1.5.5 Challenges for HRV in the perioperative setting

One of the challenges of measuring autonomic activity in the perioperative setting is achieving a standardisation of conditions when the measurements are undertaken throughout the perioperative process.[210] This includes patient, surgical, anaesthetic and environmental factors. Changes in heart rate are a common feature in the post operative period, and as already discussed above, this is potentially a major confounder in the assessment of HRV. This complexity may account for the wide variation in normal values for heart rate variability metrics in healthy controls.[211]

In addition, this large variation may be due to the lack of conformity in adherence to taskforce guidelines in measurement of HRV.[212] This lack of adherence also makes it difficult to compare studies and outcomes.

1.5.6 Heart rate recovery

In healthy individuals, the heart rate decreases rapidly after the cessation of exercise. [44] The speed of this decrease after exercise is called heart rate recovery (HRR): it can be quantified and used to measure parasympathetic reactivation.[17] Using muscarinic pharmacological blockage, it has been demonstrated that this rapid initial decrease in heart rate (heart rate recovery) is dependent on parasympathetic reactivation.[213] The arterial baroreflex is the major determinant for the increase in vagal activity [44] at the end of exercise. This is supported clinically where reduced HRR after exercise is associated with impaired baroreceptor sensitivity.[214] A potential advantage of HRR as a measure of parasympathetic function is that it is independent of the confounders of heart rate variability measures of autonomic function, such as resting heart rate [193] and respiratory rate.[215]

1.5.6.1 Heart rate recovery after exercise: cardiovascular morbidity and mortality

In a 6 year follow up study of 2428 patients with no known heart disease, impaired heart rate recovery after exercise, as defined by <12bpm one minute after the cessation of exercise, was associated with increased cardiovascular morbidity and mortality.[216] Using the same definition for HRR after exercise, a secondary analysis of 1326 patients from the UK cohort of the VISION study demonstrated that impaired heart rate after exercise prior to surgery was associated with PMI (OR 1.54 (CI 95%1.11-2.13 p=0.009).[217] A secondary analysis of two further observational studies showed that impaired HRR after exercise prior to surgery was associated with an increased risk of morbidity after surgery, including cardiovascular morbidity (RR 1.39 (CI 95% 1.15-1.69) p = <0.001).[218]

1.5.6.2 Challenges of heart rate recovery after exercise in the perioperative setting

Exercise testing to measure heart rate recovery is not always practicable before surgery. In cancer or other urgent surgery, the timeframe for perioperative assessment to surgery can be short. Exercise testing is also expensive and requires specialist equipment and expertise. Nor is it practical or possible to repeat exercise testing during the post-operative period due to the obvious mobility limitations in this period.

1.5.6.3 Heart rate recovery following an orthostatic manoeuvre

Changes to HR after postural change are mediated by vagal tone modulation of the sinus node via unloading and reloading of arterial baroreflexes.[219](Introduction section 1.2.3.1) Therefore an orthostatic manoeuvre that challenges similar baroreceptor reflex mechanisms[43, 220] to those elicited during exercise, has the potential to be utilised to measure HRR and quantify vagal activity, and thus serve as a feasible alternative to measuring HRR after exercise.

1.5.6.4 Heart rate recovery after an orthostatic manoeuvre and its association with cardiovascular morbidity and mortality

The orthostatic manoeuvre from the seated to the standing position has been shown to be a robust measurement of HRR (i.e. decrease in heart rate after standing) in the general population.[221] McCrory et al.[221] demonstrated that slower heart rate recovery is associated with higher long term mortality. Therefore, the orthostatic manoeuvre offers a potential scalable and reproducible measure of cardiac parasympathetic activity in the perioperative period that

could potentially allow for the identification of patients at risk of cardiovascular morbidity including PMI.

1.6 Cardiac vagal protective mechanisms against myocardial injury.

The population and clinical studies outlined above suggest that a loss of, or reduction in, cardiac vagal activity measured using HRV or HRR is associated with increased cardiac mortality and morbidity. I outline below the reasons why the cardiac vagal nerve may be protective in preventing adverse cardiac outcomes in the perioperative setting.

1.6.1 Haemodynamics

Tachycardia is the main cause of cardiac oxygen-supply mismatch after surgery.[72] It is therefore feasible that the negative chronotropic effect of m2AhR vagal stimulation can be protective against myocardial injury by limiting oxygen demand/supply mismatch.[222] In an experimental model examining vagal tone and an ability to exercise, an in vivo genetic model showed that silencing DVMN neurons (which innervate ventricular myocardium) impairs exercise capacity.[20] In the same study, rats that underwent DVMN silencing were given a β1 adrenergic receptor agonist (dobutamine) to model the adrenergic stimulation required to increase cardiac output (positive inotropy) to match the circulatory requirements of exercise. Dobutamine had no effect on inotropy in rats where the DVMN was silenced, suggesting that reduced vagal tone impairs myocardial contractility in response to adrenergic stimulation. It is not unfeasible to suggest that, if cardiac vagal activity is important in maintaining cardiac output to meet the circulatory requirements of exercise, then it would also be important in maintaining cardiac output when there is adrenergic stimulation during the perioperative period.

1.6.2 Cellular protective mechanisms

In a series of experiments monitoring left ventricular pressure and calcium current in isolated Langendorff-perfused rabbit heart preparations, it was demonstrated that positive contractility and increased calcium influx in response to sympathetic stimulation is reduced in the presence of vagus nerve stimulation of the heart at the level of the carotid.[223] This suggests that vagal nerve activity may have a role in attenuating calcium overload-mediated cardiomyocyte toxicity. This may be due to cholinergic stimulation of the ventricular m3AchR[224] leading to activation of antiapoptotic mediators (Bcl-2, ERK and SOD), and limiting intracellular calcium overload,[224] thus limiting oxidative stress. Activation of the m2AchR receptors by Ach also has a role in protecting cardiomyocytes from reactive oxygen species generated by damaged mitochondria. In vitro experiments have shown activation of mitophagy (mitochondria autophagy) though the PTEN-induced putative kinase 1 (PINK 1)/Parkin signalling pathway.[225] Autophagy is the evolutionary protective process whereby organelles are engulfed and recycled to remove damaged organelles before they start producing toxic mediators such as reactive oxygen species.[226] Ach can also promote cardiomyocyte mitochondrial biogenesis after reperfusion injury.[227]

The vagus nerve may also have a role in protecting against the metabolic effect of surgery on the heart: canine direct vagal nerve stimulation has also been shown to attenuate myocardial oxygen consumption and glucose oxidation in response to β adrenergic stimulation.[228]

1.6.3 Protection against arrythmias

It has been demonstrated in experimental isolated heart and in vivo animal models that vagal nerve stimulation can attenuate ventricular fibrillation.[229-231] Clinically, vagal nerve impairment, measured using HRV, is a poor prognostic indicator for morbidity associated with arrythmias in patient with heart failure.[82]

The negative chronotropic effect of vagal nerve stimulation on m2AchR receptors in the SAN is protective against arrythmias related to high heart rates.[232] DVMN vagal preganglionic motor neurons are responsible for the control of ventricular excitability, and experimental models have shown that reduced vagal activity is consistent with the development of a ventricular proarrhythmic phenotype.[19] Mechanistically, the anti-arrhythmic effects are mediated by neuronally released nitric oxide. This further facilitates the release of Ach from vagal preganglionic motor neurons via cGMP pathway increasing PKA phosphorylation of calcium channels.[233]

Clinically, non-invasive stimulation of the vagus nerve has been shown to reduce the duration and inducibility of atrial fibrillation in patients with paroxysmal atrial fibrillation.[234]

1.6.4 Cholinergic inflammatory reflex

Neuroimmune communication plays an important role in the development of all cardiovascular disease.[235] The neuroinflammatory reflex and the role of the vagal nerve activity has already been outlined in Section 1.2.3.2. Activation of the cholinergic anti-inflammatory pathway, by pharmacological and electrical vagus nerve stimulation, activates α7nAchR on macrophages[55]

which impairs leukocyte migration to sites of endothelial inflammation[236] and impairs TNF release.[237] Therefore the anti-inflammatory effects of the reflex may attenuate cardiac inflammation and limit tissue injury.[238, 239] In a cohort of patients listed for major surgery, impaired HRR after exercise (a measure of reduced vagal activity) was associated with high neutrophil to lymphocyte ratios (NLR).[240] NLR are associated with elevated cytokine levels relating to systemic inflammation.[241]

1.7 Summary

The aetiology of perioperative myocardial injury remains unclear: there is now growing evidence that perioperative myocardial injury is not the same entity as ischaemic myocardial infarction. Cardiac microRNA signatures have been used to better understand cardiovascular pathophysiology. By comparing microRNA signatures between patients with and without raised troponin levels after surgery, mechanistic insights into the aetiology of raised troponin after surgery will be elucidated. To further explore the underlying pathophysiology, cardiac vagal function will be characterised before and after surgery using HRV. In addition, a standardised orthostatic manoeuvre will be employed to assess HRR before and after surgery to evaluate parasympathetic dysfunction in patients with a raised troponin.

1.8 Research aims for thesis

Chapter 3

- Isolate and quantify levels of expression of microRNA in serum samples before and after noncardiac surgery in patients who developed perioperative myocardial injury (PMI), compared to matched controls who did not develop PMI.

- Assess whether the subgroup of patients who have a raised troponin after surgery, but who did not sustain myocardial infarction, share the same microRNA expression profiles as those seen in acute coronary syndrome.

Chapter 4

- Use heart rate variability measures to quantify cardiac vagal activity before and after elective noncardiac surgery.

- Examine if serial static measures of cardiac vagal activity are associated with PMI and noncardiac morbidity.

Chapter 5

- To use a standardised orthostatic (supine-to-sitting) manoeuvre to quantify HRR before and after elective noncardiac surgery.

- Examine if HRR responses after an orthostatic challenge differ between patients who develop PMI and those who remain PMI free.

1.9 Hypotheses for thesis

Chapter 3

Perioperative myocardial injury and acute coronary syndrome share pathophysiological mechanisms and therefore common microRNA signatures.

Chapter 4

Reduced efferent cardiac vagal activity after noncardiac surgery, as measured by heart rate variability, is associated with PMI and noncardiac morbidity.

Chapter 5

Parasympathetic dysfunction, as measured by reduced heart rate recovery after a standardised orthostatic manoeuvre, is associated with PMI.

Chapter 2
General methods

2.1 Overview

The aims and hypotheses in this thesis were explored and tested using clinical data and blood samples from patients enrolled in two prospective clinical observational studies: the **M**easurement of **E**xercise **T**olerance before **S**urgery (METS) study (Section 2.2),[242] and the Vagus (**X**)-**M**yocardial **I**njury in **N**oncardiac **S**urgery study (XMINS) (Section 2.3).[243] This section will provide an outline of each study design and its conduct with details of my involvement in each. The methodology for microRNA quantification and profiling is detailed in Section 2.6. Heart rate variability and heart rate recovery analysis was used to make serial measurements of cardiac parasympathetic function (Section 2.7).

2.2 Measurement of Exercise Tolerance before Surgery (METS) study.

2.2.1 Primary aim of the METS study

The primary aim of the METS study was to compare preoperative cardiopulmonary exercise testing (CPET) to subjective assessment for the prediction of cardiovascular morbidity and mortality within 30 days after major elective noncardiac surgery.

2.2.2 Study design

METS was an international, multicentre, prospective observational study conducted between March 1st 2013 to March 25th 2016. The study was conducted in accordance with the principles of the Declaration of Helsinki and the Research Governance Framework. Ethics approval was granted by the South East Coast (Surrey) Research Ethics Committee (13/LO/0135).

I used a nested case-control study design to test my hypotheses and the aims of this thesis using the clinical data and serum blood samples from the United Kingdom cohort of the METS study. A nested case-control study utilises an already defined cohort such as the completed METS study. Cases of interest are then selected from the cohort (i.e. patients who developed PMI) and controls (i.e. patients who did not develop PMI) are selected from the same cohort.[244] The advantage of the nested case-control study design is that the controls are from the same study population (i.e. patients undergoing noncardiac surgery). The primary METS study had been completed and its methodology published before the commencement of work towards this thesis.[242]

2.2.3 Participants

Inclusion criteria to the METS study were: age>40yrs; undergoing elective noncardiac surgery under general anaesthesia or regional (or both) with a minimum of one night overnight hospital stay; and ≥1 risk factor for cardiac complications (coronary artery disease, cardiac failure, cerebrovascular disease, diabetes mellitus, chronic renal failure, peripheral arterial disease, hypertension, a history of tobacco smoking within 12 months of surgery, or >70yrs). Exclusion criteria were: endovascular surgery; insufficient time for cardiopulmonary exercise testing (CPET) before surgery; implantable cardioverter–defibrillator; pregnancy; previous enrolment in the study; severe hypertension (>180/100 mm Hg); and/or other American Thoracic Society-defined contraindications to undertaking CPET. 620 patients were recruited into the United Kingdom arm of the study.

2.2.4 Study conduct and data and blood sample collection

Each participant underwent a preoperative CPET as per protocol previously published.[242] Researchers at each site collected data from patients and their medical records before, during, and after surgery, using a standardised case report form. Blood samples and ECGs were collected before surgery, and at 24h, 48h and 72h after surgery.

2.3 Vagus (X)-Myocardial Injury Noncardiac Surgery (XMINS) study

2.3.1 Aims of the XMINS study

The primary aim of the study was to determine whether cardiac parasympathetic dysfunction was associated with perioperative myocardial injury.

2.3.2 Study design

XMINS was a single centre, prospective, observational mechanistic cohort study conducted at University College London Hospital from 5th October 2016 to 14th January 2019. The study was approved by Stanmore Research Ethics Committee (MREC:16/LO/06/35) and conducted in accordance with the principles of the Declaration of Helsinki and the Research Governance Framework. The Strengthening and Reporting of observational Studies in Epidemiology (STROBE) guideline[245] was followed (the STROBE statement for the published study can be found in Appendix A). A pre-analysis plan was made available at www.ucl.ac.uk/anaesthesia/trials prior to completion of the study. An updated version is found in Appendix B. Written informed consent was obtained from all patients prior to surgery.

I co-designed the study and the analysis plan with my supervisor Prof. Ackland. I was lead investigator at the recruitment site. This involved the supervision of research nurses in the recruitment of patients, overseeing the recording of ECG data, obtaining blood samples, processing and uploading clinical record forms to a database, and database management.

2.3.3 Participants

The inclusion criteria for the XMINS study were adult patients >50 years old undergoing major elective noncardiac surgery with a planned overnight stay in hospital, provided they satisfied the following criteria: American Society Anaesthesiology physical status score ≥3, and major surgery with expected surgical operating time ≥ 120 min. Exclusion criteria were current atrial and/or ventricular arrhythmias (including the presence of a permanent or temporary pacemaker in-situ), and refusal of consent.

2.3.4 Study conduct and data collection

The protocol for the study is summarised in Figure 2.1. On the morning of surgery, continuous three-lead ECG recordings were made in a quiet controlled clinical environment at room temperature. After 10 minutes of recording in the supine position, the patients were given an orthostatic challenge by elevating them to a 45 degree head-up position using an electronically adjustable hospital bed (model 2232; ArjoHuntleigh, Malmo, Sweden). A further 10 minute recording was then made in the 45 degree head-up position. Blood pressure and respiratory rate observations were made at the beginning of each 10 minute recording. The protocol was then repeated 24h and 48h after surgery at the same time of the day. Blood samples were taken before surgery, and at 24h and 48h after surgery.

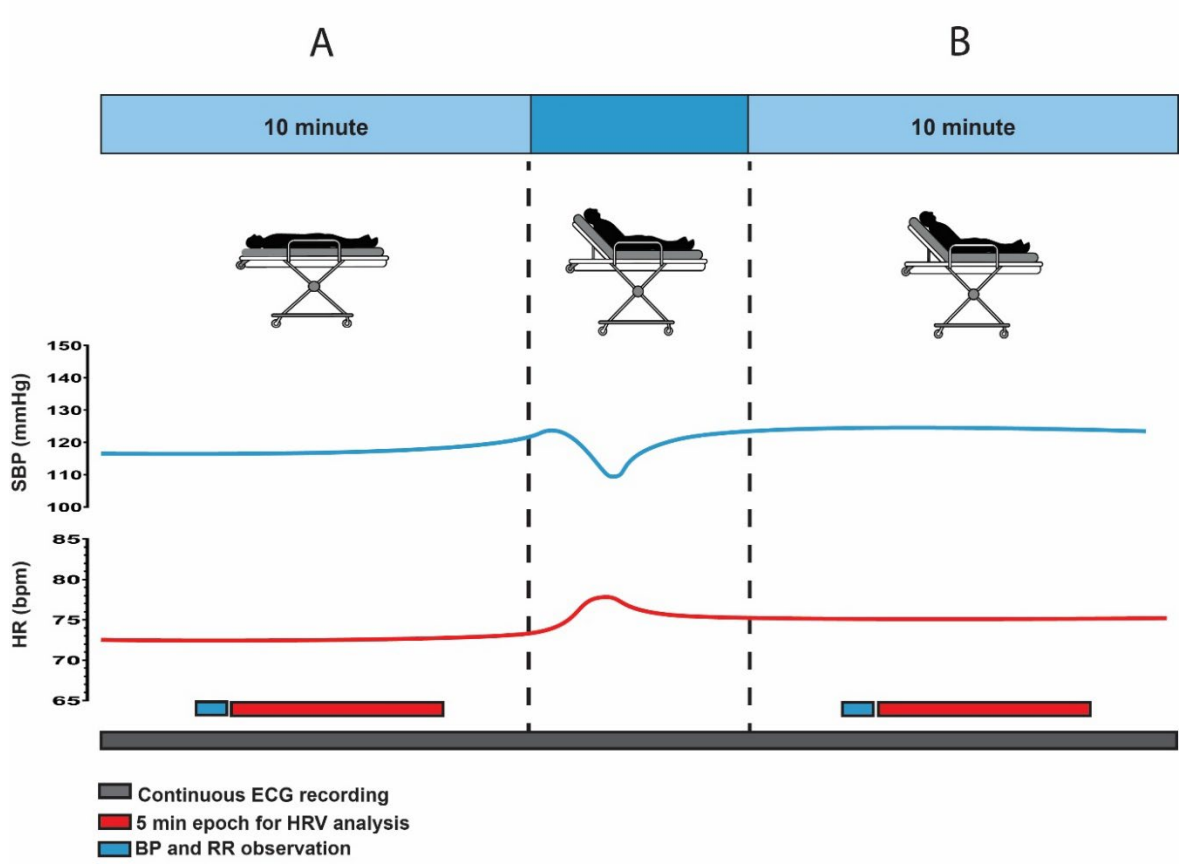

Figure 2.1 Experimental protocol

(A) 10 min supine position and (B) 10 min 45 degrees head-up position. HR (red) and systolic BP (SBP; blue) predicted response with an orthostatic challenge. HRV, HR variability; RR, respiratory rate

2.4 Collection, preparation and processing of blood samples

2.4.1 METS serum samples

Whole blood samples were taken by METS study investigators before surgery and at 24h, 48h and 72h after surgery.[242] 10ml of blood was collected in a plain tube (clotted sample). The samples were centrifuged for 10 min at 3000rpm. Serum was then alloquoted into two 2ml RNA-free cryotubes. The two alloquoted samples were then frozen at -70˚C. One aliquot of serum was sent to a laboratory for TnI quantification using Troponin-I Centaur CP Assay, (Siemens, Tarrytown ,NY, US) and the other was sent to the William Harvey Research Institute for microRNA analysis. The sample collection and processing protocol were designed prior to my thesis and therefore I did not have control over optimising microRNA yield at the time of collection.

2.4.2 XMINS study plasma samples

I developed and oversaw the protocol and processing of whole blood samples for the XMINS study. The protocol was developed in accordance with the Early Detection Research Network standard operating procedures.[246] Plasma was isolated for HsTnT assay testing and for extracellular vesicle microRNA isolation. I developed the standard operating procedure to optimise volume of plasma and microRNA yields. The research nursing staff were supervised to ensure adherence to the protocols.

On the day of surgery, and at 24h and 48h after surgery, 8ml of whole blood was collected into EDTA anticoagulant bottles by nursing staff or myself. The samples were processed within 1

hour of collection. The whole blood was centrifuged at 3500 *x g* for 10 minutes using a Cepr-AL6 Flexicool Rota (Capricorn Laboratory Equipment, Fordingbridge, UK) at the site of collection. Without disturbing the buffy coat (containing white blood cells and platelets) the upper plasma layer was filtered through a 0.8micrometre membrane filter (Starlabs, Milton Keynes, United Kingdom) and transferred to three 1 ml Eppendorf tubes. The samples were then stored in a -80˚C freezer until further processing.

2.5 Outcome measurements

2.5.1 Perioperative myocardial injury definition.

There is no consensus definition to define PMI as addressed in the General Introduction (Section 1.3.1) of this thesis.[58] The definition adopted for this thesis is from the Fourth Universal Definition of Myocardial Infarction expert consensus document where myocardial injury is defined as the "detection of an elevated cardiac troponin (cTn) value above the 99th percentile upper reference range for a given cTn assay.[60]

The METS study used the Troponin I assay (TnI) (Troponin-I Centaur CP assay, Siemens, Tarrytown, New York, USA.) whose 99th centile value is 0.04 ng.ml^{-1}. The XMINS study used the high sensitivity Troponin T assay (HsTnT) (Cobas assay, Roche Diagnostics, Mannheim, Germany) whose 99th centile value is 14 ng.L^{-1}. Patients who had a troponin result above the threshold value after surgery were considered to have developed PMI.

The term PMI is used in preference to MINS as it is more suitable when exploring all potential underlying mechanisms for myocardial injury in the perioperative period. MINS, by its own definition, assumes an ischaemic aetiology.

Patients who met the definition for myocardial infarction as per the Fourth Universal Definition of Myocardial Infarction[60] were excluded.

For the METS study, serum samples were couriered to a central laboratory at the University of Aberdeen and testing completed prior to starting this thesis. Results were made available to

me via the METS investigator database. For the XMINS study plasma samples were couriered to The Doctors Laboratory, London. I co-ordinated the transfer of samples from University College London Hospital to The Doctors Laboratory and oversaw collection of the HsTnT results of the samples. The TDL technicians were blinded to patient characteristics and holter data.

2.5.2 Morbidity

To assess short term morbidity after surgery in this thesis, the post operative morbidity survey (POMS)[247] was used on Day 3, 5 and 7 after surgery. The survey consists of 9 domains (Table 2.1) which are easily screened after surgery. The survey has been validated in the UK hospital setting to capture morbidity after surgery.[248]

Table 2.1 Postoperative morbidity survey domains and criteria

The POMS consists of 9 domains and 18 criteria.[247] For each domain morbidity is either recorded as present or absent.

Morbidity Domain	Criteria
Pulmonary	*De novo* requirement for supplemental oxygen or other respiratory support (e.g., continuous positive airway pressure therapy or intermittent positive-pressure ventilation)
Infectious	Currently on antibiotics or temperature >38°C in the last 24h
Renal	Presence of oliguria (<500 $mL.day^{-1}$), increased serum creatinine (>30% from baseline value), or urinary catheter in place for a non-surgical reasons
Gastrointestinal	Unable to tolerate an enteral diet (either by mouth or feeding tube) for any reason, including nausea, vomiting and abdominal distension
Cardiovascular	Diagnostic test or therapy in last 24 hrs for any of the following reasons: *de novo* myocardial infarction or ischemia, hypotension (requiring drug therapy or fluid >200 $mL.hr^{-1}$), atrial or ventricular arrhythmia or pulmonary oedema
Neurological	Presence of a *de novo* focal deficit, coma or confusion/delirium
Wound complications	Wound dehiscence requiring surgical exploration or drainage or pus from the wound
Haematological	Requirement for any of the following within last 24h: blood, platelets, fresh frozen plasma or cryoprecipitate
Pain	Surgical wound pain significant enough to require parenteral opiates or regional anaesthesia

2.6 Human microRNA profiling

The aim of profiling microRNA in the human samples was to see if the microRNA signatures described in acute coronary syndrome are replicated in patients who develop perioperative myocardial injury. A relatively small number of microRNA were pre-selected (as discussed in the Introduction 1.4.6) and therefore the most suitable technique to profile their expression is the real time reverse transcription quantitative polymerase chain reaction (RT-qPCR). The significant advantage of this technique is that it is an established low-cost laboratory technique used to quantify RNA, including microRNA. The technique has been shown to be accurate in detecting the small non-coding RNA molecules[249, 250] from very low starting amounts. Its main limitation as a profiling technique is that it cannot identify novel microRNA and can only process a limited number of microRNA at one time. A SYBR green-based real time quantitative polymerase chain reaction (qPCR) was used to quantify microRNA expression.[251]

The microRNA profiling workflow has multiple steps from isolation to quantification, and therefore the potential for the introduction of a large amount of technical variation between samples, thereby introducing bias to the final analysis. To address the potential for variation, quality control measures were introduced at each step of the workflow to identify and minimise the impact of variation. These were reported in accordance with Minimum Information for Publication of Quantitative Real-Time PCR Experiments (MIQE) guidelines.[252] These guidelines were published with the aim of promoting consistency and transparency between laboratories. This section will outline the steps in microRNA profiling, isolation, reverse transcription PCR (RT- PCR), and real time quantitative PCR (qPCR). For each step, a brief outline of the procedure will be given, the specific consideration taken for microRNA, and then technical details of the methodology used for this thesis.

2.6.1 Serum microRNA isolation

Considerations

For this thesis, human microRNA were isolated from serum blood samples obtained from the METS study. A serum blood sample is defined as the cell-free supernatant obtained after centrifuging blood that has been collected in the absence of anticoagulant and allowed to spontaneously clot. When isolating from serum, care must be taken to not have cellular carryover when centrifuging to prevent cell microRNA from populating the circulating microRNA. The yield of circulating microRNA from serum and plasma are low (<1-10ng) compared to fresh tissue (>1000ng).[253] The lower yields are due to the higher levels of RNase activity.[109] However, despite the higher RNAase activity, microRNA have been demonstrated to be remarkably stable from isolation to expression analysis.[109] Mixing of serum and plasma specimen types within a study is not recommended[254] but the expression of both are highly correlated.[109]

Technical details

The isolation of microRNA was carried out using the miReasy Serum/Plasma Advanced Kit (Qiagen, Denmark). Isolation protocols were carried out according to the manufacturer's instructions. 200µL of serum was thawed on melting ice and transferred to a 2ml RNase free microcentrifuge tube (StarLabs, Milton Keynes, United Kingdom). Then 60µL of guanidine-based lysis Buffer RPL was added to the mixture, vortexed for 10s and incubated for 5 min at room temperature. For quality control procedures, 1uL of spike in mixture (RNA Spike in kit, Qiagen) containing synthetic microRNA (UniSp3 (2 fmol.μL^{-1}), UniSp4 (0.02 fmol.μL^{-1}),

UniSp5 (0.00002 fmol.μL^{-1}) was added to each sample. After then addition of 20µL of Buffer RPP, the sample was vortexed for 30s and incubated at room temperature for 3 min. The sample was then centrifuged for 3 min at 11000rpm using the Prism Refrigerated microcentrifuge (Labnet International, New York, USA) to pellet the precipitate. The sample was inspected for a clear and colourless supernatant. 200µL of the supernatant was then transferred to a new 2ml RNAase free microcentrifuge tube and 200µL of isopropanol was added before vortexing for 15s. The entire sample was then transferred to a RNeasy UCP MiniElute column. The sample was then centrifuged for 15s at 11000rpm and the flow-through was discarded. 700µL of buffer RWT was added onto the RNeasy UCP MiniElute column, samples vortexed at 11000rpm and the flow-through was discarded. Then 500ul of buffer RPE was added onto the RNeasy UCP MiniElute column, samples vortexed at 11000rpm and the flow-through was discarded. Then 500ul of 80% ethanol was added onto the RNeasy UCP MiniElute column, samples vortexed at 11000rpm and the flow-through was discarded. The RNeasy UCP MiniElute columns were then placed in new 2ml collection tubes, and with the spin columns' lids open, the samples were centrifuged at 13500rpm for 5min to dry the spin columns' membranes. Finally, the RNeasy UCP MiniElute columns were placed into new 1.5 ml collection tubes. 22µL of RNase free water was directly added to the centre of the spin column membrane and allowed to incubate for 1 min. The sample was then centrifuged for 1 minute at 13500 rpm to elute the RNA. 20µL RNA in the collection tube was then stored at -20˚C. MicroRNA were isolated in batches limited by the number of slots available in the Prism Refrigerated microcentrifuge (Labnet International, New York, USA).

2.6.2 Serum microRNA reverse transcription

Considerations

The first step in quantifying microRNA expression is the synthesis of complementary DNA (cDNA) from the isolated microRNA by the process of reverse transcription. Mature microRNA sequence lengths are short after being cleaved from the 3' and 5' end of the pre-microRNA. The consequence of the short length is that it may not be long enough for primer binding. A technique to optimise the microRNA for primer binding in the qPCR process is to add a poly (A) tail to the 3' end of the mature microRNA with poly(A) polymerase. cDNA is then synthesised using oligo-dT primers (poly(T) adaptor) by reverse transcription.[255] The advantage of this technique is that multiple microRNA can be optimised within the same sample.[256] An alternative optimisation technique would be to add microRNA specific primers to the stem loop of mature microRNA. However, this technique would limit the optimised sample to quantification of that specific microRNA. Where the sample supply is finite, the poly(A) method is preferred.[256]

Technical details

2µL of RNA was reversed transcribed in a 10uL final reaction volume using the miRcury LNA RT kit (Qiagen Catalogue number 339340). Due to the low total RNA concentrations in serum samples, it is recommended by the manufacturer that RNA amounts are based on starting sample volume rather than RNA concentration. The master mix contained 2µL 5x MiRcury RT Reaction buffer, 4.5µL RNase-free water, 1µL 10x miRcury RT Enzyme Mix, 0.5µL UniSp6 Spike-in. The reactions were performed in a Primus 96 plus thermal cycler (MWG

Biotech, Ebersberg, Germany) for 60 min at 42˚C, followed by incubation (inactivation of reaction) at 95˚C for 5 min and then allowed to cool at 4˚C. The cDNA was then stored at -20˚C.

2.6.3 Real time quantitative polymerase chain reaction

Considerations

qPCR allows for the detection and quantification of small amounts of microRNA material isolated from a sample. qPCR amplifies the amount of cDNA template containing microRNA sequences that were produced at the reverse transcription step. First the cDNA is heated and split into 2 strands in a process called denaturation. Primer sequences then bind to microRNA target sequences in a process called annealing. The complementary strands are then extended with oligonucleotides and DNA polymerase to form DNA. A fluorescent dye can be incorporated into the reaction to fluoresce when DNA is produced. At the end of each amplification cycle, fluorescence intensity is directly related to the amount of DNA. The cycle at which the fluorescence meets an acceptable level above background fluorescent noise is quantification cycle (Cq). Plots of fluorescence vs cycle can be used to determine the quantification cycle. A typical amplification plot will have a background, exponential, linear and plateau phase. The background phase is during the initial PCR cycles and can be considered background noise. The exponential phase is when the reaction is at its most efficient. It is recommended to set the quantification cycles during the exponential phase to increase accuracy of microRNA quantification as it during this phase when all the reagents are in excess, and DNA polymerase is most efficient. The linear and plateau phases are where the PCR are slowing due to reagent consumption. SYBR green double stranded DNA binding dye

real time qPCR was used to quantify microRNA expression for microRNA isolated from human serum samples.

The short sequence length of microRNA also results in variation in the GC base content with the microRNA. GC content of a microRNA determines the thermostability of the microRNA with its complementary sequence a microRNA-specific primer. Therefore GC content variance results in variance in melting temperatures during the denaturing and annealing steps.

Technical details

For qualitative PCR, cDNA was diluted (1:40) and then added to a 10uL reaction containing 5µL 2 x miRCURY SYBR Green Master Mix, 0.5µL ROX Reference Dye and 0.5µL RNAse free water. The Master Mix with cDNA was added to 96 well microRNA PCR custom made plates containing pre-designed miRCURY LNA microRNA PCR Assays.

Amplification was performed using the Applied Biosystem StepOneplus RT-PCR system (Applied Biosystems, California, USA). The cycling parameters were: PCR initial heat activation at 95˚C for 2 minutes; 40 cycles of denaturation at 95˚C for 10s and annealing at 56˚C for 60s; followed by melt curve analysis from 60˚C to 95˚C. The Locked Nucleic Acid (LNA) primers overcome the challenge of varying GC content. The LNA oligonucleotides retain a higher $T_{m,}$ and therefore maintain the stability of shorter microRNA lengths. The LNA technology also standardises the melting temperature of the oligonucleotide/microRNA duplex, which overcomes the variation in duplex T_m due to GC content of the microRNA sequence. The LNA oligonucleotide also increases the affinity of the complimentary DNA strand, thus increasing sensitivity for the small microRNA sequences. The quantification cycle

(Cq) was used to quantify the PCR reactions. The log base fluorescence threshold to determine the Cq was set at the same value for each PCR and for each individual sample using the StepOne Software v.23 at 0.3 (Applied Biosystems, California, USA). An example of setting the Cq threshold is shown in Figure 2.2.

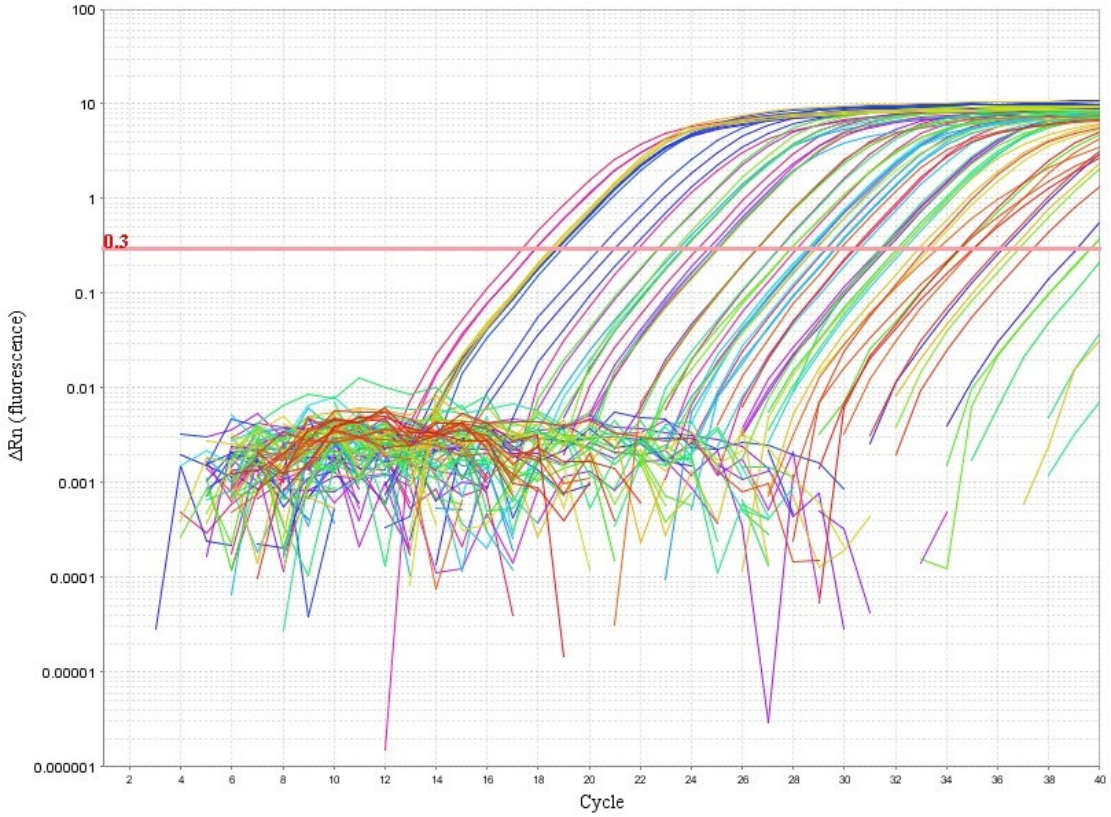

Figure 2.2 Amplification plot for customised PCR plate

This amplification plot shows the PCR cycling reaction for the different microRNA assays. The red line indicates where the threshold fluorescence value has been set (0.3). The line is shown to be crossing at the exponential phase for each PCR amplification plot.

2.6.4 Quality control assessment

2.6.4.1 microRNA isolation and reverse transcription.

As part of the isolation procedure, synthetic RNA spike-ins were added to the buffer solutions. The spike-in/technical controls are used to control for the potential variation between samples in microRNA yield, purity and integrity. The RNA spike-in templates (Un-Sp2, UniSp4 and UniSp5) are at different concentrations in 100-fold increments. UniSp2 is 100-fold higher than UniSp4 and UniSp4 is 100-fold higher than UniSp5. Therefore, UniSp2 should amplify at the level of the very abundant microRNA, and UniSp5 concentrations should correspond to the weakly expressed microRNA. The calibrated Cq data generated from the spike controls was used to compare each sample and identify outlier samples to be excluded from analysis. If the Cq values of the technical control produce similar values for each sample, isolation efficiency across all samples can be considered consistent. However, if some samples gave an outlier Cq value, it would suggest a problem in the RNA isolation procedure. For this study, UniSp5 was used as the isolation technical control. If the Cq value was ≥37, then the sample and patient was flagged as an outlier and excluded from analysis. The synthetic RNA, UniSp6, was added to the RT reaction prior to cDNA synthesis. The outlier Cq values for UniSp6 were used to evaluate RT efficiency.

2.6.4.2 Evidence of haemolysis.

Serum microRNA content is significantly altered in the presence of erythrocyte haemolysis due to contamination with erythrocyte microRNA content.[257] Although visual inspection filtered out most haemolysed serum samples, a quality control for haemolysis is still

recommended.[258] Both microRNA hsa-miR-23a and hsa-miR-451 assays were included on the miRCURY Custom PCR Panel plate to detect for haemolysis contamination. hsa-miR-451 is known to be enriched in erythrocytes, and hsa-miR-23a is stable in serum unaffected by haemolysis.[259] The ratio of Cq[hsa-miR-23a]:Cq[hsa-miR-451] of greater than 7 was used to identify high risk of haemolysis contamination[258] and those samples were excluded from analysis.

2.6.4.3 Amplification efficiency of RT PCR

The amplification efficiencies of the PCR reactions were calculated using the LinRegPCR software, Version 2017.1 (Heart Failure Research Centre, Amsterdam, the Netherlands).[260] Raw fluorescence data were obtained from Stepone Software v.23 (Life Technologies Corporation, 2012), exported as an Excel .xls file, and imported to LinRegPCR. The software determines baseline fluorescence and then uses an iterative algorithm to a set a window of linearity (W-o-L) for each assay. It uses this to calculate the PCR efficiency (E) per sample and assay. The amplification efficiency is expressed as a value between 1 and 2 and defined as the fold increase per cycle. Between 1 and 2 is the equivalent of between 0 and 1, where 1 is maximum efficiency.

2.6.4.4 Melt curve analysis

Primer sequences were not given by Qiagen as they were proprietary information. To check single targets during PCR amplification, melt curves were generated after the qPCR. For each sample the wells were heated to initially 60˚C and the fluorescence measured. The temperature was incrementally increased to 95˚C, continuously measuring fluorescence. A curve was then

generated of derivative fluorescence versus temperature. The fluorescence represents double stranded DNA. The proportion of double to single stranded DNA will depend on the temperature. Therefore, the peak of the curve represents the temperature at which 50% of the DNA is double stranded and 50% of the DNA is dissociated into single stranded DNA. This is known as the melting temperature (Tm) for the PCR reaction. Tm values are specific for microRNA primers and microRNA sequence targets. The Tm values are manufacturer proprietary information. However, melt curves can be inspected for single peaks indicating single amplicon target for that microRNA primer. Melt curves were inspected for every sample microRNA. Only microRNA that had single peaks were considered for further analysis.

2.6.5 Quantification cycle (Cq) calibration, normalisation and microRNA expression

2.6.5.1 Cq calibration

Each Cq value was then calibrated using the Cq values from the interplate calibrator (IPC) spike in, UniSP3. The UniSP3 assay is pre-aliquoted by the manufacturer and therefore the variation of these assays is minimal from well to well and from plate to plate. The mean Cq value for UniSp3 was first calculated across all plates and then deducted from the mean for each individual plate to generate a calibration factor (Appendix C). The calibration factor for the plate was then added to each Cq value for each assay on that specific plate to generate a calibrated Cq value. The calibrated Cq value was used for downstream analysis.

2.6.5.2 Cq normalisation

There is currently no consensus for a universal reference microRNA sequence for the normalisation of microRNA in expression studies.[261] It is therefore not surprising that there is no reference microRNA for testing hypotheses in experimental conditions relating to PMI after noncardiac surgery. Choosing the appropriate reference microRNA is vital to avoid misleading analysis and wrong conclusions.[262] It is recommended and important that reference microRNA are determined in preliminary experiments to establish appropriate reference microRNA in same experimental conditions as for the main study analysis.[263] The Qiagen miRCURY LNA microRNA Serum/Plasma Focus Panel was used to determine a reference microRNA for the experiments using serum microRNA. The focus panel has 179 microRNA assays commonly found in the serum and plasma. The protocol for determining the reference microRNA is found in Appendix D. The NormFinder algorithm[264] Excel add on function was used to determine the most suitable reference microRNA from Cq values.

The mathematical model used in the NormFinder algorithm divides Cq values from each 179 MicroRNA into predetermined subgroups. The variations between the different groups are then estimated and a stability value is assigned to each microRNA. The stability allows the selection of microRNA with the minimal combined inter- and intra-group expression variation. The two microRNA with the combined lowest stability value were selected as the reference microRNA for normalisation in the main analysis. MicroRNA hsa-miR-152-3p (UCAGUGCAUGACAGAACUUGG [mean Cq (SD); 30.06 (1.14)]) and hsa-miR-361-5p (UUAUCAGAAUCUCCAGGGGUAC [29.51 (1.24)]) had the lowest combined stability value (0.077).

2.6.5.3 MicroRNA expression

Expression levels for the serum microRNA Cq values were subsequently calculated using the formula:

$$\Delta Cq = Cq[microRNA] - Cq[geometric\ mean\ of\ reference\ microRNAs]$$

The ΔCq values were converted to a fold change (FC) by applying the formula of $2^{-\Delta Cq}$ [265]. Statistical analysis was performed on the ΔCq values.

2.6.6 MicroRNA function and Gene Pathway Analysis

To explore the function of differentially expressed microRNA, a web based prediction algorithm software, DNA Intelligent Analysis (DIANA)-miRPath v.3.0 (http://diana.imis.athena-innovation.gr/DianaTools/index.php), was used to derive in silico microRNA:gene target predictions.[266] User-selected microRNA names are entered into the search interface. The software then utilises an in silico miRNA target prediction algorithm (DIANA-microT-CDS) to predict the microRNA:gene interaction. It identifies microRNA targets on both the 3'untranslated region and coding sequences (microRNA recognition elements (MRE)). A score is generated for each identified MRE. An overall score, miRNA targeted genes (miTG) score, is calculated as the weighted sum of the scores of all identified MREs.[267] A prediction threshold score is set, ranging from 0 to 1, where 1 is the most conservative. A score of 0.8 is accepted as having high confidence in microRNA gene comparisons.[268] The software will then produce a list of all genes that interact with each individual microRNA with a threshold score >0.8.

To further gain insight into microRNA function, the predicted gene targets of the selected microRNA can be compared to the genes in all Known Encyclopaedia of Genes and Genomes (KEGG) pathways[269] using enrichment analysis. The algorithm produces a p value (extension of the Fischer exact test) by sampling the microRNA and calculating the probability of KEGG pathway overlap, with correction for multiple testing.

A false discovery rate (FDR) probability threshold of 0.05 is set to identify predicted pathways.[270] The online software produces a list of enrichment pathways that meet the p-value threshold, and each pathway has a list of target genes associated with the selected microRNA. The a priori analysis can overlay genes of interest on pathway wire diagrams generated from the KEGG database.

2.7 Cardiac autonomic activity measurement

The relationship between cardiac parasympathetic activity and PMI/morbidity was examined using two measurements: heart rate variability (HRV) and heart rate recovery (HRR) after an orthostatic manoeuvre. Both measures have been outlined in the Introduction section 1.5. I will now outline the technical considerations and methodology.

2.7.1 Heart rate variability

For my thesis I used serial electrocardiogram (ECG) recordings to measure heart rate variability during the perioperative period to assess changes in cardiac autonomic function. An ECG trace with its characteristic P, QRS and T waveforms can be used to analyse the fluctuations in the beat-to-beat intervals. The time between two successive R waves is known as the R-R interval and can be used to quantify the changes in beat-to beat variation.[271] Therefore HRV can be alternatively defined as the variation in R-R intervals in the ECG.

2.7.2 Acquisition of electrocardiogram recordings

Electrocardiogram recordings were made using 3-lead Lifecard CF digital Holter monitoring (Spacelabs Healthcare, Hertford UK) which had a sampling rate of 1024Hz, and were recorded onto a flash disk drive (Figure 2.3). The sampling rate of the recording device was in accordance with the recommended 500-1000Hz that facilitates accurate detection of R waves using downstream software.[182]

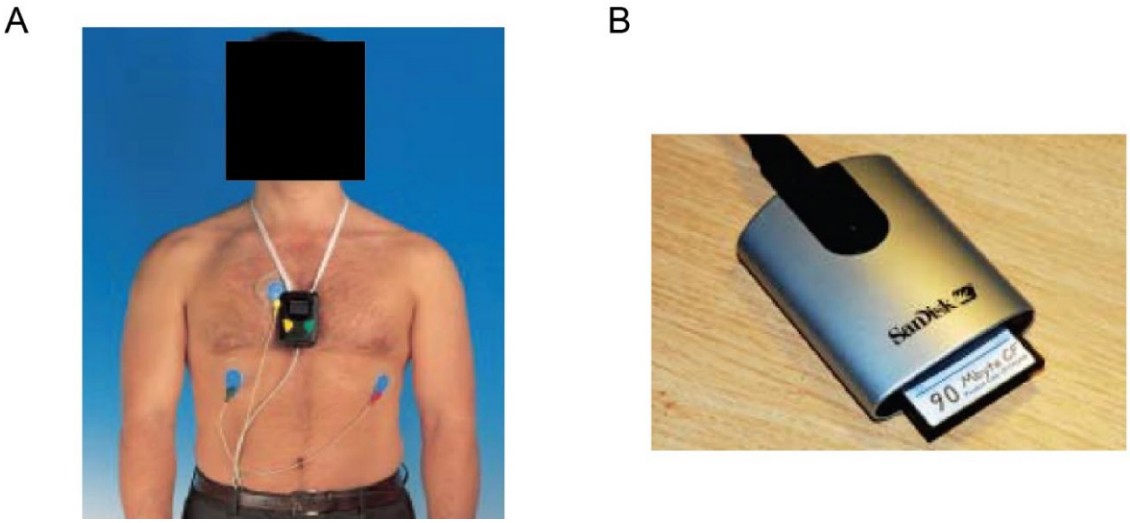

Figure 2.3 Lifecard CF digital Holter monitor (A) and flash drive and disk (B)

Images from manufacturer instruction manual.

The recordings on the flash drive were uploaded onto Sentinel V9 Cardiology information software system (Spacelabs Healthcare, Hertford, UK) and visually inspected using Pathfinder SL 1.7 Ambulatory ECG analysis system (Spacelabs Healthcare, Hertford, UK) (Figure 2.4). The file was then exported as an *.ecg file.

Figure 2.4 Screenshot from Pathfinder SL 1.7 Ambulatory ECG analysis system

Raw electrocardiogram recording taken from a patient before surgery

The *.ecg files were then batch analysed using Kubios HRV Premium software Version 3.1.0 (Kubios, Kuopio, Finland).[272] The Kubios HRV software was used for the following reasons:

1. Supported the International Society for Non-invasive Electrocardiology (ISHNE) Holter ECG data format file *.ecg
2. Able to visualise ECG trace to allow automated and manual detection of R waves
3. Manually edit R wave
4. Artefact correction algorithm availability
5. User friendly interface
6. Data export function for software package for further statistical analysis

2.7.3 R-R time series

The Kubios software uses an adapted QRS detection algorithm based on the Pan-Thomkins algorithm[273] to detect R waves and produce a R-R time series (tachogram) from the imported ECG files. An R-R times series are the R-R interval times plotted against time. All ECG recordings were visually inspected for quality of recordings and accurate R-wave detection. R waves incorrectly detected or missed were manually edited using the software (Figure 2.5).

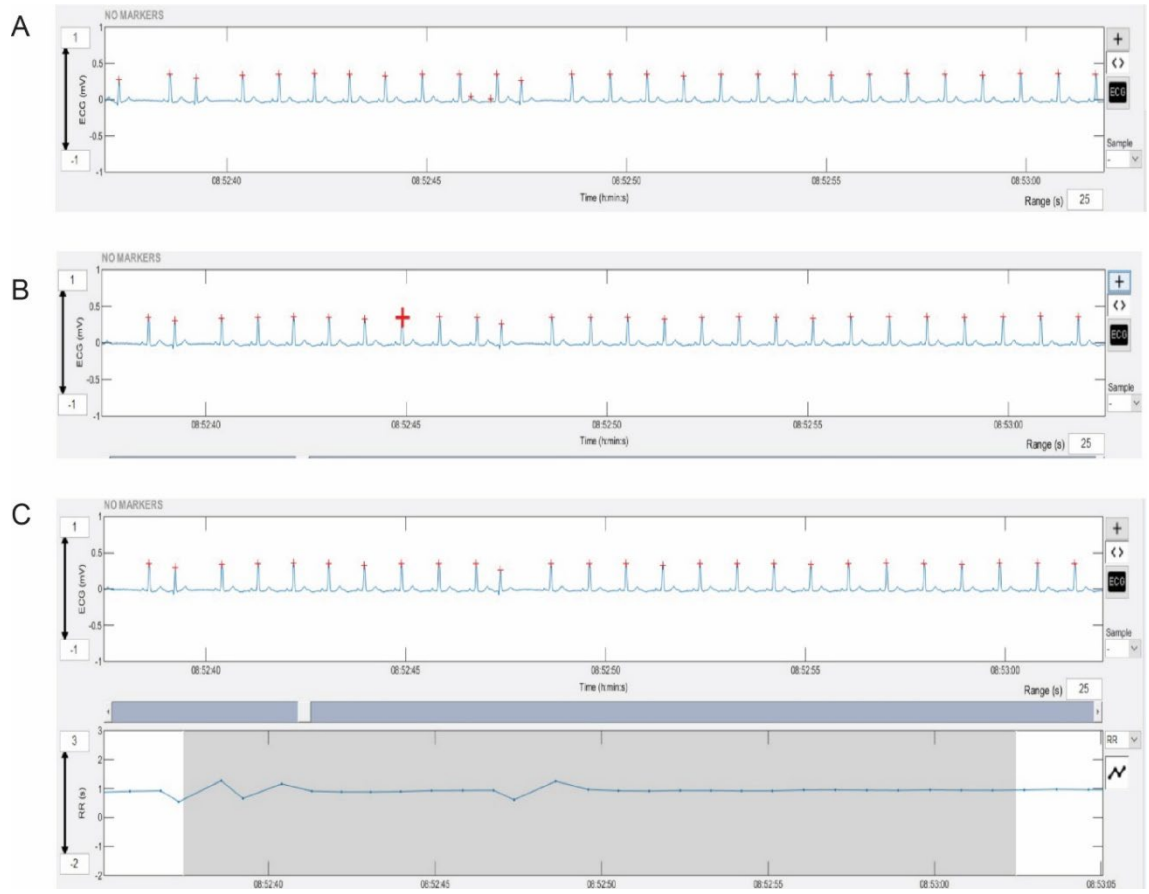

Figure 2.5 Screenshot from Kubios Software showing R wave detection

A. ECG recording with incorrect R waves detected. **B.** Incorrect R waves manually highlighted and deleted. **C.** ECG recording with accurate R wave detection with corresponding and R-R series below (25 second segment).

2.7.4 R-R segment length

5 minute (300s) segments were chosen for this thesis as they are adequate to assess vagal and sympathetic modulation of the heart.[182, 194] It is also a practical duration to perform repeated measurements in a controlled environment in the perioperative period. Longer records such as 24 hours are possible.[274] However, controlling autonomic influences such as sleep, mobility, eating and drinking for the entire duration would be practically unachievable in the perioperative setting.

The 5 minute segments were selected using the Kubios software. They were selected after a period of 150s rest to minimise external disturbance i.e. movement artefact, and to maximise a stationery time series (Figure 2.6).

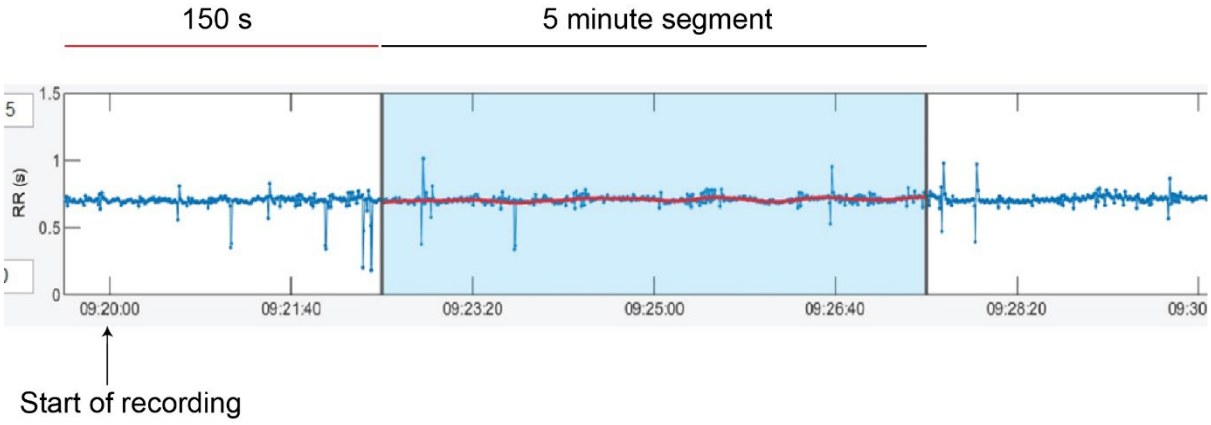

Figure 2.6 Five minute segment selection (blue-shaded area)

2.7.5 Artefact detection and correction

Artefact and its correction can have a significant effect on the HRV analysis.[275] ECG recordings can be distorted by electrical and physiological artefact. Electrical artefact includes patient movement or interference from other electrical devices, and physiological artefact includes ectopic beats. A limitation of HRV studies in the literature is the failure to report on the method of detection and management of the artefact.[212] Physiological artefacts, such as ventricular ectopics, are common in patients with cardiovascular comorbidities, including unstable angina and myocardial infarction.[276] Therefore it would be reasonable to expect ectopics in the ECG recordings from patients who experienced myocardial injury within the XMIN study recruitment cohort. The proportion of ECG recording that is artefact, i.e. the percentage of the 5 minute segment, must be reported in the HRV analysis. In addition, how the artefact is processed must also be reported.[182, 277] There are two types of methods to manage ECG artefact: deletion and interpolation. In ECG segments with a low percentage of ectopics/artefacts, an interpolation method is recommended in favour of a deletion method to preserve the segment length.[182] If the artefact within the segment is significant, it is recommended that the segment be discarded from further analysis. However in the literature, the threshold value of artefact to discard the segment has been inconsistently reported from 1% to 30%.[277] For this thesis, after manual correction, ECG recordings with movement artefact or ectopic beats were processed using the Kubios software automatic artefact detection and correction feature.[272]

Artefacts were detected from the RR time series (tachogram), using a decision algorithm that utilised a time varying threshold (Th)

A missed beat was detected if an RR interval RR (i) satisfied the following:

$$\left|\frac{RR(i)}{2} - medRR(i)\right| < 2Th$$

An extra beat was detected if two successive beats RR (i) + RR (i+1) satisfied the following:

$$|RR(i) + RR\ (i+1) - medRR(i)| < 2Th$$

Th = time varying threshold, estimated from the RR time series, for each beat a quartile deviation of the 90 surrounding beats was calculated and multiplied by 5.2.
MedRR (i) = median of the surrounding 10 RR intervals.

Detected ectopic beats were corrected by replacing the RR interval times with interpolated values using cubic spline interpolation using the automated software.[278]

For each ECG recording analysed a percentage artefact correction was calculated and documented. Time series where the percentage artefact was >5% were classified as "unsuitable quality" and excluded from further statistical analysis as per Kubios Software Manual recommendations. This was to ensure the correction algorithm did not distort and suppress variability in the recordings.

2.7.6 Heart rate variability analyses

2.7.6.1 Time Domain Analysis

The time domain analyses used in this thesis were:

- **Heart rate (bpm)**
- **SDNN (ms)**: standard deviation of the normal-to-normal RR interval
- **RMSSD (ms):** root mean square of successive RR intervals

It has been suggested that changes in heart rate variability are merely reflecting changes in the underlying heart rate.[193] Monfredi et al.[193] used intact human and animal hearts to demonstrate that there is an exponential decay-like relationship between HR and HRV. Therefore HR should be taken into consideration in both data analysis or drawing conclusions. HR is reported for all HRV analyses in this thesis.[192]

2.7.6.2 Frequency domain analyses

Power spectral analysis was performed using a fast Fourier transform.[182] The technique has good reproducibility and has the advantage of having a high processing speed allowing large numbers to be analysed.[279] To allow for the fast Fourier transform, the R-R time series needs to be equidistantly sampled. To satisfy this an artificial interpolation is applied. For this thesis, cubic spline interpolating at the sampling rate 4Hz was used to convert the R-R time series into an equidistant sampled series prior to spectrum estimation. Fast Fourier time spectrum was then calculated using Welch's Periodogram method (window width 128s with 50% overlap).

The frequency domain measures used in this thesis to assess efferent cardiac vagal activity are:

- **High frequency** (0.15-0.4Hz) ms^2
- **Low Frequency** (0.04-0.15Hz) ms^2

Absolute values were natural log transformed to comply with statistical tests.

Very low frequency was not used as it was filtered out in the process of removing stationarity trends as outlined below; in addition, it is thought to be inaccurate over shorter time periods.[182]

2.7.7 Stationarity

Spectral analysis assumes that the time series is weakly stationary.[215] Stationarity means that the statistical properties of the process generating the time series remain constant over time: i.e., in strict stationarity, the properties of mean, variance and covariance of the RR interval do not vary over time. Weak stationarity implies that only mean and covariance are constant. Non-stationarity features of a RR time series, such as the influence of respiratory sinus arrythmia over time, can alter the frequency and time domain analyses.[280] To account for non-stationarities in the recordings, slow trends (non-stationarities) were filtered out using Kubios advanced detrending method.[280] Smoothing of the data was achieved using a smoothing parameter ($\lambda = 500$) that removed slow trends below the low frequency band (<0.04Hz).

2.8 Orthostatic modulation of heart rate

2.8.1 Rationale

The heart rate variability (HRV) measurements described in the section above were taken when patients were in resting postural positions. Therefore the HRV measurements express the degree of heart rate modulation due to autonomic influences at rest.[271]

To assess cardiac vagal activity, and its dynamic response to physiological reflexes such as the baroceptor reflex, modulation of heart rate was assessed after a standardised orthostatic manoeuvre. To assess heart rate recovery (HRR) after an orthostatic manoeuvre, an orthostatic manoeuvre was incorporated into the XMINS study experimental protocol (Figure 2.1).

2.8.2 The orthostatic manoeuvre

The lying to standing manoeuvre is impractical to repeat throughout the perioperative period due to expected limitations in mobility during the recovery period after surgery.

Similar heart rate changes elicited by autonomic influences have been demonstrated using a lying to sitting manoeuvre[41] as shown in Figure 2.7, albeit with a smaller magnitude in heart rate changes. Therefore, a modification of the orthostatic manoeuvre from lying to sitting is a practical compromise for a reproducible test during the perioperative period.

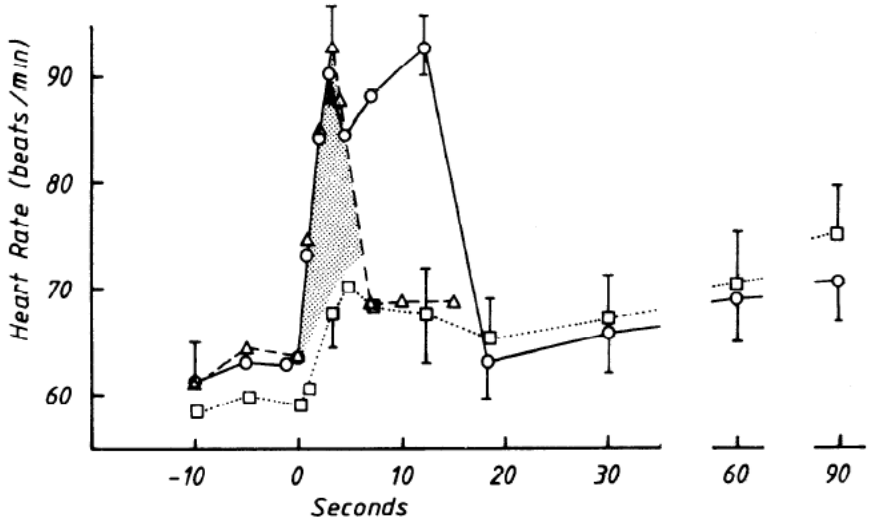

Figure 2.7 Heart rate changes to active and passive changes in posture

Heart rate changes (mean ±SE) induced in trained subjects (n =10) by standing (O), handgrip (Δ), and 70-degree head-up head tilt (□). Image and caption adapted from Borst et al.[41]

The orthostatic manoeuvre is described as follows: after 10 minutes in the supine position, patients were elevated to a 45-degree head-up position using an electronically adjustable hospital bed (Model 2232, ArjoHuntleigh, Malmo, Sweden) (Figure 2.8). The Model 2232 adjustable bed was used for all patients on the day of surgery in the pre-assessment ward. A standard long-stay adjustable hospital bed was used for 24h and 48h hours after surgery. It would have been impractical in the first 48 hours of surgery to move patients to the preassessment area to repeat the manoeuvre using the Model 2232. However, the challenge was standardised to take no more than 10s to achieve the change in posture. As bed rest is known to influence the heart rate response, the challenge was only performed after 10 minutes of bed rest in the supine patient.[41] To standardise the challenge before, 24h and 48h after surgery, the same bed was used for each patient to perform the standardised challenge.

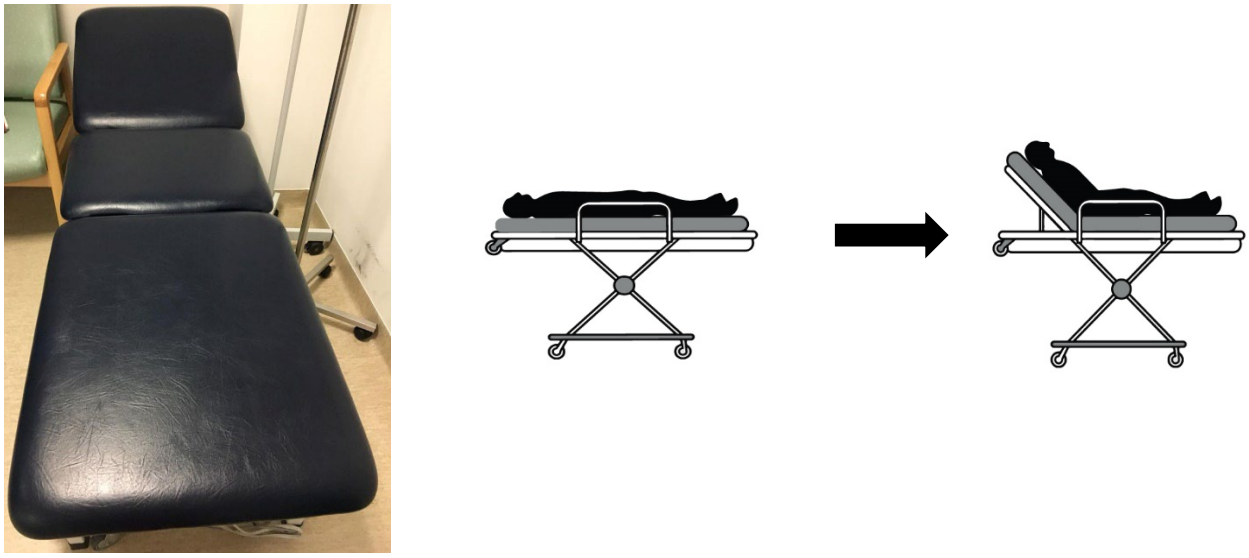

Figure 2.8 Orthostatic manoeuvre using adjustable hospital bed (Model 2232, ArjoHuntleigh, Malmo, Sweden)

Patients were elevated from a supine position to a 45-degree head up position using the motorised bed function.

2.8.3 Heart rate data acquisition

The same ECG recordings used to acquire heart rate variability measures were used to assess the HR during the orthostatic manoeuvre. The ECG recordings were time stamped and research staff made a record of the time (t = 0s) at which the patient reached the sitting position once the orthostatic manoeuvre had been initiated. ECG recording segments from 120s before and 120s after t = 0s were analysed. The HR data was then processed using the Kubios software and Microsoft Excel. For every patient that had an orthostatic manoeuvre, RR interval data (in seconds) measured using the Kubios software (Figure 2.9) was exported into a Microsoft Excel spreadsheet with its corresponding time stamp (in seconds) (Figure 2.10). The time was then converted into the hh:mm:ss format and RR interval (in seconds) converted into HR (bpm). The heart rate was then averaged for 3 consecutive beats (Figure 2.10 and Table 2.2). The

average HR at 10 second intervals, 120s before and after the orthostatic challenge (t =0), were exported to a new Excel spreadsheet (Figure 2.11).

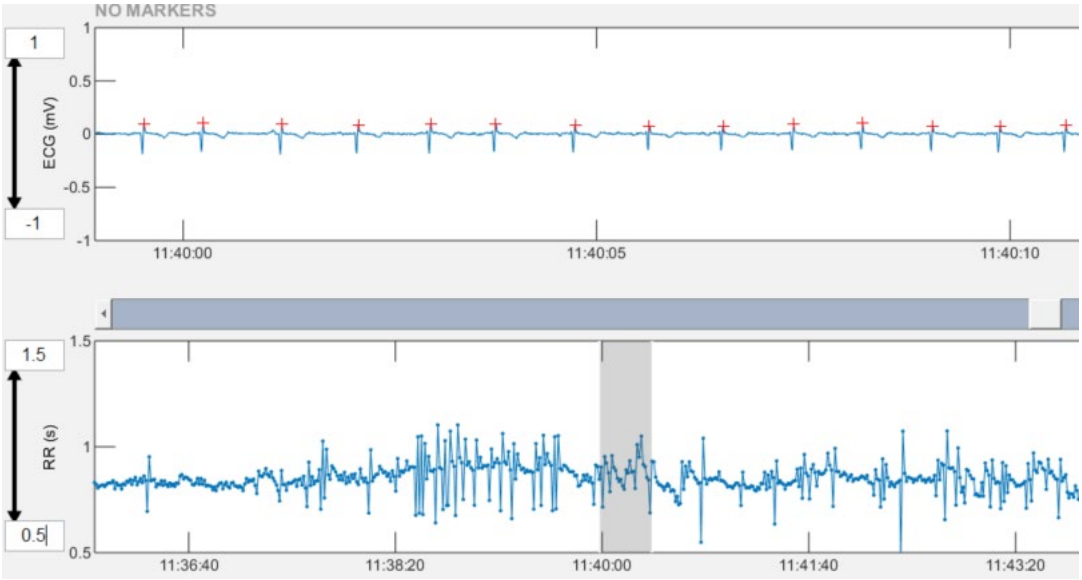

Figure 2.9 Screenshot for ECG recording and RR interval data series as shown in the Kubios software

Kubios Import		Excel Conversion		
Time (s)	RR interval (s)	Time (hh:mm:ss)	HR	Average HR
42000.22	0.714	11:40:00	84.0336	
42001.17	0.953	11:40:01	62.9591	
42002.1	0.926	11:40:02	64.7948	70.60
42002.98	0.876	11:40:03	68.4932	65.42
42003.76	0.786	11:40:04	76.3359	69.87
42004.72	0.958	11:40:05	62.6305	69.15
42005.62	0.902	11:40:06	66.5188	68.50
42006.51	0.887	11:40:07	67.6437	65.60

Figure 2.10 Screenshot image of Microsoft excel spreadsheet

RR interval and time (s) were extracted from the Kubios software for each orthostatic test. Formulae were used to convert time and RR into HR. Average HR was calculated from the 3 previous HR values and rounded to the nearest beat.

Table 2.2 Explanation of cell contents for calculating HR

Cell Column	Explanation
Time (hh:mm:ss)	t (s) divided by 86400
HR (heart rate; beats per minute)	1 divided by RR interval (s) multiple by 60
Average HR	Heart rate average for 3 consecutive beats

Recruit	-120	-110	-100	-90	-80	-70	-60	-50	-40	-30	-20	-10	0	10	20	30	40	50	60	70	80	90	100	110	120
XMIN 007	69.22638	64.499	66.19464	63.223	69.59649	72.91476	73.6696	72.104	61.8884	74.2382	68.562	79.0962	72.004	71.9017	70.8838	73.5448	66.7798	65.0176	70.1589	71.1983	72.0291	70.3683	71.1792	66.7163	70.2357
XMIN 019	72.35307	76.99311	72.5084	74.05638	72.17463	72.47861	72.6513	73.9103	73.2921	76.7703	70.8161	73.1114	69.181	74.5053	73.3865	72.1454	72.8942	83.2238	77.6886	66.8444	67.9229	74.1173	66.6472	65.7551	68.2846
XMIN 020	74.9201	81.66943	97.94022	94.73753	93.91055	84.34868	88.1967	89.3586	81.5558	82.9617	82.539	92.983	94.7482	82.9635	97.9426	104.054	92.8055	84.8647	93.3325	90.8226	91.8911	94.99	91.6966	93.6044	97.1456
XMIN 021	76.74764	75.72646	78.24205	77.51998	80.27095	75.44073	78.2962	86.6013	84.8241	83.3173	76.5105	77.7539	81.416	80.1674	84.2552	89.3157	77.3878	78.5437	80.2154	81.1945	80.358	84.3445	80.8279	76.0457	75.0321
XMIN 022	51.6395	51.24096	48.69852	51.48918	52.85415	52.53106	52.9641	58.1314	48.209	49.8759	47.6831	48.8816	49.7116	52.2191	48.2361	54.6961	52.4983	51.9488	53.0512	50.7585	48.6784	49.0516	49.5865	50.4346	50.8948
XMIN 023	90.03846	109.597	116.2083	99.06619	92.91469	89.88918	96.9337	105.763	90.5259	96.6711	122.54	107.928	103.967	112.791	95.9538	100.92	97.5622	114.599	98.0399	108.831	91.3393	113.153	96.9837	97.8265	102.489
XMIN 024	118.656	113.1365	111.9406	109.7562	107.5949	102.9168	104.958	102.623	105.325	101.409	101.187	104.05	116.23	112.053	114.505	108.313	105.148	104.287	98.363	92.4509	95.5941	92.7363	89.0353	92.9766	93.9988
XMIN 025	86.54354	84.99172	88.76687	82.95253	83.07779	79.06915	83.4557	83.0396	86.0095	81.9978	85.9013	85.4716	97.0896	87.8182	86.749	85.9605	89.4687	94.4402	90.1396	84.2351	81.129	82.1316	82.314	80.7925	82.0536

Figure 2.11 Screenshot from Excel spreadsheet with 10s interval HR measurements for each patient's orthostatic challenge

2.8.4 Determination of heart rate recovery after the orthostatic manoeuvre

During exercise testing, HRR is commonly defined as the heart rate change at a defined time point after the termination of exercise.[281] It is assumed that at the point of termination of exercise, the heart rate is at its peak rate.[44]

As described in Section 2.8.3, ECG recordings were time stamped when patients reached their sitting position after the orthostatic manoeuvre. A population cohort study characterising BP

and HR changes after a lying to standing orthostatic challenge demonstrated that HR responses to the challenge varied according to age and sex.[282]

Compared to an orthostatic manoeuvre from the lying to standing position, the heart rate increases more gradually from lying to sitting position.[41] Combined with the population study findings, it can be assumed that reaching peak heart rate is not uniform for all patients at t=0. Peak heart rate for this study was defined as the highest heart rate within 50 seconds after completing the orthostatic challenge, i.e., from t=0. The peak heart rate was identified for each patient using the Excel spreadsheet function *=MAX (number1, [number2])*, where number 1 and number 2 are the specified range in which the MAX value is identified. Using the spreadsheet in Figure 2.11 as an example, the function can identify the highest heart rate for each row (patient) for the range of time values 0s, 10s, 20s, 30s, 40s, 50s. Further examples are shown in Appendix E.

HRR recovery values were then then calculated as the difference between peak heart rate and heart rate at each 10s time interval after the time peak heart rate was identified for each individual patient.

2.8.5 Curve fitting for the orthostatic challenge

To further analyse HRR after peak heart rate and investigate its relationship with PMI, time constants were obtained using curve fitting analysis of the heart rate after sitting.

The assumption was made that heart rate declined gradually and exponentially after reaching peak heart rate.[41, 213] This contrasts with the more rapid decline that is observed after standing

from the supine position. The change in heart rate associated with change in posture is thought to be mediated by vagal tone modulation of the sinus node via unloading and reloading of arterial baroreflexes.[219] To obtain time constants for decay, heart rate after peak were fitted to the exponential equation:

$$Y=A\ Exp(-BX)$$

Where Y is heart rate (at 10 second intervals), A is peak heart rate, X is time after peak and B is the rate in change in heart rate of peak (decay).

Heart rate values were natural logarithm transformed to allow for the exponential curve fit.[213] NCSS 12 (Kaysville, UT, USA) statistical software was used for the curve fitting analysis. Using a pre-set mathematical model that expresses the relationship between dependent Y variable and independent variable X, the software is able to estimate values of the parameter of the model (A and B) using non-linear regression. [283]

2.9 Statistical and data methods

The statistical analyses and power calculations for chapters 3-5 are outlined in each chapter. Below is a general overview of the data handling and statistical methods used in this thesis.

2.9.1 Software packages

I used Microsoft Excel (Microsoft, Redmond, USA) to clean, manage and process data for the XMINS and METS databases. All statistical analyses and graphs were performed and produced using NCSS 12 (Kaysville, UT, USA) and GraphPad Software Version 8, La Jolla, California, USA). Graphical illustrations were created using Biorender.com. Illustrations and graphs were edited using Adobe Illustrator 22 (San Jose, California, USA). Journal articles references were managed using Endnote version X8.2 (Thomson Reuters, New York, USA).

2.9.1.1 Data management

I received the METS database in Microsoft Excel format. I then imported the database into NCSS statistical software package. Data was then cleaned in the package by assigning variable names, assigning data types, checking categorical variable coding and category labels, and generating new variables required for analysis. Manual and automated validation checks of data were undertaken using the data screening function in the NCSS software.

I created and managed the database for the XMINS study on Microsoft Excel. The column fields on the database matched those for the study case report form. The research nurses and I performed data input. Data from the ECG recordings and heart rate variability analysis were

merged with the clinical database on Microsoft Excel. I then imported the database into NCSS statistical software package, and the same procedures were performed as described above for the METS study.

2.9.2 Statistical analyses

Statistical analysis was performed using NCSS Version 12 (Kaysville, UT, USA) unless otherwise stated. Categorical data are summarised as absolute values (%). Continuous data are presented as mean (95% confidence interval), or median [interquartile range], unless stated otherwise. Distributions of data were assessed using the Shapiro-Wilk test. Statistical tests and power calculations used throughout the thesis are stated in each chapter with statistical significance set at $p<0.05$.

2.9.2.1 Repeated measures statistical analysis

Within this thesis, experimental designs use repeated observations or measurements of a variable for the same individual over a period of time. The main advantage of this experimental design is that individuals serve as their own control. To analyse these observations and measurements, a mixed model repeated measures approach was used, as opposed to repeated measures analysis of variance (ANOVA). Mixed model is a mathematical extension of the general linear repeated measure ANOVA model.[284] It can also be referred to as multilevel models, hierarchical linear models, mixed models or random coefficient models.[284] The different names reflect the different scientific fields in which they were first developed, and their application varies depending on the statistical package used in analysis. For this thesis, NCSS Version 12 (Kaysville, UT, USA) mixed model repeated measures application was used

for mixed model analysis. The term mixed model refers to the use of both fixed effects and random effects in the same analysis. A fixed effects (or factor) is a variable that is of interest in the study and is fixed for each individual. Each factor will have levels (i.e. group and time points) of interest, for which tests of hypotheses are performed. The fixed factors and their levels are described in each results chapter. The random effects are factors that cause variability in the responses within the sample i.e. patients/subjects.[285] Repeated measures ANOVA analysis does not have the flexibility to include random effects and assumes all effects are fixed.[286]

Missing data is sometimes unavoidable in clinical studies due to unforeseen circumstances.[287] Mixed model analysis makes the assumption that missing data is independent of unobserved measurements but dependent on observed measurements,[287] i.e. observed values can be used by the analysis package to predict the missing values.[285] Repeated measures analysis makes the assumption that missing values are missing completely at random, and most analysis packages will remove subjects that have missing values, thus decreasing the power of the analysis. NCSS-mixed model analysis is able to make estimates for missing data, therefore allowing all subjects to be retained in the analysis and improving overall power.[285]

The mixed model also does not assume that the repeated measures have equal variance, and that all paired measurements have the same covariance at different time points. Where multiple observations are incorporated into a mixed model analysis, a covariant pattern can be selected that is appropriate for the study observations. Mixed model analysis allows the flexibility to consider a wide variety of correlation patterns in repeated measures, whereas in repeated measures ANOVA it is fixed. [288]

2.9.2.2 Multiple testing corrections

Where a large number of statistical tests are carried out simultaneously in this thesis (e.g., microRNA differential expression in the NGS analysis and q-PCR analysis) p-values have been adjusted in order to control for false positive, i.e. Type 1, errors using the Benjamini and Hochberg method.[289] This p-value is referred to as the false discovery rate (FDR).

Chapter 3
microRNA and perioperative myocardial injury

Results in this chapter have been published in the British Journal of Anaesthesia (2020) 125(5), 661-671

3.1 Background

The pathological mechanisms contributing to perioperative myocardial injury remain unclear. The assumption that, in the absence of evidence of a Type 1 myocardial infarction, the cause of a rise in troponin after noncardiac surgery is ischaemic in nature requires further evaluation (Introduction Section 1.3.5). MicroRNA are small, non-coding RNA which regulate post-translational gene expression[109] and molecular signatures of cardiovascular disease can be revealed by detecting circulating serum microRNA.[148] Acute coronary syndrome (ACS), an ischaemic aetiology, is associated with specific microRNA signatures.[172] Selected microRNA associated with ACS have not been previously profiled in patients who develop perioperative myocardial injury (PMI) after noncardiac surgery.

If ACS and PMI share pathological mechanisms, then microRNA expression profiles after noncardiac surgery should be common to both, and may help reveal potential mechanistic pathways for PMI.

3.1.1 Hypotheses

Perioperative myocardial injury and acute coronary syndrome share pathophysiological mechanisms, and therefore common microRNA signatures.

3.1.2 Aims and objectives

- Isolate and quantify levels of expression of microRNA in serum samples before and after noncardiac surgery in patients who developed PMI, compared to matched controls who did not develop PMI.

- Assess whether the subgroup of patients who have a raised troponin after surgery, but who did not sustain myocardial infarction, share the same microRNA expression profiles as those seen in acute coronary syndrome.

3.2 Methods

3.2.1 Study participants

This was a nested case-control study using blood samples from UK patients that had been enrolled in the METS study. The METS study has been outlined in General Methods Section 2.2.

3.2.2 Inclusion/exclusion criteria for the nested case control study

620 patients were recruited into the UK arm of the METS study cohort between 1st March 2013 and 25th March 2016. Patients who developed PMI were identified using Troponin I assay results. PMI was defined as Troponin I (TnI) >99th centile (>0.04 $ng.ml^{-1}$; Troponin-I Centaur CP assay, Siemens, United Kingdom) within three days of surgery. All patients with confirmed PMI had an ECG reviewed by an independent adjudication committee as part of the METS study. Patients with clinically confirmed myocardial infarction and/or pulmonary embolus, those receiving renal replacement therapy, and patients with elevated TnI >99th centile before surgery were excluded from this study. Patients with missing samples before or after surgery were also excluded. Serum samples of the patients identified as having developed PMI were then screened for any obvious red discolouration as evidence for haemolysis. These samples (and patients) were excluded as they would almost certainly fail quality control measures for microRNA expression analysis. After passing exclusion criteria, patients who developed PMI were matched by age, sex, and revised cardiac risk index score[290] to patients who did not develop PMI. Potential matches were only considered if they had TnI ≤0.04 $ng.ml^{-1}$ for all 3 days of sampling after surgery.

3.2.3 MicroRNA selection

The microRNA selected for quantification are listed with their sequence below (Table 3.1). Justification for the selection of microRNA has been outlined in Introduction section 1.4.6. The nomenclature and sequence for each microRNA was crosschecked using the miRBase database (www.miRBase.org).[117]

Table 3.1 List of microRNA selected for quantification.

Each microRNA is listed with its corresponding miRbase nomenclature and sequence.

MicroRNA	miRBase nomenclature	Sequence
miR-1	hsa-miR-1-3p	UGGAAUGUAAAGAAGUAUGUAU
miR-21	hsa-miR-21-5p	UAGCUUAUCAGACUGAUGUUGA
miR-499	hsa-miR-499a-5p	UUAAGACUUGCAGUGAUGUUU
miR-146	hsa-miR-146a-5p	UGAGAACUGAAUUCCAUGGGUU
miR-133	hsa-miR-133a-3p	UUUGGUCCCCUUCAACCAGCUG
miR-208a	hsa-miR-208a-3p	AUAAGACGAGCAAAAAGCUUGU
miR-208b	hsa-miR-208b-3p	AUAAGACGAACAAAAGGUUUGU

3.2.4 microRNA quantification and expression

Detailed methodology and propriety references for microRNA isolation and quantitative RT-PCR are outlined in General Methods Section 2.6.1 and Section 2.6.3.

Quality control measures for microRNA isolation, reverse transcription, evidence of haemolysis, amplification efficiency and melt curve analysis have been described in detail in General Methods Section 2.6.4**.** MicroRNA were defined as detected if the calibrated Cq value was <37. MicroRNA hsa-miR-152-3p and hsa-miR-361-5p were identified as reference

microRNA **(**methodology and results in Appendix D). Expression levels of microRNA were then compared using the relative Cq method calculated using the formula:

$$\Delta Cq = Cq[microRNA] - Cq[geometric\ mean\ of\ reference\ microRNA].$$

The ΔCq values were converted to a fold change (FC) by applying the formula of $2^{-\Delta Cq}$ [265].

3.2.5 MicroRNA pathway analysis

DNA Intelligent Analysis (DIANA)-miRPath v.3.0 pathway analysis[266] was used to predict which transcriptomic processes may be altered by microRNA changes after surgery (General Methods Section 2.6.6). The workflow for pathway analysis is summarised in Figure 3.1:

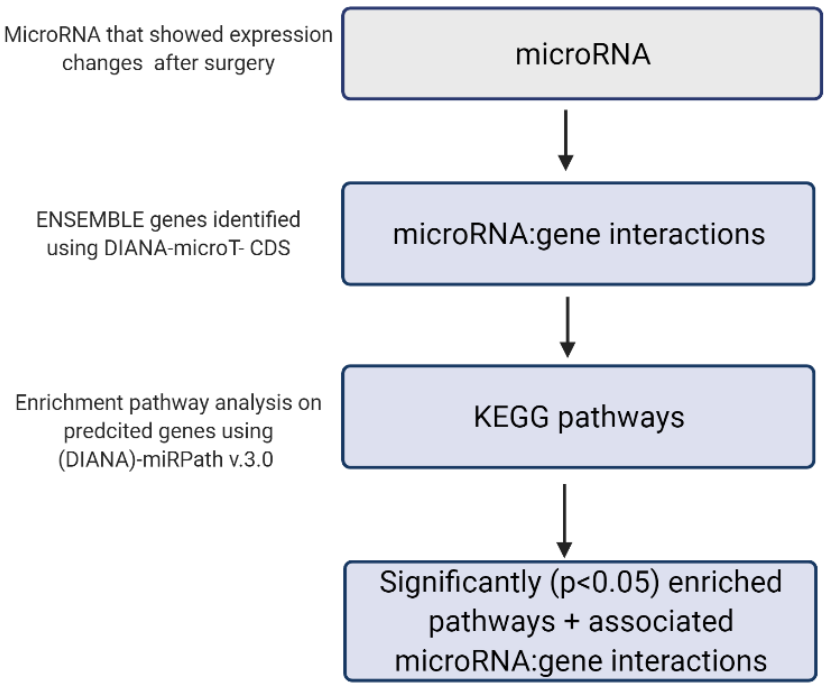

Figure 3.1 Workflow for pathway analysis

3.2.6 Statistical analysis

Clinical characteristics of the patients were stratified according to the presence or absence of troponin elevation: TnI ≥0.04ng.mL^{-1} (>99th centile value). The ΔCq values were checked for normality using the Shapiro–Wilk test for normality. For microRNA assays that were expressed in >95% across all samples, changes in ΔCq values were analysed using a mixed repeated measures model (General Methods Section 2.9.2.1). The levels examined were perioperative myocardial injury (TnI ≥0.04ng.mL^{-1} and TnI <0.04ng.mL^{-1}), and sampling time related to surgery (before or after surgery). Individual comparisons between groups were calculated using post-hoc Bonferroni tests. It was anticipated from the literature that the detection rate of some microRNA may be low,[172] and therefore required a statistical contingency plan. For microRNA expressed in <95% samples, Chi-Squared analysis was performed to assess proportions between groups. Pearson's test was used to test for correlations. P<0.05 was considered statistically significant. All statistical analyses were undertaken using NCSS 12 (Kaysville, UT, USA).

3.2.7 Sample size calculation

Receiver operating character curve analysis has demonstrated that miR-499, miR-1-3 and miR-21 can be used to identify patients with acute coronary syndrome, area under the curve (AUC) = 0.89.[175] The assumption was made that if these microRNA are potentially predictive for diagnosing acute coronary syndrome, then presuming the pathophysiological mechanism is the same for PMI, the AUC value could be used to calculate the required sample size in this study. Assuming a significance level of $\alpha = 0.01$ and $1-\beta = 0.9$, a minimum of 12 patients would be needed in each group to detect a difference in relative expression of the microRNA after

surgery. The sample size calculation was performed by the pROC package,[291, 292] using R software Version 3.4.3.

3.3 Results

3.3.1 Patient characteristics

After exclusion criteria was met, 24 patients recruited from the METS study who developed PMI were matched with clinically similar patients who did not develop PMI after noncardiac surgery (Figure 3.2 and Table 3.2). Patients' clinical characteristics such as age, sex, and BMI were similar in both groups. Both groups were low risk for cardiovascular complications as assessed by RCRI. The type of surgical and anaesthesia was similar in both groups. Patients who developed PMI had a median TnI of 0.08 $ng.ml^{-1}$, interquartile range: 0.05-0.13 $ng.ml^{-1}$, on the day they first developed PMI.

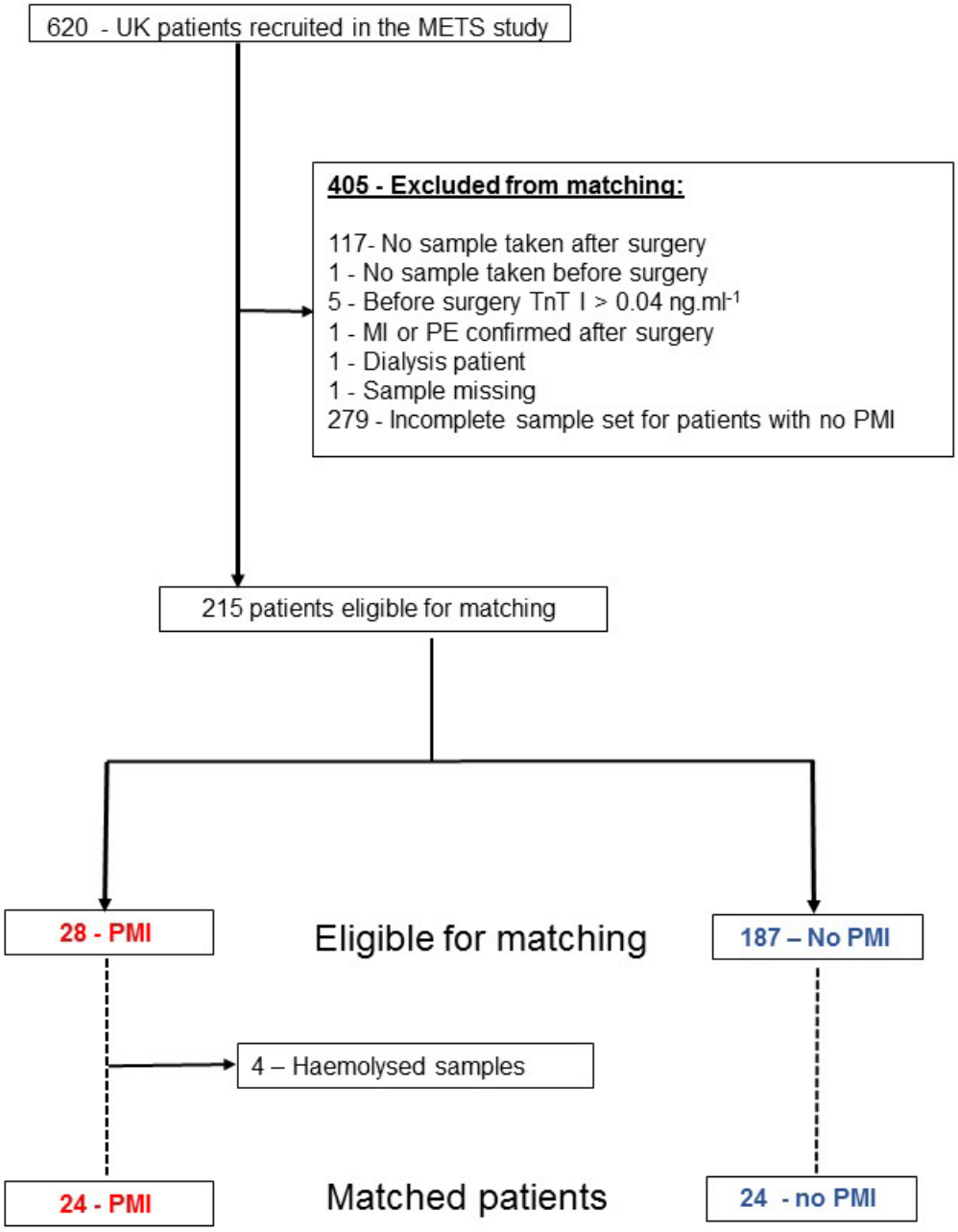

Figure 3.2 Sample selection flow diagram

The flow diagram illustrates patient sample selection from the UK METS study.

MI: myocardial infarction. PE: pulmonary embolus.

Table 3.2 Patient characteristics for study

Data is presented as mean with standard deviations (SD) for parametric data and as median (25th-75th interquartile range) for non-parametric data. Frequencies are presented with percentages (%). Age is rounded to the nearest year. Perioperative myocardial injury (PMI) was defined as troponin I (TnI) >99th centile (>0.04 ng.ml^{-1}) after surgery. eGFR: estimated glomerular filtration rate. RCRI: Revised cardiac risk index score. ACE-I: Angiotensin converting enzyme inhibitor. ARB: angiotensin receptor blocker. Other units as indicated. #Previous diagnosis of asthma, reactive airways disease, chronic obstructive lung disease, chronic bronchitis, or emphysema. *Indication for surgery was for treatment of cancer.

	Whole cohort n=48	No PMI n =24	PMI n=24
Troponin level ng ml^{-1}		≤0.04	0.08 (0.05-0.13)
Clinical Characteristics			
Age (yr)	67 (61-75)	67 (60-74)	66 (61-76)
Male sex (n;%)	22 (45.8%)	11 (45.8%)	11 (45.8%)
Body Mass Index (kg m^{-2})	27 (5)	27(5)	27 (5)
Before surgery eGFR(ml.min.1.73m^2)	87 (76-96)	84 (72-94)	90 (79-103)
Haemoglobin (g dl^{-1})	130 (22)	128 (16)	131 (26)
Co-morbidities (n; %)			
RCRI ≥2	4 (8.3%)	2 (8.3%)	2 (8.3%)
Coronary artery disease	5 (10.4%)	3 (12.5%)	2 (8.3%)
Congestive heart failure	0 (0.0%)	0 (0.0%)	0 (0.0%)
Cerebrovascular disease	1 (2.1%)	1 (4.2%)	0 (0.0%)
Diabetes Mellitus	10 (20.8%)	5(20.8%)	5 (20.8%)
Peripheral vascular disease	1 (2.1%)	0 (0.0%)	1 (4.2%)
Hypertension	24 (50.0%)	11(45.8%)	13 (54.2%)
Obstructive lung disease#	5 (10.4%)	3 (12.5%)	2 (8.3%)
Significant malignancy*	34 (70.8%)	18 (75.0%)	16 (66.7%)
Preoperative medications			
Beta blocker	6 (12.5%)	4 (16.7%)	2 (8.3%)
Calcium channel blocker	5 (10.4%)	3 (12.5)	2 (8.3%)
ARB/ACE-I	19 (39.5%)	8 (33.3%)	11 (45.8%)
Aspirin	8 (16.7%)	4 (16.7%)	4 (16.7%)
Surgical Procedure type (n; %)			
Intraperitoneal or retroperitoneal	30 (62.5%)	17 (70.8%)	13 (54.2%)
Urology or gynaecological	15 (31.3%)	6 (25.0%)	9 (37.5%)
Orthopaedic	3 (6.2%)	1 (4.2%)	2 (8.3%)
Anaesthesia Type (n; %)			
General Anaesthesia alone	24 (50.0%)	13(54.2%)	11 (45.8%)
General + regional anaesthesia	24 (50.0%)	11 (45.8%)	13 (54.2%)

3.3.2 Quality control (QC) assessment

3.3.2.1 MicroRNA Isolation, reverse transcription and evidence of haemolysis

MicroRNA was isolated from 96 patient serum samples (24 paired samples from patients who did and not develop PMI). 2 samples failed the haemolysis QC and 5 failed the isolation QC. The outlier samples identified in the reverse transcription QC had also been identified in the isolation QC (Sample 44). The 7 samples that failed the QC were excluded from the microRNA expression analysis (Figure 3.3).

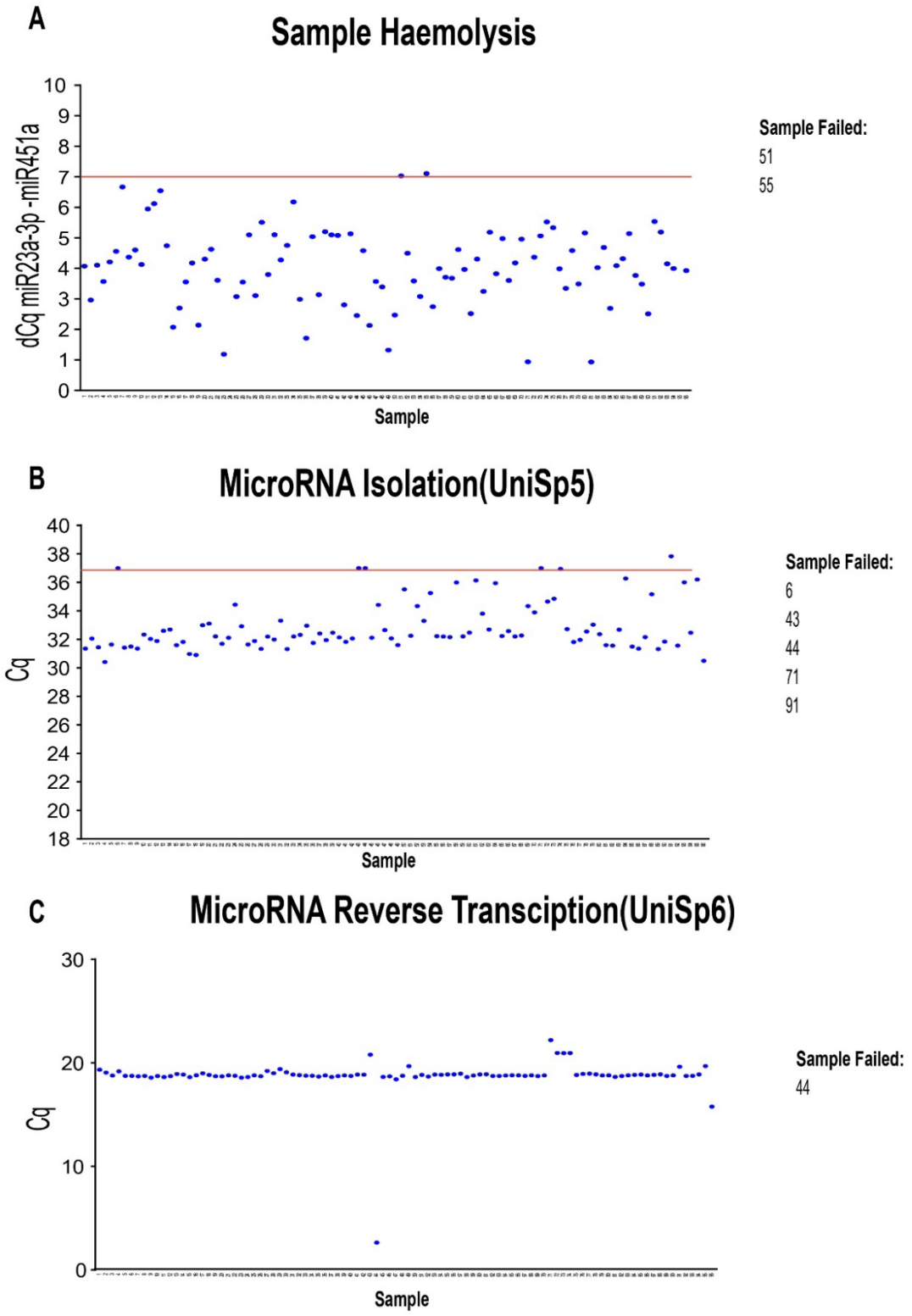

Figure 3.3 Quality control (QC) analysis for each sample

A: Haemolysis QC: Ratio of Cq miR23a-3p-miR451a. Samples with ΔCq ≥7 (red line) failed QC. **B: Isolation QC:** Spike in UniSp5. Samples Cq≥37 (red line) failed QC. **C: Reverse Transcription QC:** Spike in UniSp6.

3.3.2.2 Amplification efficiency

The amplification efficiency was 90% for microRNA:1-3p, 21-5p, 146a-5p, 133a-3p. MicroRNA with low detection rates had lower amplification rates (Table 3.3)

Table 3.3 Sample detection and amplification efficiency

MicroRNA was defined as detected in a sample if the calibrated Cq value was <37. Amplification efficiency is expressed as mean across all samples (standard deviation). The amplification efficiency is expressed as a value between 1 and 2 and defined as the fold increase per cycle. Between 1 and 2 is the equivalent of between 0 and 1.

MicroRNA	Samples detect (Cq<37)	Amplification efficiency (E)
UniSp5	89/89 (100%)	1.9 (0.2)
hsa-miR-1-3p	89/89 (100%)	1.9 (0.1)
hsa-miR-21-5p	89/89 (100%)	1.9 (0.1)
hsa-miR-146a-5p	89/89 (100%)	1.9 (0.1)
hsa-miR-133a-3p	88/89 (99%)	1.9 (0.1)
hsa-miR-499a-5p	47/89 (53%)	1.6 (0.4)
hsa-miR-208a-3p	4/89 (4%)	1.5 (0.4)
hsa-miR-208b-3p	39/89 (44%)	1.4 (0.4)
hsa-miR-152-3p	89/89 (100%)	1.9 (0.1)
hsa-miR-361-5p	89/89 (100%)	1.9 (0.1)

3.3.2.3 Melt curve analysis:

Visual inspection of melt curve analysis revealed single peaks in all samples that had a Cq <37. Melt curves for one sample are shown in Figure 3.4.

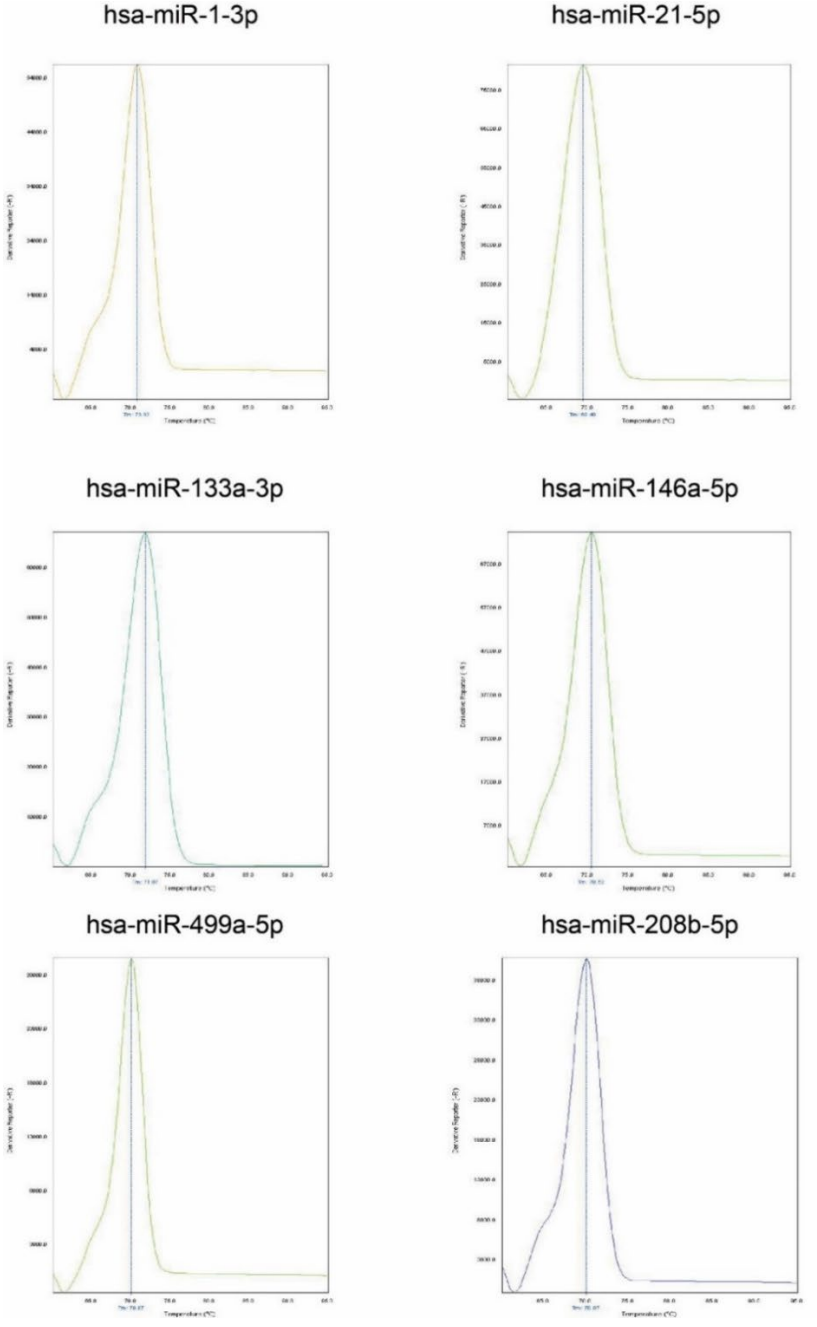

Figure 3.4 Melt curve analysis

Example of melt curve analysis for each tested microRNA from a sample. A single peak indicates a single PCR product for the microRNA assay.

3.3.2.4 Reference MicroRNA

There were no significant differences between surgery and between PMI group for the reference microRNA hsa-miR-152-3p and hsa-miR-361-5p Cq values, indicating the microRNA were stable to be used as reference microRNA for the microRNA expression study. (Table 3.4)

Table 3.4 Cq values for reference candidate microRNA hsa-miR-152-3p and hsa-miR-361-5p

Data are presented as mean Cq values (95%CI) for before and after surgery for patients who did and did not develop PMI. There were no statistical differences ($p>0.05$) in Cq values between surgery and PMI group when analysed using repeated measures ANOVA. PMI: perioperative myocardial injury.

	NO PMI		PMI	
MicroRNA	Before Surgery	After Surgery	Before Surgery	After Surgery
hsa-miR-152-3p	29.41(28.82-29.99)	29.94(29.38-30.50)	29.93(29.26-30.60)	30.19(29.46-30.91)
hsa-miR-361-5p	28.72(28.18-29.27)	28.83(28.22-29.43)	29.27(28.58-29.96)	29.01(28.31.29.71)

3.3.3 MicroRNA expression

The calibrated Cq values for the detected circulating microRNA are presented in Figure 3.5. The ΔCq values, normalised to the geometric mean of the reference microRNA Cq are shown in the heatmap Figure 3.6. No correlation was observed between fold change expression in microRNA after surgery and TnI levels for all microRNA that were detected before and after surgery (Figure 3.8). Details of mixed model analysis are found in Appendix F.

3.3.3.1 hsa-miR-1-3p

There was an increase in hsa-miR-1-3p expression levels in both patients who developed PMI (mean fold-change:3.99 (95%CI: 1.95-8.19); $F_{[1,47.5]}$ =24.16; p<0.001) and those that remained free from PMI (mean fold-change:2.47 (95%CI: 1.44-4.01); $F_{[1,44.2]}$ =11.95; p=0.002) (Figure 3.6**A** and Figure 3.7**A**).

3.3.3.2 hsa-miR-133-3p

Similar to hsa-miR-1-3p, there was an increase in circulating hsa-miR-133-3p expression levels in both patients who developed PMI (mean fold-change :5.67 (95%CI: 2.94-10.91); $F_{[1,42]}$ = 31.13; p<0.001) and those that remained free from PMI (mean fold-change: 3.10 (95%CI: 1.79-5.37); $F_{[1,42]}$ = 17.54; p<0.001) (Figure 3.6**B** and Figure 3.7**B**).

3.3.3.3 hsa-miR-146a-5p

Expression levels of hsa-miR146a-5p decreased after surgery in patients who developed PMI after surgery (mean fold-change: 0.74 (95%CI: 0.64-0.84) and those that remained free of PMI (mean fold-change: 0.90 (95%CI: 0.72-1.12); ($F_{[1,33.5]}$=5.70, p=0.023 (Figure 3.6**C** and Figure 3.7**C**).

3.3.3.4 hsa-miR-21-5p

There was no change in expression for hsa-miR-21-5p after surgery in either group of patients (Figure 3.6**D** and Figure 3.7**D**).

3.3.3.5 hsa-miR-208b-3p and hsa-miR-208a-3p

hsa-miR-208b-3p was detected in a higher proportion of patients who developed PMI compared to those who remained free from PMI in samples collected after surgery (odds ratio (OR):4.11 (95%CI:1.01-23.09); p=0.032). In patients who developed PMI, there was an increase in the proportion detected after surgery compared to before surgery (odds ratio (OR):20.56 (95%CI:4.08-185.44); p<0.001) (Figure 3.9). An increase after surgery was not observed in patients who remained free of PMI. Circulating hsa-miR-208b-3p was not detected for all samples before and after surgery, therefore only a correlation between circulating levels after surgery and Troponin I levels was investigated. No correlation was observed between circulating levels after surgery and Troponin I levels (Figure 3.10). No differences in detection were observed for hsa-miR-208a-3p (Figure 3.11).

3.3.3.6 hsa-miR-499a-5p

There was an increase in proportion of hsa-miR-499a-5p detected after surgery compared to before surgery for patients that developed PMI ((OR):1.82 (95%CI:1.11-3.28); $p<0.013$) (Figure 3.9). No correlation was observed between circulating levels after surgery and Troponin I levels (Figure 3.10).

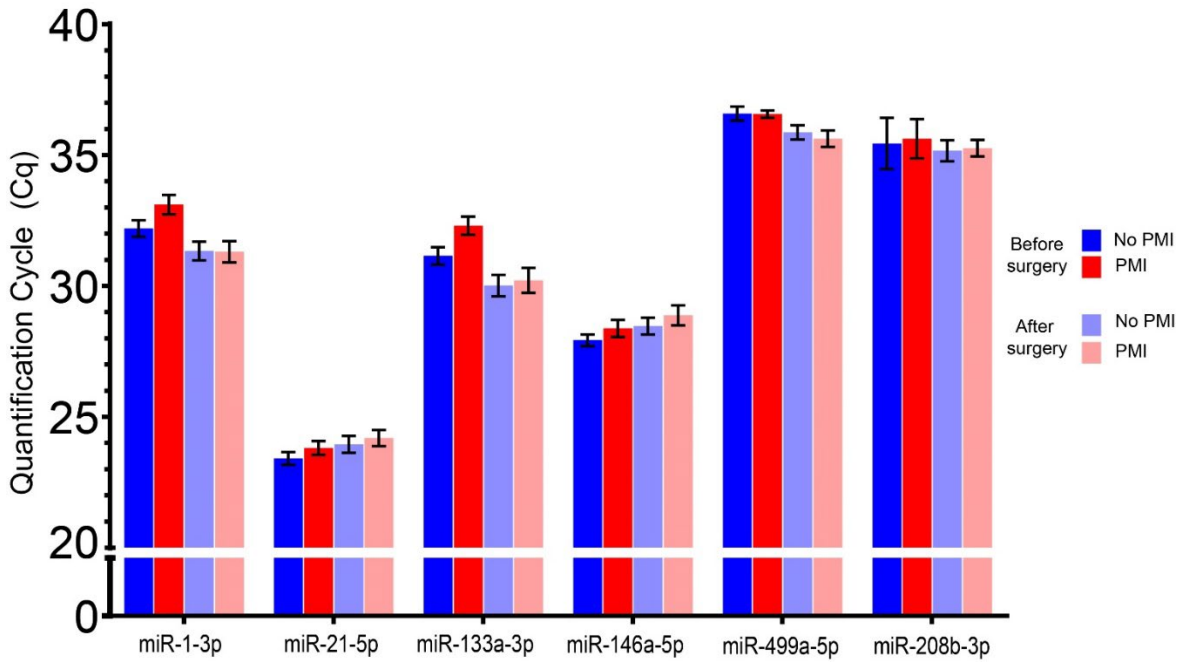

Figure 3.5 Calibrated Cq values for serum circulating microRNA

The data presented are calibrated Cq values (mean ±SEM). The data presented are prior to normalisation of the Cq values, and therefore no statistical comparisons have been performed on this data set. Cq; quantification cycle, the cycle number at a set fluorescence threshold for the real-time PCR.

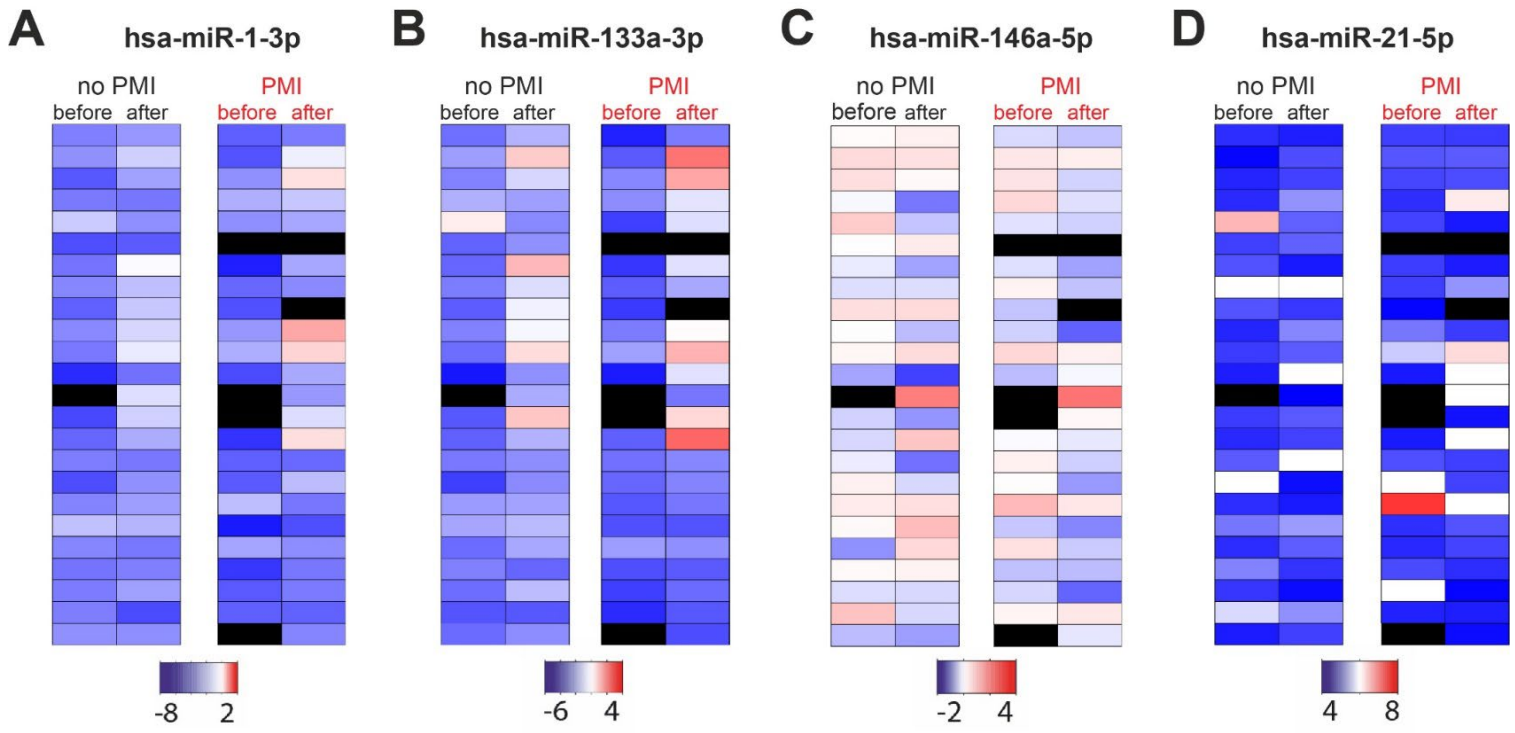

Figure 3.6 A-D Heatmaps showing relative expression levels (fold change) of detectable serum microRNA before and after noncardiac surgery, in relation to the development of myocardial injury

Heatmap showing relative serum expression levels for each matched sample using the relative Cq method. MicroRNA Cq values were normalised to the geometric mean of the reference microRNA Cq values to give ΔCq values. The ΔCq values were converted to a fold change (FC) by applying the formula of $2^{-\Delta Cq}$. Each row represents microRNA expression of a patient sample before and surgery. Bars below each microRNA heatmap indicate range of fold-change expression (log_2 scaled). Black bars denote sample that failed quality control threshold.

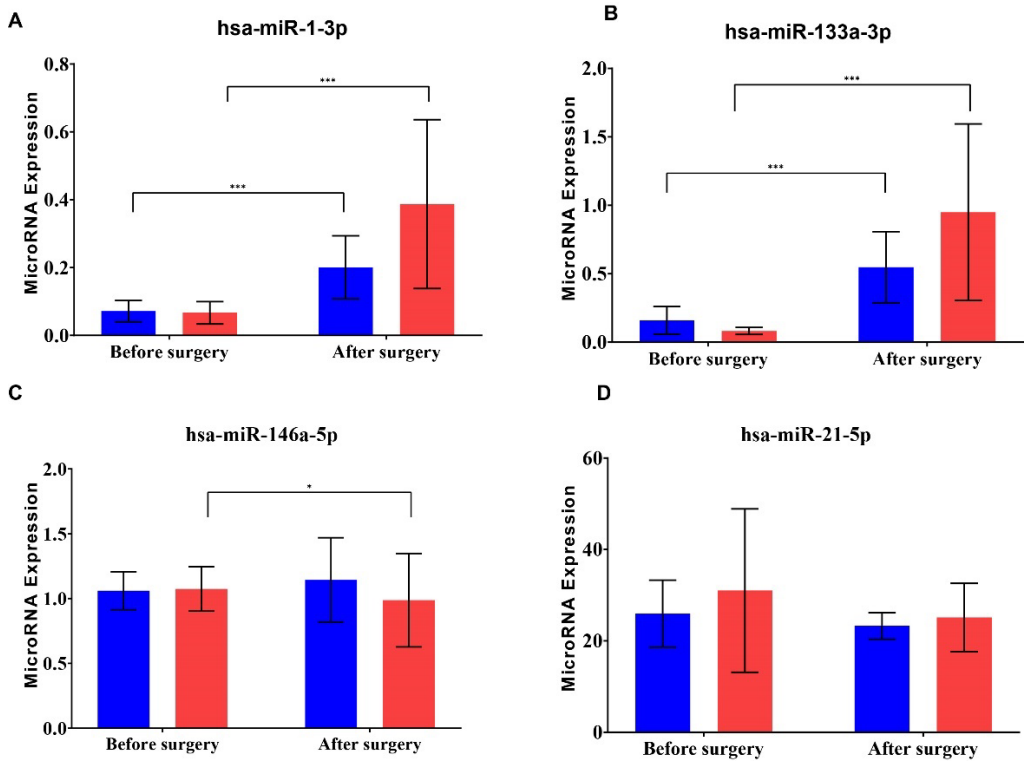

Figure 3.7 Bar graph showing relative expression levels (fold change relative to reference microRNA) of detectable serum microRNA before and after noncardiac surgery, in relation to the development of myocardial injury

Data are presented as mean microRNA expression values with 95% confidence intervals. MicroRNA expression calculated using relative Cq method and normalised to reference microRNA. P value refers to before surgery versus after surgery (mixed model analysis) * $p<0.05$ and ***$p<0.001$

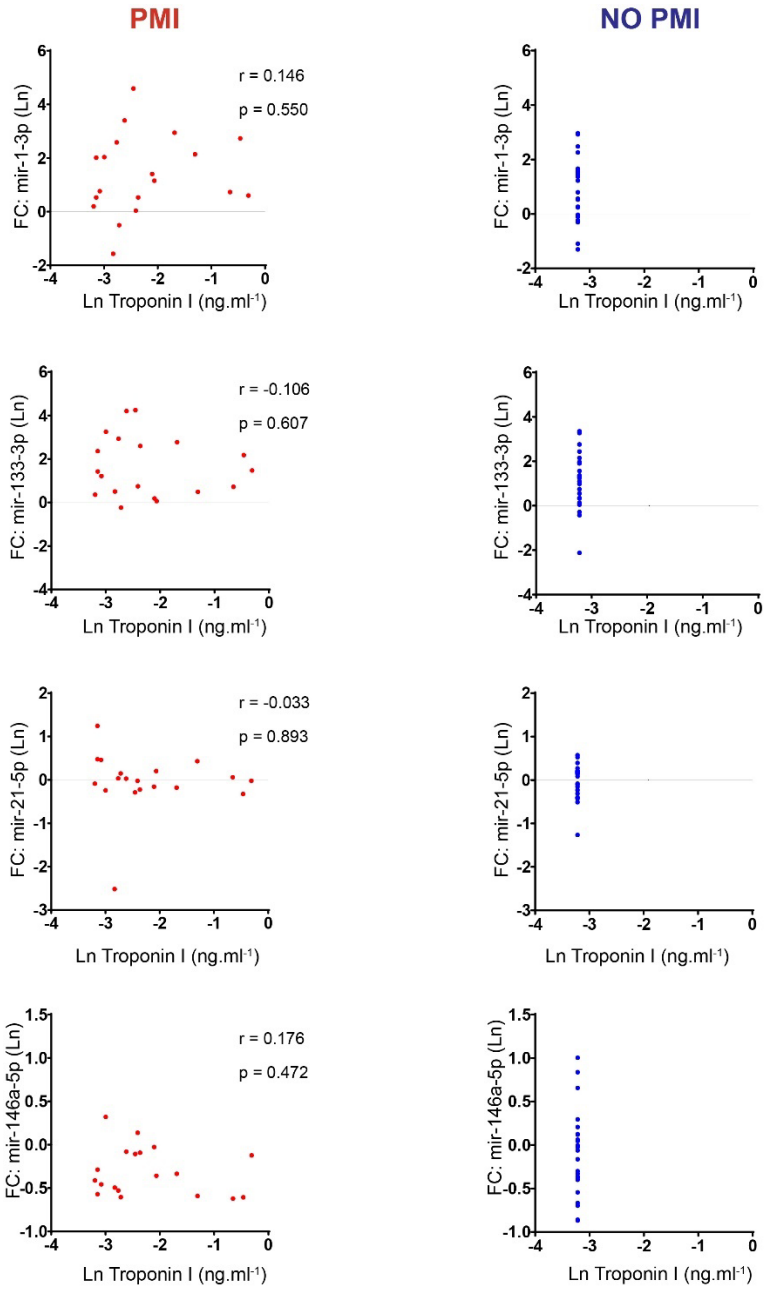

Figure 3.8 Correlation between fold change of circulating microRNA after surgery and troponin I

Pearson correlation was used to compare fold change after surgery with Troponin I after natural logarithmic transformation for patients who had Troponin I >0.04ng.ml^{-1}. No statistical test was performed on samples where Troponin I <0.04 ng.ml^{-1}, as the relationship is a vertical line. r value is the correlation coefficient, and p-value is testing the null hypothesis that the correlation coefficient is zero.

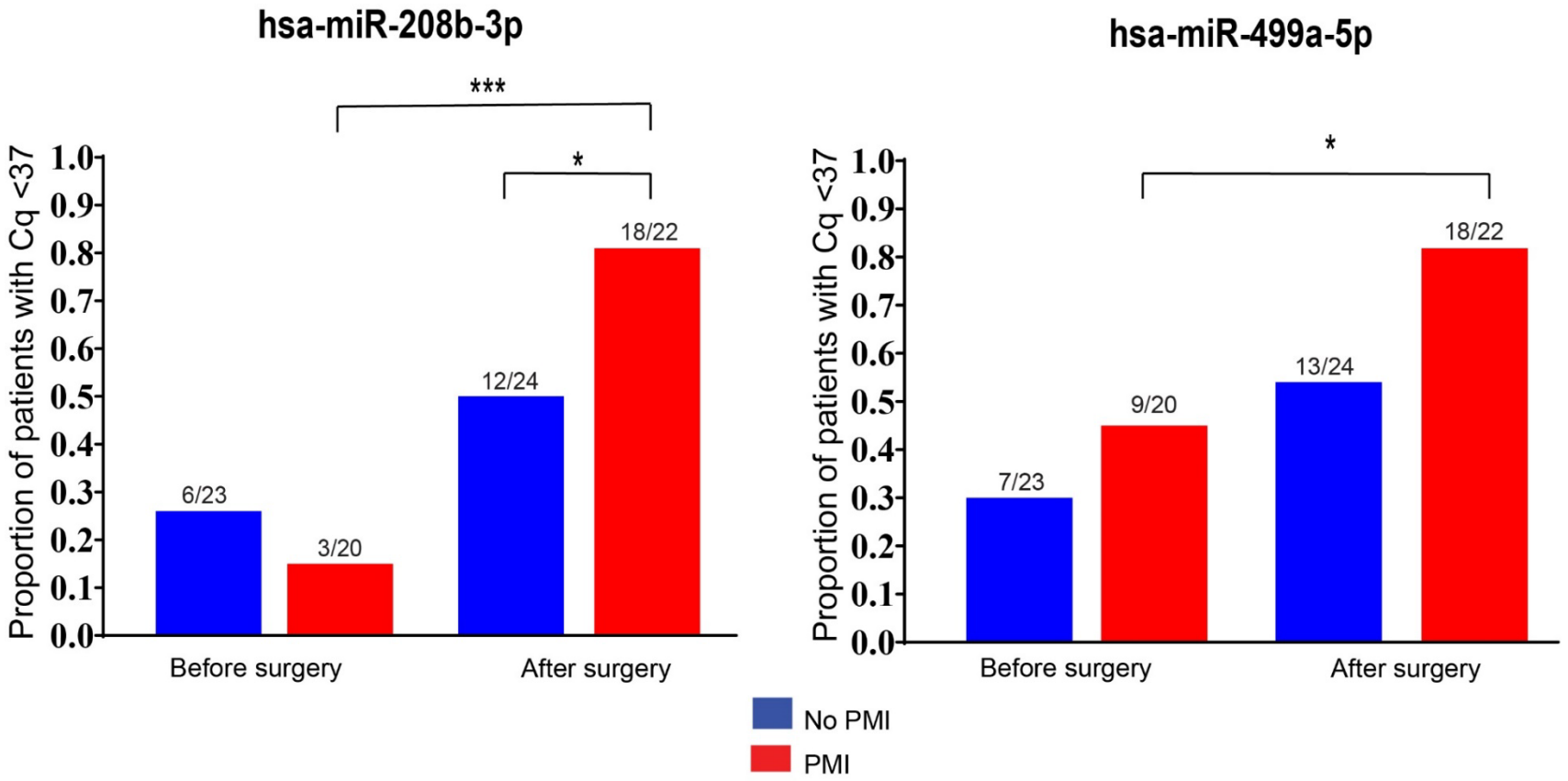

Figure 3.9 Proportion of patient serum samples in which hsa-miR-208b-3p and has-miR-499a-5p were detected

P-value refers to before surgery vs after surgery, and PMI vs no PMI (X^2 test). *P<0.05, ***P<0.001.

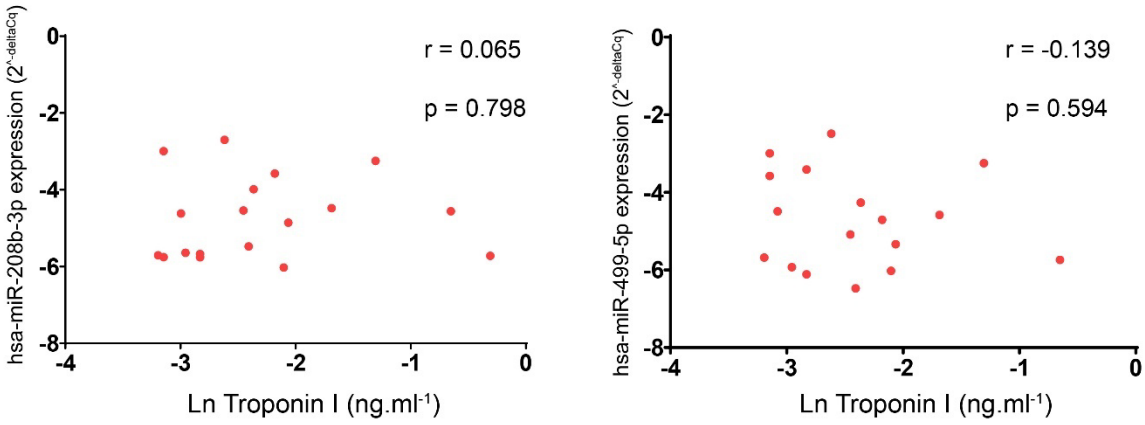

Figure 3.10 No correlation between hsa-miR-208b-3p and has-miR-499-5p expression after surgery with Troponin I for patient who develop PMI

Pearson correlation was used to compare hsa-miR-208b-3p expression after surgery with Troponin I ($ng.ml^{-1}$) after natural logarithmic transformation. The comparison with fold change after surgery has not been analysed, as some patients had no detectable levels below the Cq threshold of 37. r value is the correlation coefficient, and p-value is testing the null hypothesis that the correlation coefficient is zero.

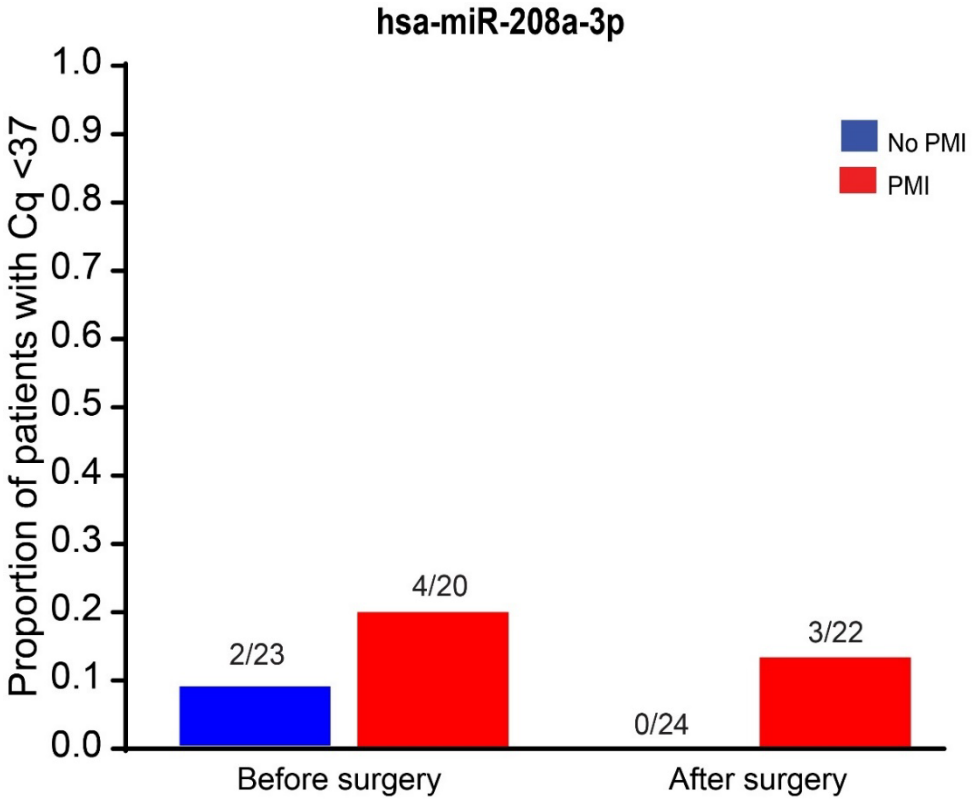

Figure 3.11 Proportion of patient serum samples in which hsa-miR-208a-3p was detected

No differences in detection were observed between groups, X^2 test.

3.3.4 MicroRNA predicted gene pathways and enrichment pathway analysis

Circulating microRNA that changed after surgery were entered onto the online DNA Intelligent Analysis (DIANA)-miRPath v.3.0 pathway analysis tool. The number of genes predicted to interact with each microRNA are listed in Table 3.5.

Table 3.5 MicroRNA with the number of predicted target genes

The DNA Intelligent Analysis (DIANA)-miRPath v.3.0 produces a list of genes (proteins) that are predicted to interact with each individual microRNA (miRNA targeted genes (miTG) score threshold >0.8).

MicroRNA	Number of predicted target genes
hsa-miR-1-3p	634
hsa-miR-133-3p	608
hsa-miR-146a-5p	413
hsa-miR-208b-3p	691
hsa-miR-499-5p	534

Using an a priori analysis methodology, 17 signalling pathways were identified by the DIANA in silico pathway analysis (FDR <0.05) for the selected microRNA that showed changes after surgery (Table 3.6)

The overriding aim of this thesis is to obtain a better understanding of the mechanisms underlying perioperative myocardial injury. MicroRNA and their targeted proteins were found to be associated with the adrenergic signalling pathway in cardiomyocytes (Table 3.6; hsa04261; p=0.006), thus identifying this pathway as a potential mechanism for further exploration.

KEGG pathway (pathway map code)	FDR	No. of genes	hsa-miR-1 3p	hsa-miR-133-3p	hsa-miR146a-5p	hsa-miR-499a-5p	hsa-miR-208b-3p
Glioma (hsa05214)	0.001	18					
Biotin metabolism (hsa00780)	0.001	1					
Hippo signalling pathway (hsa04390)	0.001	32					
Thyroid hormone synthesis (hsa04918)	0.001	15					
Gap junction (hsa04540)	0.004	21					
Endocytosis (hsa04144)	0.004	43					
Adrenergic signalling in cardiomyocytes (hsa04261)	0.005	29					
Arrhythmogenic right ventricular cardiomyopathy (hsa05412)	0.007	13					
Regulation of actin cytoskeleton (hsa04810)	0.007	44					
ECM-receptor interaction (hsa04512)	0.009	14					
Nicotinate and nicotinamide metabolism (hsa00760)	0.010	8					
Long-term potentiation (hsa04720)	0.013	19					
Amphetamine addiction (hsa05031)	0.013	17					
Transcriptional mis regulation in cancer (hsa05202)	0.020	37					
Glycosphingolipid biosynthesis (hsa00601)	0.021	3					
Axon guidance (hsa04360)	0.034	26					
Adherens junction (hsa04520)	0.046	20					

Table 3.6 KEGG pathways identified by DIANA-miRPath v.3.0

Each significant enriched pathway is listed with its KEGG pathway map identifier code. P values are generated by sampling the microRNA and calculating the probability of KEGG pathway overlap (extension of the Fischer exact test), then corrected for multiple testing. Pathways that are significantly enriched ($p<0.05$) are listed. The number of genes refers to the number of genes predicted by the selected microRNA that are enriched by their associated pathway. MicroRNA that are linked to the pathway are highlighted in green, and those with no predicted genes in red. Cardiomyocyte specific pathways are highlighted in purple. hsa: homo sapien. FDR: false discovery rate.

3.3.5 Adrenergic signalling in cardiomyocyte pathway

The adrenergic signalling pathway was predicted by all 5 of the selected microRNA that showed a change in expression after surgery (Table 3.6). The 5 microRNA were predicted to target 29 proteins (genes). Some microRNA were predicted to interact with the same genes, and therefore the gene lists for each microRNA were cross-referenced to identify which genes are targeted by more than 1 microRNA. The gene lists are summarised in Figure 3.12.

Genes that were predicted targets of more than 1 microRNA were: SLC8A1 (hsa-miR-1-3p, hsa-miR-133a-3p, hsa-miR-208b-5p, hsa-miR-499-5p), TPM4 (hsa-miR-1-3p, hsa-miR-133a-3p), ATF2 (hsa-miR-1-3p and hsa-miR-499-5p) and CREB5 (hsa-miR-1-3p, hsa-miR-133a-3p). The function of each target gene within the adrenergic pathway is outlined below and summarised in Figure 3.13

Gene Abbreviation	Protein Coding
ADCY1	Adenylate Cyclase 1
ADCY3	Adenylate Cyclase 3
AGTR2	Angiotensin II receptor type 2
ATF2	Activating Transcription Factor 2
ATGR1	Angiotensin II receptor type 1
ATP1A4	ATPase Na+/K+ Transporting Subunit Alpha 4
ATP1B4	ATPase Na+/K+ Transporting Subunit Beta 4
ATP2B1	ATPase Plasma Membrane Ca2+ Transporting 1
ATP2B3	ATPase Plasma Membrane Ca2+ Transporting 3
CACNB2	Calcium Voltage-Gated Channel Auxiliary Subunit Beta 2
CALM1	Calmodulin 1
CALM2	Calmodulin 2
CAMK2D	Calcium/Calmodulin Dependent Protein Kinase II Delta
CAMKB	Calcium/Calmodulin Dependent Protein Kinase Beta
CREB32	CAMP Responsive Element Binding Protein 32
CREB5	CAMP Responsive Element Binding Protein 5
GNAQ	G Protein Subunit Alpha Q
PIK3R1	Phosphoinositide-3-Kinase Regulatory Subunit 1
PPP1CB	Protein Phosphatase 1 Catalytic Subunit Beta
PPP2CA	Protein Phosphatase 2A Catalytic Subunit C α
PPP2CB	Protein Phosphatase 2A Catalytic Subunit Cβ
PPP2R2D	Protein Phosphatase 2A Regulatory Subunit B 2δ
PPP2R3A	Protein Phosphatase 2A Regulatory Subunit B 3α
PPP2R5A	Protein Phosphatase 2A Regulatory Subunit B 5α*
PPP2R5E	Protein Phosphatase 2 Regulatory Subunit 5 Epsilon
PRKACB	Protein Kinase CAMP-Activated Catalytic Subunit Beta
SLC8A1	Sodium/Calcium Exchanger Protein 1
TPM3	Tropomyosin 3
TPM4	Tropomyosin 4

*also the alpha subunit of the regulatory subunit B56

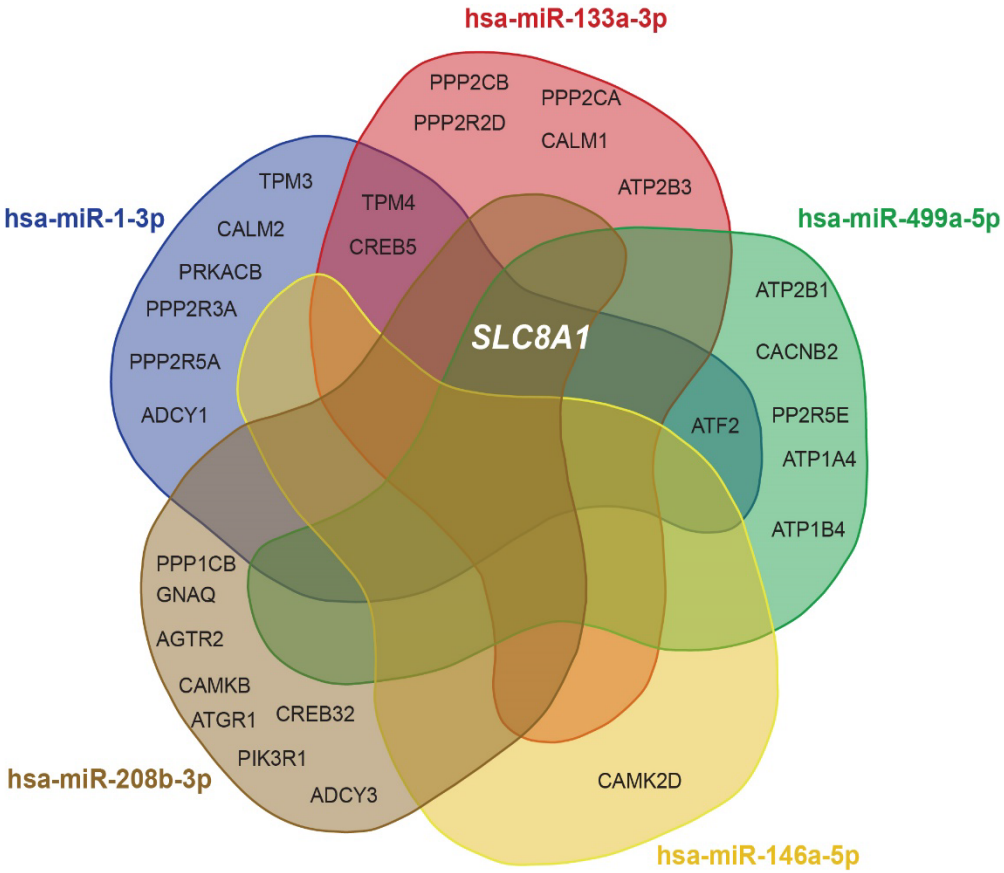

Figure 3.12 Venn diagram showing predicted microRNA:gene interaction for microRNA that changed after surgery for the adrenergic signalling pathway in cardiomyocytes

The Venn diagram shows each microRNA and their predicted gene interaction with overlap between microRNA. The table lists the genes in Venn diagram and the protein it encodes. Gene names are derived from ENSEMBL annotation directory.[293]

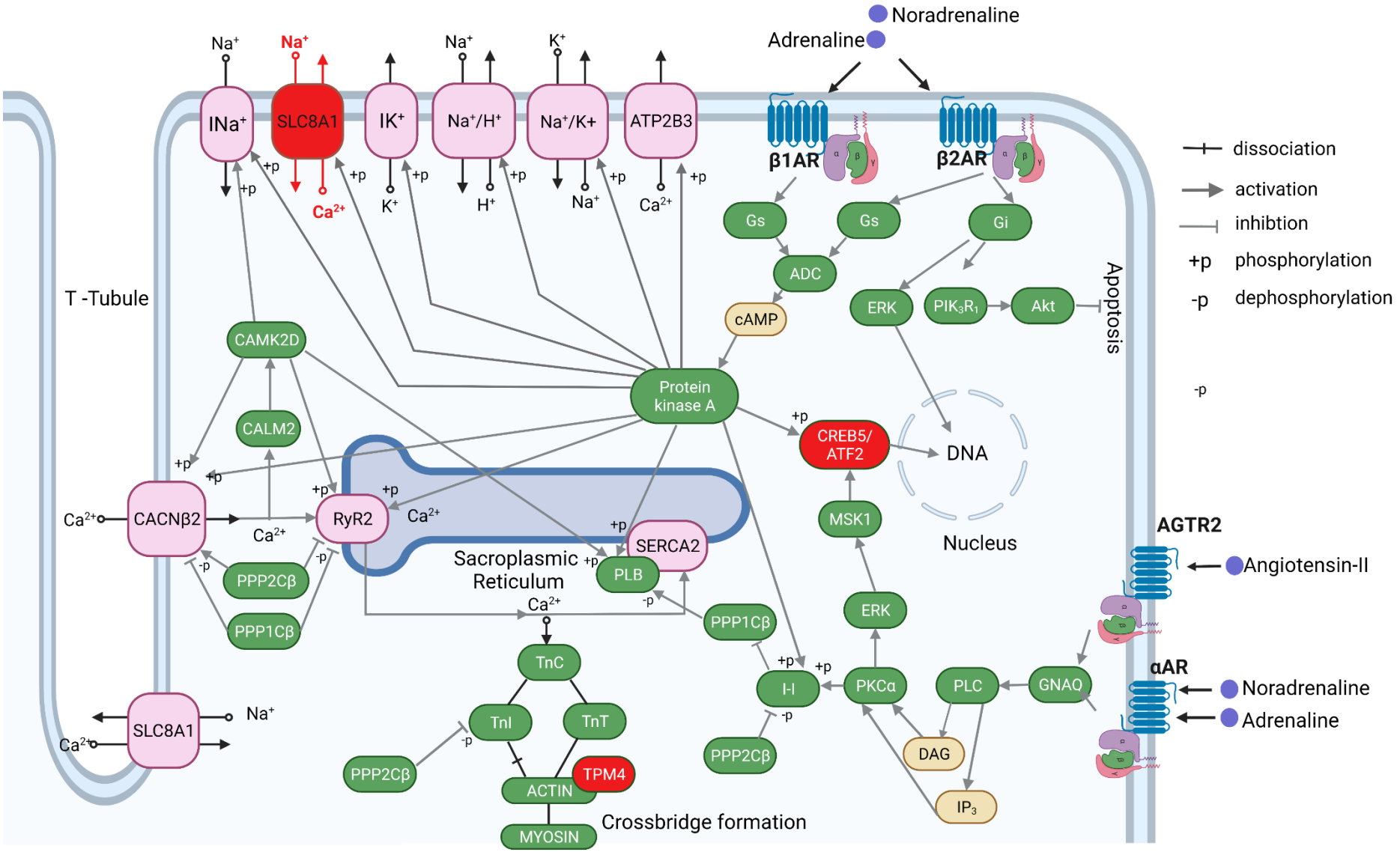
Noradrenaline
Adrenaline
INa+
SLC8A1
IK+
Na+/H+
Na+/K+
ATP2B3
β1AR
β2AR
Gs
Gs
Gi
ADC
cAMP
ERK
PIK3R1
Akt
Apoptosis
T -Tubule
CAMK2D
CALM2
Protein kinase A
CREB5/ ATF2
DNA
Nucleus
CACNβ2
RyR2
Sacroplasmic Reticulum
SERCA2
PLB
PPP2Cβ
PPP1Cβ
MSK1
ERK
PKCα
PLC
GNAQ
I-I
DAG
IP3
TnC
TnI
TnT
TPM4
ACTIN
MYOSIN
Crossbridge formation
AGTR2
Angiotensin-II
αAR
Noradrenaline
Adrenaline
dissociation
activation
inhibtion
+p phosphorylation
-p dephosphorylation

Figure 3.13 Adrenergic and calcium signalling in cardiomyocyte adapted from KEGG pathway wire diagram

This schematic of the sarcolemma (cardiomyocyte plasma membrane) shows the interaction of proteins after adrenergic receptor stimulation (e.g., perioperative surgical stress). The genes highlighted in **RED** were targeted by ≥2 microRNA. SLC8A1: Na^{+}/Ca^{2+} exchanger. TPM4: tropomyosin 4. CREB5: cyclic AMP responsive element binding protein 5. ATF2: activating transcription factor 2. INa+: voltage gated inward sodium channel. IK+: voltage gated potassium channel. Na+/H+: sodium/hydrogen exchanger. Na+/K+: sodium/potassium ATPase exchanger. ATP2B1: ATPase plasma membrane Ca^{2+} transporting 1. β1-AR: beta 1 adrenergic receptor. β2-AR: beta 2 adrenergic receptor. α-AR: alpha adrenergic receptor. AGTR2: angiotensin II receptor type 2. Gs: guanine nucleotide-binding protein G(s) subunit alpha. Gi: guanine nucleotide-binding protein G(i) subunit alpha. ADC: adenylate cyclase 1/3. cAMP: cyclic adenosine monophosphate. ERK: extra-signalling regulating kinase. PIK3R1: phosphoinositide-3-kinase regulatory subunit 1. AKt: AKT serine/threonine kinase 3. MSK1: mitogen stress activated kinase 1. GNAQ: G-protein subunit alpha Q. PLC: phosphatidylinositol phospholipase C. IP3: inositol 1,4,5-trisphosphate. DAG: diacylglycerol. PKCα: protein kinase A alpha subunit. I-1: inhibitor 1 protein/protein phosphatase regulatory inhibitor. PPP1Cβ: Protein phosphatase 1 catalytic subunit Beta. PPP2Cβ: Protein phosphatase 2 catalytic subunit Beta. TnI: Troponin I. TnC: Troponin C. TnT: Troponin T. PLB: phospholamban. SERCA2: sarcoplasmic/endoplasmic reticulum Ca2+ ATPase. RyR2: ryanodine receptor 2. CACNβ2: calcium voltage-gated channel auxiliary subunit beta 2. CALM2: calmodulin 2. CAMK2D: calcium calmodulin dependent protein kinase II delta. (Adapted from KEGG pathway wire diagram-hsa04261)

3.3.5.1 SLC8A1

The SLC8A1 gene encodes for the sodium-calcium exchange (NCX) antiporter membrane protein which is widely distributed in the sarcolemma.[294] It is responsible for the counter transport of three Na^+ ions into the cell for one Ca^{2+} ion using the Na^+ gradient.[294] Calcium overload after excitation is primarily removed from the cardiomyocyte by NCX.[295]

3.3.5.2 TPM4

Tropomyosin 4 (TPM4) is one of 4 genes that encode for the protein tropomyosin.[296] Tropomyosin binds to actin filaments and plays an important role in calcium-dependent muscle contraction by forming the tropomyosin-troponin complex. However, TPM4 isoform expression in the human heart is low, and the role of this specific isoform in calcium-dependent contractility is unclear.[297]

3.3.5.3 ATF2

Activating transcription factor 2 shares homology with CREB and is also activated by cAMP-dependent pathways.[298]

3.3.5.4 CACNB2

L-type voltage gated calcium channels in the heart consist of an α pore subunit and an axillary β unit.[299] The predominant gene that encodes for the β unit in mammalian hearts is the

CACNB2 (calcium voltage-gated channel auxiliary subunit Beta 2). It enhances calcium current via phosphorylation.[300]

3.3.5.5 CREB5

cAMP response element body protein (CREB) is a nuclear transcription factor that is activated by cAMP-dependent pathways such as protein kinase A.[298]

3.3.5.6 ADCY1 and ADCY3

Adenylate cyclase type 1 and type 3 are two of the nine known isoforms of the membrane-associated adenylate cyclase enzyme.[301] In the cardiomyocyte, adenylate cyclase production is coupled to G-protein coupled receptors (i.e. β1/β2 adrenoreceptors). They catalyse the formation of cyclic adenosine monophosphate (cAMP), a universal secondary messenger, from ATP. cAMP then acts on effectors: protein kinase A (PKA), exchange protein activated by cAMP (EPAC), hyperpolarization-activated cyclic nucleotide–gated (HCN) channels, cyclic nucleotide-regulated ion channels, and phosphodiesterases.[302] ADCY1 modulates the funny (I*f)* current in pacemaker cells.[303]

3.3.5.7 AGTR1 and AGTR2

Angiotensin II type 1 (AGTR1) and type 2 (AGTR1) receptors found in the myocardium are G-protein coupled receptors. Stimulation of Gq-coupled AGTR1, via angiotensin II, is responsible for increased calcium mobilisation and SERCA activation via secondary messengers phospholipase C and inositol triphosphate.[304] Chronic stimulation can lead to

hypertrophy, fibrosis and inflammation.[305] The signalling mechanisms of AGTR2 remain controversial but are thought to oppose the effects of AGTR1.[306]

3.3.5.8 ATP2B3

The ATPase plasma membrane Ca^{2+} transporting protein is a plasma membrane calcium ATPase: its function is to remove Ca^{2+} from the cardiomyocyte.[307]

3.3.5.9 CALM1 AND CALM2

CALM1 and CALM2 genes encode the same calmodulin protein. Calmodulin is a calcium sensing and signalling molecule that can affect over 300 target proteins.[308] It has been shown to regulate ion channels: the L-type Ca^{2+}channel, the ryanodine receptor, and the IP3 receptor.[309] Therefore its signalling function plays an important role in action potential generation, calcium induced calcium release, and modulating the ryanodine receptor.

3.3.5.10 CAMKB and CAM2KD

Calmodulin Kinase II has 4 gene isoforms (α, β, δ, γ). The predominant isoform in the heart is CAM2KD. The protein is activated by an increase in intracellular calcium, and regulates key proteins in excitation and contraction coupling within the cardiomyocyte.[310] These include L-type receptors, ryanodine receptors and the regulation of calcium reuptake from the cytoplasm by SERCA, via its inhibitory effects on phospholabin (PLB). PLB tonically inhibits SERCA. Phosphorylation by CAMK2 removes the inhibitory effect, allowing SERCA to remove calcium to allow cardiomyocyte relaxation.[311]

3.3.5.11 CREB32

cAMP response element body protein (CREB) is a nuclear transcription factor that is activated by cAMP and is induced at translational level during endoreticular stress.[312]

3.3.5.12 GNAQ

G protein subunit α encodes for the effector subunit of the Gq heterotrimeric coupled G protein. Gq coupled receptors for the cardiomyocyte include: α adrenergic (1 and 2) receptors, muscarinic receptors (M1, M3 and M5), endothelial receptors, histamine, and vasopressin.[313]

3.3.5.13 PI3KR1

Phosphoinositide 3-kinase regulatory subunits are activated by the βγ subunit of the G-protein coupled β2 adrenoceptors,[314] leading to recruitment and activation of Akt/protein kinase B. Akt/protein kinase B regulates myocardial contractility and contractile strength.[315]

3.3.5.14 PPP1CB, PPP2CA, PPP2CB, PPP2R2D, PPP2R3A, PPP2R5A, PPP2R5E

Protein phosphatases consist of structural, catalytic and regulatory subunits. Protein phosphatase 1 (PP1) catalytic subunit is encoded by 3 genes: PPP1CA, **PPP1CB** and PPP1CC. Protein phosphatase 2 (PP2A) consists of a catalytic C subunit (**PPP2CA**, **PPP2CB**), scaffold A subunit, and a regulatory B subunit (PPP2R2A, PPP2R2B, PPP2R2C, **PPP2R2D**, **PPP2R5A**, PPP2R5B, PPP2R2C, PPP2R5D, PPP2R5E, **PPP2R3A**, PPP2R3B, PPP2R3C).[316]

The literature can be confusing because the isoforms for the regulatory units have alternative names. For example, **PPP2R5A's** alternative name in the literature is B56α.[317]

Activation of the actin- myosin contractile apparatus is dependent on the dephosphorylation of the inhibitory contractile protein TnI. PP1 preferentially dephosphorylates TnI in response to a rise in intracellular calcium.[318]

3.3.5.15 PRKACB

PRKACB encodes for the catalytic subunit Cβ of protein kinase A. The catalytic subunit phosphorylates key substrates for excitation-contraction coupling: calcium ion channels, RyR, PLB and TnI. Adrenergic stimulation of β adrenergic G protein coupled receptors (Gs) causes its alpha-GTP complex to dissociate from the receptor. The alpha subunit then stimulates the production of adenylate cyclase to increase the levels of cAMP from ATP. Increased cAMP levels then increase the phosphorylation activity of protein kinase A.[6]

Inotropic effects are mediated by the phosphorylation of ion channel increasing the inward calcium current and the release of Ca^{2+} from the SR. Lusitropic effects are mediated by the phosphorylation of PLB and TnI.[319]

3.3.5.16 TPM3

There are 4 isoforms of the Tropomyosin protein (1-4). TPM3 encodes for Tropomyosin 3. Tropomyosin 1 and 2 are predominantly found in the heart and TPM 3 is found in striated

muscle.[296] Transgenic mice expressing TPM 3 in the heart showed reduced myofilament Ca^{2+} sensitivity.[320]

3.4 Discussion

The principle finding of this study was that microRNA expression in patients with PMI was independent of troponin concentrations, suggesting that, in this cohort of patients, the microRNA represent a generalised stress/injury response to surgery, rather than a Type II myocardial infarction. Cardiac-specific microRNA were isolated from serum samples taken from matched patients before and after noncardiac surgery. This approach allowed changes in microRNA expression after surgery to be attributed to physiological/pathophysiological processes occurring during surgery. Moreover, all patients before surgery were "PMI free" with TnI levels <0.04. The experimental design took into consideration the many methodological limitations of previous studies isolating and measuring microRNA in acute coronary syndrome. Stable endogenous reference controls were selected from the same experimental conditions to reduce biological variation, and robust quality control analysis was performed to reduce technical variation.

Main findings (Summarised in Figure 3.14):

- Expression levels for microRNAs hsa-miR-1-3p and hsa-miR-133a-3p, usually associated with acute myocardial ischaemia, increased after noncardiac surgery, independent of troponin elevation.

- Expression of hsa-miR-146a-5p decreased after surgery, independent of troponin elevation.

- MicroRNA hsa-miR-499a-5p and hsa-miR-208b-3p detection increased after noncardiac surgery in patients who had elevated troponin.

- Bioinformatic analyses identified signalling pathways associated with cellular stress: these involved adrenergic signalling in the cardiomyocyte, and proteins regulating cardiomyocyte calcium homeostasis.

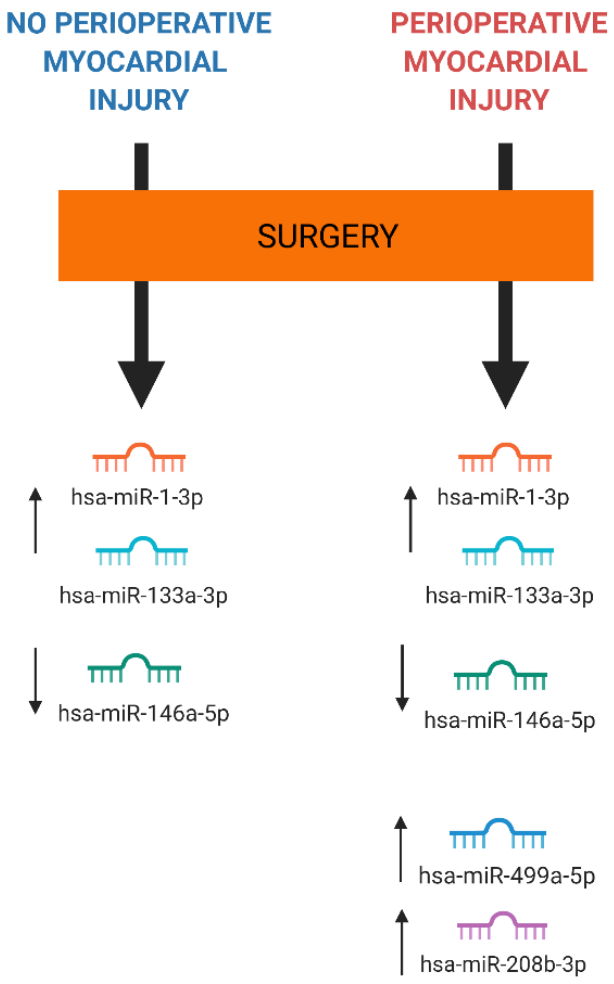

Figure 3.14 Cardiac-specific microRNA changes after noncardiac surgery

Schematic illustrating the change in microRNA expression before and after noncardiac surgery in patients who developed PMI and those that remained free of PMI.

3.4.1 hsa-miR-1-3p and hsa-miR-133a-3p

MicroRNA hsa-miR-1-3p and hsa-miR-133a-3p expression increased after noncardiac surgery irrespective of whether patients did or did not develop PMI (TnI >0.04 ng.ml-1). MicroRNA expression levels after noncardiac surgery did not correlate with troponin concentrations. In clinical studies investigating ACS, an ischaemic aetiology, both these microRNA are upregulated in patients with raised troponins compared to controls.[172] It has therefore been inferred that these microRNA are associated with acute myocardial ischaemia. However, the findings from my study population, in which increased expression has no relationship with increased troponin, suggest that this inference is too narrow in its assumption of ischaemic aetiology. My results instead suggest that the increased expression of these cardiac-specific microRNA represents a generalised physiological cardiac stress/injury response.

Hypothalamic-pituitary-adrenal axis activation during periods of surgical stress leads to the activation of the sympathetic nervous system with increased secretion of catecholamines from the adrenal medulla, and noradrenaline from the presynaptic nerve terminals. An increase in catecholamines and noradrenaline results in increased stimulation of cardiomyocyte β-adrenoreceptors which increase heart rate and contractility, and therefore cardiac output, to meet the metabolic demands of surgery.[80] The α subunit of G protein-coupled β-adrenoreceptors activates adenylate cyclase leading to an increase in cAMP levels. cAMP activates PKA signalling pathways to phosphorylate L-type calcium channels, phospholabin, Troponin I, RyR and NCX,[4, 321] resulting in calcium influx and increased contractility. An imbalance between the signalling pathways can lead to elevated cytosolic calcium levels, which impairs contractility.[322] In vivo and loss of function cardiomyocyte cell experiments have demonstrated that miR-133 targets β_1 adrenoreceptor signalling pathways at the level of

adenylate cyclase and PKA,[323] and that overexpression of miR-133 protects against β_1 adrenoreceptor dependent apoptosis.[324] In vivo rat experiments have shown that carvedilol, a beta antagonist, increases miR-133 expression, and is cardioprotective against oxidative stress.[325] This is mediated by downregulating pro-apoptotic genes Caspase-9[326] and Caspase-3.[325] Experimental models of remote ischaemic injury have shown that overexpression of miR-1 augments cardiac injury by downregulating protective anti-apoptotic genes, such as heat shock protein 60 and protein kinase C epsilon.[327] Overexpression of microRNA -1 has also been shown to induce apoptosis in response to H_2O_2.[135]

Further evidence that the increased expression of hsa-miR-1-3p and hsa-miR-133a-3p after surgery is not related to ischaemia, is the lack of correlation with TnI levels. In clinical studies that did show a correlation between these same cardiac microRNA and troponin concentrations in patients presenting with myocardial infarction, correlation was improved at higher troponin concentrations but inconsistent at lower troponin concentrations.[328] It has been suggested that, at these lower troponin concentrations, increased expression of hsa-miR-1-3p and hsa-miR-133a-3p represent cardiac pathology/myocardial injury rather than myocardial infarction.[144, 328]

3.4.2 hsa-miR-146a-5p

hsa-miR-146a-5p expression was decreased after surgery, both in patients who developed PMI and in those that remained free of PMI. In contrast, hsa-miR-146a-5p shows increased expression levels in ACS patients, compared to controls.[175] The PMI observed in patients after noncardiac surgery may be due to the loss of the anti-inflammatory function of hsa-miR-146a-5p. hsa-miR-146a-5p has been shown to have a role in the expression of IL-1 receptor associated kinase (IRAK1), TNF receptor-associated factor 6 (TRAF6) and nuclear factor

kappa b (NFkb);[329] it therefore has a potential regulatory role in suppressing the production of key pro-inflammatory cytokines which promote myocardial injury.[330]

hsa-miR-146a-5p has also been shown to have a role of downregulating Fos gene expression in cardiomyocytes.[143] Fos is a gene that regulates inflammation in response to cardiac stress.[125, 331] Ackland et al.[332] demonstrated that an elevated neutrophil:lymphocyte ratio, a marker of sub-clinical systemic inflammation, is associated with PMI. Therefore, reduced expression of hsa-miR-146a-5p indicates that the dysregulation of inflammation after surgery may contribute to myocardial injury.

3.4.3 hsa-miR-499-5p and hsa-miR-208b-3p

Both hsa-miR-499a-5p and hsa-miR-208b-3p were detected in higher proportions after surgery compared to before surgery in patients who developed PMI.

This is consistent with the literature, where these microRNA are commonly shown to have increased expression in ACS patients with myocardial injury. [176] [129, 175, 328, 333] However, in this cohort, expression levels for both microRNA did not correlate with troponin concentration (Figure 3.10).

In patients who develop acute myocardial infarction, the correlation between troponin concentration and miR-208b and miR-499 is "hockey stick" shaped, and Cq values correlate better at higher troponin concentrations.[328] The troponin concentrations in this study, although above the 99th centile, are at comparable levels to those where no correlation is observed between microRNA and troponin concentrations in patients with myocardial infarction.[157, 328,

[334] Both these microRNA are cardiac-specific, therefore detection at low levels of troponin may signify myocardial damage, rather than an underlying pathological process.

3.4.4 Pathway analyses

Pathway analysis of the microRNA:gene interactions for the microRNA that were upregulated or downregulated after surgery identified signalling pathways associated with cellular stress (i.e. proteins regulating cardiomyocyte calcium homeostasis), and with adrenergic signalling in the cardiomyocyte (Figure 3.13). The pathway analysis would therefore suggest that adrenergic activation in the cardiomyocyte, a common feature of the surgical stress response, is a factor driving PMI in this study cohort.

The four microRNA that were upregulated after surgery converged on the gene transcription target SLC8A1 (Figure 3.12), which encodes the Na^+/Ca^{2+} exchanger 1 (NCX) within the cardiomyocyte.[294] In the heart, the NCX plays a crucial role in calcium homeostasis and excitation-contraction coupling.[134] Under normal physiological conditions, NCX removes intracellular calcium after each heartbeat to ensure relaxation and restoration of calcium intracellular balance. This is achieved by the counter transport of 1 Ca^{2+} for 3 Na^+ using the energy of the Na^+ gradient.[294, 295]

Under certain pathophysiological conditions, the NCX can be inhibited or even go into reverse mode.[335] Hypoxia and ischaemia/reperfusion have been demonstrated to inhibit and/or reverse the NCX mechanism.[336, 337] Cardiomyocyte hypoxia leads to ATP depletion and intracellular acidosis. This in turn results in an increase in intracellular Na^+, driven by Na^+/K^+ ATPase inhibition; in addition, the acidosis drives the Na^+/H^+ antiporter. The increase in intracellular

sodium reduces or reverses the driving mechanism for NCX, leading to cardiomyocyte calcium overload.[337] An increase in intracellular calcium leads to cardiac injury mediated by excessive myofilament activation, mitochondrial dysfunction, and excessive activation of Ca^{2+}-activated intracellular proteases which destroy cellular structures.[338] Adaptively, an increase in NCX can be protective against these effects, as demonstrated by transgenic mice with overexpression of NCX that have preserved contractility in response to hypoxic conditions.[339]

Multiple catalytic and regulatory subunits for protein phosphatase 1 and protein phosphatase 2 were also identified by the pathway analysis (Figure 3.12). Protein phosphatases 1 and 2 account for 90% of dephosphorylation activity in the heart.[316] Reversible protein phosphorylation is essential for excitation-contraction coupling, calcium regulation, cell signalling, myofilament contraction, and membrane protein control (e.g. NCX). [317] The diversity of roles for the protein phosphatases within the cardiomyocyte is due to the number of combinations of the subunits.[317]

The PP2A B56α subunit is a confirmed gene target for miR-1.[161] Rat isolated cardiomyocytes with adenoviral-mediated overexpression of miR-1 show reduced expression of the B56α regulatory subunit. This in turn inhibits the dephosphorylation activity of PP2A of RyR2 and L-type Calcium channel. Consequently, there is hyperphosphorylation of the RyR2 and L-type Calcium channel by CAMKII, elevating intracellular calcium.[161]

In mouse cardiomyocyte models, the regulatory subunit B56α (PPP2R5A**)** has also been shown to have a role in modulating cardiomyocyte calcium signalling. Subunit overexpression models showed a decrease in PP2A activity, resulting in increased phosphorylation of RyR2;[340] whereas a loss of the B56α subunit attenuates the inotropic response to acute B-AR stimulation

with dobutamine (sympathetic stimulation).[341] PP2A phosphorylation of TnI also involves the regulatory subunit B56α; the degree of phosphorylation is mediated by β-adrenergic stimulation.[342]

3.4.5 Strengths and limitations of the study

The emphasis of this study was to probe the mechanisms underlying PMI: it was not a diagnostic or prognostic study. In the ACS literature evaluating microRNA, there is a high degree of heterogeneity in study design. In particular, there is variation in the comparator control group. The comparator groups are predominantly either healthy volunteers or patients with stable coronary disease.[172] The experimental design for this study, of isolating microRNA from serum samples from matched patients before and after noncardiac surgery, allowed microRNA function to be attributed specifically to the perioperative period and the postulation of an adrenergic stress injury hypothesis.

In addition to the strength of the experimental design, the other main strength of this study was the selection of microRNA used to normalise the calibrated Cq values. These were selected from a pool of 176 microRNA that underwent the same experimental conditions used in the main experiment and were validated in the main study (Appendix D**)**. A further strength of this work is the utilisation of spike-in microRNA at isolation, reverse transcription and the PCR stage, which allowed the identification of outliers and minimised technical variation within the experiments. In addition, amplification efficiencies were reported in keeping with the MIQE guidelines.[252] The low efficiency values for hsa-miR-208b-3p (0.4) and hsa-miR499a-5p (0.4) are consistent, given the low detection rates for both.[252] For the microRNA that were detected in all samples, the Cq values were consistent with values reported in the literature.[129, 328]

The low detection rates for hsa-miR-208b-3p (52%) and hsa-miR499a-5p (60%) are consistent with low detection rates reported in the literature: this is due to the low levels of both in the plasma/serum.[343] Detection rates in samples reported in the literature range between 14-57%

for both microRNA.[175, 333] In fact, the detection threshold in these clinical studies use a much higher threshold of Cq>50, compared to Cq>37, as utilised in this study.[333] The low levels may also be due to the timing of sample collection relative to developing PMI, as lower levels in plasma or serum after ACS have been reported in relation to when the samples were taken.[130]

The lack of correlation between microRNA expression and troponin concentration may also be due to temporal factors. MicroRNA were isolated and expression levels measured from samples taken at the same time as the troponin sample. Schulte et al.[328] have demonstrated that the correlation of troponin concentration with microRNA expression improves at higher troponin concentrations. It is therefore possible that the correlation may have improved had microRNA been isolated from samples taken at the time of peak troponin level after noncardiac surgery.

A potential disadvantage of using a nested case control study in a study population with a lower incidence of PMI was the risk of having insufficient cases or controls to power the study. The incidence of PMI in the UK METS cohort (28/620 = 4.5%) was lower than 25% quoted elsewhere in the thesis for the incidence of PMI. However, the power calculation demonstrates the number of PMI and controls obtained from the UK METS cohort was adequate to power the study.

A candidate driven approach to microRNA studies can lead to biases in repeatedly reporting popular microRNA.[172] The circulating serum microRNA utilised in this study were selected due to their acceptance in the literature as established signatures for ACS and myocardial injury. A selection bias for these microRNA cannot be excluded in this study. In addition, the limited nature of this selection cannot exclude the possibility that other microRNA may be

involved in PMI. However, this selection sufficed for the aim of this exploratory study: to investigate whether established ischaemic-related microRNA are present in the context of troponin elevation after noncardiac surgery.

However, in samples taken from the prospective XMINS study, next generation microRNA sequencing was used to compare plasma samples of patients with troponin elevation to those with no elevation after surgery. 345 microRNA were identified between the groups. Consistent with the results in this chapter, bioinformatic analysis of the differentially expressed sequenced microRNA identified signalling pathways related to cardiomyocyte calcium signalling.[344] In this same next generation study, the expression of microRNA hsa-miR-208b-3p, hsa-miR499a-5p, hsa-miR-146a-5p, hsa-miR-1-3p and hsa-miR-133a-3p after surgery were compared between patients who developed PMI versus those who remained free of PMI after surgery. After taking account multiple testing no significant difference was found between the groups for these microRNA[344]. Due to the high running costs of NGS, comparisons were not made before and after surgery between groups and therefore this cannot be considered a true validation study.

Finally, it should be cautioned that microRNA:gene interactions and subsequent pathway analysis are only in silico predictions, and therefore their interactions require further experimental validation.

3.4.6 Conclusion

Levels of circulating microRNA that are elevated in ACS also increase after noncardiac surgery; however, this pattern does not appear to be confined to only patients with PMI (as

defined by a TnI >99th centile). This would suggest that the changes in microRNA expression occur due to (perioperative) adrenergic stress rather than an exclusively myocardial ischaemic event.

Chapter 4
Cardiac parasympathetic dysfunction and perioperative myocardial injury

Results in this chapter have been published in the British Journal of Anaesthesia (2019) 123(6), 758-767

4.1 Background

The results in Chapter 3 suggest that a generalised cardiac stress response occurs during noncardiac surgery in all patients, independent of troponin rise. However, this does not explain why some patients do develop a raised troponin after surgery and why they have an increased associated risk of morbidity and mortality. A plausible explanation is that, whilst all patients experience a generalised cardiac stress response, troponin release only occurs in patients who lack cardioprotective compensatory mechanisms to cope with the physiological stress of surgery. The vagus nerve has a chronotropic, dromotropic and inotropic effect on the heart[4] and is part of the afferent and efferent limbs of the cholinergic anti-inflammatory reflex.[47] Clinical observational studies have demonstrated an association between cardiac vagal dysfunction and PMI. In the METS study (described in General Methods 2.2), delayed heart rate recovery (HRR) before surgery, a measure of cardiac vagal activity,[216] was shown to be independently associated with myocardial injury after noncardiac surgery.[217] Similarly, resting heart rate before surgery, which is chiefly determined by cardiac vagal tone, is independently associated with myocardial injury after surgery.[345, 346] Cardiac vagal impairment contributes to baroreflex dysfunction,[347] and when demonstrated to be present in patients before surgery, has been shown to predispose patients to haemodynamic compromise and morbidity after

noncardiac surgery.[348] In vivo experimental studies have demonstrated that the stimulation of the vagus nerve confers anti-inflammatory properties[238] through its parasympathetic activity by mediating the cholinergic anti-inflammatory reflex.[349] Stimulation of the vagus has also been shown to maintain normal calcium handling[350] after myocardial ischaemia by restoring function of SERCA2a and NCX.

Taken together, these studies suggest that patients with impaired cardiac vagal activity are at particular risk of sustaining PMI. A loss of cardiac vagal activity has been previously demonstrated after noncardiac surgery.[204, 206] An increase in cardiac vagal activity after elective orthopaedic surgery has been shown to be associated with reduced morbidity after surgery.[206]

However, what has not been previously demonstrated is whether the loss of cardiac vagal activity, and its cardioprotective properties, contributes to developing PMI.

4.1.1 Hypothesis

Reduced efferent cardiac vagal activity after noncardiac surgery, as measured by heart rate variability, is associated with PMI and noncardiac morbidity.

4.1.2 Aims

- Use heart rate variability measures to quantify cardiac vagal activity before and after elective noncardiac surgery.
- Examine if serial static measures of cardiac vagal activity are associated with PMI and noncardiac morbidity.

4.2 Methods

4.2.1 Study design and participants

The study design and participants have been described in General Methods Section 2.3.

4.2.2 Heart rate recording

Three lead electrocardiogram (ECG) recordings were captured using Lifecard CF digital Holter monitors (Spacelabs Healthcare, Hertford, UK), with a sampling rate of 1024Hz.

4.2.3 Assessment of cardiac autonomic activity

R-R intervals from ECG data were analysed using Kubios HRV Premium software Version 3.1.0 (Kubios, Kuopio, Finland).[272] Holter data cleaning and analysis were undertaken blinded to troponin levels, perioperative data and outcomes. Heart rate variability analysis was calculated for 5 minute segments of ECG recordings according to taskforce guidelines.[182] Serial measures of cardiac autonomic activity were quantified using established heart rate variability measures of cardiac autonomic activity. These were time domain and frequency domain analyses. Further detailed methodology is outlined in the General Methods Section 2.7.

4.2.4 Experimental protocol

The protocol for the study is outlined in Figure 4.1. On the morning of surgery, continuous three lead electrocardiogram recordings were made in a quiet, controlled, clinical environment at room temperature. After 10 minutes recording in the supine position, patients were positioned to a 45-degree head up position using an electronically adjustable hospital bed (Model 2232, ArjoHuntleigh, Malmo, Sweden). A further 10 minute recording was then made in the 45-degree head up position. Blood pressure and respiratory rate observations were made at the beginning of each 10 minute recording. The protocol was then repeated 24h and 48h after surgery at the same time of day. The serial measurement of ECGs on patients allowed each patient to act as their own control in the analysis of HRV. Blood samples were taken on the day of surgery, 24h and 48 after surgery, after completion of the protocol. Whole blood was processed as described in General Methods Section 2.2.4.

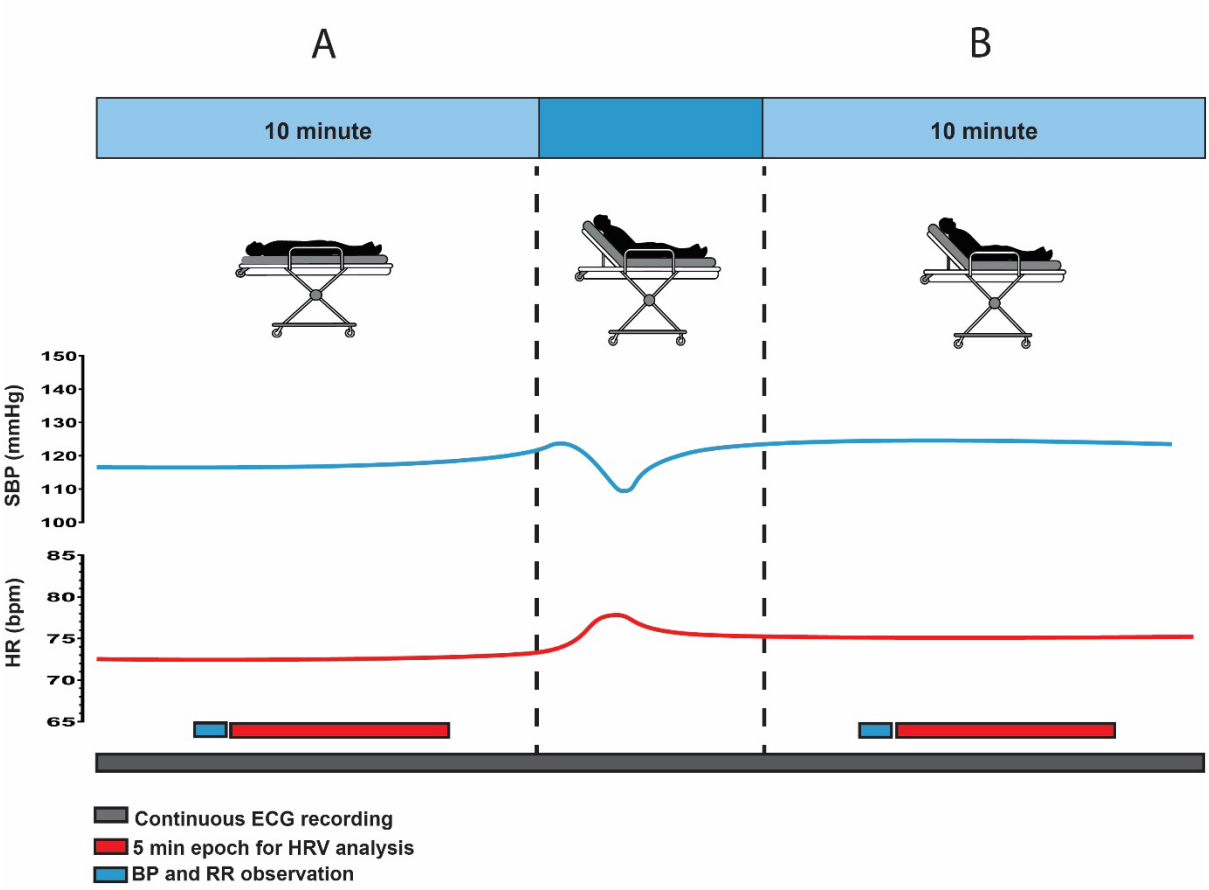

Figure 4.1 :Experimental protocol

(A) 10 minute supine position and (B) 10 minute 45-degree head-up position. HR (red) and systolic BP (SBP; blue) predicted response with an orthostatic challenge. HRV, heart rate variability; RR, respiratory rate.

4.2.5 Perioperative management

I had no involvement in the perioperative decision making or the postoperative care of the patients recruited into the study. The patients' anaesthetic and surgical teams provided perioperative and postoperative care, in accordance with the usual standard of care for the hospital. Admission to the critical care unit was at the discretion of the anaesthetic and surgical team. Postoperative management was conducted according to local enhanced recovery clinical guidelines. Free fluids or light diet was permitted on the day of surgery if tolerated. There was no protocolised postoperative fluid administration regime. Early mobilisation was encouraged in parallel with routine physiotherapy and acute pain reviews as per hospital guidelines. All clinicians were blinded to Holter data and outcome data.

4.2.6 Primary outcome

The primary outcome of the study was perioperative myocardial injury, as defined by plasma high sensitivity troponin level (HsTnT) $\geq 15 ng.L^{-1}$ within two days of surgery. The cut off value is above the limit for the normal range for the Troponin-T high sensitivity Cobas® assay.[351] The cut off value for the Cobas® assay was the same for male and female patients. Plasma troponin levels were batch analysed by an independent laboratory (The Doctors Laboratory, United Kingdom) after patients were discharged from the hospital. Investigators, patients and attending clinical staff were masked to troponin data, which were only revealed at the end of the study.

4.2.7 Secondary outcomes

The secondary outcome was all-cause postoperative morbidity within 7 days after surgery, assessed using the Post Operative Morbidity Survey[352] (as described in General Methods Section 2.5), which was collected prospectively on day 3, 5 and 7 after surgery. The time to become morbidity-free and the length of hospital stay were also calculated.

4.2.8 Explanatory variables

The relationships between cardiac autonomic activity and primary and secondary outcomes were examined using heart rate variability measures outlined in General Methods Section 2.7.

1. *Time domain measures:*

- The square root of the mean of the sum of the squares of the successive differences between adjacent beat-to beat intervals (RMSSD) ms
- Standard deviation of the N-N interval (SDNN) ms

2. *Frequency domain measures:*

- High frequency (0.15-0.4Hz)
- Low frequency (0.04-0.15Hz)

Comparisons with population HRV values are challenging due to the inconsistency of HRV measurement acquisition.[212] When using raw RMSSD values it has been previously demonstrated that values below what is considered to be a population norm (RMSSD <19ms), taken from a surgical cohort before surgery, are associated with delayed heart rate recovery

before surgery, a marker of cardiac vagal dysfunction.[214] To compare the current study with population normal values (19-75ms),[211] the proportion of patients with RMSSD <19ms was calculated. Log transformation of these measures was performed to transform skewed data to approximately conform to normality.

4.2.9 Statistical analysis

Patients' characteristics were stratified by the primary outcome (PMI). Continuous longitudinal data were analysed using a mixed repeated measures model, as outlined in Methods Section 2.9.2. The levels examined were: perioperative myocardial injury (hsTnT $\geq$15ng.L^{-1} and hsTnT $\leq$14ng.L^{-1}); day relating to surgery (day of surgery, 24h after surgery and 48h after surgery); and body position (supine and 45-degrees sitting). Body position was included in the model because autonomic influences for body posture have been shown to affect HRV measures.[271] Individual comparisons between groups were calculated using post hoc Bonferroni tests. Length of hospital stay and time to become morbidity free were analysed using Kaplan-Meier estimates. p <0.05 was considered statistically significant. All statistical analyses were undertaken using NCSS 12 (Kaysville, UT, USA).

4.2.10 Sensitivity analysis

Heart rate variability measures may be influenced by regional anaesthesia technique delivered for noncardiac surgery. [353-355] This was addressed by repeating the primary analysis for high frequency heart rate variability measurements and excluding patients who had received only a general anaesthetic.

4.2.11 Sample size calculation

A comparison of two proportions was utilised to calculate a sample size to adequately detect parasympathetic dysfunction from heart rate variability measures in patients who developed PMI versus those who did not develop PMI.[356] The hypothesis that reduced efferent cardiac vagal activity after noncardiac surgery, as measured by heart rate variability, is associated with PMI and noncardiac morbidity had not been tested before, therefore assumptions and proportions from previous related work would need to be utilised for the calculation. Firstly, Ackland et al. have previously demonstrated that cardiac vagal dysfunction, as defined by abnormal heart rate recovery ≤12 beats minute^{-1}, is present in ~35% of surgical patients.[214] Perioperative myocardial injury occurs in ~25% of noncardiac surgical patients.[357] In METS, a 50% increase in myocardial injury was observed in patients with preoperative vagal dysfunction (OR:1.54 (1.11-2.13); p=0.009).[217] Using these assumptions it was calculated that ≥152 patients would be required to detect differences in ECG-derived measures of parasympathetic dysfunction, accounting for α= 0.05 and 1-β=0.1.[356] Allowing for ~15% dropout rate, and/or ~25% incomplete ECG data,[358] it was estimated that at least 210 patients would be required.

4.3 Results

Patient characteristics

210 patients were recruited into the study between 5th October 2016 and 14th January 2019 (Figure 4.2). Data was analysed from 189 participants, of whom 174/189 (92.1%) had a RCRI score <2 (Table 4.1). Age ($p<0.001$) and duration of surgery ($p<0.001$) was higher in patients who developed PMI. There was a greater proportion of male patients ($p =0.004$) and patients with active cancer ($p = 0.049$) who developed PMI after surgery. Resting respiratory rate, SBP and DBP measures were similar before surgery. Respiratory rate increased similarly in both groups ($p<0.001$), whereas SBP and DBP decreased similarly 48h after surgery ($p<0.001$) (Figure 4.3).

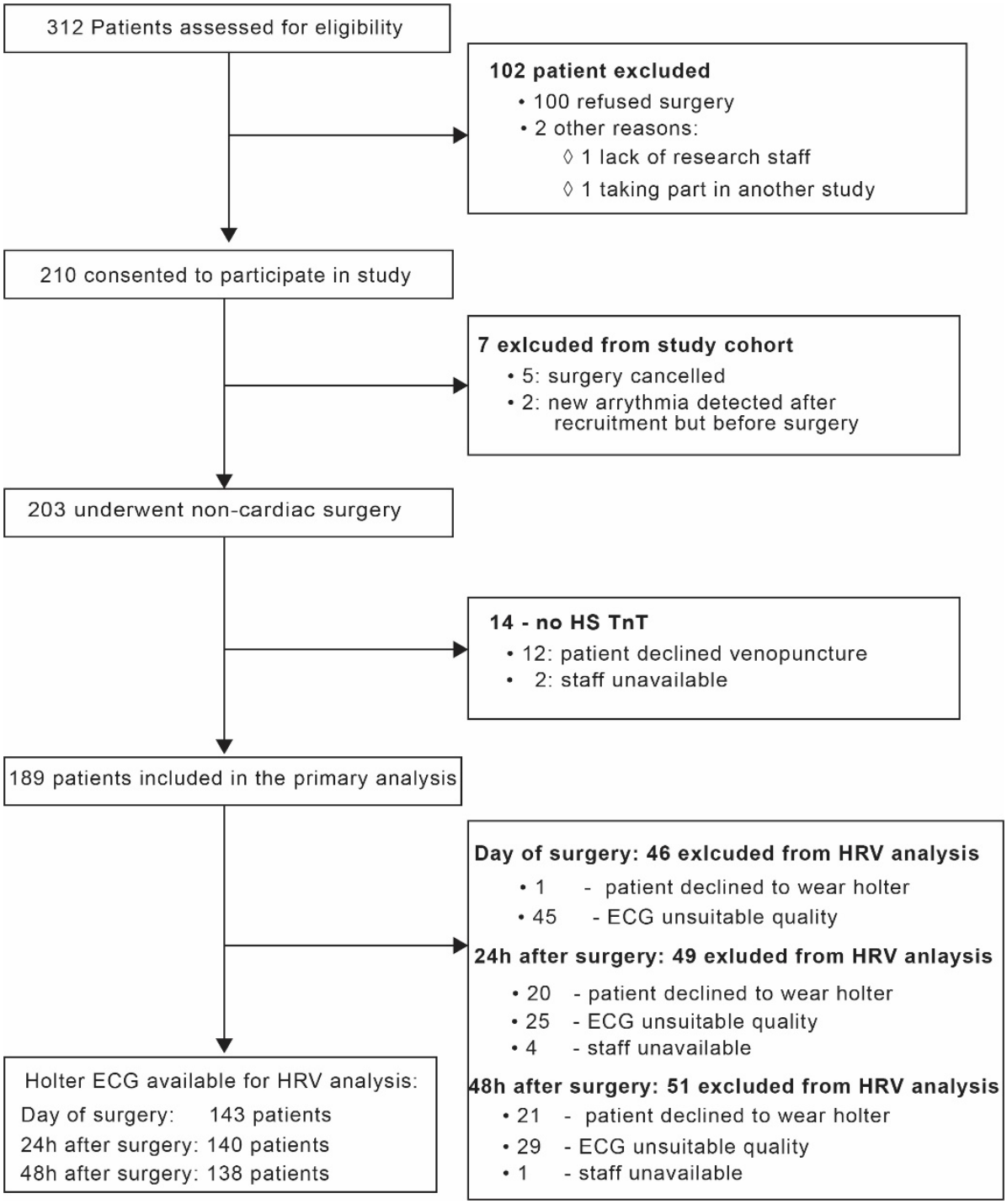

Figure 4.2 Consolidated Standards of Reporting Trials diagram showing patients included in the analysis

HRV, Heart Rate variability; HsTnT, high sensitivity troponin T assay.

Table 4.1 Patient characteristics

Data is presented as mean with standard deviations (SD) for parametric data and as median (25th-75th interquartile range) for non-parametric data. Frequencies are presented with percentages (%). Age is rounded to the nearest year. CKD: chronic kidney disease. Stage is defined as per KDIGO recommendations.[359] RCRI: Revised cardiac risk index score. ACE-I: angiotensin converting enzyme inhibitor. ARB: angiotensin receptor blocker. Intraoperative hypotension is defined as ≥1 intraoperative episode of systolic blood pressure <90mmHg after induction of anaesthesia. Other units as indicated. Statistical analysis using Student's unpaired t-test for continuous data and the χ^2 test for categorical data.

	Whole cohort n =189	hsTnT ≤14ng L^{-1} n= 141	hsTnT ≥15ng L^{-1} n= 48	p-value
Troponin ng L^{-1}	9 (15-22)	7 (5-11)	21 (17-23)	
Clinical Characteristics				
Age (yr)	67 (60-76)	66 (58-72)	74 (66-78)	<0.001
Male sex (n;%)	81 (42.9%)	52 (36.9%)	29 (60.4%)	0.004
Body Mass Index (kg m^{-2})	27.5 (24.4-31.3)	28.0(24.6-31.4)	26.1 (24.1-31.2)	0.131
CKD Stage ≥2 (n;%)	110 (58.2%)	80 (57.6%)	30 (62.5%)	0.485
Haemoglobin (g L^{-1})	13.1 (11.7-14.1)	13.2 (12.2-14.2)	12.2 (11.1-13.8)	0.054
Co-morbidities (n; %)				
RCRI ≥2	15 (7.9%)	8 (5.8%)	7 (14.6%)	0.049
Chronic obstructive airway disease	15 (7.9%)	12 (8.5%)	3 (6.3%)	0.617
Asthma	29 (15.3%)	21 (14.9%)	8 (16.7%)	0.769
Ischaemic heart disease	11 (5.8%)	6 (4.3%)	5 (10.4%)	0.115
Diabetes mellitus	41 (21.7%)	32(22.7%)	9 (18.8%)	0.567
Congestive heart failure	2 (1.1%)	1 (0.7%)	1 (2.1%)	0.422
Cerebral vascular disease	11 (5.8%)	6 (4.3%)	5 (10.4%)	0.115
Peripheral vascular disease	7 (3.7%)	5 (3.6%)	2 (4.2%)	0.844
Hypertension	104 (55.0%)	74 (52.5%)	30 (62.5%)	0.228
Active cancer	106 (56.1%)	73 (51.8%)	33 (68.8%)	0.041
At least one cardiovascular medication (n;%)	92 (48.7%)	66 (46.8%)	26 (54.2%)	0.378
Beta blocker	21 (11.1%)	12 (8.5%)	9 (18.8%)	
Calcium channel blocker	49 (25.9%)	35 (24.82%)	14 (29.2%)	
Doxazosin	9 (4.8%)	5 (3.6%)	4 (8.3%)	
ARB/ACE-I	53 (28.0%)	37 (26.2%)	16 (33.3%)	
Type of surgery (n; %)				
Gastrointestinal	95 (50.3%)	66 (46.8%)	29 (60.4%)	0.103
Urology/gynaecological	51 (29.9%)	41 (29.1%)	10 (20.8%)	0.266
Head/neck/ear, nose, throat	2 (1.1%)	2 (1.4%)	0 (0.0%)	0.407
Orthopaedic	41 (21.7%)	32 (22.7%)	9 (18.8%)	0.567
Type of anaesthesia (n; %)				
General	56 (29.6%)	47 (33.3%)	9 (18.8 %)	0.056
General + epidural	90 (47.6%)	62 (44.0%)	28 (58.3%)	0.085
General anaesthesia + spinal	30 (15.9%)	24 (17.0%)	6 (12.5%)	0.717
Neuroaxial only	13 (6.9%)	8 (5.7%)	5 (10.4%)	0.154
Intraoperative events				
Duration of surgery (minutes)	296 (135-300)	184 (129-260)	255 (169-383)	0.001
Intraoperative hypotension (n; %)	114 (60.3%)	84 (59.6%)	30 (62.5%)	0.721

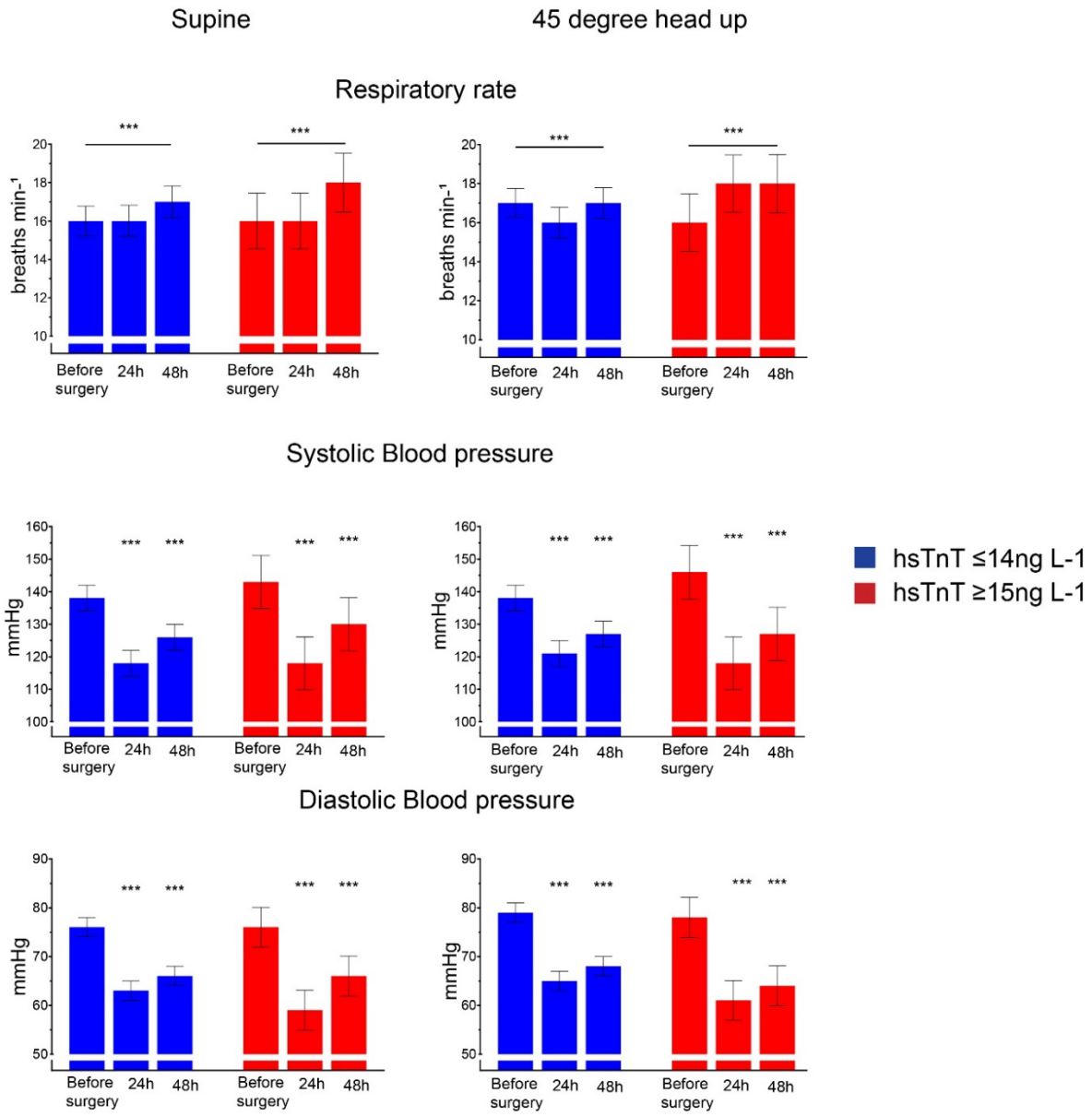

Figure 4.3 Serial resting respiratory and haemodynamic variables

Data are presented as mean values with 95% confidence interval. P-value refers to before surgery compared to 24h after surgery, and before surgery vs 48h after surgery (analysed by mixed-model repeated measures and Bonferroni test). ***P<0.001. No differences were observed between the two groups before and after surgery.

4.3.1 Primary outcome: perioperative myocardial injury

48 out of 189 (25%) patients sustained perioperative myocardial injury within 48h after surgery. Median troponin values were 21ng L^{-1} (IQR:17-23ng.L^{-1}) in patients with perioperative myocardial injury, compared with a median of 7 ng L^{-1} [IQR: 5-11 ng.L^{-1}], p <0.001 in patients without perioperative myocardial injury (plasma troponin remained lower than the 99th centile value).

4.3.2 Secondary outcome: postoperative morbidity.

Patients who developed perioperative myocardial injury after surgery sustained more POMS-defined morbidity (41/48 [85.4%]), compared with those who did not develop perioperative myocardial injury (91/141 [64.5%]; OR: 3.41[95% CI:1.29-9.09]; p=0.007).

27 out of 48 (56%) patients with raised troponin after surgery had a higher proportion of cardiovascular associated POMS-defined morbidity within 7 days after surgery, compared to 29 out of 141 (20.5%) patients who had no troponin elevation (OR: 4.88 [95% CI:2.32-10.62]; p<0.001) (Table 4.2). Patients who developed PMI also took longer to become free from post-surgery morbidity (Figure 4.4). There were no myocardial infarctions or acute coronary syndrome events reported after surgery for any of the patients with a recorded raised troponin. PMI was associated with prolonged length of stay: the median (IQR) length of stay for patients who developed PMI was 9 (6-20) compared to 6 (4-10) in patients who remained free of PMI (Hazard ratio: 1.8 (95% CI:1.34–2.41); P <0.001; log-rank test) (Figure 4.5).

Table 4.2 POMS defined morbidity within 7 days after surgery

Morbidity defined by Postoperative Morbidity Survey (POMS), compared between patients with HsTnT ≤14ng L^{-1} versus HsTnT ≥15ng L^{-1}. Data are presented as n (%). All comparisons made by two-tailed Fisher's exact test. OR; odds ratio; CI; confidence interval.

	HsTnT ≤14ng.L^{-1} *n* = 141	HsTnT ≥15ng.L^{-1} *n* = 48	OR (95% CI)	P-value
Any POMS, n (%)	91 (64)	41 (85)	3.05 (1.29-9.09)	0.007
Infection, n (%)	40 (28)	26 (54)	2.95 (1.44-6.09)	0.001
Pulmonary, n (%)	61 (43)	29 (60)	1.98 (0.98-4.15)	0.04
Cardiovascular, n (%)	29 (21)	27 (56)	4.88 (2.32-10.62)	<0.001
Renal, n (%)	62 (44)	33 (69)	2.99 (1.46-6.56)	0.001
Gastrointestinal, n (%)	56 (40)	25 (52)	1.78 (0.88-3.63)	0.08
Wound, n (%)	3 (2)	1 (23)	1.25 (0.02-12.53)	0.98
Neurological, n (%)	7 (5)	11 (23)	5.79 (1.94-19.35)	<0.001
Haematology, n (%)	3 (2)	8 (17)	8.31 (2.06-55.49)	<0.001
Pain, n (%)	56 (40)	28 (58)	2.10 (1.04-4.38)	0.025

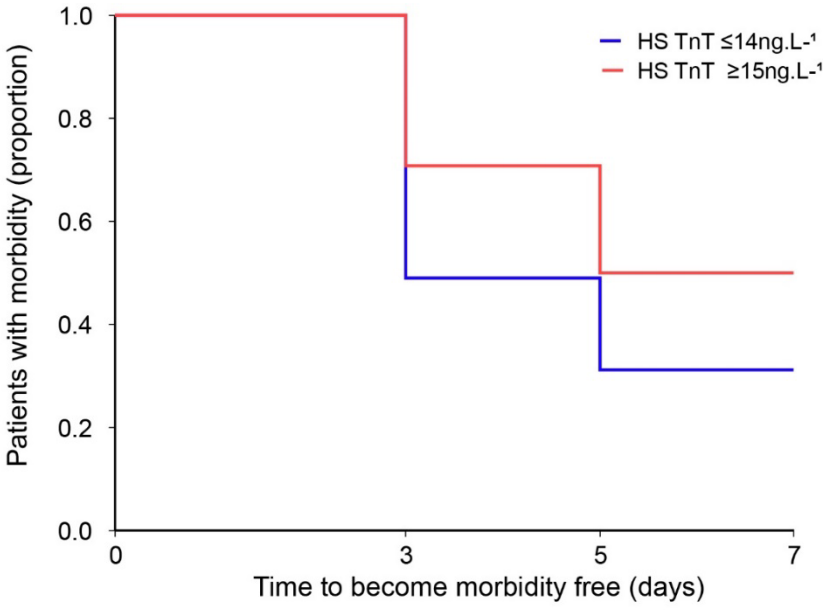

Figure 4.4 Time to become morbidity free within 7 days of surgery, in relation to developing PMI after surgery

Kaplan-Meier plot showing the effect of PMI status on time to become morbidity free (unadjusted hazard ratio 1.28 (95%CI 0.94-1.75); p = 0.1373; log rank test.

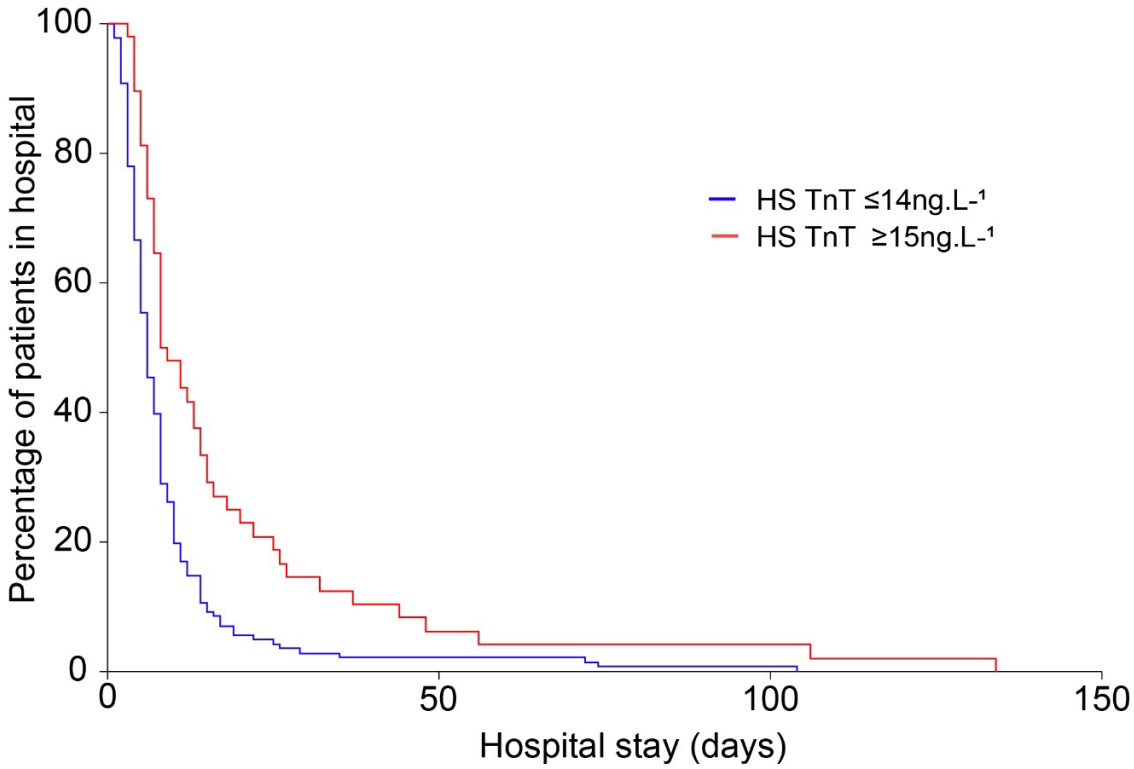

Figure 4.5 Perioperative myocardial injury and length of stay

Kaplan-Meier plots of hospital length of stay in patients with and without PMI. Hazard ratio: 1.8 (95% CI:1.34–2.41); p <0.001; log-rank test.

4.3.3 Technical features of autonomic measures

There was no difference between time of day for the ECG recordings before, 24h and 48h after surgery (Table 4.3). 99 of the 583 patient ECGs analysed (17%) had >5% artefact detected by the Kubios software and were excluded from further analysis (Figure 4.2). 45 out of the 189 patients (23.5%) included in the primary analysis had no artefact detected for all their ECG recordings. For patients who had less than <5% artefact detected, the mean (95%CI) artefact was 0.49% (0.40-0.60%).

Table 4.3 Time of day for ECG recordings

The start time of the ECG recordings was categorised to morning (*07:00-12:00*) or afternoon (*12:01-17:00*).

	Time of Day for ECG recording	
	07:00-12:00	*12:01-17:00*
Day of surgery (n =143)	94 (65.7%)	49 (34.3%)
24h after surgery (n =140)	100 (71.4%)	40 (28.5%)
48h after surgery (n =138)	93 (67.4%)	45 (32.6%)

4.3.4 Explanatory autonomic measures for perioperative myocardial injury

4.3.4.1 Time domain measures.

Resting heart rate was similar in both groups before surgery and was increased 48h after surgery ($p<0.001$; Figure 4.6). LnRMSSD and LnSDNN in the supine and head up position declined 24h after surgery in patients who developed perioperative myocardial injury ($p<0.01$) (Figure 4.7 and Figure 4.8). 62 out of 143 (43%) patients with suitable ECG recordings had RMSSD <19ms before surgery (Appendix H). A full report of the mixed model analysis can be found in Appendix I.

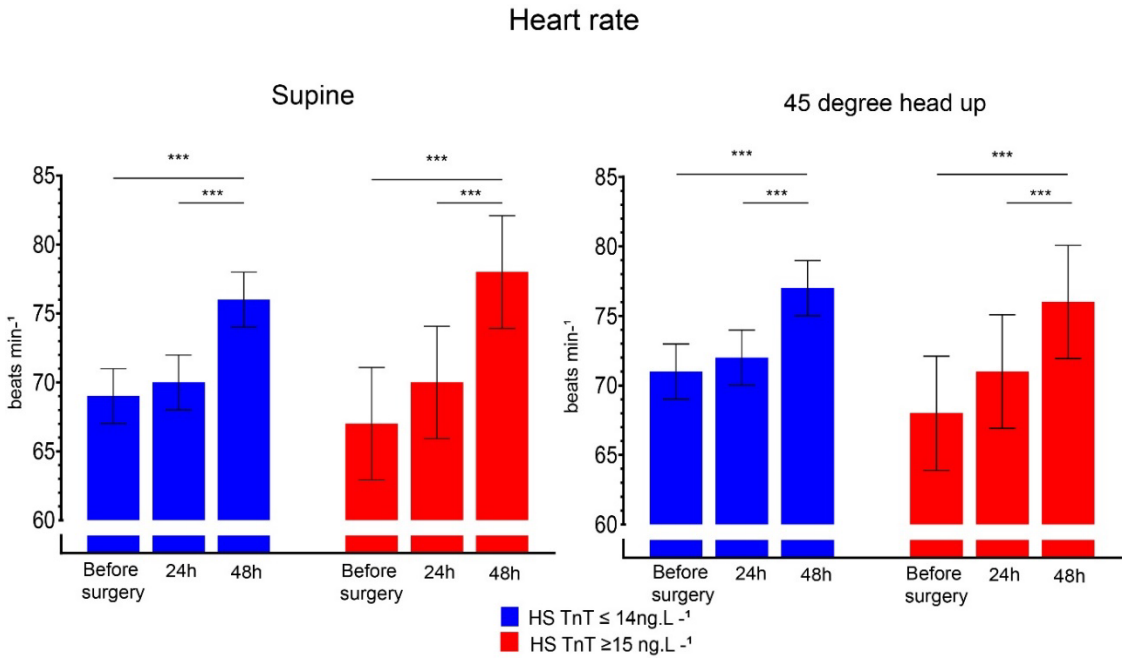

Figure 4.6 Serial resting heart rate measurements in the supine and 45 degree head up positions

Data is presented as mean values with 95% confidence interval. P-value refers to before surgery vs 48 h after surgery, and 24h versus 48h after surgery (analysed by mixed-model repeated measures and Bonferroni test). ***P<0.001. No differences were observed between the two groups before and after surgery.

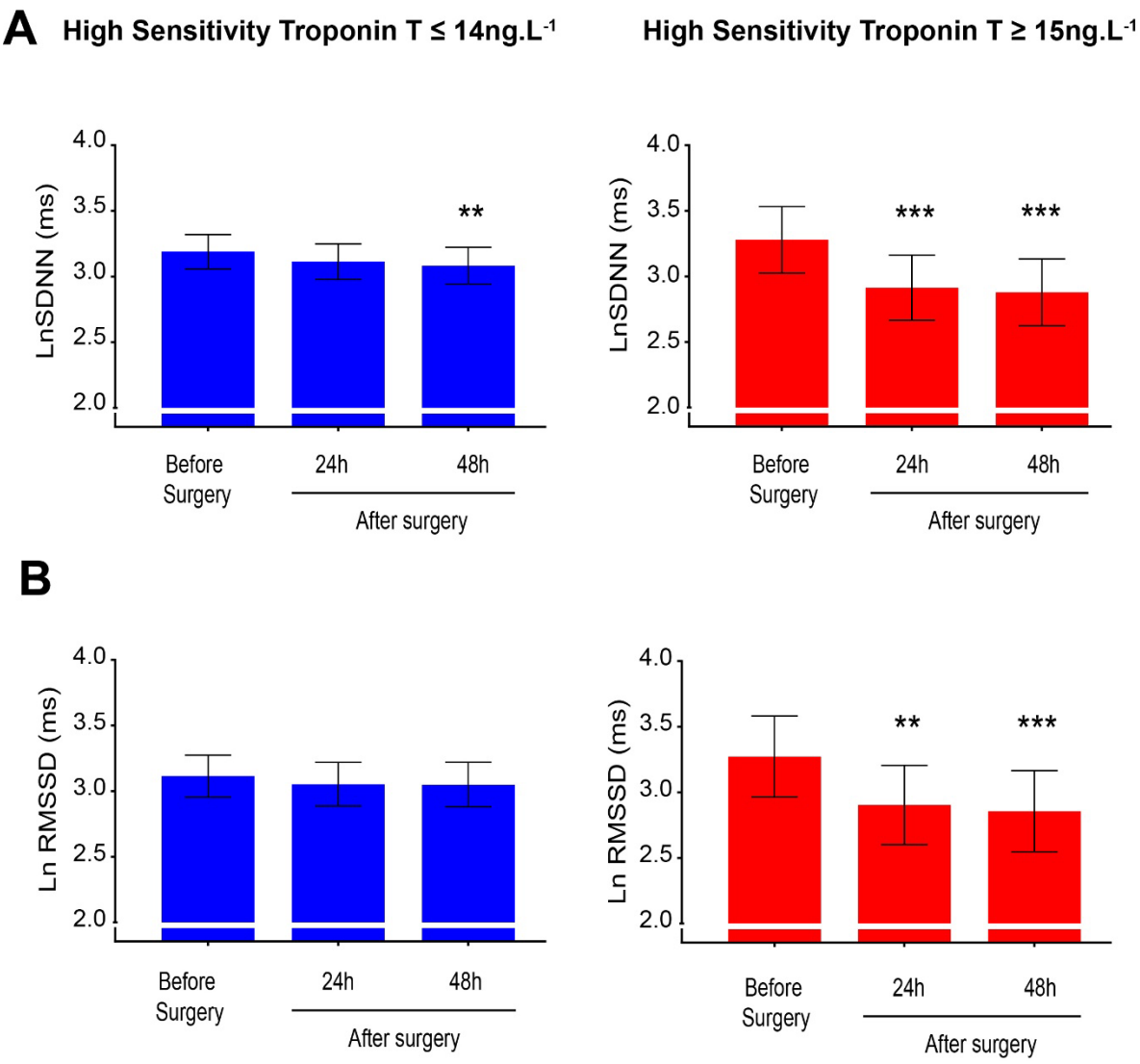

Figure 4.7 Supine serial changes in time domain HRV measures

(A) Standard deviation of the heart NN interval (SDNN). (B) Root mean square of the standard deviation of the heart NN interval (RMSSD). Data are presented as natural logarithmic transformed mean values with 95% confidence interval. P-value refers to before surgery vs 24 h after surgery, and before surgery vs 48 h after surgery comparisons. **P<0.01; ***P<0.001 (analysed by mixed-model repeated measures and Bonferroni test).

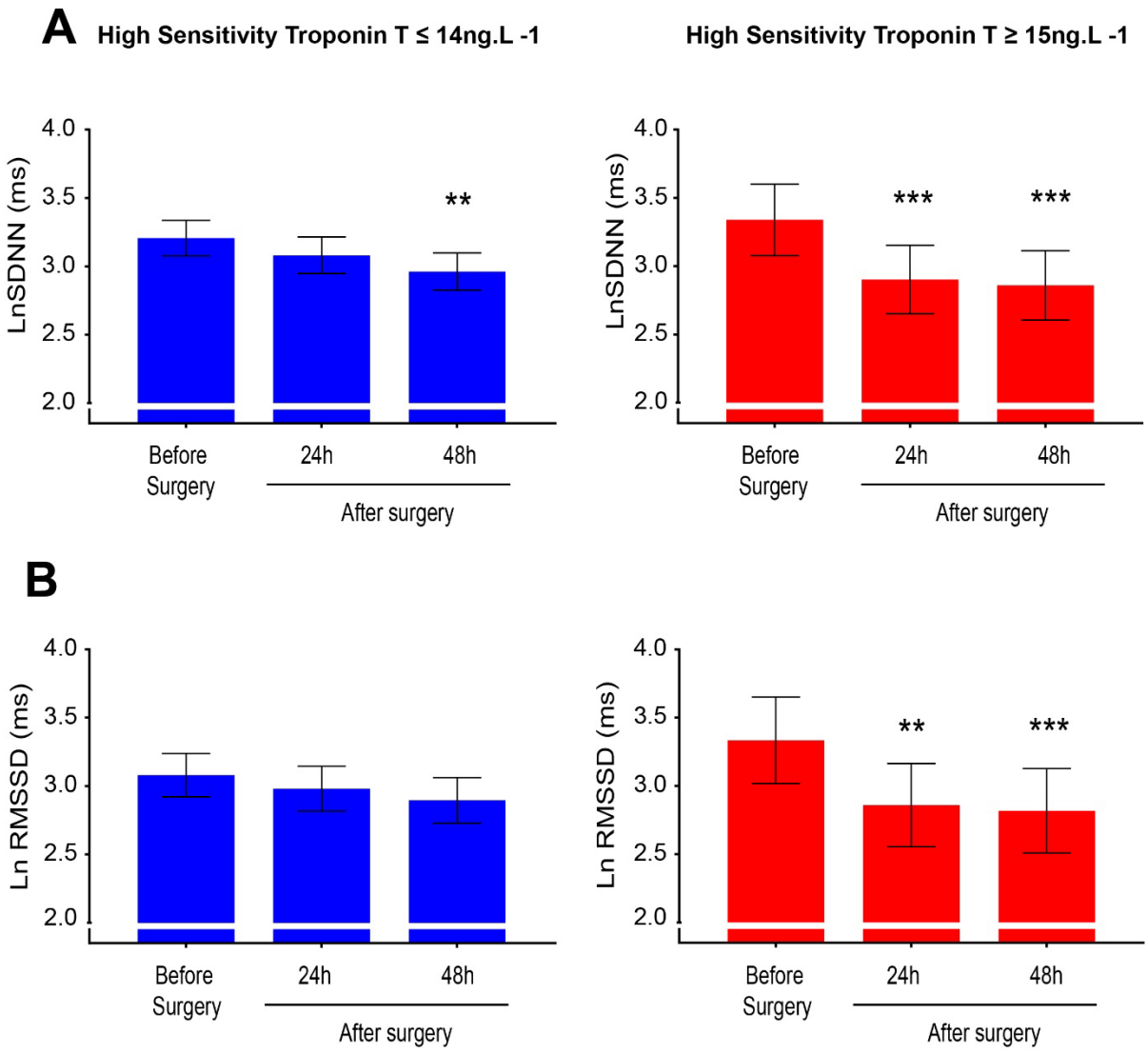

Figure 4.8 45-degree head up position serial changes in time domain HRV measures

(A) Standard deviation of the heart NN interval (SDNN). (B) Root mean square of the standard deviation of the heart NN interval (RMSSD). Data are presented as natural logarithmic transformed mean values with 95% confidence interval. P-value refers to before surgery vs 24 h after surgery, and before surgery vs 48 h after surgery comparisons. **P<0.01; ***P<0.001 (analysed by mixed-model repeated measures and Bonferroni test).

4.3.4.2 Frequency domain measures.

High frequency power decreased 24h after surgery only in patients who developed perioperative myocardial injury ($p < 0.01$) (Figure 4.9A and Figure 4.10A). The low frequency power spectral band decreased in patients both with and without perioperative myocardial injury after surgery (Figure 4.9B and Figure 4.10B).

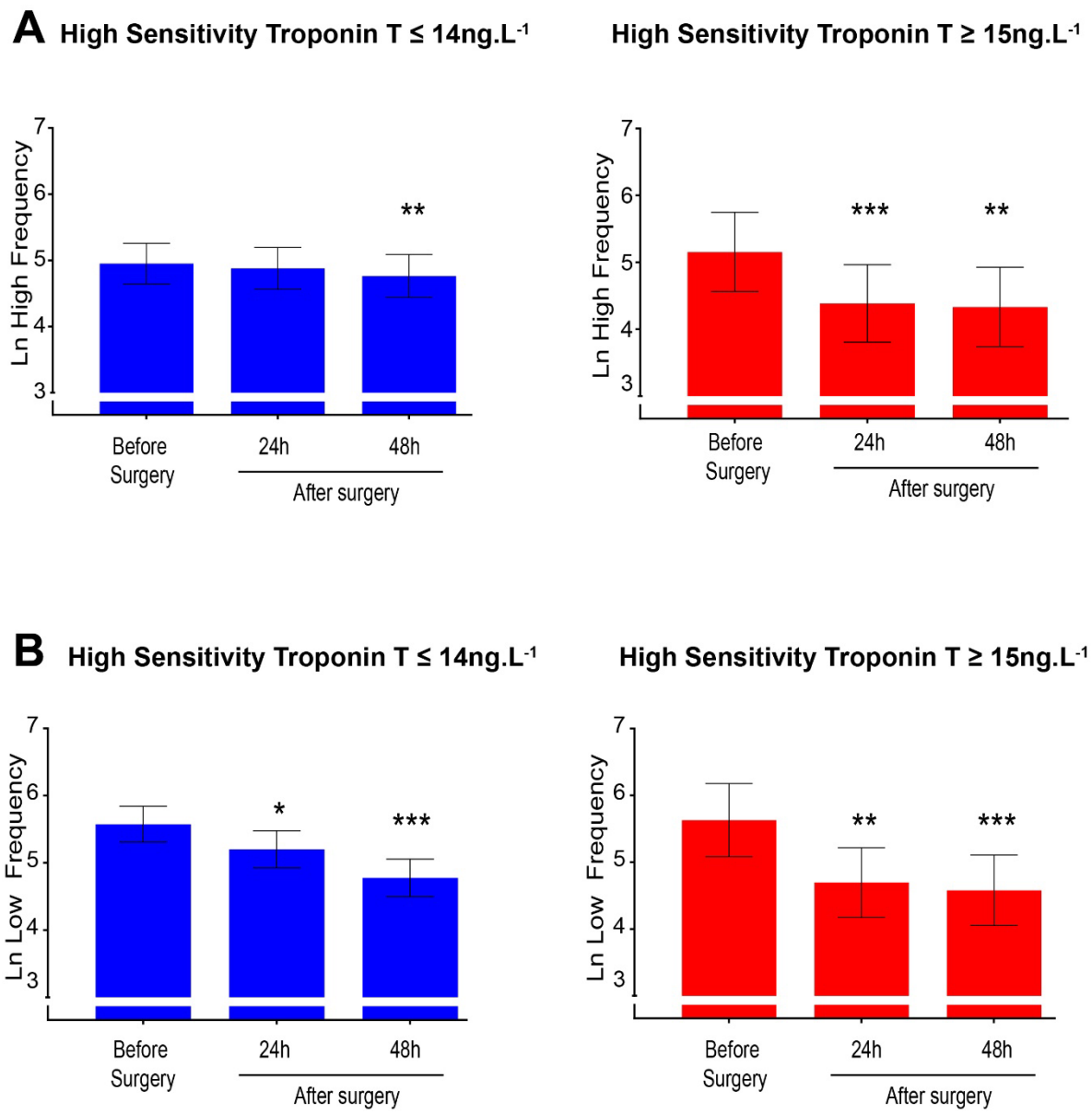

Figure 4.9 Supine position serial changes in frequency HRV measures

(A) High frequency power spectral analysis. (B) Low frequency power spectral analysis. Data are presented as natural logarithmic transformed mean values with 95% confidence interval. P-value refers to before surgery vs 24 h after surgery, and before surgery vs 48 h after surgery comparisons. **P<0.01; ***P<0.001 (analysed by mixed-model repeated measures and Bonferroni test).

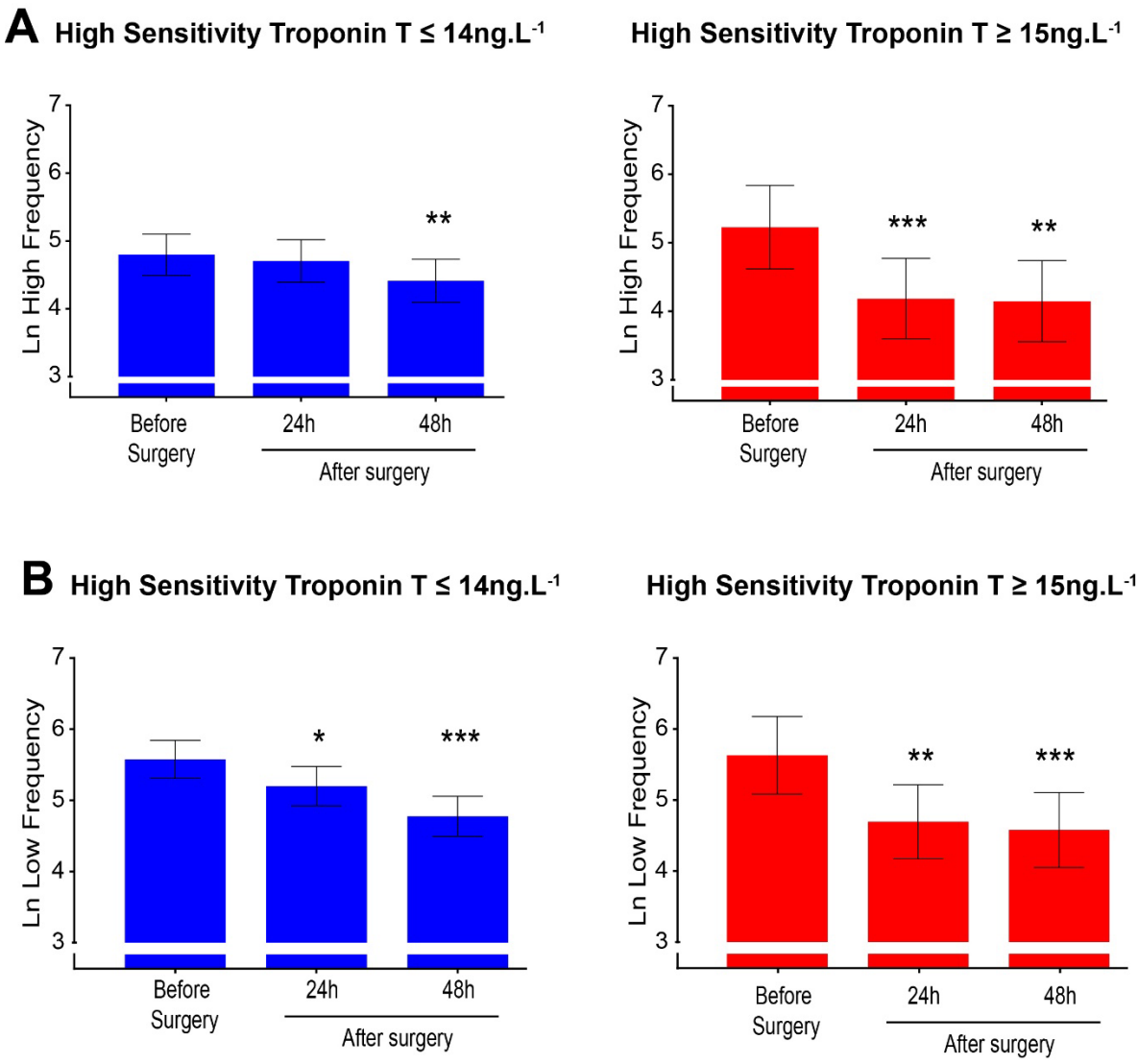

Figure 4.10 45-degree head up position serial changes in frequency HRV measures

(A) High frequency power spectral analysis. (B) Low frequency power spectral analysis. Data are presented as natural logarithmic transformed mean values with 95% confidence interval. P-value refers to before surgery vs 24 h after surgery, and before surgery vs 48 h after surgery comparisons. **P<0.01; ***P<0.001 (analysed by mixed-model repeated measures and Bonferroni test).

4.3.5 Explanatory autonomic measures for postoperative morbidity

4.3.5.1 Time domain measures

Resting heart rate was similar before surgery in patients who did and did not develop POMS morbidity. Heart rate increased in both groups 48h after surgery p<0.001; Figure 4.11). LnRMSSD and LnSDNN values in the supine and head up position did not change after surgery (Figure 4.12 and Figure 4.13).

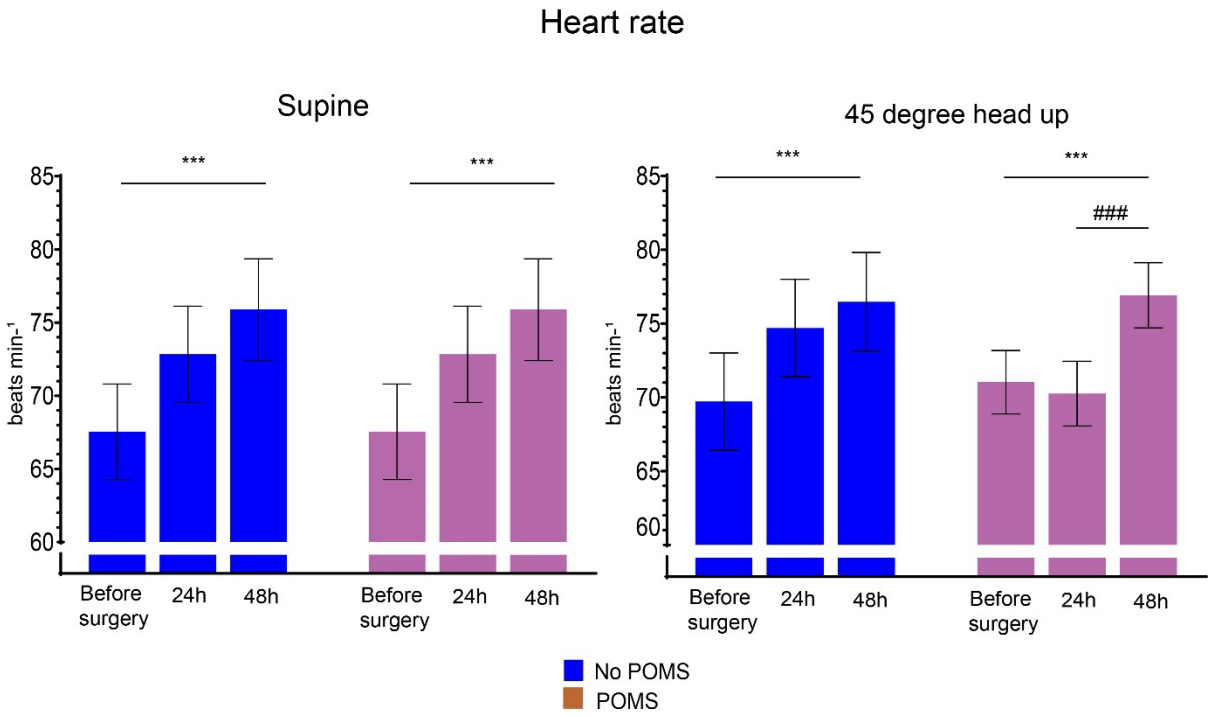

Figure 4.11 Serial resting heart rate measurements in the supine and 45-degree head up positions

Data is presented as mean values with 95% confidence interval. ***P<0.001 refers to before surgery vs 48 h after surgery (analysed by mixed-model repeated measures and Bonferroni test). ###P<0.001 refers to 24h vs 48h after surgery.

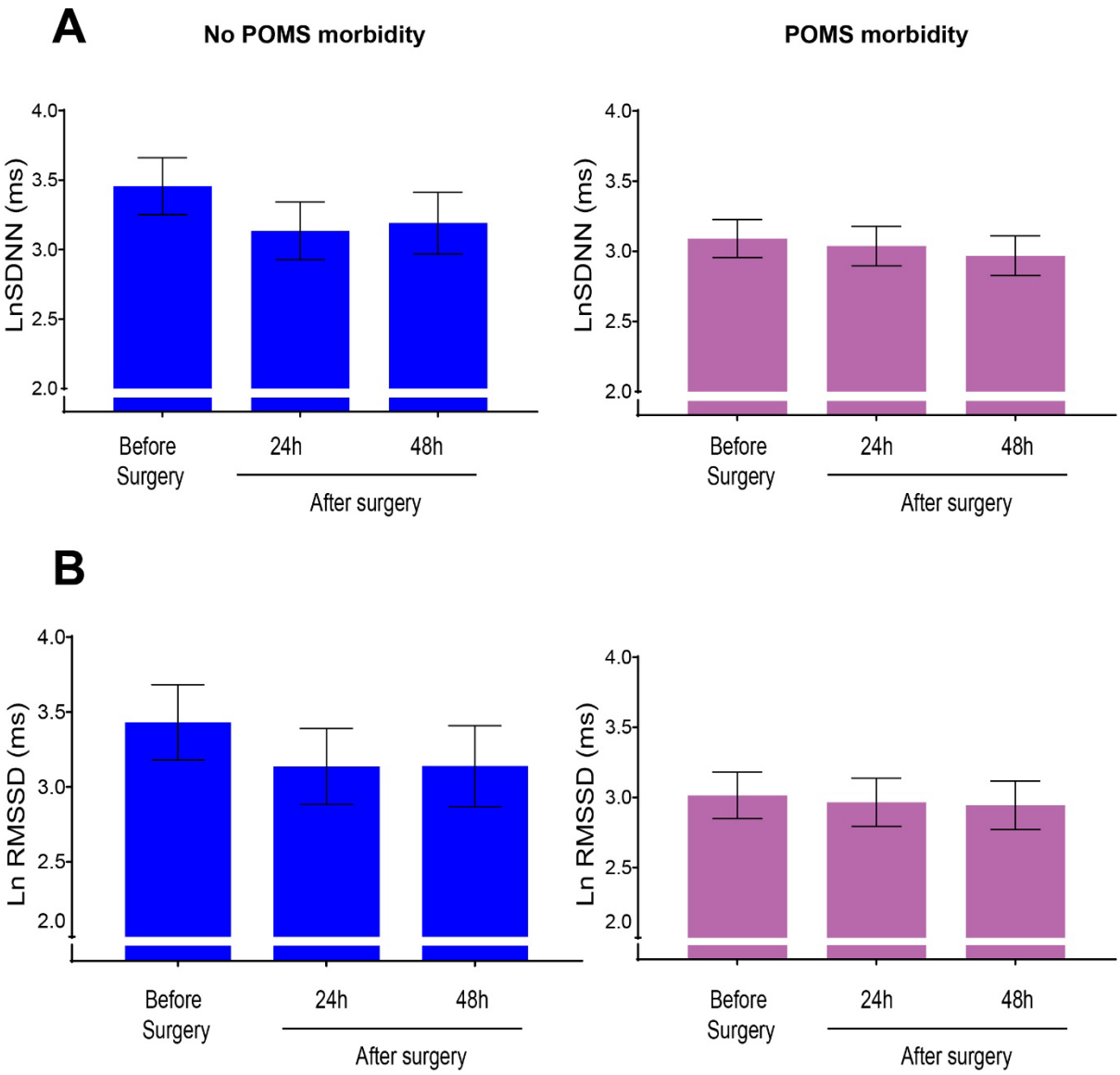

Figure 4.12 Supine serial changes in time domain HRV measures

(A) Standard deviation of the heart NN interval (SDNN). (B) Root mean square of the standard deviation of the heart NN interval (RMSSD). Data are presented as natural logarithmic transformed mean values with 95% confidence interval.

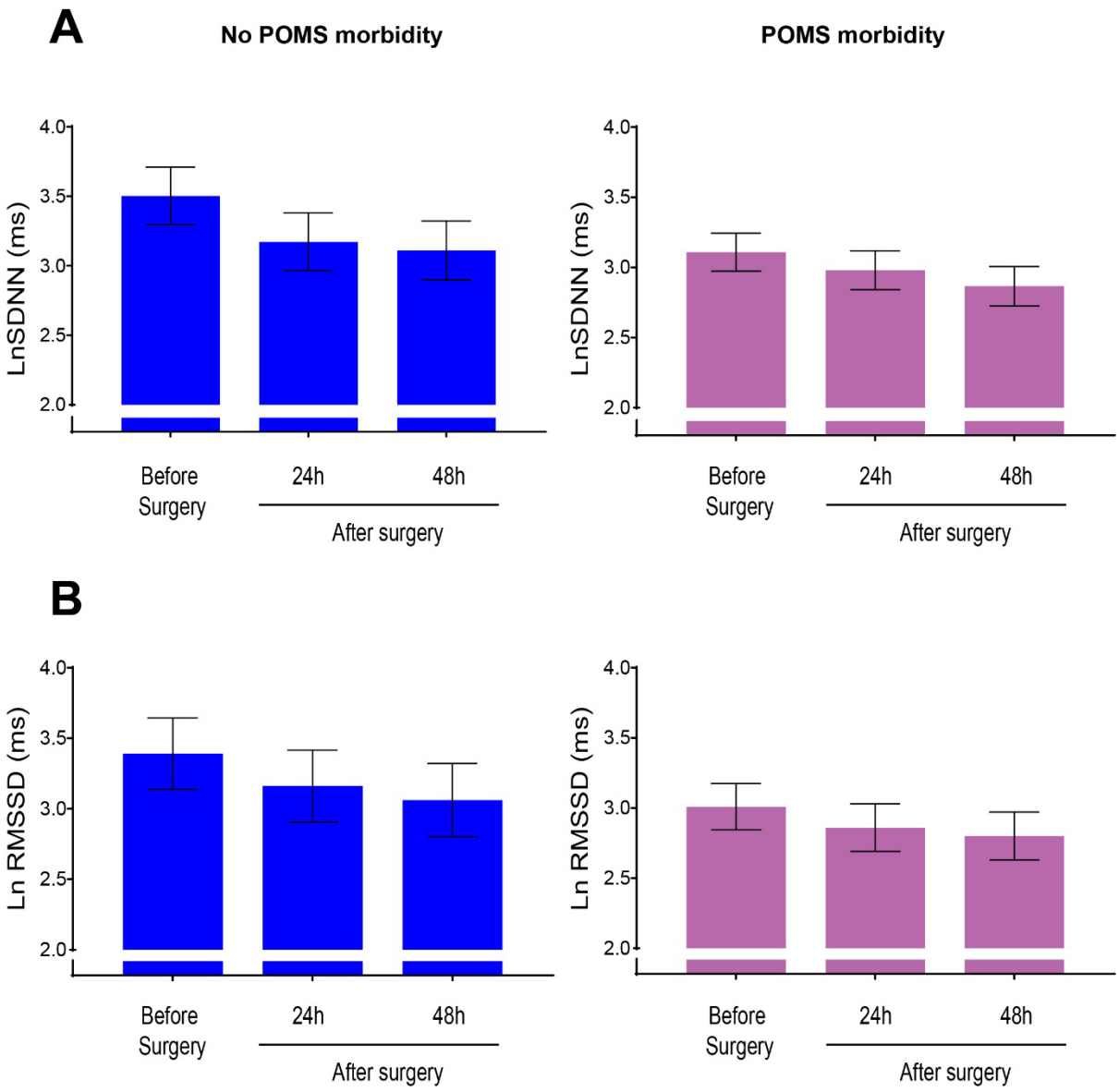

Figure 4.13 45-degree head up position serial changes in time domain HRV measures

(A) Standard deviation of the heart NN interval (SDNN). (B) Root mean square of the standard deviation of the heart NN interval (RMSSD). Data are presented as natural logarithmic transformed mean values with 95% confidence interval.

4.3.5.2 Frequency domain measures

No changes in high frequency power spectral band were observed in either group after surgery. The low frequency power spectral band decreased in patients with and without POMS morbidity after surgery (Figure 4.14B and Figure 4.15B).

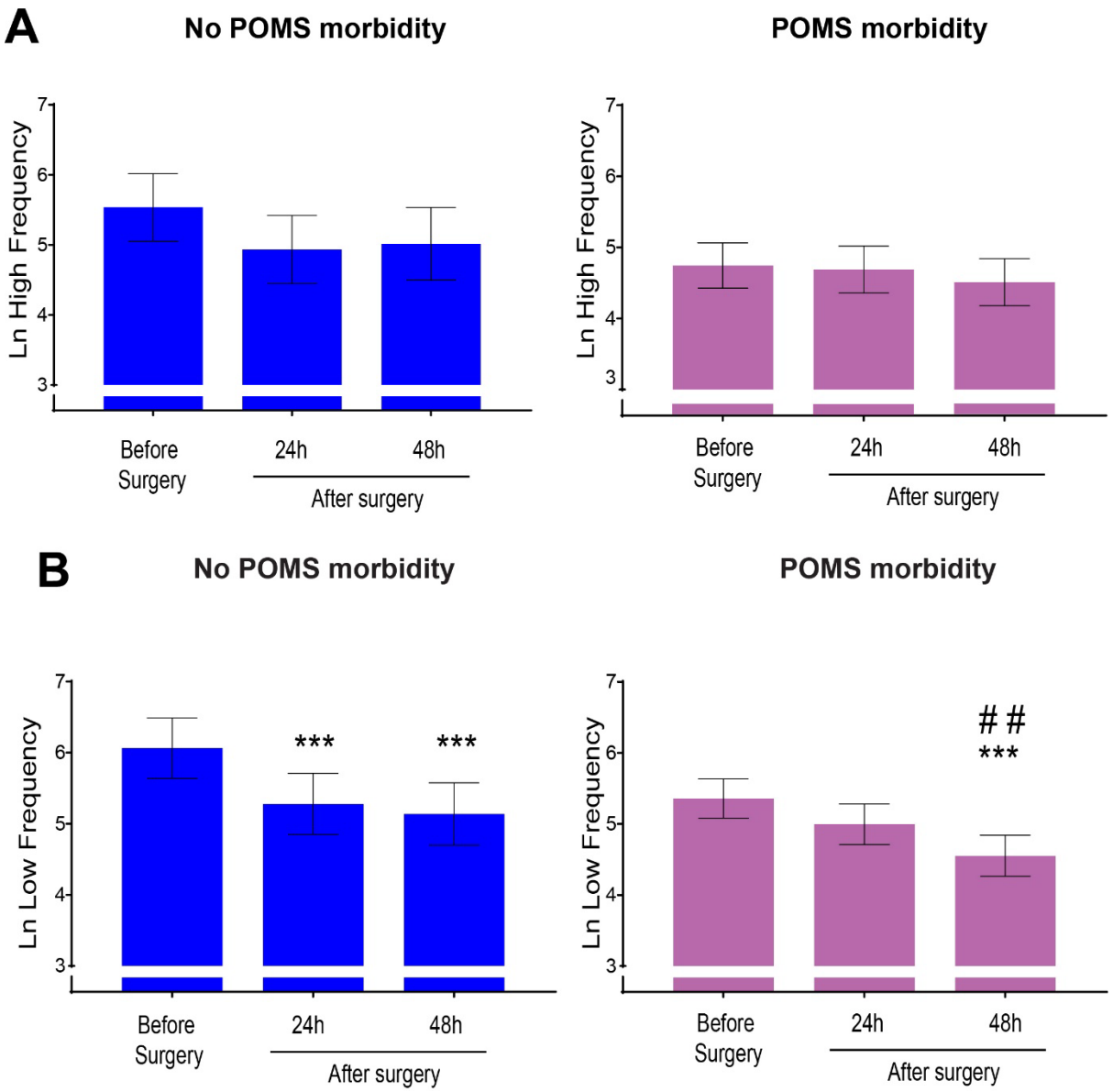

Figure 4.14 Supine serial changes in frequency position HRV measures

(A) High frequency power spectral analysis. (B) Low frequency power spectral analysis. Data are presented as natural logarithmic transformed mean values with 95% confidence interval. ***P<0.001 refers to before surgery vs 24 h after surgery, and before surgery vs 48 h after surgery comparisons. ##P<0.01 refers to 24h vs 48h after surgery comparisons (analysed by mixed-model repeated measures and Bonferroni test).

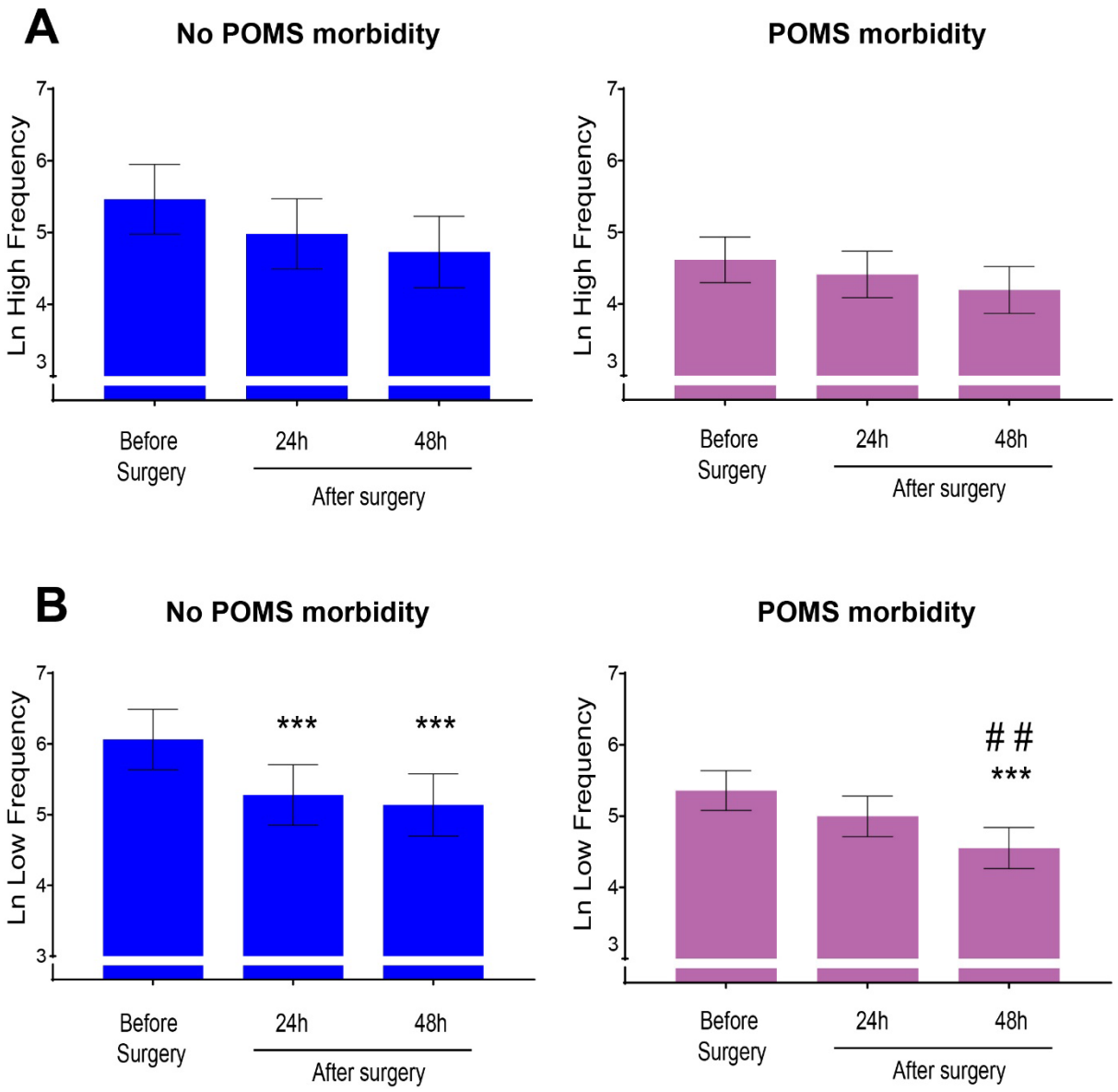

Figure 4.15 Supine serial changes in frequency position HRV measures

(A) High frequency power spectral analysis. (B) Low frequency power spectral analysis. Data are presented as natural logarithmic transformed mean values with 95% confidence interval. ***P<0.001 refers to before surgery vs 24 h after surgery, and before surgery vs 48 h after surgery comparisons. ##P<0.01 refers to 24h vs 48h after surgery comparisons (analysed by mixed-model repeated measures and Bonferroni test).

4.3.6 Sensitivity analysis

When the primary analysis was repeated excluding patients who had received only a general anaesthetic, the results for the heart rate variability measurements were similar to the original primary analysis. In patients with HsTnT≥15ng.L^{-1}, HF_{Ln} declined from 5.34 [95%CI: 4.66-6.01] before surgery to 4.06 [95%CI:3 .42-4.71]; p<0.001 24h after surgery. In patients who remained free of myocardial injury, HF_{Ln} did not change (4.84 [95% CI: 4.46-5.22] before surgery versus 4.77 [95%CI: 4.37-5.18] after surgery) (Figure 4.16).

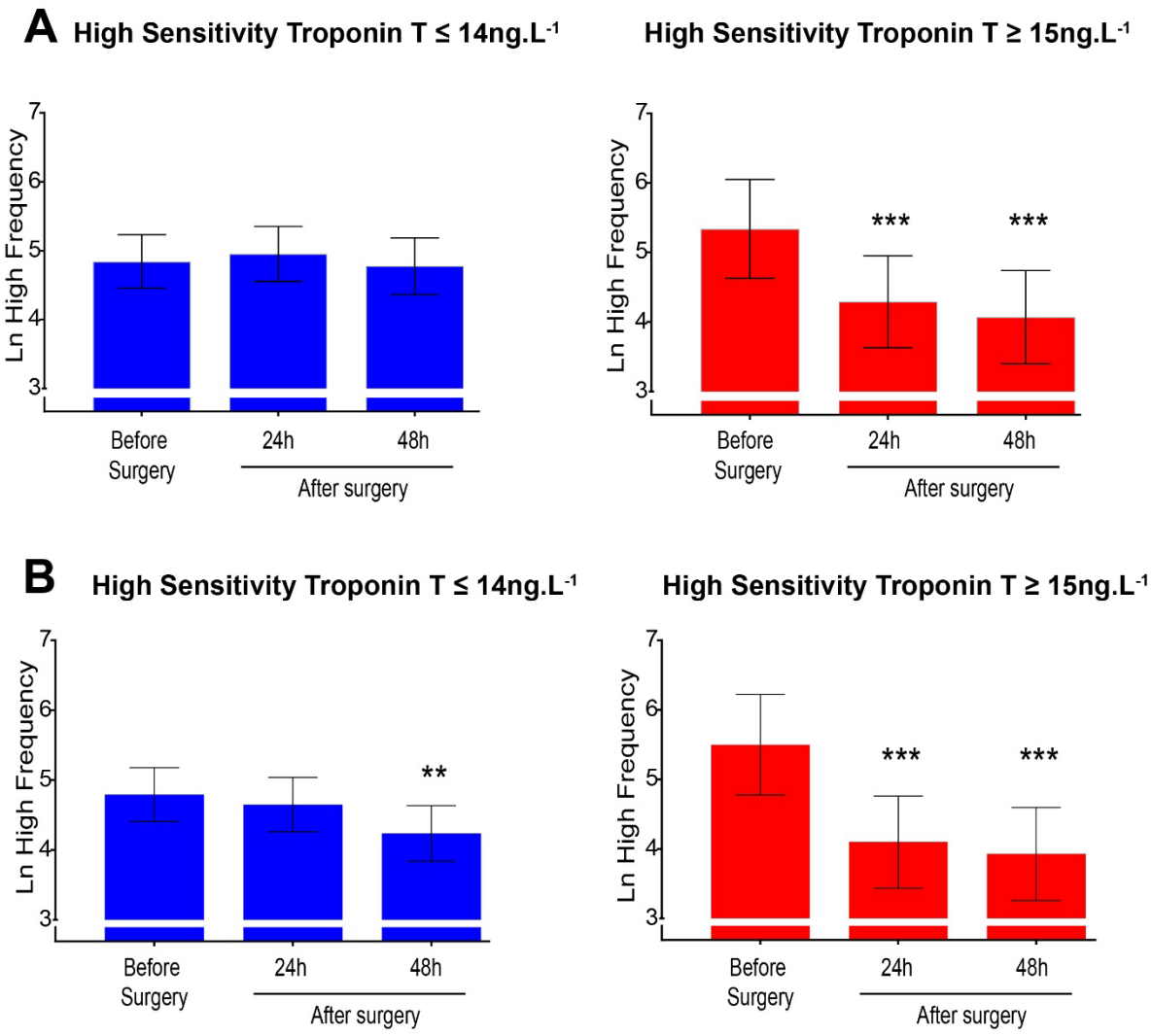

Figure 4.16 Serial changes in high frequency HRV measures (excluding patients who received a general anaesthetic)

(A) Supine. (B) 45-degree head up position. Data are presented as natural logarithmic transformed mean values with 95% confidence interval. P-value refers to before surgery vs 24 h after surgery, and before surgery vs 48 h after surgery comparisons. **P<0.01; ***P<0.001 (analysed by mixed-model repeated measures and Bonferroni test).

4.4 Discussion

The aim of this study was to assess whether acquired cardiac vagal dysfunction is associated with perioperative myocardial injury and postoperative morbidity. Cardiac vagal dysfunction was quantified before and after surgery using standardised electrocardiogram recordings and heart rate variability analysis. This approach allowed each patient to serve as their own control. The cohort of patients in the study were at low risk of cardiovascular complications, as indicated by 92% (174/189) of the patients having a RCRI <2 before surgery. Patients who had an elevated troponin after surgery showed no clinical evidence of heart failure or myocardial infarction, suggesting that the elevation in troponin is subclinical.

The main findings of the study described in this chapter are:

- PMI is associated with a loss of efferent cardiac vagal activity 24 hours after surgery.
- PMI was associated with noncardiac morbidity after noncardiac surgery.
- Low frequency power spectrum decreases after noncardiac surgery.

4.4.1 PMI was associated with a loss of efferent cardiac vagal activity within 24h of surgery

This longitudinal observational cohort study is the first to demonstrate that a loss of efferent cardiac vagal activity after noncardiac surgery, as measured by HRV, is associated with the development of PMI. This was demonstrated in the time-domain (Ln RMSSD and Ln SDNN) and the high frequency heart rate variability measurements.

A loss of efferent cardiac vagal activity within 24 hours suggests that it is the early loss of efferent vagal activity that contributes to the development of PMI. However, at 48 hours after surgery, a decrease in cardiac parasympathetic activity was evident in both groups of patients. This is consistent with the loss of parasympathetic function previously demonstrated in patients after orthopaedic[206] and major abdominal surgery.[204]

92% (174/189) of the patients in this study had a revised cardiac risk index score of <2 before surgery, and therefore can be considered at low risk for developing cardiovascular complications prior to surgery.[290] The comorbidities between patients who developed PMI and those who remained free from PMI were similar. A possible explanation for why patients who are at apparently low risk for perioperative cardiovascular events go on to develop PMI, is that acquired parasympathetic dysfunction, and hence a loss of cardiac vagal protective mechanisms, is a key contributory mechanism in PMI.

A rise in troponin after noncardiac surgery has been previously reported in young healthy adults with no cardiovascular comorbidities[360] (i.e., low risk for elevated troponin after surgery), further suggesting the loss of cardioprotective mechanisms can be acquired during surgery.

To compare the current study with population normal values (19-75ms),[211] the proportion of patients with RMSSD <19ms was calculated. In this study cohort, 44% of the patients who did not develop PMI had a raw RMSSD value <19 compared to 41% who developed PMI (Appendix H). The similarity of raw RMSSD values before surgery between the two groups suggests that it is an acute loss of cardioprotective vagal mechanisms in the perioperative period that contributes to PMI. When considering the entire study cohort, 44% of the patients had a raw RMSSD <19, suggesting that a proportion of this ostensibly low-risk population may already have an established autonomic phenotype associated with a higher risk of developing morbidity, including PMI, after noncardiac surgery. This is supported by previous work by Abbott et al.,[217] where impaired cardiac vagal function, as defined by impaired HRR after CPET before surgery, was associated with the development of PMI after noncardiac surgery.

The implication of the association stated above is that a loss of cardiac vagal activity is contributing to PMI. In the absence of controlled experimental intervention it would not be unreasonable to suggest that PMI may be contributing to the loss of cardiac vagal activity after surgery. In controlled canine experiments, it was demonstrated that following myocardial infarction, the conscious dogs had a decrease in baroreceptor sensitivity compared to before the induced myocardial infarction, suggesting that myocardial infarction modifies baroreceptor reflex.[361] The baroreceptor reflex receives afferent inputs and efferent inputs from the vagus nerve. Therefore it is possible that myocardial injury may involve damage to the vagus nerve at cardiac level[362] and therefore reduce efferent cardiac vagal activity as revealed by reduced HF. The results presented in this study are unable to differentiate potential causality.

Potential explanatory mechanisms for the loss of efferent cardiac vagal activity

The early loss of efferent cardiac activity may due to circulating inflammatory mediators such as TNF-α, which inhibits dorsal vagal motor neurons.[363] In addition, pharmacological agents commonly used in the perioperative period have been shown experimentally to modulate vagal outflow. At low concentrations, propofol has been shown to potentiate GABAergic inhibitory pathways to cardiac vagal neurons in the nucleus ambiguus, thus decreasing efferent cardiac vagal activity.[364] At higher concentrations, propofol decreases GABAergic neurotransmission to cardiac vagal neurons, which increases the activity of the cardiac parasympathetic neurons.[364]

Opioid administration may also reduce vagal activity: experimentally, stimulation of δ_1 opioid receptors on the SAN attenuated the bradycardic effects of vagal stimulation.[365] Activation of μ opioid receptors has been shown to centrally inhibit DVMN projections.[366] Commonly used muscle relaxants that exhibit M2 muscarinic blockade can also attenuate vagal activity to the heart.[367]

Acquired loss of cardiac vagal protective mechanisms leading to PMI

Adrenergic cardiac stress is a common feature of the physiological response to surgery.[344] cAMP-mediated increases in intracellular calcium produce an increase in heart rate and contractility, and hence in cardiac output, to meet the elevated metabolic demands due to the surgical insult. A loss of cardioprotective mechanisms may promote the likelihood of a cardiomyocyte cAMP-mediated calcium overload, resulting in mitochondrial dysfunction, degradation of the myofibril complex, and ultimately cell death. This would manifest clinically

as a rise in the serum of cTn, a component of the myofibril complex. If the vagus nerve confers cardioprotective mechanisms to prevent myocardial injury, an acquired loss of cardiac vagal nerve activity may result in the development of PMI in the presence of adrenergic cardiac stress. These protective mechanisms have been outlined in the Introduction Section 1.6. In summary, vagally-mediated cardioprotection may be conferred in several ways, including: lowering heart rate;[222, 345] reducing oxidative stress;[368] activating mitophagy;[225] promoting mitochondrial biogenesis;[227] remote ischaemic preconditioning;[369] maintaining cardiac output;[20] minimising inflammation;[238, 239] and via anti-arrhythmic effects.[19, 370] Experimental models have demonstrated that neurotransmitters released by the vagus nerve confer cardioprotection through both muscarinic and nicotinic acetylcholine receptors.[371]

This study demonstrated the loss of efferent cardiac vagal activity. If inflammatory cytokines are able to inhibit vagal activity centrally,[363] then it is not unreasonable to assume that vagal activity from other central projections is also attenuated during surgery. This may therefore also include vagal-splenic communication in the cholinergic anti-inflammatory reflex. A reduction in vagal efferent outflow to splenic cholinergic fibres would attenuate the anti-inflammatory effects of macrophage n7AchR activation[55] (Introduction Section 1.2.3.2). This may result in increased inflammation of the heart and in tissue injury.[238, 239]

This would be consistent with data from human subjects in which it was demonstrated that reduced HRR, a measure of vagal dysfunction, was associated with systemic inflammation by assessing the neutrophil-lymphocyte (NRL) ratio.[240]

4.4.2 PMI was associated with noncardiac morbidity after noncardiac surgery

Patients who developed PMI after surgery had a higher proportion of all cause morbidity within 7 days after surgery as adjudged by POMS including cardiovascular comorbidities, compared with patients who did not develop PMI.

Patients who developed PMI were also associated with an increased length of stay in hospital. These findings are consistent with the findings from the UK cohort (4335 patients) of the VISION study[3] where a rise in troponin within 24h of noncardiac surgery was associated with cardiovascular morbidity.[70] The association with elevated troponin within 24 hours of surgery is significant, as it would suggest that the cardiac parasympathetic protective mechanisms, outlined above, are reduced in the early perioperative period.

No difference in the occurrence of intraoperative blood pressure (defined as >1 episode of intraoperative of systolic blood pressure of <90mmHg after induction of anaesthesia) was found between patients who developed PMI and those that remained free from PMI. In cohort studies showing an association between perioperative hypotension[372, 373] and PMI there is a wide variation in the definition of perioperative hypotension.[374] It is feasible that the definition used in the XMINS study was not robust enough to elicit an association with PMI. However, random controlled trials targeting specific blood pressure targets have failed to demonstrate improved outcomes, including the prevention of PMI.[375] In addition to inconsistent definitions, this would suggest that hypotension and its effects on end organ damage is more complex and multifactorial than targeting specific BP numbers.[376] Hypotension leads to a decrease in perfusion pressure. However it does not always lead to organ hypoperfusion, as organ perfusion is also determined by peripheral vascular resistance.[374] The XMINS study did not

measure other haemodynamic variables relating to intraoperative blood pressure such as cardiac output, systemic vascular resistance or stroke volume. In view of inconsistencies within the literature and lack of direct evidence of end organ hypoperfusion in this study, it not surprising that hypotension as defined for the XMINs study was not associated with PMI.

4.4.3 Low frequency power spectrum decreases after noncardiac surgery

Low frequency power spectrum decreased within 24 hours of noncardiac surgery both in patients who developed PMI and in those who remained free of PMI. This ubiquitous decrease in low frequency after noncardiac surgery is consistent with previous studies measuring frequency domains of heart rate variability after surgery. Amar et al.[204] demonstrated a decrease in low frequency 24 hours after surgery that persisted for the 72 hours during which measurements were taken.

In the General Introduction Section 1.5.1.2 , I discussed canine pharmacological studies which suggested that low frequency corresponds with baroreceptor function rather than solely sympathetic function.[188, 189] Cardiac neuroimaging in human subjects, using ^{18}F fluorodopamine, has shown that LF power is not related to cardiac sympathetic innervation of the intraventricular septum and left ventricular wall.[188, 189] However in these studies, LF power did correlate to baroreflex cardiac gain at rest and during Valsalva manoeuvres, irrespective of cardiac sympathetic innervation of the heart.[188, 189] This would suggest that LF power reflects autonomic outflow by the baroreceptor reflex, and not solely cardiac sympathetic activity.[377]

Therefore, if LF power is representative of the baroreceptor function, then the decrease in LF power after noncardiac surgery would suggest that there is an attenuation in baroreceptor function 24 hours after surgery. Baroreceptor dysfunction, measured by baroreceptor sensitivity, is associated with increased cardiac morbidity[348]. However, LF in this study was not associated with morbidity, as measured by the development of POMS after noncardiac surgery.

4.4.4 Strengths and limitations of the study

The study and analyses were not designed to establish benchmark values for time and frequency heart rate variability measures in the perioperative period; however, this work is the largest observational study measuring serial heart rate variability and its components in the perioperative period. The main strength of this study was that serial heart rate recordings were made at standardised times before and after surgery, enabling intra-individual changes to be assessed, and for each patient to serve as their own control in the analysis. In addition, technical specifications on how the HRV measures were analysed were considered prior to analysis and transparently reported rather than relying on software automation. The loss of ECG data was predictable from previous longitudinal studies in similar settings.[212] However, in contrast to preceding studies[358, 378] where loss of ECG data exceeded 30%, this study captured a higher proportion of data of sufficient quality to enable heart rate variability analyses. This capture of data was consistent with the estimates for the sample size power calculation. Furthermore, a 48/189 (25.4%) rate of PMI in the cohort was consistent with power calculation estimates. As already discussed, comparisons with population HRV values is challenging due to the inconsistency of HRV measurements, and therefore using a comparable HRV metric in this study to justify the estimates used in the power calculation is challenging. For completion of assessing the estimates for the power calculation, 43% of patients had a RMSSD value <19ms, a threshold associated with delayed heart rate recovery before surgery,[214] compared to the 35% estimation.

HRV analysis was conducted before troponin and clinical outcome data were revealed. The masking of high-sensitivity troponin results to investigators, patients and attending clinicians was also a strength of this study.

It was highlighted in the introduction (section 1.5.2) that there is controversy as to whether HRV parameter are surrogates for autonomic activity or intrinsic cardiac heart rate. HRV parameters in the study were also reported alongside heart rate and respiratory rate, as has been recommended.[192, 195] It was beyond the scope of the study to disentangle whether it was efferent cardiac activity or change in intrinsic heart rate that was driving the decrease in cardiac vagal efferent components of HRV. Heart rate increased in both groups after surgery, suggesting HR was not influencing the differences in vagal parameters of HRV observed between the two groups.

The confounding influences of comorbidities[379, 380] and cardiac medications[381] are potential limitations, as both can influence HRV analysis. In addition the comorbidities such as age, length of surgery and male sex (Table 4.1) have been shown to be associated with an increased risk of the primary outcome, PMI.[345] It is recognised that these are potential confounders in observational studies.[382] The design of the study mitigated potential confounding factors, since each patient served as their own control in the mixed model analysis. Both groups experienced a similar frequency of intraoperative hypotension, suggesting that preoperative medications were not likely to contribute to the overall outcome. Despite best efforts to record patients' heart rate in standardised conditions throughout the perioperative period, this was, in practice, not always achievable due to the unpredictability of a clinical environment. Reassuringly, however, studies comparing standardised and non-standardised conditions using healthy and diabetic neuropathic patients showed an acceptable agreement in heart rate variability measurements.[383]

Previous work by Abbott et al [345] had shown than increased HR (>96bpm) was associated with PMI. The fact that the HRV results in this study were unable to inform on preoperative risk

was not a surprise as this study was a single centre hypothesis driven mechanistic study assessing for an association of PMI and HRV after surgery. In contrast, the Abbott et al [345] study was a large international multicentre population-based study of over 16000 patients that was able to use multivariate logistic regression to take into account potential confounders, with the aim to specifically assess the association of preoperative HR and PMI.

4.4.5 Conclusions

The observational data support the hypothesis that impaired cardiac vagal activity contributes to perioperative myocardial injury.

Chapter 5
Perioperative orthostatic modulation of heart rate

Results from the data presented in this chapter have been published in the British Journal of Anaesthesia (2019) 123(6), 758-767

5.1 Background

The results in Chapter 4 have demonstrated that a loss of efferent cardiac vagal activity after surgery is associated with PMI, using heart rate variability as a measurement of vagal activity. An alternative method of quantifying cardiac vagal activity is to measure the degree of vagal recruitment after peak exercise.[384] Cardiopulmonary exercise testing (CPET) is a common test employed before surgery to risk stratify patients for postoperative complications.[375] However, CPET is expensive, and requires specialist equipment and expertise. Nor would it be practicable to repeat exercise testing during the postoperative period due to the obvious limitations to mobility at this time. An orthostatic manoeuvre, that challenges similar baroreceptor reflex mechanisms to those elicited during exercise, has the potential to be utilised to measure heart rate recovery (HRR) and to quantify vagal activity. A lying to standing orthostatic manoeuvre has previously been demonstrated to be a robust measure of HRR in the general population,[221] and therefore has the potential to be implemented before and immediately after surgery in a standardised protocol. A further advantage of HRR is that it is not affected by the confounders of heart rate variability measures of autonomic function, such as resting heart rate[193] and respiratory rate.[215]

5.1.1 Hypothesis

Parasympathetic dysfunction, as measured by reduced heart rate recovery after a standardised orthostatic manoeuvre, is associated with PMI.

5.1.2 Aims

- To use a standardised orthostatic (supine-to-sitting) manoeuvre to quantify HRR before and after elective noncardiac surgery.

- Examine if HRR responses after an orthostatic challenge differ between patients who develop PMI and those who remain PMI free.

5.2 Methods

5.2.1 Study participants

Patients underwent an orthostatic challenge as part of the XMINS study protocol on the day of surgery, 24h and 48h after surgery (Figure 5.1 and Figure 5.2). The study protocol has been described in General Methods Section 2.3.

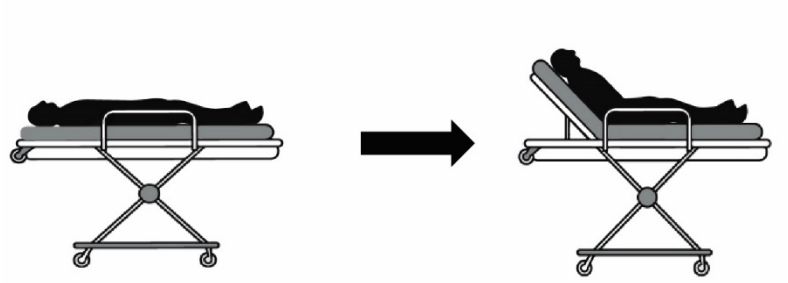

Figure 5.1 Orthostatic manoeuvre: supine to 45-degree head-up position

After 10 minutes in the supine position, patients were elevated to a 45-degree head-up position using an electronically adjustable hospital bed. To ensure standardisation of the test, the same bed was used for each test on each patient.

Figure 5.2 Adjustable hospital bed (Model 2232, ArjoHuntleigh, Malmo, Sweden)

5.2.2 Primary outcome

The primary outcome was perioperative myocardial injury, as defined by plasma HsTnT ≥15mg.L^{-1} within 48 hours of surgery. Patients, attending clinical staff, and myself were masked to troponin data, which were revealed only at the end of the study.

5.2.3 Heart rate

Heart rate recordings and data acquisition were made for all patients with available ECG data as outlined in General Methods Section 2.8. Heart rate is represented at 10s interval as an average of three consecutive beats. Baseline heart rate prior to the orthostatic challenge was calculated as the average of the 10s intervals for 1 minute before the orthostatic challenge. Peak heart rates were manually identified within the first 50 seconds of 10s intervals after the orthostatic challenge had been completed.

5.2.4 Heart rate recovery

HRR recovery values were calculated as the difference between peak heart rate and heart rate at each 10s time interval after the time that peak heart rate was identified for each individual patient.

5.2.5 Time constant analysis

In addition to heart rate recovery after peak heart rate at 70 seconds, time constants for the rate of change of heart rate were obtained from analysis of the heart rate decay by applying the equation detailed in General Methods Section 2.8:

$$Y=A\ Exp\ (-BX)$$

where Y is heart rate (at 10 second intervals), A is peak heart rate, X is time after peak and B is the rate in change in heart rate of peak (decay).

5.2.6 Statistical analysis

All values were assessed for normality using the Shapiro-Wilk test before statistical analysis. Comparisons between baseline heart rate and peak heart rate were analysed using a multi-level mixed model as outlined in General Methods Section 2.9.2.1. The levels examined were perioperative myocardial injury (HsTnT $\geq$15ng.L^{-1} and HsTnT $\leq$14ng.L^{-1}), and day relative to surgery (day of surgery, 24h after surgery and 48h after surgery). Individual comparisons between groups were calculated using post hoc Bonferroni tests when significance between terms was $p < 0.05$. Comparisons for time to reach peak heart rate were made using log rank tests. A comparison of the speed of HRR between patients who developed PMI versus those that remained free was made at 70s after peak using the Mann-Whitney U statistical test. 70 seconds was chosen as the comparator time point to minimise missing data points in the analysis, after taking into consideration the adjustment of the peak heart rate time. HRR values had been calculated using a peak heart rate selected from a time point after the completion of

orthostatic manoeuvre between 0 and 50 seconds (i.e., 0, 10, 20, 30, 40 or 50s). HR values had been processed for 120s after the completion of the orthostatic manoeuvre. Therefore, a participant who had a peak heart rate at 0s would have complete HR data for the full 120s. Whereas a participant who had a peak heart rate after 50s would have only complete data for the following 70s and would have missing values if a comparator value was set at 80s, 90s, 100s, 110s or 120s.

To take into account changes in initial HR response to the orthostatic challenge following surgery, analysis of HRR after 70 seconds was reanalysed using Analysis of Covariance (ANCOVA). ANCOVA is useful in studying a set of independent variables (PMI) on a response variable (HRR at 70 seconds) by improving precision by removing variation by including a covariate (change in HR from baseline to peak HR).[385] The ANCOVA uses multiple regression techniques to estimate model parameters to estimate least square means. A t-test is then used to calculate the difference between the group means having been adjusted for the covariate. To comply with the assumptions of normality for ANCOVA, data was natural log transformed. Statistical significance for tests was $p < 0.05$.

A randomisation statistical test was used to compare the model parameters and fitted curve equivalence between PMI groups. A randomisation test is a permutation test in which all possible permutations of the group variable are investigated. For each permutation, the difference between the estimated group parameters is calculated. The number of permutations greater than or equal to the actual sample are counted. This count is then divided by the number of permutations to give the significance of the test.[386] These tests assess for model parameter and curve equivalence without making unrealistic assumptions about constant variance, normality or model accuracy.[387] Statistical significance was $p < 0.05$.

5.3 Results

5.3.1 Patient characteristics and primary outcome.

ECG data from 189 patients was analysed (Figure 5.3). 48 out of 189 patients (25.4%) had sustained PMI by 48 hours after surgery (Chapter 4: Table 4.1). 93 patients had complete data sets for before, 24h and 48h after surgery.

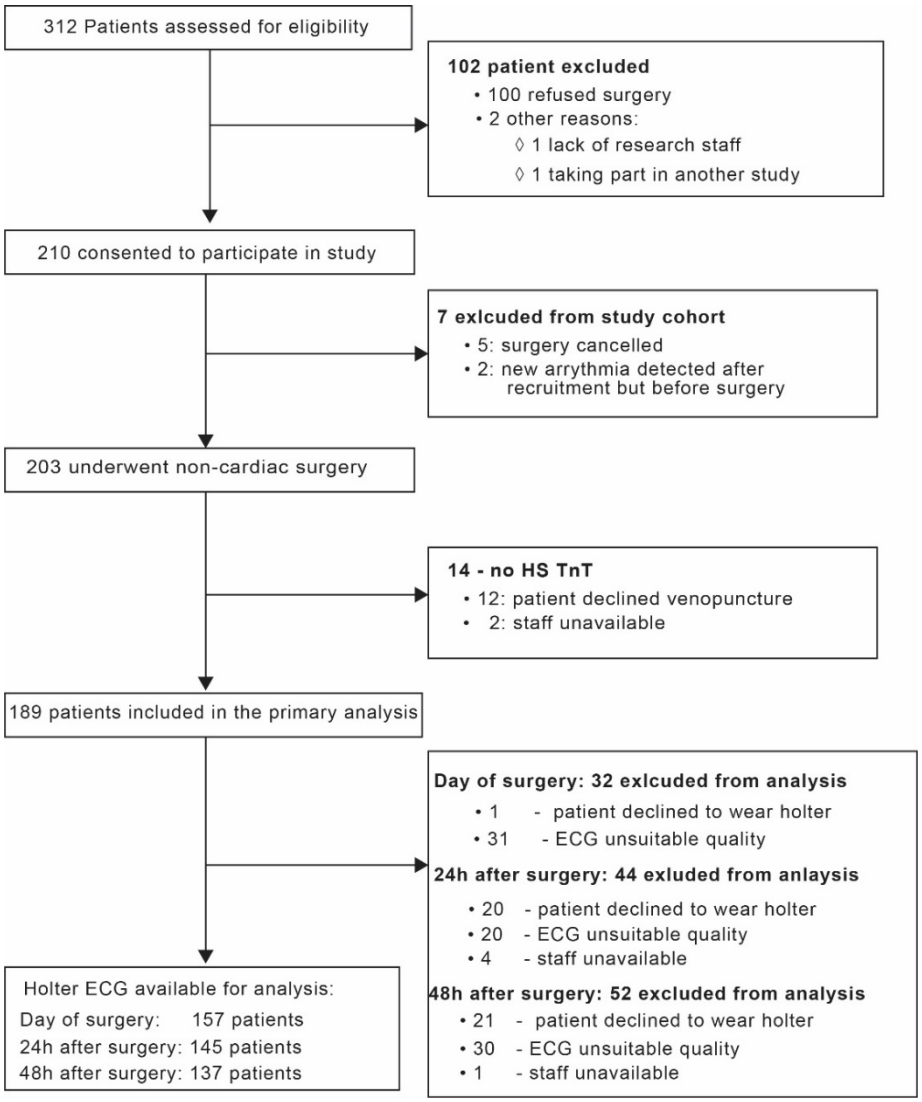

Figure 5.3 Consolidated standards of reporting trials diagram showing patients included in the analysis

5.3.2 Heart rate response to orthostatic manoeuvre

The mean heart rate responses to the orthostatic manoeuvre for all patients before surgery, and at 24h and 48 h after surgery, are represented in Figure 5.4**A-C**. The baseline heart rate prior to initiating the manoeuvre increased at 48hours after surgery, compared to before surgery and at 24h after surgery ($p<0.001$; Figure 5.5**A**). No differences in the peak heart rate achieved after the manoeuvre was completed were observed after surgery (Figure 5.5**B**). The peak heart rate compared to baseline heart rat, in response to the orthostatic challenge, declined from a mean increase of 11bpm (95%CI 10-13) to 5bpm (95%CI 4-6); $p<0.001$ (Figure 5.5**C).**

There was no difference in baseline heart rate prior to the orthostatic challenge between groups before surgery, and at 24h and 48h after surgery (Figure 5.7A). There was also no difference in peak heart rate before surgery, and at 24h and 48h after surgery (Figure 5.7 B). The time to reach peak heart rate was similar in both groups of patients at all time points ($p = >0.05$ by log rank test) (Figure 5.9 A-B).

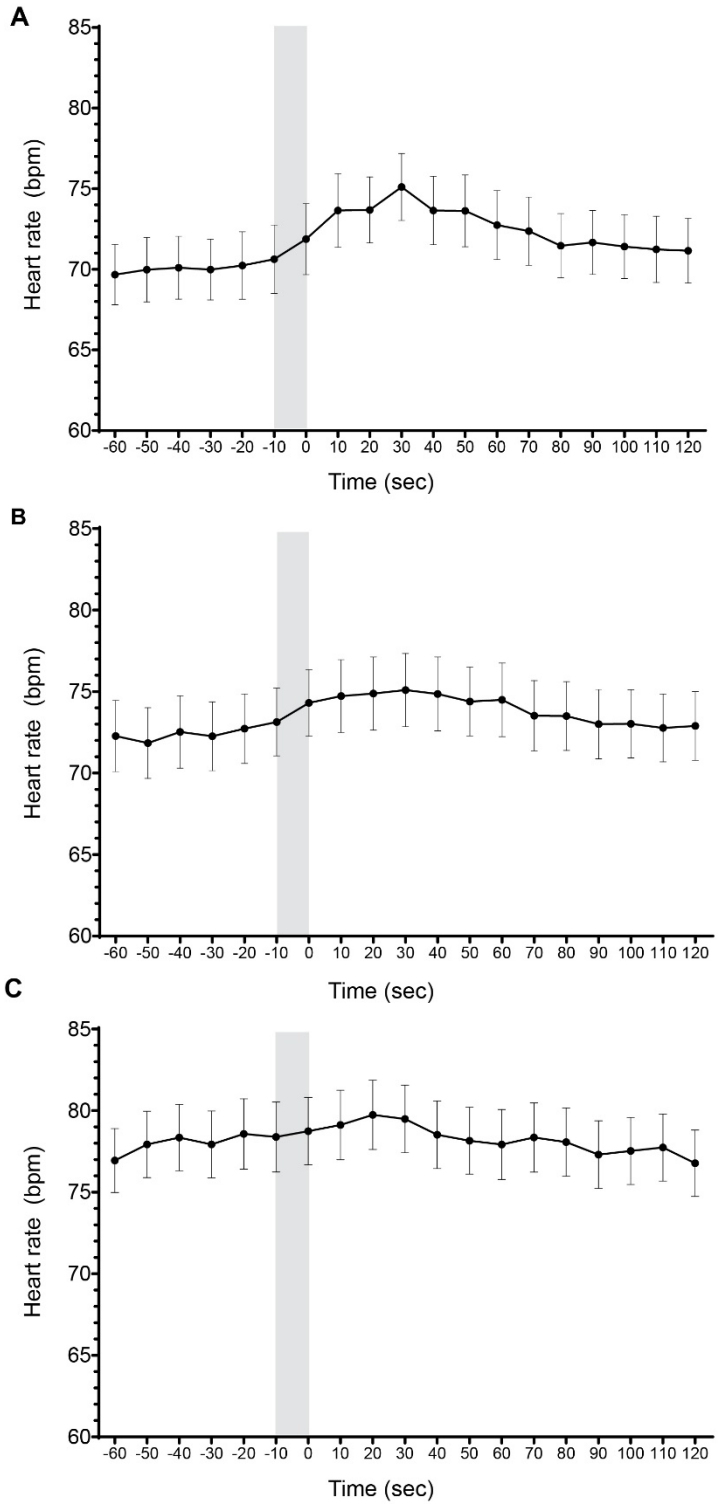

Figure 5.4 HR changes during a standardised orthostatic manoeuvre

Before surgery (**A**), 24h (**B**) and 48h (**C**) after surgery. Values are mean HR (95% CI) at 10s intervals before and after the standardised manoeuvre (grey shaded area).

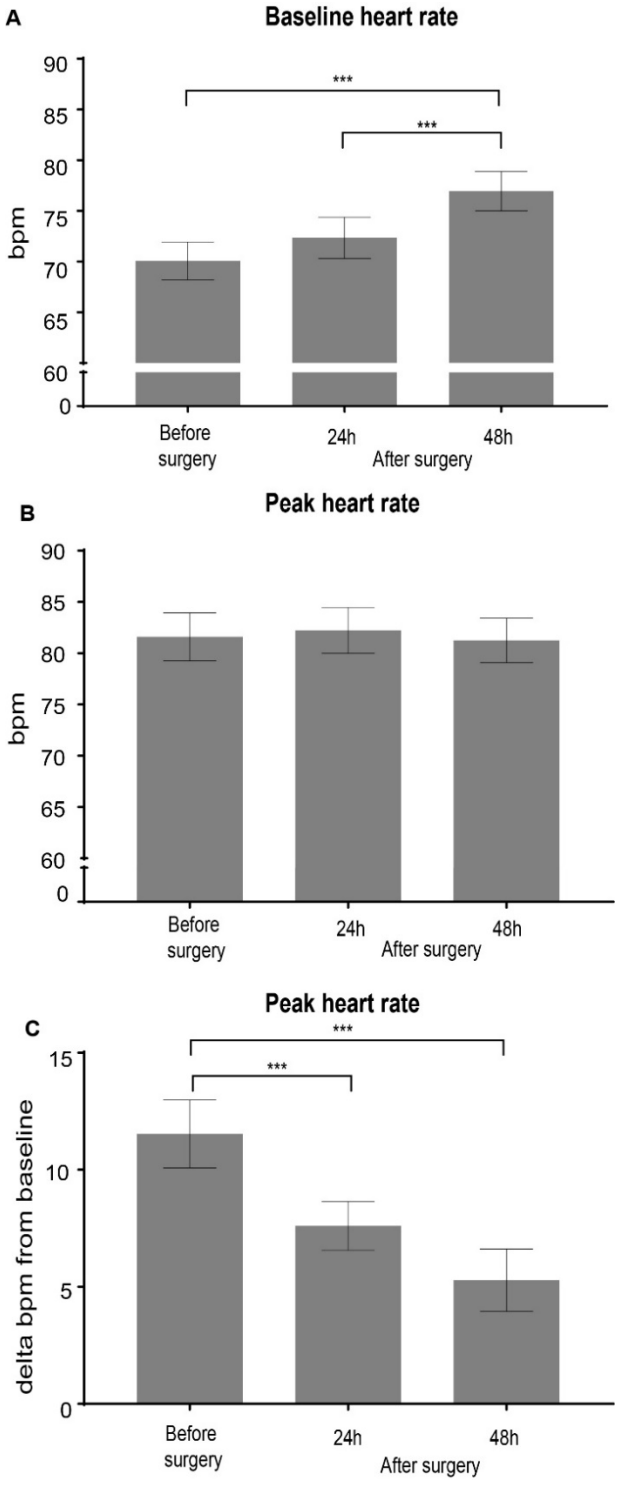

Figure 5.5 Baseline heart rate and peak heart rate

A-C: Baseline HR before orthostatic challenge and peak HR after the challenge. Data are presented as mean values with 95% CI. P value refers to before surgery vs 24 h after surgery, before surgery vs 48 h after surgery, and 24 h vs 48 h after surgery (analysed by mixed-model repeated measures and Bonferroni test). ***P<0.001.

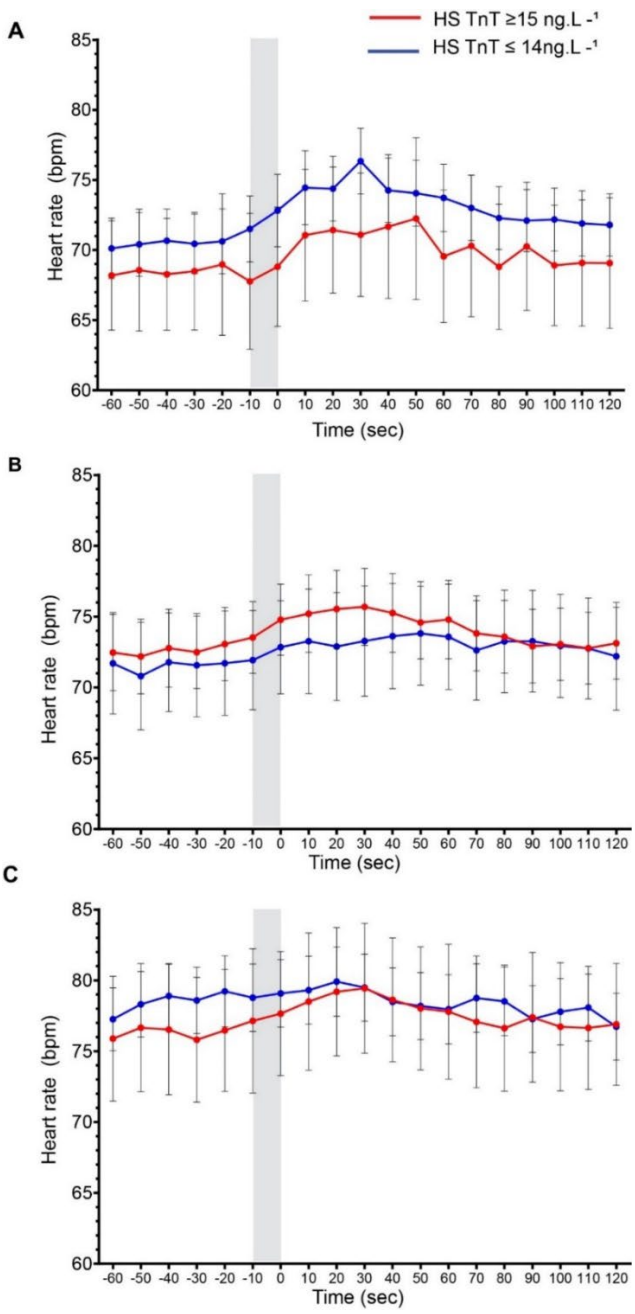

Figure 5.6 : HR changes during standardised orthostatic manouevre

Before surgery (**A**), 24h (**B**) and 48h (**C**) after surgery. Values are mean HR (95% CI) at 10s intervals before and after the standardised manouevre (grey shaded area).

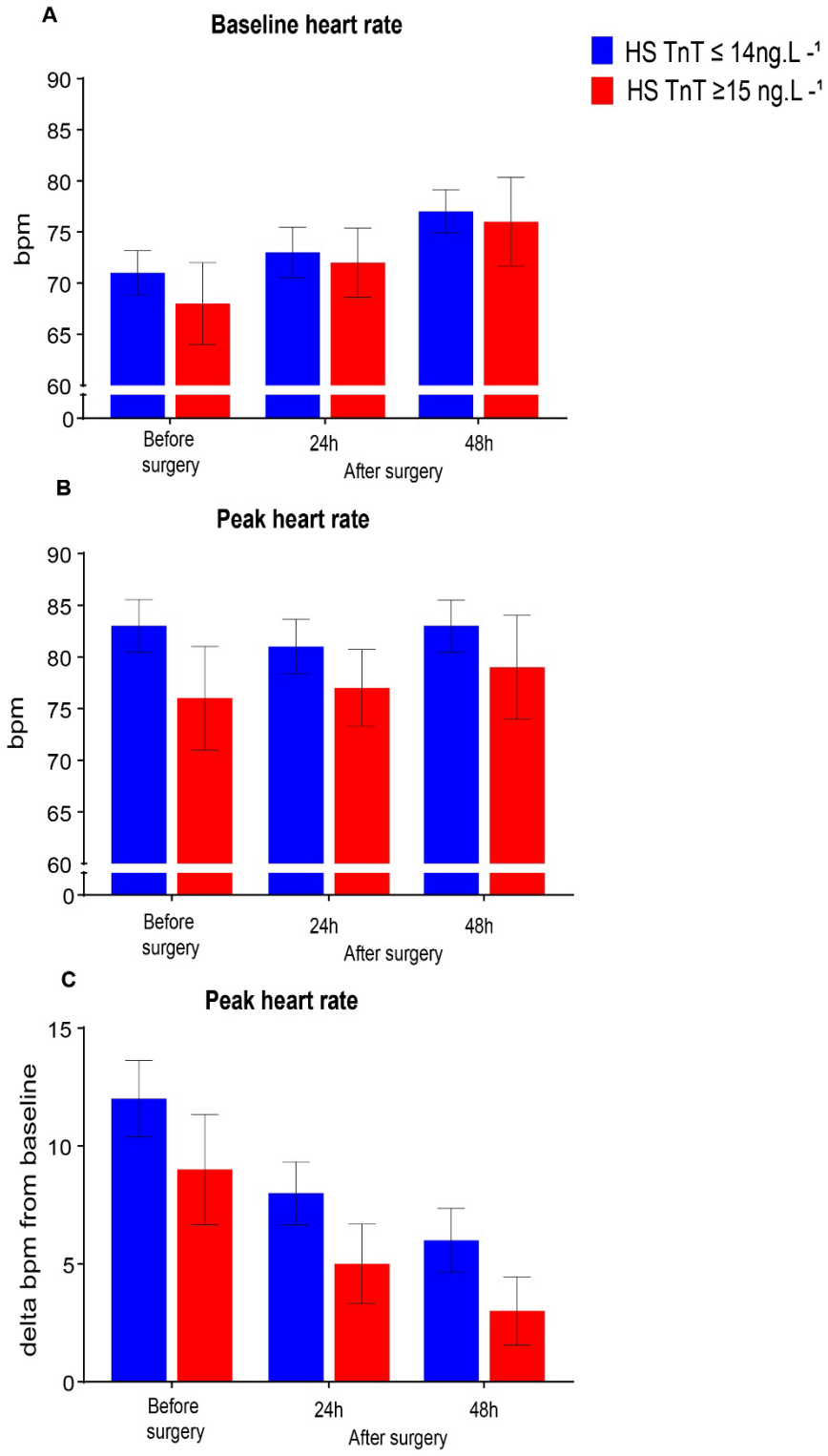

Figure 5.7 Baseline heart rate and peak heart rate

A-C: Baseline HR before orthostatic challenge and peak HR after the challenge. Data are presented as mean values with 95% CI. No statistical significance when analysed by mixed model analysis.

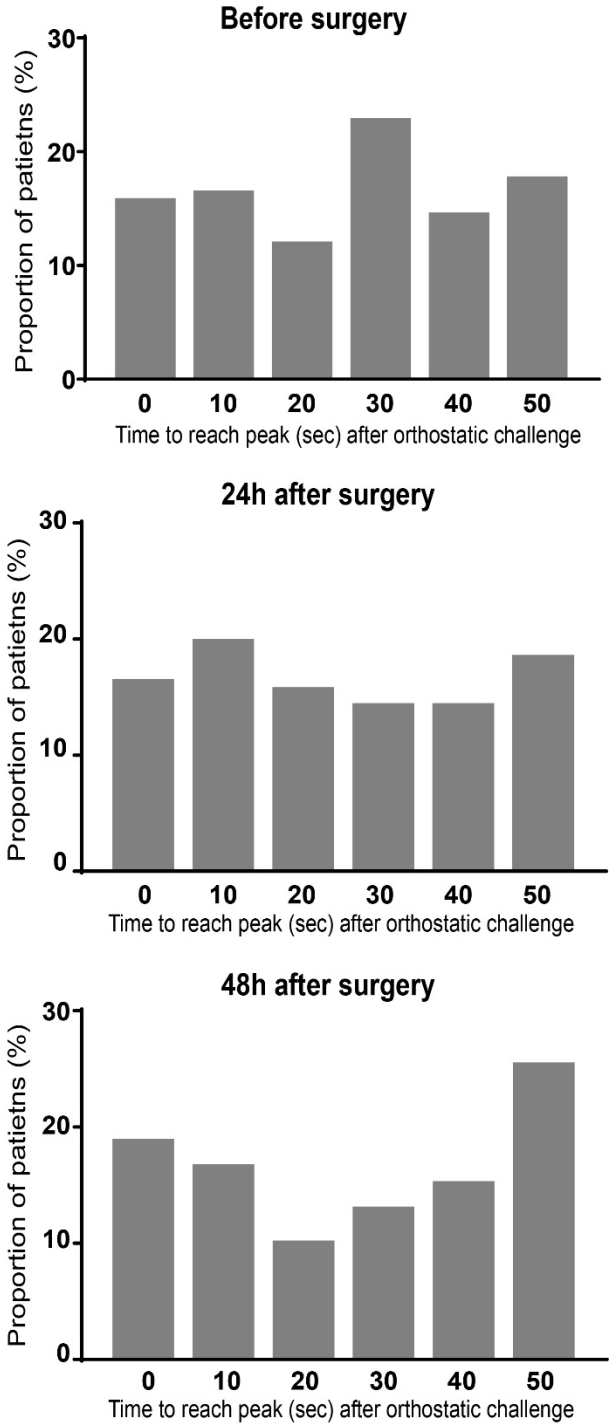

Figure 5.8 Distribution of time(s) to reach peak heart rate

Bar graph indicates proportion of patients reaching peak heart rate at times(s) after orthostatic manoeuvre.

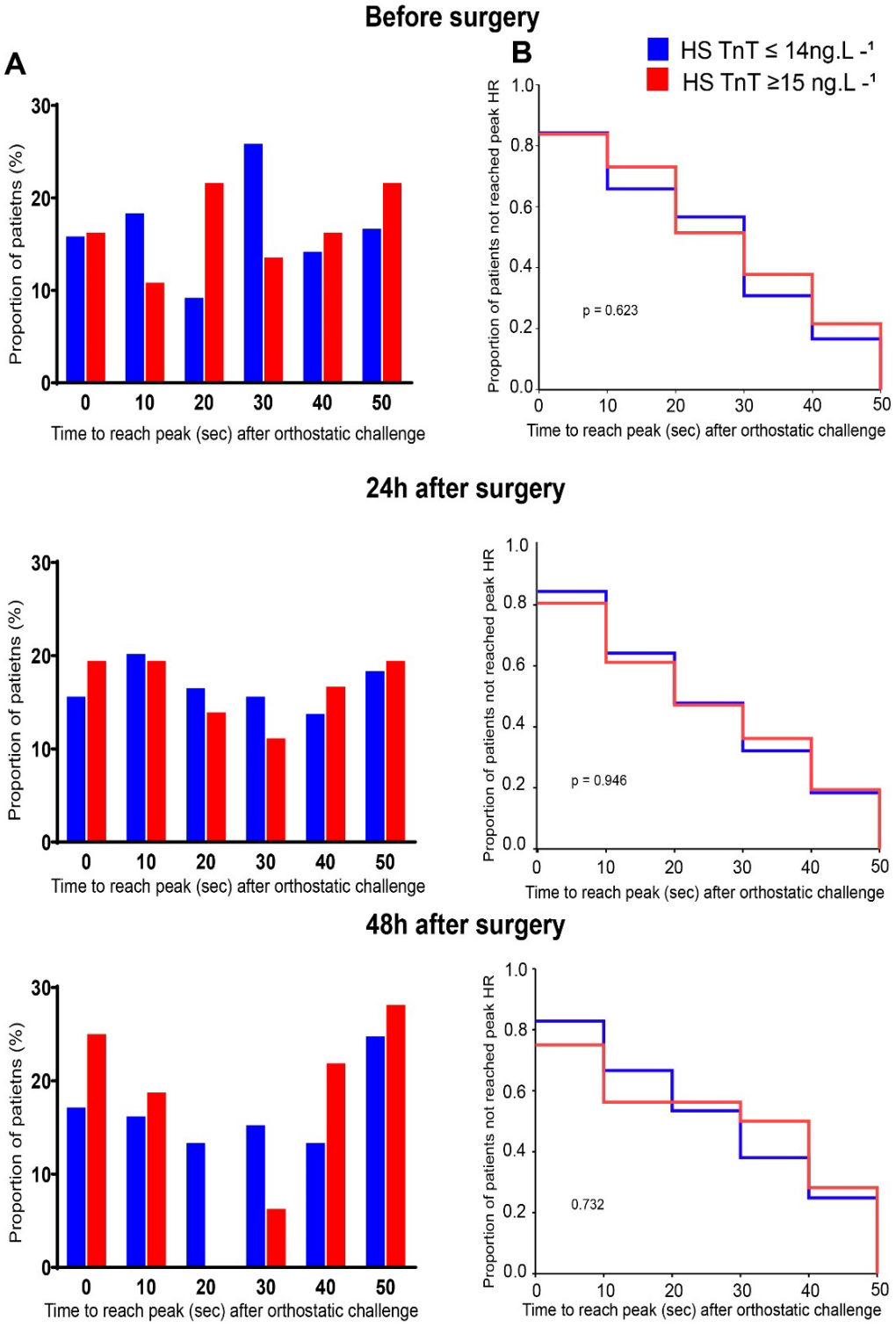

Figure 5.9 Time to reach peak heart rate

A: Bar graph indicates proportion of patients reaching peak heart rate at times(s) after orthostatic manoeuvre. **B**: Comparison of times to reach peak heart rate using log rank test. P>0.05.

5.3.3 Heart rate recovery

The speed of heart rate recovery 0-70s after peak heart rate is shown for all patients in relation to the day of surgery in Figure 5.10. Figure 5.11 shows the speed of heart rate recovery by day of surgery for HSTnT≥15ng.L^{-1} versus HSTnT≤14ng.L^{-1}.

At 24 hours after surgery, HRR at 70s was slower in patients with hsTnT≥15ng.L^{-1} (3 beats $minute^{-1}$ [IQR 1-9]), compared to a faster HRR in patients who remained free of myocardial injury (7 beats $minute^{-1}$ [IQR 1-9]; p = 0.001) (Figure 5.12). However, there was no difference in the speed of HRR after peak heart rate when comparing patients who developed PMI and those who remained free of PMI, either before surgery or at 48 hours after surgery. This result was consistent with the ANCOVA analysis that showed there was a significant effect of PMI on LnHRR at 70s, at 24 hours after surgery when controlling for changes in HR from baseline to peak heart rate for each patient (F[1,144] =7.393, p = 0.007). 24 hours after surgery, the mean (adjusted for the covariant) LnHRR at 70 was slower in patients with hsTnT≥15ng.L^{-1} (0.057 [Standard error +/- 0.079]), compared to a faster HRR in patients who remained free of myocardial injury (0.094 [standard error +/- 0.014]). (Figure 5.13). There was no significant difference observed before surgery and 48h after surgery.

The time constant analysis using the function $Y = A\ exp\ (-XB)$ showed that the peak heart rate (A) after the orthostatic challenge was higher on the day of surgery in patients who remained free of PMI (p = 0.003, randomisation test) (Figure 5.13 and Table 5.1).

The probability levels for the randomisation tests for comparing fitted curves for HR after peak heart rate following orthostatic manoeuvre for participants who had HsTnT ≥15 ngL^{-1} versus

HsTnT ≤14 ng L^{-1} after surgery are shown in Table 5.2. The probability levels for the day of surgery and after surgery are $p<0.05$, meaning the null hypothesis that the curves are equal/coincide can be rejected (Figure 5.13).

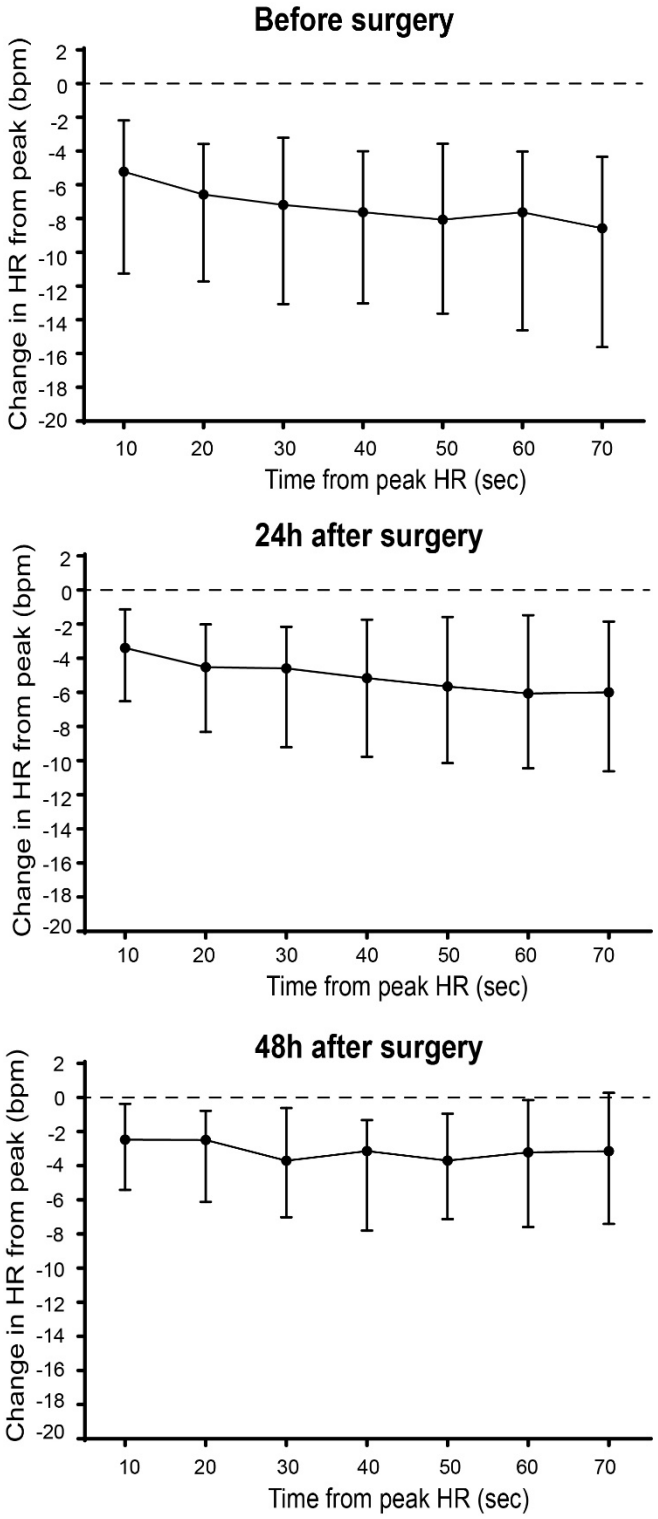

Figure 5.10 Speed of heart rate recovery after orthostatic challenge by day for all patients.

Median (IQR) change in HR (bpm) from peak heart rate for all patients before, 24h and 48h after surgery. Dashed line represents peak heart rate.

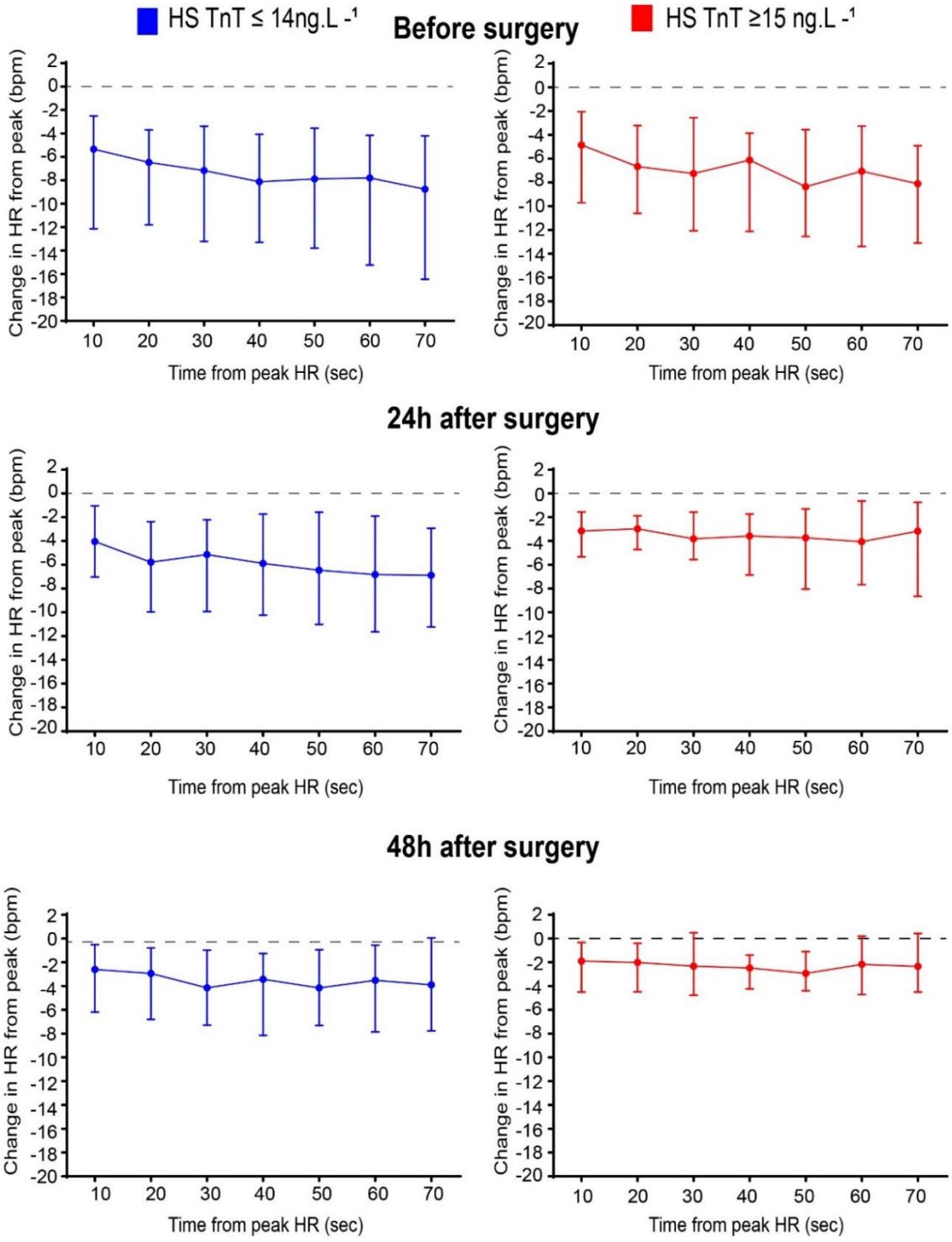

Figure 5.11 Speed of heart rate recovery after the orthostatic challenge before and after surgery for patients who developed PMI (HS TnT ≥ 15ng.L^{-1}) versus those that remained free of PMI (HS TnT ≤14ng.L^{-1}.)

Median (IQR) change in HR (bpm) from peak heart rate for patients who developed PMI and those who remained free of PMI. Dashed line represents peak heart rate.

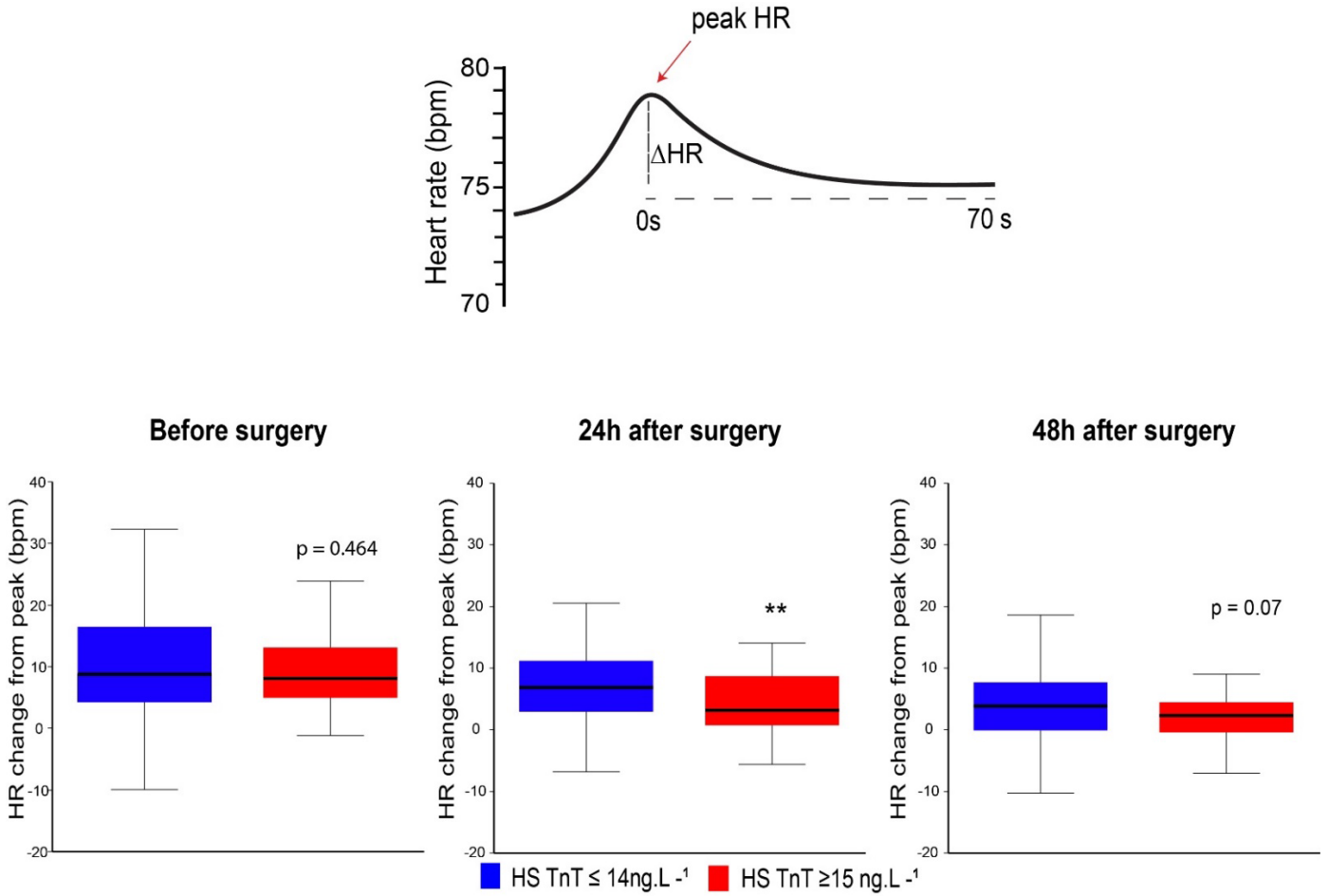

Figure 5.12 Heart rate recovery 70s after peak heart rate

Median (IQR) heart rate recovery values 70s after peak heart rate. P-values refer to HsTnT ≥15 ng L^{-1} vs HsTnT ≤14 ng L^{-1} (Mann-Whitney U test). **P<0.01.

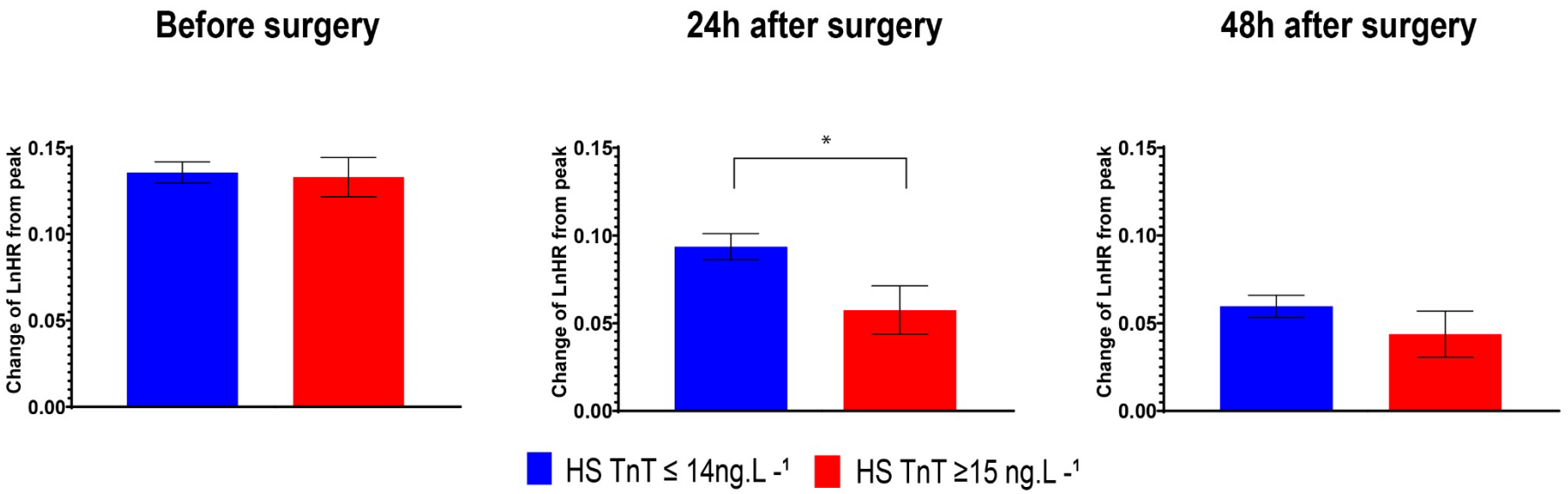

Figure 5.13 Heart rate recovery 70s after peak heart rate; ANCOVA analysis

Data presented are adjusted (ANCOVA) logarithmic transformed mean values with standard error. P values refers to P-values refer to HsTnT ≥15 ng L^{-1} vs HsTnT ≤14 ng L^{-1}. **P<0.01 (T-test for covariate adjusted means).

A

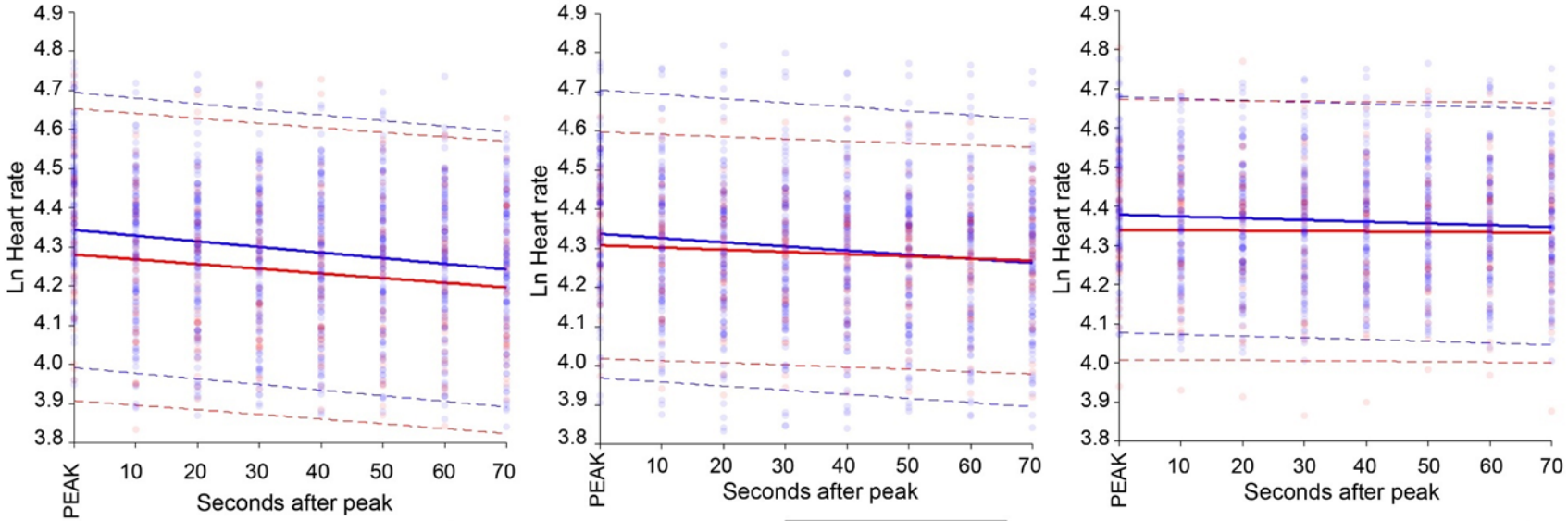

	Model R-squared value
hsTnT ≤14ng L^{-1}	0.03
hsTnT ≥15ng L^{-1}	0.02

	Model R-squared value
hsTnT ≤14ng L^{-1}	0.02
hsTnT ≥15ng L^{-1}	0.01

	Model R-squared value
hsTnT ≤14ng L^{-1}	0.004
hsTnT ≥15ng L^{-1}	0.0002

B Equation parameters for heart rate changes after orthostatic challenge *y = A exp (-BX)*

	HSTnT ≤14ng.L^{-1}		HSTnT≥15ng.L^{-1}	
	A	B	A	B
Before Surgery	4.34 (4.32-4.36)	0.0003 (0.0002-0.0004)	4.28 (4.24-4.32)	0.0003(0.0001-0.0005)
24h after surgery	4.33 (4.31-4.36)	0.0003 (0.0001-0.0004)	4.30 (4.28-4.34)	0.0001(-0.00004 – 0.0003)
48h after surgery	4.38 (4.36-4.40)	0.0001 (0.0000-0.0002)	4.34 (4.30-4.38)	0.00002(-0.0002-0.0002)

HS TnT ≤ 14ng.L -¹
HS TnT ≥15 ng.L -¹

Figure 5.14 Heart rate change after peak heart following orthostatic manoeuvre

A: Fitted curves for HR after peak HR following orthostatic manoeuvre**.** Each dot denotes individual heart rate. Heart rate values were natural logarithm transformed to allow for the exponential curve fit.[213] Solid lines denote fitted curve, $Y = A\ exp\ (-XB)$. Dotted lines denote 95% CI of fitted curve function. The R squared values indicate how well the model works for the data: a value near to zero indicates that the model does not fit the data well. **Red**: HsTnT ≥15 ngL^{-1}. **Blue**: HsTnT ≤14 ng L^{-1}.

B: Table of equation parameters for heart rate changes after orthostatic manoeuvre. Values are mean (95% CI).

Table 5.1 Parameter inequality randomization tests

Comparison of parameters A and B for HR after peak heart rate following orthostatic challenge for patients who had HsTnT ≥15 ng.L^{-1} versus HsTnT ≤14 ng.L^{-1} after surgery.

A is peak heart rate, X is time after peak, and B is the rate of change in heart rate following peak heart rate (decay).

	Parameter A Randomization Probability	Parameter B Randomization Probability
Before surgery	0.003	0.651
24hr after surgery	0.189	0.336
48h after surgery	0.062	0.513

Table 5.2 Curve inequality randomization tests

Comparing fitted curves for HR after peak heart rate following orthostatic manoeuvre for patients who had HsTnT ≥15 ng.L^{-1} versus HsTnT ≤14 ng.L^{-1} after surgery.

	Randomization Probability	No. of points compared along the curve
Before surgery	<0.001	8
24hr after surgery	0.464	8
48h after surgery	0.026	8

5.4 Discussion

5.4.1 Main findings

The primary aim of this part of the XMINS study was to evaluate whether a standardised orthostatic manoeuvre can be used to evaluate heart rate recovery (HRR) in the perioperative setting. The results presented in this chapter demonstrate that, in 157 patients undergoing noncardiac surgery, an orthostatic manoeuvre from the supine to sitting position can be used to elicit heart rate responses that can then be used to quantify HRR. HRR was used as a measure of cardiac vagal activity as part of the baroreceptor reflex, and was compared between patients who developed PMI and those remained free from PMI.

The main findings of the study described in this chapter are:

- An orthostatic challenge can be employed in the perioperative setting to quantity HRR.

- HRR is slower at 24 hours after surgery in patients who develop PMI compared to patients who remain free from PMI.

5.4.2 Orthostatic challenge can be used to quantity HRR in the perioperative setting

This study has demonstrated that an orthostatic manoeuvre can be used to modulate heart rate before and after surgery, which can then be analysed to quantify heart rate recovery. Patient willingness to participate before and after surgery was high, as indicated by participants only

declining to wear a Holter monitor on 42 occasions out of the 567 (7.4%) eligible Holter reading events (Figure 5.3).

5.4.3 HRR is slower at 24 hours after surgery in patients who develop PMI

HRR 70 seconds after the orthostatic challenge was slower in the patients that developed PMI 24h after surgery. This delay in HRR was not observed before surgery or at 48h after surgery. HR changes after a change in posture are mediated by vagal modulation of the sinus node via the unloading and reloading of the arterial baroreflex, and therefore the slower HRR may reflect early loss of vagal modulation after surgery. Therefore the orthostatic challenge is able to assess cardiac vagal activity in response to dynamic physiological changes. The HRV analysis is unable to do this as measurements are taken at a resting state. The loss of vagal modulation of heart rate may also be inferred to signify a loss of other protective mechanisms that the vagus nerve provides the heart during surgery. These mechanisms have already been outlined in Introduction Section 1.6 and in the Discussion of Chapter 4. The association of delayed HRR with PMI is consistent with a clinical study in which baroreceptor insensitivity was associated with increased cardiovascular complications after surgery.[348] In this study, Toner et al[348] measured baroreflex dysfunction using the spontaneous baroreflex sensitivity (BRS) method. Baroreflex dysfunction (BRS <6mmHg s^{-1}) after surgery was associated with cardiovascular morbidity (RR 2.39 (95% CI: 1.22–4.71), p=0.008).

There was no difference in HRR values at 70s when measured before surgery between patients who developed PMI and those that remained free of PMI. This observation is not consistent with previous studies examining HRR after CPET prior to noncardiac surgery, where HRR was

calculated as the difference between heart rate at the end of the exercise and heart rate 1 minute after recovery.[217, 218]

Abbott et al[217] showed that HRR<12bpm before surgery was associated with PMI after noncardiac surgery (OR 1.54 (CI 95%1.11-2.13 p=0.009). Similar results were observed in a secondary analysis of two observational studies where impaired HRR before surgery was associated with increased risk of cardiovascular morbidity after noncardiac surgery (RR 1.39 (CI 95% 1.15-1.69) p = <0.001).[217]

However, the randomisation tests for curve fitting equality would suggest that curves for the modulation of heart rate between the patients who develop PMI and those who remain free are unequal before surgery (Table 5.1). This may reflect a higher peak heart rate after the orthostatic manoeuvre in patients who did not develop PMI (Table 5.1; A variable, p =0.003).

5.4.4 Strengths and limitations of the study

A strength of the study was that peak heart rate following the orthostatic challenge was identified for each individual patient. In a previous population study, HRR was measured as the delta HR from 10 to 20 seconds after the orthostatic challenge.[221] The previous study made two assumptions: firstly, that peak heart rate occurs immediately following the completion of the orthostatic challenge; and secondly, that peak heart rate is achieved at the same time for each patient. The distribution of times to reach peak heart rate in this study, as shown in Figure 5.8, clearly shows that the time to reach peak heart rate is not uniform for all patients. This lack of uniformity is consistent with a population cohort study that showed variation in haemodynamic responses to an orthostatic challenge across 4475 participants.[282] The patient-

specific, individual selection of peak heart rate within 50 seconds of the orthostatic manoeuvre, provided a more accurate calculation of HRR for each individual patient. However, it is recognised that smoothing HR over 3 minutes and then binning into 10s when analysing the time course of HR recovery may have minimised the peak amplitude (heart rate) detection and may have potentially prolonged the time course of recovery.

The selection of 70 seconds after the orthostatic manoeuvre as a threshold to assess HRR requires further evaluation as it was necessarily curtailed by the length of HR recordings. This could be achieved by comparing against the "gold-standard" exercise-induced HRR calculated with CPET in patients before surgery.

The small effect on the curve fitting parameters (Table 5.1) between PMI groups may reflect the nature of the orthostatic manoeuvre employed in this study. This is not surprising, as smaller differences in heart rate responses between passive (head-up tilt to 70-degrees) and standing manoeuvres have previously been observed in healthy volunteers.[41] A lying-to-standing orthostatic manoeuvre also elicits a more significant drop in blood pressure compared to supine-to-sitting, and therefore a greater challenge (offloading) to the baroreceptor reflex.[388] However, as previously highlighted in General Methods Section 2.8, it would not be practical to perform a standing orthostatic manoeuvre for all patients after major surgery. It is also recognised that the exponential decay equation may be a gross simplification of the autonomic components influencing change in heart rate after an orthostatic challenge.[213] This is reflected in the low R-squared values, which indicate a poor curve fit.

A further limitation of the study was that HR was the only cardiovascular variable captured during the manoeuvre in real time. Beat-to-beat arterial blood pressure measurements were

not measured. Beat-to-beat blood pressure monitoring using invasive arterial blood pressure measurement would not be clinically justifiable for all patients undergoing major noncardiac surgery. A possible alternative to allow the non-invasively measurement of beat-to-beat arterial blood pressure is the use of a device that utilises Finapres technology.[388]

Although successfully demonstrated that an orthostatic manoeuvre can be used to modulate heart rate before and after surgery, it should also be noted that there are some drawbacks to performing an orthostatic challenge in the perioperative period. The procedure is time consuming and requires dedicated personnel with holter monitoring equipment expertise. Currently, intensive manual analysis is required to analyse HRR that, as shown in this analysis, has large variance in measure and a small signal.

The impracticality of using the Model 2232 adjustable bed before and after surgery is a limitation of performing protocols in a perioperative clinical environments. However attempts were made to mitigate for this by standardising the time to achieve the change in posture (i.e. 10s).

5.4.5 Conclusions

Using a real-time orthostatic challenge before and after surgery, the study has demonstrated that delayed HRR is associated with perioperative myocardial injury.

Chapter 6
Conclusions and future work

6.1 Summary of key findings

Elevated troponin after surgery is a biomarker for poor outcomes after noncardiac surgery.[64] Given the frequent apparent absence of clinical myocardial ischemia, the rationale for why this should be the case remains unclear. Very modest increases in high-sensitivity troponin levels within 24 hours of noncardiac surgery have been demonstrated to precede subsequent morbidity and mortality in up to ~25% patients.[64, 70] Unravelling the enigma of why early elevated troponin occurs, and how it may be linked to cardiovascular and non-cardiovascular complications, may elucidate the underlying mechanisms that cause a substantial subset of patients to experience a more complicated recovery or death after noncardiac surgery.

Although an elevated troponin is useful in identifying those patients who have developed myocardial injury, and are at increased risk of morbidity and mortality, troponin alone cannot be used to explain why myocardial injury occurs. High sensitivity tests can detect very low concentrations of troponin that may represent causes of myocardial injury other than ischaemia (General Introduction 1.3.5).

To investigate whether a rise in troponin after surgery simply represents occult ischaemic episodes, this thesis explored whether molecular microRNA signatures that are common and specific for acute coronary syndrome and ischaemia, can be detected before and after surgery. MicroRNA are small non-coding RNA molecules which are synthesised in the nucleus of cells

and regulate post-translational gene expression. They are released by injured tissue and can be detected and quantified in the plasma or serum. MicroRNA signatures exist for acute coronary syndrome and have been investigated both as potential biomarkers and as tools to better understand the underlying pathophysiology. I therefore hypothesised that if perioperative myocardial injury and acute coronary syndrome share pathophysiological mechanisms (i.e., ischaemia), they should therefore share common microRNA signatures.

MicroRNA expression level was quantified before and after surgery using real-time polymerase chain reaction with robust quality controls. Patients were matched for age, sex and revised cardiac risk index score. Assuming the hypothesis to be true, the expectation was to observe the same microRNA signature in the PMI group as is seen in ACS. However, after mixed model analysis, changes in the expression levels of microRNA associated with ACS (hsa-miR-1-3p, hsa-miR-133a-3p and hsa-146a-5p) were similar in both patients who developed PMI and those that remained PMI-free. This suggested that these microRNA are features of generalised stress or injury in response to surgery rather than myocardial ischaemia. The increase after surgery in detected levels of cardiomyocyte enriched microRNAs, hsa-miR-499a-5p and hsa-208b-5p, in patients who had developed myocardial injury, indicates that cardiac injury has occurred at these low troponin concentrations.

Pathway analyses (DIANA miRPath v3.0.) identified signalling pathways associated with cellular stress: these included adrenergic signalling in the cardiomyocyte, and the regulation of cardiomyocyte calcium homeostasis (NCX1 (sodium/calcium exchange transporter) encoded by the SLC8A1 gene). The pathway analysis therefore suggests that the changes in microRNA expression reflect a generalised cardiac adrenergic stress response during noncardiac surgery in all patients, that is independent of an elevated troponin.

However, it remains the case that some of these patients do have a raised troponin, and these patients have an increased risk of morbidity and mortality. I therefore postulated that, whilst all patients experience a generalised cardiac adrenergic stress response, troponin release only occurs in patients who lack the necessary protective compensatory mechanisms to cope with the physiological stress of surgery.

As outlined in the Introduction, the vagus nerve can confer protection against the adrenergic stimulation which occurs during the physiological stress of surgery. It has also been previously demonstrated that pre-existing vagal dysfunction is associated with elevated troponin after surgery.[217] Experimental data demonstrate that increasing cardiac vagal activity maintains normal calcium handling after myocardial injury by restoring function of NCX^{350} and limits myocardial damage.[371] It has not been previously demonstrated that the loss of cardiac parasympathetic activity is associated with an elevated troponin in the perioperative period. I therefore hypothesised that an acquired loss of protective cardiac vagal signalling promotes troponin elevation after noncardiac surgery.

To test this hypothesis, serial cardiac autonomic measurements were made using 5-minute ECG recordings. Measurements were taken before and after noncardiac surgery so that each patient could serve as their own control. Efferent cardiac vagal activity was quantified by heart rate, heart rate variability and heart rate recovery after a standardised orthostatic manoeuvre. Both measures found that cardiac vagal activity, as measured by high frequency power domain and heart rate recovery, was reduced 24 hours after surgery in patients who developed PMI. The loss of cardiac vagal activity within 24 hours of noncardiac surgery would support the hypothesis that it is the loss of compensatory mechanisms that contributes to the early

development of an elevated troponin. The loss of compensatory vagal mechanisms may also explain why an early rise in troponin after surgery has been shown to be associated with increased postoperative morbidity and requirement for intensive care interventions.[70]

Viewed together, the temporal changes in microRNA expression perioperatively and the loss in cardiac vagal tone indicate that a more considered approach is required when interpreting an elevated troponin after surgery; the results also reveal novel potential mechanisms contributing to perioperative myocardial injury, and challenge the assumption that PMI has a purely ischaemic aetiology. The conclusions can be summarised as a refined hypothesis for the development of perioperative myocardial injury (Figure 6.1). Adrenergic stress is a common feature of the perioperative period, which can lead to the release of specific microRNA from cardiomyocytes. In individuals that are at higher risk of having an elevated troponin after surgery (e.g., older patients, patients with heart failure or renal disease), pre-existing or acquired loss of cardioprotective vagal signalling promotes the likelihood of calcium overload from adrenergic stimulation during the perioperative period. This results in myocardial dysfunction and cell apoptosis which manifests clinically as an elevated troponin in the plasma or serum.[344]

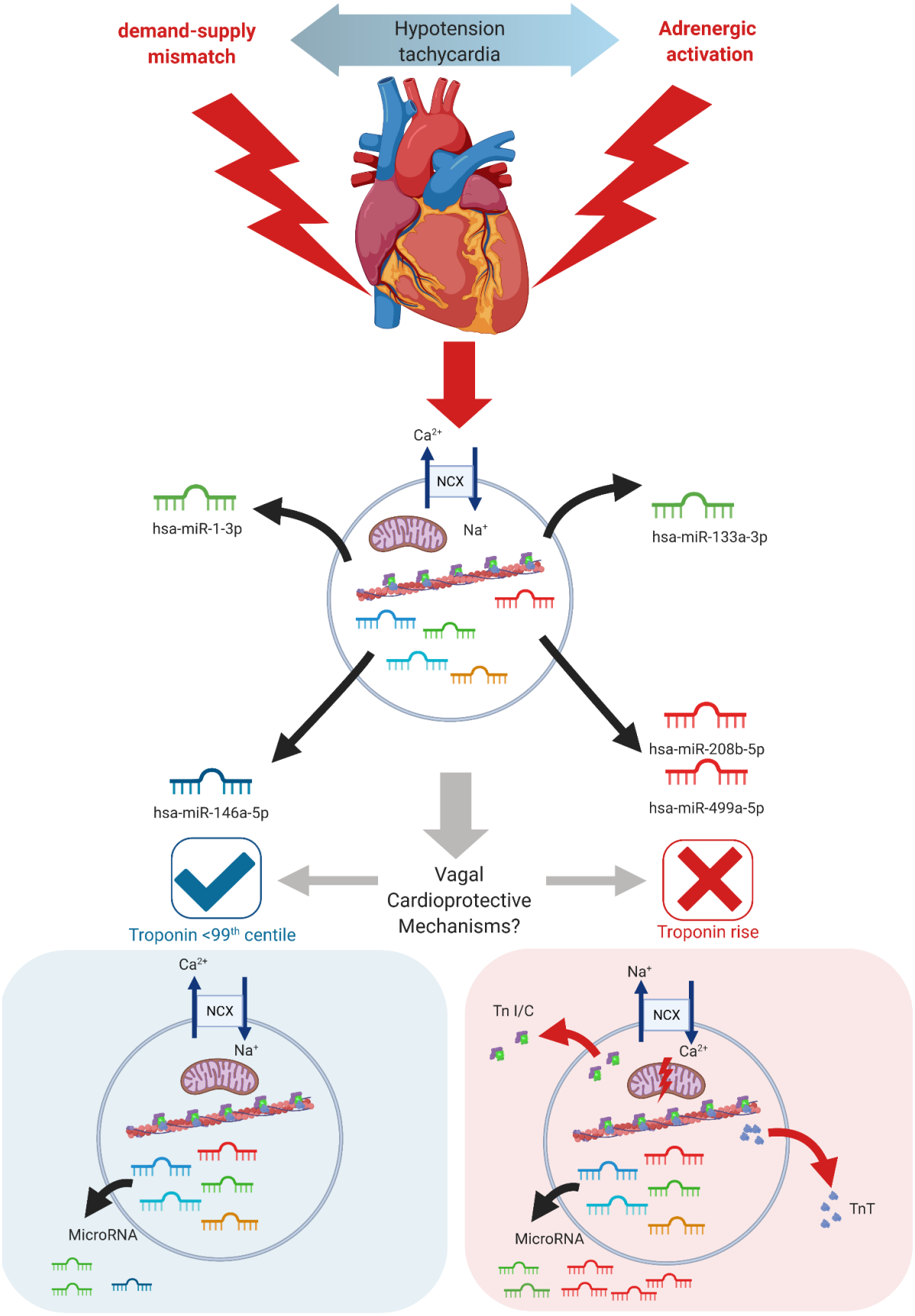
demand-supply mismatch
Hypotension tachycardia
Adrenergic activation
Ca2+
NCX
Na+
hsa-miR-1-3p
hsa-miR-133a-3p
hsa-miR-208b-5p
hsa-miR-499a-5p
hsa-miR-146a-5p
Vagal Cardioprotective Mechanisms?
Troponin <99th centile
Troponin rise
MicroRNA
Tn I/C
TnT

Figure 6.1 Potential mechanisms contributing to perioperative myocardial injury

This figure summarises the microRNA findings in the potential role for cardioprotection. hsa-miR-1-3p, hsa-miR-133a-3p and hsa-146a-5p expression changes are common to all patients undergoing noncardiac surgery. The expression of hsa-miR-499a-5p and hsa-208b-5p increases after surgery in patients who develop PMI. Adrenergic stress is a common feature of the perioperative period, leading to the release of these microRNA from cardiomyocytes. In individuals at greatest risk of elevated troponin, the pre-existing or acquired loss of parasympathetic cardioprotective signalling promotes the likelihood of calcium overload from adrenergic stress, resulting in mitochondrial dysfunction and cell apoptosis. This myocardial injury manifests itself clinically by a rise in Troponin I or T in the plasma.

Tn I: Troponin I; Tn C: Troponin C; TnT: Troponin T; NCX, sodium-calcium exchanger.

To test this hypothesis, further work is required to assess the microRNA investigated in this thesis in murine models of cardiac injury and noncardiac surgery. In addition, it should also be determined if other microRNA, not confined to the cardiovascular literature, are implicated in PMI. The role of these microRNA and those evaluated in this thesis should be investigated in loss of function models to explore other potential mechanisms underlying myocardial injury. The identification of new therapeutic targets by these novel insights into the underlying pathophysiological mechanisms provides an opportunity for the development of treatments which might reduce postoperative morbidity.

Postoperative surveillance of troponin after surgery has been recommended by the Canadian Cardiovascular Society. In their 2017 guideline, "perioperative cardiac risk assessment and management for patients who undergo noncardiac surgery", it was recommended that patients at risk of cardiovascular complications should have daily troponin measurements 48-72hr after surgery.[103] The potential benefits of such surveillance would be to improve the survival of patients that experience a myocardial infarction after surgery where failure to rescue after an MI is estimated to be 1 in 5.[389] This would be achieved by targeting resources such as cardiac monitoring and interventions such as invasive coronary angiogram towards patients with a rise in troponin after surgery. The recommendations are a result of the findings in the prospective observational VISION study, where a raised troponin after surgery was associated with an increased risk of morbidity and mortality[3]. However, measurement of troponin after surgery is not routinely performed clinically in the perioperative setting outside of research studies. The main reasons for this are considerable gaps in the evidence that have been highlighted in a recent expert consensus review on perioperative myocardial injury screening in noncardiac surgery by Puelacher et al in 2021.[58] As was highlighted in the introduction to this thesis, there is no consensus for the definition of PMI and the thresholds for troponin assays to diagnose it.

There is no evidence for the utility of targeted management strategies and their cost effectiveness in the perioperative setting. The assumption made by the authors of both the VISION study and the Canadian Cardiovascular Society guideline is that a rise in troponin is caused by myocardial injury of an asymptomatic ischaemic aetiology, also known as MINS (myocardial injury after noncardiac surgery). The results in this thesis have demonstrated that a more considered approach is required when interpreting an elevated troponin after surgery and that the assumption that myocardial injury is ischaemic, made with the MINS definition, is misleading. In view of the lack of evidence for interventional management strategies, the lack of consensus for the definition of PMI, and the ongoing research to fully elucidate the mechanism of PMI, it would be premature to implement a guideline advocating postoperative troponin surveillance.

Finally, as a non-invasive assessment of parasympathetic function, the orthostatic manoeuvre allows for the identification of patients at risk of troponin rise and therefore increased risk of morbidity and mortality, but requires further validation. The details of potential future work and therapeutic avenues are outlined in the next section.

6.2 Future work

6.2.1 Next generation sequencing

The microRNA investigated in this thesis are limited to six cardiac-specific microRNA. The limited selection cannot exclude the possibility that other microRNA may be significant in patients with an elevated troponin after surgery. A discovery technique such as next generation sequencing (NGS) could be utilised to identify novel microRNAs associated with PMI after noncardiac surgery. NGS is a term used to describe a range of new techniques that are used to sequence RNA or DNA at a high throughput, and are more efficient than the previous Sanger's sequencing technique. The technology analyses small fragments of DNA or RNA in parallel, and then uses bioinformatics to map these small fragments to a reference genome, such as the human genome. The advantage of using NGS is that it confers high accuracy in detecting microRNA in a low yield sample such as plasma, and can aid in the discovery of new microRNA. [253]

Collaborative work by our research laboratory has used next generation sequencing on 11 samples taken after surgery, and has been used to compare patients with and without PMI. To identify further mechanistic pathways, it would be beneficial to extend this work and replicate the experimental design utilised in Chapter 3. This would involve sequencing samples taken before and after noncardiac surgery, allowing the identification of microRNA that are up- or down-regulated after the insult of surgical stress. A major limiting factor to implementing this work is the very high cost of the NGS technique.[253]

6.2.2 Murine experimental models

Knockout models are in development in which the m2AchR receptor can be targeted and silenced: m2AchR floxed mice are injected with adeno-associated virus to deliver Cre-recombinase under the control of a cardiac-specific promoter such as cTnT.[390] This knockout model will allow for the longitudinal assessment of the effects of reduced cardiac vagal function before and after a surgical intervention in a controlled environment. Other methodologies are available to assess the effects of increasing cardiac vagal activity: optogenetically stimulating the DMNV has been shown to preserve left ventricular function after acute myocardial infarction in rats.[391] These animal models could be used with a noncardiac surgical protocol to assess cardiac vagal activity and its association with perioperative myocardial injury after noncardiac surgery. In addition, microRNA PCR panels with selected microRNA could be used to assess changes in microRNA expression within cardiac tissue and circulating plasma and serum.

6.2.3 Antimirs

MicroRNA loss of function studies could be used to further interrogate the function of the microRNA that demonstrated changes in expression after noncardiac surgery. An example of one such loss of function technique is the "silencing" of microRNA in vivo, using chemically engineered microRNA known as antimiRs.[392] AntimiRs are single stranded oligonucleotides that bind to mature microRNA in competition with the cellular targets of the microRNA, and prevent loading onto the RISC complex (General Introduction 1.4.3).[393] This leads to the functional inhibition of the microRNA and its mRNA targets.

Experimentally, antimiRs have been used to demonstrate both microRNA function and their potential in their own right as a therapeutic intervention. Cardiac miR-1 levels have been shown to increase after myocardial infarction in rats, increasing the risk of pathogenic arrythmia by targeting ion channels GJA1 (encodes connexin 43, responsible for intracellular conductance in ventricles) and KCNJA (encodes Kir2.1, main K^+ channel subunit).[140] By using the antimiR for miR-1 to reduce miR-1 levels, ischaemic arrythmias were inhibited after myocardial infarction.[140] Intravenous injection of antimiR-208 over 6 weeks into rats subjected to hypertension-induced heart failure prevented cardiac remodelling, and improved cardiac function and survival.[394] The authors of this study were also able to demonstrate that sustained inhibition of miR-208, using antimiR-208, led to reduced expression of the myosin heavy chain in the cardiomyocyte. In a study investigating the role of miR-34, a microRNA involved in apoptosis, mice were injected with the antimiR Ant-34. The investigators were able to demonstrate that Ant-34 reduced cardiac expression of miR-34. They then induced an acute myocardial infarction in the mice and found that contractility was greater in mice treated with Ant-34. Histological findings confirmed that Ant-34 reduced cell death and fibrosis following acute myocardial infarction.[149]

These studies demonstrate the potential of antimiRs, together with loss of function experiments, to elucidate microRNA function. Known cardiac microRNA and microRNA identified from NGS could be inhibited using antimiRs in a murine model of noncardiac surgery, to better understand the role of microRNA and the underlying cellular mechanisms involved in surgical cardiac stress and the development of PMI.

AntimiRs could also be deployed as a therapeutic intervention. Phase I and phase II trials are in progress for diseases such as hepatitis C (miR-122), multiple cancers (miR-155), Alport

syndrome (miR-21), and heart failure (miR-132).[395] Further investigation into microRNA function and cellular targets in PMI may reveal new therapeutic avenues to reduce postoperative morbidity.

6.2.4 *Orthostatic manoeuvre validation*

The orthostatic manoeuvre utilised in this thesis is a potential alternative test to assess parasympathetic function based on heart rate recovery. Previous work has shown that CPET testing can be used to quantify heart rate recovery[214] and that delayed heart rate recovery is associated with PMI and post-operative morbidity.[217] However, CPET testing is expensive, resource-intensive, and there is usually limited time and opportunity before surgery to perform testing. To adopt the highly scalable and reproducible orthostatic test as a diagnostic test for cardiac parasympathetic function, it would be prudent to validate the autonomic response to a standardised orthostatic manoeuvre, as demonstrated in this thesis, against CPET-evoked heart rate recovery measures.

The lying to sitting methodology was adopted for this thesis as it allowed assessment of the manoeuvre throughout the perioperative period. Previous studies assessing orthostatic manoeuvres/challenges have used a lying to standing manoeuvre,[221] which may elicit a more robust autonomic response to the postural change.[41] Therefore it may be useful to validate a lying to standing manoeuvre and a lying to sitting manoeuvre against CPET HRR to assess the robustness of the various autonomic responses.

6.2.5 Perioperative autonomic neuromodulation.

The results in this thesis have demonstrated that a loss of cardiac efferent vagal activity is associated with PMI. Experimental studies have shown that preserving vagal nerve activity is cardioprotective (General Introduction 1.6). It is therefore feasible that increasing or preserving vagal activity in the perioperative period may reduce myocardial injury. Vagal nerve stimulation can be achieved via the costly and invasive technique of implanting cervical vagal nerve stimulators, or the non-invasive and cheaper methods of transcutaneous auricular or cervical nerve stimulation.[396] A recent systematic review and meta-analysis by Patel et al. showed that non-invasive neuromodulation strategies, aimed at preserving vagal activity in non-surgical clinical settings, have the potential to reduce perioperative organ injury, i.e., myocardial injury.[397] However their conclusions were limited, due to the low quality in study design and lack of concordance with minimum reporting standards.[396]

There is therefore an unmet need for definitive clinical studies in the perioperative period that are well designed and meet recommended reporting standards. This would facilitate testing the hypothesis that preserving or increasing vagal activity by non-invasive vagal nerve stimulation can prevent or limit perioperative myocardial injury.

References

1. Weiser, T.G., et al., Estimate of the global volume of surgery in 2012: an assessment supporting improved health outcomes. The Lancet, 2015. 385: p. S11.
2. International Surgical Outcomes Study, g., Global patient outcomes after elective surgery: prospective cohort study in 27 low-, middle- and high-income countries. Br J Anaesth, 2016. 117(5): p. 601-609.
3. Vascular Events in Noncardiac Surgery Patients Cohort Evaluation Study, I., Association between complications and death within 30 days after noncardiac surgery. CMAJ, 2019. 191(30): p. E830-E837.
4. Herring, N., D.J. Paterson, and J.R. Levick, Levick's introduction to cardiovascular physiology. Sixth edition. ed. 2018, Boca Raton, FL: CRC Press.
5. Greaser, M.L. and J. Gergely, Purification and properties of the components from troponin. J Biol Chem, 1973. 248(6): p. 2125-33.
6. Rang, H.P., et al., Rang & Dale's pharmacology. Eighth edition. ed. 2016, United Kingdom: Churchill Livingstone.
7. Hamill, R.W., R.E. Shapiro, and M.A. Vizzard, Chapter 4 - Peripheral Autonomic Nervous System, in *Primer on the Autonomic Nervous System (Third Edition)*, D. Robertson, et al., Editors. 2012, Academic Press: San Diego. p. 17-26.
8. Kalia, M. and M.M. Mesulam, Brain stem projections of sensory and motor components of the vagus complex in the cat: I. The cervical vagus and nodose ganglion. J Comp Neurol, 1980. 193(2): p. 435-65.
9. Kalia, M. and J.M. Sullivan, Brainstem projections of sensory and motor components of the vagus nerve in the rat. J Comp Neurol, 1982. 211(3): p. 248-65.
10. Berthoud, H.R. and W.L. Neuhuber, Functional and chemical anatomy of the afferent vagal system. Auton Neurosci, 2000. 85(1-3): p. 1-17.
11. Taylor, E.W., D. Jordan, and J.H. Coote, Central control of the cardiovascular and respiratory systems and their interactions in vertebrates. Physiol Rev, 1999. 79(3): p. 855-916.
12. Bieger, D. and D.A. Hopkins, Viscerotopic representation of the upper alimentary tract in the medulla oblongata in the rat: The nucleus ambiguus. Journal of Comparative Neurology, 1987. 262(4): p. 546-562.
13. Gourine, A.V., et al., Cardiac vagal preganglionic neurones: An update. Auton Neurosci, 2016. 199: p. 24-8.
14. Altschuler, S.M., et al., The central organization of the vagus nerve innervating the colon of the rat. Gastroenterology, 1993. 104(2): p. 502-509.
15. Powley, T.L., Vagal circuitry mediating cephalic-phase responses to food. Appetite, 2000. 34(2): p. 184-8.
16. Drew, R.C. and L.I. Sinoway, Chapter 36 - Autonomic Control of the Heart, in *Primer on the Autonomic Nervous System (Third Edition)*, D. Robertson, et al., Editors. 2012, Academic Press: San Diego. p. 177-180.
17. Coote, J.H., Myths and realities of the cardiac vagus. J Physiol, 2013. 591(17): p. 4073-85.
18. Massari, V.J., T.A. Johnson, and P.J. Gatti, Cardiotopic organization of the nucleus ambiguus? An anatomical and physiological analysis of neurons regulating atrioventricular conduction. Brain Research, 1995. 679(2): p. 227-240.
19. Machhada, A., et al., Control of ventricular excitability by neurons of the dorsal motor nucleus of the vagus nerve. Heart Rhythm, 2015. 12(11): p. 2285-93.

20. Machhada, A., et al., Vagal determinants of exercise capacity. Nat Commun, 2017. 8: p. 15097.
21. Gilbey, M.P., et al., Synaptic mechanisms involved in the inspiratory modulation of vagal cardio-inhibitory neurones in the cat. J Physiol, 1984. 356: p. 65-78.
22. Anrep, G.V., W. Pascual, and R. Rossler, Respiratory Variations of the Heart Rate. II.--The Central Mechanism of the Respiratory Arrhythmia and the Inter-Relations between the Central and the Reflex Mechanisms. Proceedings of the Royal Society of London. Series B, Biological Sciences, 1936. 119(813): p. 218-230.
23. Japundzic, N., et al., Spectral analysis of blood pressure and heart rate in conscious rats: effects of autonomic blockers. Journal of the Autonomic Nervous System, 1990. 30(2): p. 91-100.
24. Paton, J.F.R. and A.E. Pickering, Chapter 31 - Cross-talk Between Body Systems: Respiratory-Cardiovascular Coupling in Health and Disease, in *Primer on the Autonomic Nervous System (Third Edition)*, D. Robertson, et al., Editors. 2012, Academic Press: San Diego. p. 151-155.
25. Farmer, D.G., et al., Brainstem sources of cardiac vagal tone and respiratory sinus arrhythmia. J Physiol, 2016. 594(24): p. 7249-7265.
26. Spyer, K.M., Annual review prize lecture. Central nervous mechanisms contributing to cardiovascular control. J Physiol, 1994. 474(1): p. 1-19.
27. Hayano, J., et al., Respiratory Sinus Arrhythmia. Circulation, 1996. 94(4): p. 842-847.
28. Lewis, M.E., et al., Vagus nerve stimulation decreases left ventricular contractility in vivo in the human and pig heart. J Physiol, 2001. 534(Pt. 2): p. 547-52.
29. Saternos, H.C., et al., Distribution and function of the muscarinic receptor subtypes in the cardiovascular system. Physiol Genomics, 2018. 50(1): p. 1-9.
30. Coote, J.H. and R.A. Chauhan, The sympathetic innervation of the heart: Important new insights. Auton Neurosci, 2016. 199: p. 17-23.
31. Mohl, M.C. and R.M. Graham, Chapter 9 - α1-Adrenergic Receptors, in *Primer on the Autonomic Nervous System (Third Edition)*, D. Robertson, et al., Editors. 2012, Academic Press: San Diego. p. 51-54.
32. Wang, Q., Chapter 10 - α2-Adrenergic Receptors, in *Primer on the Autonomic Nervous System (Third Edition)*, D. Robertson, et al., Editors. 2012, Academic Press: San Diego. p. 55-58.
33. Woodcock, E.A., et al., Cardiac α1-adrenergic drive in pathological remodelling. Cardiovascular Research, 2007. 77(3): p. 452-462.
34. Brack, K.E., J.H. Coote, and G.A. Ng, The effect of direct autonomic nerve stimulation on left ventricular force in the isolated innervated Langendorff perfused rabbit heart. Auton Neurosci, 2006. 124(1-2): p. 69-80.
35. Vincent, N.H. and S. Ellis, Inhibitory effect of acetylcholine on gylcogenolysis in the isolated guinea-pig heart. Journal of Pharmacology and Experimental Therapeutics, 1963. 139(1): p. 60-68.
36. Levy, M.N. and H. Zieske, Effect of enhanced contractility on the left ventricular response to vagus nerve stimulation in dogs. Circ Res, 1969. 24(3): p. 303-11.
37. Dampney, R.A., Central neural control of the cardiovascular system: current perspectives. Adv Physiol Educ, 2016. 40(3): p. 283-96.
38. Mayer, E.A., Gut feelings: the emerging biology of gut-brain communication. Nat Rev Neurosci, 2011. 12(8): p. 453-66.
39. Tracey, K.J., The inflammatory reflex. Nature, 2002. 420(6917): p. 853-9.
40. Dampney, R.A., Functional organization of central pathways regulating the cardiovascular system. Physiol Rev, 1994. 74(2): p. 323-64.

41. Borst, C., et al., Mechanisms of initial heart rate response to postural change. Am J Physiol, 1982. 243(5): p. H676-81.
42. Raven, P.B., P.J. Fadel, and S. Ogoh, Arterial baroreflex resetting during exercise: a current perspective. Exp Physiol, 2006. 91(1): p. 37-49.
43. Borst, C., et al., Mechanisms of Initial Blood Pressure Response to Postural Change. Clinical Science, 1984. 67(3): p. 321-327.
44. Coote, J.H., Recovery of heart rate following intense dynamic exercise. Exp Physiol, 2010. 95(3): p. 431-40.
45. Rowell, L.B., Chapter 2: Reflex control during homeostasis, in *Human Cardiovascular Control* 1993, Oxford University Press: New York. p. 37-80.
46. Pavlov, V.A. and K.J. Tracey, Neural regulation of immunity: molecular mechanisms and clinical translation. Nat Neurosci, 2017. 20(2): p. 156-166.
47. Chavan, S.S., V.A. Pavlov, and K.J. Tracey, Mechanisms and Therapeutic Relevance of Neuro-immune Communication. Immunity, 2017. 46(6): p. 927-942.
48. Medzhitov, R., Origin and physiological roles of inflammation. Nature, 2008. 454(7203): p. 428-35.
49. Akira, S., S. Uematsu, and O. Takeuchi, Pathogen recognition and innate immunity. Cell, 2006. 124(4): p. 783-801.
50. Goehler, L.E., et al., Interleukin-1β in Immune Cells of the Abdominal Vagus Nerve: a Link between the Immune and Nervous Systems? The Journal of Neuroscience, 1999. 19(7): p. 2799-2806.
51. Hosoi, T., et al., Novel pathway for LPS-induced afferent vagus nerve activation: possible role of nodose ganglion. Auton Neurosci, 2005. 120(1-2): p. 104-7.
52. Goehler, L.E., et al., Vagal immune-to-brain communication: a visceral chemosensory pathway. Autonomic Neuroscience, 2000. 85(1-3): p. 49-59.
53. Bellinger, D.L., et al., Origin of noradrenergic innervation of the spleen in rats. Brain Behav Immun, 1989. 3(4): p. 291-311.
54. Rosas-Ballina, M., et al., Acetylcholine-synthesizing T cells relay neural signals in a vagus nerve circuit. Science, 2011. 334(6052): p. 98-101.
55. Wang, H., et al., Nicotinic acetylcholine receptor alpha7 subunit is an essential regulator of inflammation. Nature, 2003. 421(6921): p. 384-8.
56. Pavlov, V.A., et al., The cholinergic anti-inflammatory pathway: a missing link in neuroimmunomodulation. Mol Med, 2003. 9(5-8): p. 125-34.
57. Kox, M., et al., alpha7 nicotinic acetylcholine receptor agonist GTS-21 attenuates ventilator-induced tumour necrosis factor-alpha production and lung injury. Br J Anaesth, 2011. 107(4): p. 559-66.
58. Puelacher, C., et al., Expert consensus on peri-operative myocardial injury screening in noncardiac surgery: A literature review with expert consensus. Eur J Anaesthesiol, 2021.
59. Chew, M.S., et al., Identification of myocardial injury using perioperative troponin surveillance in major noncardiac surgery and net benefit over the Revised Cardiac Risk Index. British Journal of Anaesthesia, 2021.
60. Thygesen, K., et al., Fourth universal definition of myocardial infarction (2018). European Heart Journal, 2018.
61. Beattie, W.S., The emergence of a postoperative myocardial injury epidemic: true or false? Can J Anaesth, 2021. 68(8): p. 1109-1119.
62. Devereaux, P.J., et al., Characteristics and short-term prognosis of perioperative myocardial infarction in patients undergoing noncardiac surgery: a cohort study. Ann Intern Med, 2011. 154(8): p. 523-8.

63. Botto, F., et al., Myocardial injury after noncardiac surgery: a large, international, prospective cohort study establishing diagnostic criteria, characteristics, predictors, and 30-day outcomes. Anesthesiology, 2014. 120(3): p. 564-78.
64. Devereaux, P.J., et al., Association of Postoperative High-Sensitivity Troponin Levels With Myocardial Injury and 30-Day Mortality Among Patients Undergoing Noncardiac Surgery. Jama, 2017. 317(16): p. 1642.
65. Puelacher, C., et al., Perioperative Myocardial Injury After Noncardiac Surgery: Incidence, Mortality, and Characterization. Circulation, 2018. 137(12): p. 1221-1232.
66. Vascular Events In Noncardiac Surgery Patients Cohort Evaluation Study, I., et al., Association between postoperative troponin levels and 30-day mortality among patients undergoing noncardiac surgery. JAMA, 2012. 307(21): p. 2295-304.
67. Beattie, W.S., et al., Implication of Major Adverse Postoperative Events and Myocardial Injury on Disability and Survival: A Planned Subanalysis of the ENIGMA-II Trial. Anesth Analg, 2018. 127(5): p. 1118-1126.
68. Smilowitz, N.R., et al., Myocardial Injury After Noncardiac Surgery: A Systematic Review and Meta-Analysis. Cardiol Rev, 2019. 27(6): p. 267-273.
69. Beattie, W.S., et al., Survival After Isolated Post-Operative Troponin Elevation. J Am Coll Cardiol, 2017. 70(7): p. 907-908.
70. Ackland, G.L., et al., Early elevation in plasma high-sensitivity troponin T and morbidity after elective noncardiac surgery: prospective multicentre observational cohort study. Br J Anaesth, 2020. 124(5): p. 535-543.
71. Nathoe, H.M., W.A. van Klei, and W.S. Beattie, Perioperative troponin elevation: always myocardial injury, but not always myocardial infarction. Anesth Analg, 2014. 119(5): p. 1014-6.
72. Landesberg, G., et al., Perioperative myocardial infarction. Circulation, 2009. 119(22): p. 2936-44.
73. Thygesen, K., et al., Third universal definition of myocardial infarction. Eur Heart J, 2012. 33(20): p. 2551-67.
74. Abbott, T.E.F., et al., A Prospective International Multicentre Cohort Study of Intraoperative Heart Rate and Systolic Blood Pressure and Myocardial Injury After Noncardiac Surgery: Results of the VISION Study. Anesth Analg, 2018. 126(6): p. 1936-1945.
75. Park, K.C., et al., Cardiac troponins: from myocardial infarction to chronic disease. Cardiovasc Res, 2017. 113(14): p. 1708-1718.
76. Sheth, T., et al., Prognostic capabilities of coronary computed tomographic angiography before non-cardiac surgery: prospective cohort study. BMJ, 2015. 350: p. h1907.
77. Cohen, M.C. and T.H. Aretz, Histological Analysis of Coronary Artery Lesions in Fatal Postoperative Myocardial Infarction. Cardiovascular Pathology, 1999. 8(3): p. 133-139.
78. Devereaux, P.J., et al., Aspirin in patients undergoing noncardiac surgery. N Engl J Med, 2014. 370(16): p. 1494-503.
79. Dunser, M.W. and W.R. Hasibeder, Sympathetic overstimulation during critical illness: adverse effects of adrenergic stress. J Intensive Care Med, 2009. 24(5): p. 293-316.
80. Desborough, J.P., The stress response to trauma and surgery. Br J Anaesth, 2000. 85(1): p. 109-17.
81. Landesburg, G., W. Zhou, and T. Aversano, Tachycardia-Induced Subendocardial Necrosis in Acutely Instrumented Dogs with Fixed Coronary Stenosis. Anesthesia & Analgesia, 1999. 88(5): p. 973-979.

82. Herring, N., M. Kalla, and D.J. Paterson, The autonomic nervous system and cardiac arrhythmias: current concepts and emerging therapies. Nat Rev Cardiol, 2019. 16(12): p. 707-726.
83. Shiferaw, Y., G.L. Aistrup, and J.A. Wasserstrom, Intracellular Ca2+ waves, after depolarizations, and triggered arrhythmias. Cardiovasc Res, 2012. 95(3): p. 265-8.
84. Mann, D.L., et al., Adrenergic effects on the biology of the adult mammalian cardiocyte. Circulation, 1992. 85(2): p. 790-804.
85. Ellison, G.M., et al., Acute beta-adrenergic overload produces myocyte damage through calcium leakage from the ryanodine receptor 2 but spares cardiac stem cells. J Biol Chem, 2007. 282(15): p. 11397-409.
86. Zhang, Q., et al., Beta(2)-adrenoceptor agonist clenbuterol reduces infarct size and myocardial apoptosis after myocardial ischaemia/reperfusion in anaesthetized rats. Br J Pharmacol, 2010. 160(6): p. 1561-72.
87. Zhang, X., et al., Cardiotoxic and cardioprotective features of chronic beta-adrenergic signaling. Circ Res, 2013. 112(3): p. 498-509.
88. Mair, J., et al., How is cardiac troponin released from injured myocardium? Eur Heart J Acute Cardiovasc Care, 2018. 7(6): p. 553-560.
89. Hessel, M.H., et al., Release kinetics of intact and degraded troponin I and T after irreversible cell damage. Exp Mol Pathol, 2008. 85(2): p. 90-5.
90. Wu, A.H., et al., Characterization of cardiac troponin subunit release into serum after acute myocardial infarction and comparison of assays for troponin T and I. American Association for Clinical Chemistry Subcommittee on cTnI Standardization. Clin Chem, 1998. 44(6 Pt 1): p. 1198-208.
91. Katrukha, I.A. and A.G. Katrukha, Myocardial Injury and the Release of Troponins I and T in the Blood of Patients. Clin Chem, 2021. 67(1): p. 124-130.
92. Hammarsten, O., et al., Possible mechanisms behind cardiac troponin elevations. Biomarkers, 2018. 23(8): p. 725-734.
93. Piper, H., The calcium paradox revisited An artefact of great heuristic value. Cardiovascular Research, 2000. 45(1): p. 123-127.
94. Piper, H.M., K. Meuter, and C. Schäfer, Cellular mechanisms of ischemia-reperfusion injury. The Annals of Thoracic Surgery, 2003. 75(2): p. S644-S648.
95. Ganote, C.E., Contraction band necrosis and irreversible myocardial injury. J Mol Cell Cardiol, 1983. 15(2): p. 67-73.
96. Imahashi, K., et al., Cardiac-specific ablation of the Na+-Ca2+ exchanger confers protection against ischemia/reperfusion injury. Circ Res, 2005. 97(9): p. 916-21.
97. Weil, B.R., et al., Troponin Release and Reversible Left Ventricular Dysfunction After Transient Pressure Overload. J Am Coll Cardiol, 2018. 71(25): p. 2906-2916.
98. Weil, B.R., et al., Brief Myocardial Ischemia Produces Cardiac Troponin I Release and Focal Myocyte Apoptosis in the Absence of Pathological Infarction in Swine. JACC Basic Transl Sci, 2017. 2(2): p. 105-114.
99. Vallins, W.J., et al., Molecular cloning of human cardiac troponin I using polymerase chain reaction. FEBS Letters, 1990. 270(1-2): p. 57-61.
100. Melanson, S.E., M.J. Tanasijevic, and P. Jarolim, Cardiac troponin assays: a view from the clinical chemistry laboratory. Circulation, 2007. 116(18): p. e501-4.
101. Taggart, C., et al., Diagnosis, Investigation and Management of Patients with Acute and Chronic Myocardial Injury. J Clin Med, 2021. 10(11).
102. Wereski, R., et al., Cardiac Troponin Thresholds and Kinetics to Differentiate Myocardial Injury and Myocardial Infarction. Circulation, 2021. 144(7): p. 528-538.

103. Duceppe, E., et al., Canadian Cardiovascular Society Guidelines on Perioperative Cardiac Risk Assessment and Management for Patients Who Undergo Noncardiac Surgery. Can J Cardiol, 2017. 33(1): p. 17-32.
104. Lee, R.C., R.L. Feinbaum, and V. Ambros, The C. elegans heterochronic gene lin-4 encodes small RNAs with antisense complementarity to lin-14. Cell, 1993. 75(5): p. 843-854.
105. Beermann, J., et al., Non-coding RNAs in Development and Disease: Background, Mechanisms, and Therapeutic Approaches. Physiol Rev, 2016. 96(4): p. 1297-325.
106. van Rooij, E., The Art of MicroRNA Research. Circulation Research, 2011. 108(2): p. 219-234.
107. Creemers, E.E., A.J. Tijsen, and Y.M. Pinto, Circulating microRNAs: novel biomarkers and extracellular communicators in cardiovascular disease? Circ Res, 2012. 110(3): p. 483-95.
108. Bartel, D.P., Metazoan MicroRNAs. Cell, 2018. 173(1): p. 20-51.
109. Mitchell, P.S., et al., Circulating microRNAs as stable blood-based markers for cancer detection. Proc Natl Acad Sci U S A, 2008. 105(30): p. 10513-8.
110. Ha, M. and V.N. Kim, Regulation of microRNA biogenesis. Nat Rev Mol Cell Biol, 2014. 15(8): p. 509-24.
111. Lee, Y., et al., The nuclear RNase III Drosha initiates microRNA processing. Nature, 2003. 425(6956): p. 415-9.
112. Lund, E., et al., Nuclear export of microRNA precursors. Science, 2004. 303(5654): p. 95-8.
113. Ketting, R.F., et al., Dicer functions in RNA interference and in synthesis of small RNA involved in developmental timing in C. elegans. Genes Dev, 2001. 15(20): p. 2654-9.
114. Chendrimada, T.P., et al., TRBP recruits the Dicer complex to Ago2 for microRNA processing and gene silencing. Nature, 2005. 436(7051): p. 740-4.
115. Paroo, Z., et al., Phosphorylation of the human microRNA-generating complex mediates MAPK/Erk signaling. Cell, 2009. 139(1): p. 112-22.
116. Jonas, S. and E. Izaurralde, Towards a molecular understanding of microRNA-mediated gene silencing. Nat Rev Genet, 2015. 16(7): p. 421-33.
117. Kozomara, A., M. Birgaoanu, and S. Griffiths-Jones, miRBase: from microRNA sequences to function. Nucleic Acids Res, 2019. 47(D1): p. D155-D162.
118. Bartel, D.P., MicroRNAs. Cell, 2004. 116(2): p. 281-297.
119. Bartel, D.P., MicroRNAs: target recognition and regulatory functions. Cell, 2009. 136(2): p. 215-33.
120. Ludwig, N., et al., Distribution of miRNA expression across human tissues. Nucleic Acids Res, 2016. 44(8): p. 3865-77.
121. Treiber, T., N. Treiber, and G. Meister, Regulation of microRNA biogenesis and its crosstalk with other cellular pathways. Nat Rev Mol Cell Biol, 2019. 20(1): p. 5-20.
122. Coulthard, L.R., et al., p38(MAPK): stress responses from molecular mechanisms to therapeutics. Trends Mol Med, 2009. 15(8): p. 369-79.
123. Yang, Q., et al., Stress induces p38 MAPK-mediated phosphorylation and inhibition of Drosha-dependent cell survival. Mol Cell, 2015. 57(4): p. 721-734.
124. Shen, J., et al., EGFR modulates microRNA maturation in response to hypoxia through phosphorylation of AGO2. Nature, 2013. 497(7449): p. 383-7.
125. Shieh, J.T., et al., Elevated miR-499 levels blunt the cardiac stress response. PLoS One, 2011. 6(5): p. e19481.
126. Liang, Y., et al., Characterization of microRNA expression profiles in normal human tissues. BMC Genomics, 2007. 8: p. 166.

127. Huang, Y. and J. Li, MicroRNA208 family in cardiovascular diseases: therapeutic implication and potential biomarker. J Physiol Biochem, 2015. 71(3): p. 479-86.
128. Zhao, Y., E. Samal, and D. Srivastava, Serum response factor regulates a muscle-specific microRNA that targets Hand2 during cardiogenesis. Nature, 2005. 436(7048): p. 214-20.
129. Wang, G.K., et al., Circulating microRNA: a novel potential biomarker for early diagnosis of acute myocardial infarction in humans. Eur Heart J, 2010. 31(6): p. 659-66.
130. Chistiakov, D.A., A.N. Orekhov, and Y.V. Bobryshev, Cardiac-specific miRNA in cardiogenesis, heart function, and cardiac pathology (with focus on myocardial infarction). J Mol Cell Cardiol, 2016. 94: p. 107-121.
131. Piubelli, C., et al., microRNAs and Cardiac Cell Fate. Cells, 2014. 3(3): p. 802-23.
132. Tritsch, E., et al., An SRF/miR-1 axis regulates NCX1 and annexin A5 protein levels in the normal and failing heart. Cardiovasc Res, 2013. 98(3): p. 372-80.
133. Belevych, A.E., et al., MicroRNA-1 and -133 increase arrhythmogenesis in heart failure by dissociating phosphatase activity from RyR2 complex. PLoS One, 2011. 6(12): p. e28324.
134. Harada, M., et al., MicroRNA regulation and cardiac calcium signaling: role in cardiac disease and therapeutic potential. Circ Res, 2014. 114(4): p. 689-705.
135. Tang, Y., et al., MicroRNA-1 regulates cardiomyocyte apoptosis by targeting Bcl-2. Int Heart J, 2009. 50(3): p. 377-87.
136. Wang, J., et al., miR-499 protects cardiomyocytes from H 2O 2-induced apoptosis via its effects on Pdcd4 and Pacs2. RNA Biol, 2014. 11(4): p. 339-50.
137. Huang, W., et al., Combination of microRNA-21 and microRNA-146a Attenuates Cardiac Dysfunction and Apoptosis During Acute Myocardial Infarction in Mice. Mol Ther Nucleic Acids, 2016. 5: p. e296.
138. Yin, C., X. Wang, and R.C. Kukreja, Endogenous microRNAs induced by heat-shock reduce myocardial infarction following ischemia-reperfusion in mice. FEBS Lett, 2008. 582(30): p. 4137-42.
139. Li, S., et al., Overexpression of microRNA-133a inhibits ischemia-reperfusion-induced cardiomyocyte apoptosis by targeting DAPK2. Journal of Human Genetics, 2015. 60(11): p. 709-716.
140. Yang, B., et al., The muscle-specific microRNA miR-1 regulates cardiac arrhythmogenic potential by targeting GJA1 and KCNJ2. Nat Med, 2007. 13(4): p. 486-91.
141. Gryshkova, V., et al., miR-21-5p as a potential biomarker of inflammatory infiltration in the heart upon acute drug-induced cardiac injury in rats. Toxicol Lett, 2018. 286: p. 31-38.
142. Williams, Andrew E., et al., Role of miRNA-146a in the regulation of the innate immune response and cancer. Biochemical Society Transactions, 2008. 36(6): p. 1211-1215.
143. Palomer, X., et al., miR-146a targets Fos expression in human cardiac cells. Dis Model Mech, 2015. 8(9): p. 1081-91.
144. Kuwabara, Y., et al., Increased microRNA-1 and microRNA-133a levels in serum of patients with cardiovascular disease indicate myocardial damage. Circ Cardiovasc Genet, 2011. 4(4): p. 446-54.
145. Gupta, S.K., C. Bang, and T. Thum, Circulating microRNAs as biomarkers and potential paracrine mediators of cardiovascular disease. Circ Cardiovasc Genet, 2010. 3(5): p. 484-8.

146. Valadi, H., et al., Exosome-mediated transfer of mRNAs and microRNAs is a novel mechanism of genetic exchange between cells. Nat Cell Biol, 2007. 9(6): p. 654-9.
147. Arroyo, J.D., et al., Argonaute2 complexes carry a population of circulating microRNAs independent of vesicles in human plasma. Proc Natl Acad Sci U S A, 2011. 108(12): p. 5003-8.
148. Navickas, R., et al., Identifying circulating microRNAs as biomarkers of cardiovascular disease: a systematic review. Cardiovasc Res, 2016. 111(4): p. 322-37.
149. Boon, R.A., et al., MicroRNA-34a regulates cardiac ageing and function. Nature, 2013. 495(7439): p. 107-10.
150. Heymans, S., et al., Macrophage microRNA-155 promotes cardiac hypertrophy and failure. Circulation, 2013. 128(13): p. 1420-32.
151. Gao, H., et al., Plasma Levels of microRNA-145 Are Associated with Severity of Coronary Artery Disease. PLoS One, 2015. 10(5): p. e0123477.
152. Gao, W., et al., Plasma levels of lipometabolism-related miR-122 and miR-370 are increased in patients with hyperlipidemia and associated with coronary artery disease. Lipids Health Dis, 2012. 11: p. 55.
153. Devaux, Y., et al., Diagnostic and prognostic value of circulating microRNAs in patients with acute chest pain. J Intern Med, 2015. 277(2): p. 260-71.
154. Jakob, P., et al., Profiling and validation of circulating microRNAs for cardiovascular events in patients presenting with ST-segment elevation myocardial infarction. Eur Heart J, 2017. 38(7): p. 511-515.
155. Li, C., et al., Circulating microRNAs as novel and sensitive biomarkers of acute myocardial Infarction. Clin Biochem, 2012. 45(10-11): p. 727-32.
156. Zeller, T., et al., Assessment of microRNAs in patients with unstable angina pectoris. Eur Heart J, 2014. 35(31): p. 2106-14.
157. De Rosa, S., et al., Transcoronary concentration gradients of circulating microRNAs. Circulation, 2011. 124(18): p. 1936-44.
158. Zhao, Y., et al., Dysregulation of cardiogenesis, cardiac conduction, and cell cycle in mice lacking miRNA-1-2. Cell, 2007. 129(2): p. 303-17.
159. Xie, C., et al., MicroRNA-1 regulates smooth muscle cell differentiation by repressing Kruppel-like factor 4. Stem Cells Dev, 2011. 20(2): p. 205-10.
160. Kim, G.H., MicroRNA regulation of cardiac conduction and arrhythmias. Transl Res, 2013. 161(5): p. 381-92.
161. Terentyev, D., et al., miR-1 overexpression enhances Ca(2+) release and promotes cardiac arrhythmogenesis by targeting PP2A regulatory subunit B56alpha and causing CaMKII-dependent hyperphosphorylation of RyR2. Circulation research, 2009. 104(4): p. 514-521.
162. Aronsen, J.M., F. Swift, and O.M. Sejersted, Cardiac sodium transport and excitation-contraction coupling. J Mol Cell Cardiol, 2013. 61: p. 11-9.
163. Espinoza-Lewis, R.A. and D.Z. Wang, MicroRNAs in heart development. Curr Top Dev Biol, 2012. 100: p. 279-317.
164. Cheng, Y. and C. Zhang, MicroRNA-21 in cardiovascular disease. J Cardiovasc Transl Res, 2010. 3(3): p. 251-5.
165. Dong, S., et al., MicroRNA expression signature and the role of microRNA-21 in the early phase of acute myocardial infarction. J Biol Chem, 2009. 284(43): p. 29514-25.
166. Cheng, Y., et al., Ischaemic preconditioning-regulated miR-21 protects heart against ischaemia/reperfusion injury via anti-apoptosis through its target PDCD4. Cardiovasc Res, 2010. 87(3): p. 431-9.
167. Liu, N., et al., microRNA-133a regulates cardiomyocyte proliferation and suppresses smooth muscle gene expression in the heart. Genes Dev, 2008. 22(23): p. 3242-54.

168. Xiao, J., et al., MicroRNA miR-133 represses HERG K+ channel expression contributing to QT prolongation in diabetic hearts. J Biol Chem, 2007. 282(17): p. 12363-7.
169. Oliveira-Carvalho, V., V.O. Carvalho, and E.A. Bocchi, The emerging role of miR-208a in the heart. DNA Cell Biol, 2013. 32(1): p. 8-12.
170. Callis, T.E., et al., MicroRNA-208a is a regulator of cardiac hypertrophy and conduction in mice. J Clin Invest, 2009. 119(9): p. 2772-86.
171. Cheng, C., et al., MiRNAs as biomarkers of myocardial infarction: a meta-analysis. PLoS One, 2014. 9(2): p. e88566.
172. Kaur, A., et al., Systematic review of microRNA biomarkers in acute coronary syndrome and stable coronary artery disease. Cardiovascular Research, 2019.
173. Kumar, A. and C.P. Cannon, Acute coronary syndromes: diagnosis and management, part I. Mayo Clinic proceedings, 2009. 84(10): p. 917-938.
174. Fuster, V., et al., The pathogenesis of coronary artery disease and the acute coronary syndromes (1). N Engl J Med, 1992. 326(4): p. 242-50.
175. Oerlemans, M.I., et al., Early assessment of acute coronary syndromes in the emergency department: the potential diagnostic value of circulating microRNAs. EMBO Mol Med, 2012. 4(11): p. 1176-85.
176. Corsten, M.F., et al., Circulating MicroRNA-208b and MicroRNA-499 reflect myocardial damage in cardiovascular disease. Circ Cardiovasc Genet, 2010. 3(6): p. 499-506.
177. D'Alessandra, Y., et al., Circulating microRNAs are new and sensitive biomarkers of myocardial infarction. Eur Heart J, 2010. 31(22): p. 2765-73.
178. Chapleau, M.W. and R. Sabharwal, Methods of assessing vagus nerve activity and reflexes. Heart Fail Rev, 2011. 16(2): p. 109-27.
179. Akselrod, S., et al., Power spectrum analysis of heart rate fluctuation: a quantitative probe of beat-to-beat cardiovascular control. Science, 1981. 213(4504): p. 220-222.
180. Malpas, S.C., Neural influences on cardiovascular variability: possibilities and pitfalls. Am J Physiol Heart Circ Physiol, 2002. 282(1): p. H6-20.
181. Billman, G.E., Heart rate variability - a historical perspective. Front Physiol, 2011. 2: p. 86.
182. Task Force of the European Society of Cardiology the North American Society of Pacing Electrophysiology, Heart Rate Variability: Standards of Measurement, Physiological Interpretation, and Clinical Use. Circulation Research, 1996(93): p. 1043-1065.
183. Bilchick, K.C., et al., Prognostic value of heart rate variability in chronic congestive heart failure (Veterans Affairs' Survival Trial of Antiarrhythmic Therapy in Congestive Heart Failure). The American Journal of Cardiology, 2002. 90(1): p. 24-28.
184. Nolan, J., et al., Prospective Study of Heart Rate Variability and Mortality in Chronic Heart Failure : Results of the United Kingdom Heart Failure Evaluation and Assessment of Risk Trial (UK-Heart). Circulation, 1998. 98(15): p. 1510-1516.
185. Kleiger, R.E., et al., Decreased heart rate variability and its association with increased mortality after acute myocardial infarction. The American Journal of Cardiology, 1987. 59(4): p. 256-262.
186. Billman, G.E., The LF/HF ratio does not accurately measure cardiac sympatho-vagal balance. Front Physiol, 2013. 4: p. 26.
187. Randall, D.C., et al., SA nodal parasympathectomy delineates autonomic control of heart rate power spectrum. American Journal of Physiology-Heart and Circulatory Physiology, 1991. 260(3): p. H985-H988.

188. Rahman, F., et al., Low frequency power of heart rate variability reflects baroreflex function, not cardiac sympathetic innervation. Clin Auton Res, 2011. 21(3): p. 133-41.
189. Moak, J.P., et al., Supine low-frequency power of heart rate variability reflects baroreflex function, not cardiac sympathetic innervation. Heart Rhythm, 2007. 4(12): p. 1523-9.
190. Malliani, A., et al., Cardiovascular neural regulation explored in the frequency domain. Circulation, 1991. 84(2): p. 482-492.
191. Eckberg, D.L., Sympathovagal Balance. A Critical Appraisal, 1997. 96(9): p. 3224-3232.
192. Boyett, M., Y. Wang, and A. D'Souza, CrossTalk opposing view: Heart rate variability as a measure of cardiac autonomic responsiveness is fundamentally flawed. J Physiol, 2019.
193. Monfredi, O., et al., Biophysical characterization of the underappreciated and important relationship between heart rate variability and heart rate. Hypertension, 2014. 64(6): p. 1334-43.
194. Malik, M., et al., CrossTalk proposal: Heart rate variability is a valid measure of cardiac autonomic responsiveness. J Physiol, 2019.
195. de Geus, E.J.C., et al., Should heart rate variability be "corrected" for heart rate? Biological, quantitative, and interpretive considerations. Psychophysiology, 2019. 56(2): p. e13287.
196. Hillebrand, S., et al., Heart rate variability and first cardiovascular event in populations without known cardiovascular disease: meta-analysis and dose-response meta-regression. Europace, 2013. 15(5): p. 742-9.
197. Tsuji, H., et al., Reduced heart rate variability and mortality risk in an elderly cohort. The Framingham Heart Study. Circulation, 1994. 90(2): p. 878-83.
198. Fei, L., et al., Short- and long-term assessment of heart rate variability for risk stratification after acute myocardial infarction. The American Journal of Cardiology, 1996. 77(9): p. 681-684.
199. Rovere, M.T.L., et al., Baroreflex sensitivity and heart-rate variability in prediction of total cardiac mortality after myocardial infarction. The Lancet, 1998. 351(9101): p. 478-484.
200. Bigger, J.T., et al., The ability of several short-term measures of RR variability to predict mortality after myocardial infarction. Circulation, 1993. 88(3): p. 927-934.
201. Kato, M., et al., Spectral analysis of heart rate variability during isoflurane anesthesia. Anesthesiology, 1992. 77(4): p. 669-74.
202. Galletly, D.C., et al., Heart rate variability during propofol anaesthesia. Br J Anaesth, 1994. 72(2): p. 219-20.
203. Inoue, K. and J.O. Arndt, Efferent vagal discharge and heart rate in response to methohexitone, althesin, ketamine and etomidate in cats. Br J Anaesth, 1982. 54(10): p. 1105-16.
204. David Amar, M.M.F., PhD; Carol B. Pantuck, BA; Harry Shamoon, MD; Hao Zhang, MD; Nancy Roistacher, MD; Denis H. Y. Leung, PhD; Ilana Ginsburg, RN; Richard M. Smiley, MD, PhD, Persistent Alterations of the Autonomic Nervous System after Noncardiac Surgery. Anesthesiology, 1998. 89: p. 30-42.
205. Marsch, S.C., et al., Prolonged decrease in heart rate variability after elective hip arthroplasty. Br J Anaesth, 1994. 72(6): p. 643-9.
206. Karmali, S., et al., Randomized controlled trial of vagal modulation by sham feeding in elective non-gastrointestinal (orthopaedic) surgery. Br J Anaesth, 2015. 115(5): p. 727-35.

207. Laitio, T., et al., The role of heart rate variability in risk stratification for adverse postoperative cardiac events. Anesth Analg, 2007. 105(6): p. 1548-60.
208. Filipovic, M., et al., Heart rate variability and cardiac troponin I are incremental and independent predictors of one-year all-cause mortality after major noncardiac surgery in patients at risk of coronary artery disease. J Am Coll Cardiol, 2003. 42(10): p. 1767-76.
209. Stein, P.K., et al., Association between heart rate variability recorded on postoperative day 1 and length of stay in abdominal aortic surgery patients. Crit Care Med, 2001. 29(9): p. 1738-43.
210. Stein, P.K., Challenges of heart rate variability research in the ICU. Crit Care Med, 2013. 41(2): p. 666-7.
211. Nunan, D., G.R. Sandercock, and D.A. Brodie, A quantitative systematic review of normal values for short-term heart rate variability in healthy adults. Pacing Clin Electrophysiol, 2010. 33(11): p. 1407-17.
212. Karmali, S.N., et al., Heart rate variability in critical care medicine: a systematic review. Intensive Care Med Exp, 2017. 5(1): p. 33.
213. Imai, K., et al., Vagally mediated heart rate recovery after exercise is accelerated in athletes but blunted in patients with chronic heart failure. Journal of the American College of Cardiology, 1994. 24(6): p. 1529-1535.
214. Ackland, G.L., et al., Molecular Mechanisms Linking Autonomic Dysfunction and Impaired Cardiac Contractility in Critical Illness. Crit Care Med, 2016. 44(8): p. e614-24.
215. Berntson, G.G., et al., Heart rate variability: Origins, methods, and interpretive caveats. Psychophysiology, 1997. 34(6): p. 623-648.
216. Cole, C.R., et al., Heart-rate recovery immediately after exercise as a predictor of mortality. N Engl J Med, 1999. 341(18): p. 1351-7.
217. Abbott, T.E.F., et al., Cardiac vagal dysfunction and myocardial injury after non-cardiac surgery: a planned secondary analysis of the measurement of Exercise Tolerance before surgery study. Br J Anaesth, 2019. 122(2): p. 188-197.
218. Ackland, G.L., et al., Heart rate recovery and morbidity after noncardiac surgery: Planned secondary analysis of two prospective, multi-centre, blinded observational studies. Plos One, 2019. 14(8).
219. Ewing, D.J., et al., Autonomic mechanisms in the initial heart rate response to standing. Journal of Applied Physiology, 1980. 49(5): p. 809-814.
220. Furlan, R., et al., Oscillatory patterns in sympathetic neural discharge and cardiovascular variables during orthostatic stimulus. Circulation, 2000. 101(8): p. 886-92.
221. McCrory, C., et al., Speed of Heart Rate Recovery in Response to Orthostatic Challenge. Circ Res, 2016. 119(5): p. 666-75.
222. Gajewski, M., et al., The neuromodulation aspects of ischaemic myocardium: the importance of cholinergic system. J Physiol Pharmacol, 1995. 46(2): p. 107-25.
223. Brack, K.E., J.H. Coote, and G.A. Ng, Vagus nerve stimulation inhibits the increase in Ca2+ transient and left ventricular force caused by sympathetic nerve stimulation but has no direct effects alone--epicardial Ca2+ fluorescence studies using fura-2 AM in the isolated innervated beating rabbit heart. Exp Physiol, 2010. 95(1): p. 80-92.
224. Yang, B., et al., Choline produces cytoprotective effects against ischemic myocardial injuries: evidence for the role of cardiac m3 subtype muscarinic acetylcholine receptors. Cell Physiol Biochem, 2005. 16(4-6): p. 163-74.

225. Sun, L., et al., Acetylcholine Attenuates Hypoxia/Reoxygenation Injury by Inducing Mitophagy Through PINK1/Parkin Signal Pathway in H9c2 Cells. J Cell Physiol, 2016. 231(5): p. 1171-81.
226. Lu, H., et al., Regulation and function of mitophagy in development and cancer. Autophagy, 2013. 9(11): p. 1720-36.
227. Sun, L., et al., Cardioprotection by acetylcholine: a novel mechanism via mitochondrial biogenesis and function involving the PGC-1alpha pathway. J Cell Physiol, 2013. 228(6): p. 1238-48.
228. Vimercati, C., et al., Acute vagal stimulation attenuates cardiac metabolic response to beta-adrenergic stress. J Physiol, 2012. 590(23): p. 6065-74.
229. Ng, G.A., et al., Autonomic modulation of electrical restitution, alternans and ventricular fibrillation initiation in the isolated heart. Cardiovasc Res, 2007. 73(4): p. 750-60.
230. Vanoli, E., et al., Prediction of unexpected sudden death among healthy dogs by a novel marker of autonomic neural activity. Heart Rhythm, 2008. 5(2): p. 300-305.
231. De Ferrari, G.M., et al., Pharmacologic modulation of the autonomic nervous system in the prevention of sudden cardiac death. Journal of the American College of Cardiology, 1993. 22(1): p. 283-290.
232. Laurita, K.R. and D.S. Rosenbaum, Cellular mechanisms of arrhythmogenic cardiac alternans. Prog Biophys Mol Biol, 2008. 97(2-3): p. 332-47.
233. Kalla, M., et al., Protection against ventricular fibrillation via cholinergic receptor stimulation and the generation of nitric oxide. J Physiol, 2016. 594(14): p. 3981-92.
234. Stavrakis, S., et al., Low-level transcutaneous electrical vagus nerve stimulation suppresses atrial fibrillation. J Am Coll Cardiol, 2015. 65(9): p. 867-75.
235. Carnevale, D. and G. Lembo, Neuroimmune interactions in cardiovascular diseases. Cardiovasc Res, 2021. 117(2): p. 402-410.
236. Saeed, R.W., et al., Cholinergic stimulation blocks endothelial cell activation and leukocyte recruitment during inflammation. J Exp Med, 2005. 201(7): p. 1113-23.
237. Bernik, T.R., et al., Pharmacological stimulation of the cholinergic antiinflammatory pathway. J Exp Med, 2002. 195(6): p. 781-8.
238. Zhang, Y., et al., Chronic vagus nerve stimulation improves autonomic control and attenuates systemic inflammation and heart failure progression in a canine high-rate pacing model. Circ Heart Fail, 2009. 2(6): p. 692-9.
239. Leib, C., et al., Role of the cholinergic antiinflammatory pathway in murine autoimmune myocarditis. Circ Res, 2011. 109(2): p. 130-40.
240. Ackland, G.L., et al., Autonomic regulation of systemic inflammation in humans: a multi-center, blinded observational cohort study. Brain, Behavior, and Immunity, 2017.
241. Chen, Z.Y., et al., Cytokine profile and prognostic significance of high neutrophil-lymphocyte ratio in colorectal cancer. Br J Cancer, 2015. 112(6): p. 1088-97.
242. Wijeysundera, D.N., et al., Measurement of Exercise Tolerance before Surgery (METS) study: a protocol for an international multicentre prospective cohort study of cardiopulmonary exercise testing prior to major non-cardiac surgery. BMJ Open, 2016. 6(3): p. e010359.
243. May, S.M., et al., Acquired loss of cardiac vagal activity is associated with myocardial injury in patients undergoing noncardiac surgery: prospective observational mechanistic cohort study. Br J Anaesth, 2019. 123(6): p. 758-767.
244. Ernster, V.L., Nested Case-Control Studies. Preventive Medicine, 1994. 23(5): p. 587-590.

245. von Elm, E., et al., The Strengthening the Reporting of Observational Studies in Epidemiology (STROBE) statement: guidelines for reporting observational studies. J Clin Epidemiol, 2008. 61(4): p. 344-9.
246. Tuck, M.K., et al., Standard operating procedures for serum and plasma collection: early detection research network consensus statement standard operating procedure integration working group. J Proteome Res, 2009. 8(1): p. 113-7.
247. Bennett-Guerrero, E., et al., The Use of a Postoperative Morbidity Survey to Evaluate Patients with Prolonged Hospitalization After Routine, Moderate-Risk, Elective Surgery. Anesthesia & Analgesia, 1999. 89(2): p. 514-519.
248. Grocott, M.P., et al., The Postoperative Morbidity Survey was validated and used to describe morbidity after major surgery. J Clin Epidemiol, 2007. 60(9): p. 919-28.
249. Mestdagh, P., et al., High-throughput stem-loop RT-qPCR miRNA expression profiling using minute amounts of input RNA. Nucleic Acids Res, 2008. 36(21): p. e143.
250. Jensen, S.G., et al., Evaluation of two commercial global miRNA expression profiling platforms for detection of less abundant miRNAs. BMC Genomics, 2011. 12: p. 435.
251. Fu, H.-J., et al., A Novel Method to Monitor the Expression of microRNAs. Molecular Biotechnology, 2006. 32(3): p. 197-204.
252. Bustin, S.A., et al., The MIQE guidelines: minimum information for publication of quantitative real-time PCR experiments. Clin Chem, 2009. 55(4): p. 611-22.
253. Pritchard, C.C., H.H. Cheng, and M. Tewari, MicroRNA profiling: approaches and considerations. Nat Rev Genet, 2012. 13(5): p. 358-69.
254. Kroh, E.M., et al., Analysis of circulating microRNA biomarkers in plasma and serum using quantitative reverse transcription-PCR (qRT-PCR). Methods, 2010. 50(4): p. 298-301.
255. Dellett, M. and D.A. Simpson, Considerations for optimization of microRNA PCR assays for molecular diagnosis. Expert Rev Mol Diagn, 2016. 16(4): p. 407-14.
256. Moldovan, L., et al., Methodological challenges in utilizing miRNAs as circulating biomarkers. J Cell Mol Med, 2014. 18(3): p. 371-90.
257. Kirschner, M.B., et al., Haemolysis during sample preparation alters microRNA content of plasma. PLoS One, 2011. 6(9): p. e24145.
258. Blondal, T., et al., Assessing sample and miRNA profile quality in serum and plasma or other biofluids. Methods, 2013. 59(1): p. S1-6.
259. Rasmussen, K.D., et al., The miR-144/451 locus is required for erythroid homeostasis. J Exp Med, 2010. 207(7): p. 1351-8.
260. Ruijter, J.M., et al., Amplification efficiency: linking baseline and bias in the analysis of quantitative PCR data. Nucleic Acids Res, 2009. 37(6): p. e45.
261. Peltier, H.J. and G.J. Latham, Normalization of microRNA expression levels in quantitative RT-PCR assays: identification of suitable reference RNA targets in normal and cancerous human solid tissues. RNA, 2008. 14(5): p. 844-52.
262. Bas, A., et al., Utility of the housekeeping genes 18S rRNA, beta-actin and glyceraldehyde-3-phosphate-dehydrogenase for normalization in real-time quantitative reverse transcriptase-polymerase chain reaction analysis of gene expression in human T lymphocytes. Scand J Immunol, 2004. 59(6): p. 566-73.
263. Vandesompele, J., et al., Accurate normalization of real-time quantitative RT-PCR data by geometric averaging of multiple internal control genes. Genome Biol, 2002. 3(7): p. research0034.1-research0034.11.
264. Andersen, C.L., J.L. Jensen, and T.F. Orntoft, Normalization of real-time quantitative reverse transcription-PCR data: a model-based variance estimation approach to identify genes suited for normalization, applied to bladder and colon cancer data sets. Cancer Res, 2004. 64(15): p. 5245-50.

265. Livak, K.J. and T.D. Schmittgen, Analysis of relative gene expression data using real-time quantitative PCR and the 2(-Delta Delta C(T)) Method. Methods, 2001. 25(4): p. 402-8.
266. Vlachos, I.S., et al., DIANA-miRPath v3.0: deciphering microRNA function with experimental support. Nucleic Acids Res, 2015. 43(W1): p. W460-6.
267. Maragkakis, M., et al., DIANA-microT web server: elucidating microRNA functions through target prediction. Nucleic Acids Res, 2009. 37(Web Server issue): p. W273-6.
268. Alexiou, P., et al., Lost in translation: an assessment and perspective for computational microRNA target identification. Bioinformatics, 2009. 25(23): p. 3049-55.
269. Kanehisa, M., et al., New approach for understanding genome variations in KEGG. Nucleic Acids Research, 2018. 47(D1): p. D590-D595.
270. Papadopoulos, G.L., et al., DIANA-mirPath: Integrating human and mouse microRNAs in pathways. Bioinformatics, 2009. 25(15): p. 1991-3.
271. Malik, M. and A.J. Camm, Components of heart rate variability — what they really mean and what we really measure. The American Journal of Cardiology, 1993. 72(11): p. 821-822.
272. Tarvainen, M.P., et al., Kubios HRV--heart rate variability analysis software. Comput Methods Programs Biomed, 2014. 113(1): p. 210-20.
273. Pan, J. and W.J. Tompkins, A real-time QRS detection algorithm. IEEE Trans Biomed Eng, 1985. 32(3): p. 230-6.
274. Shaffer, F. and J.P. Ginsberg, An Overview of Heart Rate Variability Metrics and Norms. Front Public Health, 2017. 5: p. 258.
275. Alcantara, J.M.A., et al., Impact of Using Different Levels of Threshold-Based Artefact Correction on the Quantification of Heart Rate Variability in Three Independent Human Cohorts. J Clin Med, 2020. 9(2).
276. Oliveira, R.S., et al., Ectopic beats arise from micro-reentries near infarct regions in simulations of a patient-specific heart model. Sci Rep, 2018. 8(1): p. 16392.
277. Peltola, M.A., Role of editing of R-R intervals in the analysis of heart rate variability. Front Physiol, 2012. 3: p. 148.
278. Lipponen, J.A. and M.P. Tarvainen, A robust algorithm for heart rate variability time series artefact correction using novel beat classification. Journal of Medical Engineering & Technology, 2019. 43(3): p. 173-181.
279. Li, K., H. Rudiger, and T. Ziemssen, Spectral Analysis of Heart Rate Variability: Time Window Matters. Front Neurol, 2019. 10: p. 545.
280. Tarvainen, M.P., P.O. Ranta-Aho, and P.A. Karjalainen, An advanced detrending method with application to HRV analysis. IEEE Trans Biomed Eng, 2002. 49(2): p. 172-5.
281. Morshedi-Meibodi, A., et al., Heart rate recovery after treadmill exercise testing and risk of cardiovascular disease events (The Framingham Heart Study). The American Journal of Cardiology, 2002. 90(8): p. 848-852.
282. Finucane, C., et al., Age-related normative changes in phasic orthostatic blood pressure in a large population study: findings from The Irish Longitudinal Study on Ageing (TILDA). Circulation, 2014. 130(20): p. 1780-9.
283. NCSS-Statistical-Software, Introduction to Curve Fitting 2021. p. 1-10.
284. Brown, H. and R. Prescott, Applied Mixed Models in Medicine. 2014, New York, USA: John Wiley & Sons, Incorporated.
285. NCSS-Statistical-Software, Mixed Models – Repeated Measures. 2021. p. 222-1 to 222 -30.
286. Detry, M. and Y. Ma, Analyzing Repeated Measurements Using Mixed Models. JAMA, 2016. 315(4): p. 407-408.

287. Newgard, C. and R. Lewis, Missing Data How to Best Account for What Is Not Known. JAMA, 2015. 314(9): p. 940-941.
288. Lu, K. and D.V. Mehrotra, Specification of covariance structure in longitudinal data analysis for randomized clinical trials. Stat Med, 2010. 29(4): p. 474-88.
289. Benjamini, Y. and Y. Hochberg, Controlling the False Discovery Rate: A Practical and Powerful Approach to Multiple Testing. Journal of the Royal Statistical Society: Series B (Methodological), 1995. 57(1): p. 289-300.
290. Lee, T.H., et al., Derivation and Prospective Validation of a Simple Index for Prediction of Cardiac Risk of Major Noncardiac Surgery. Circulation, 1999. 100(10): p. 1043-1049.
291. Robin, X., et al., pROC: an open-source package for R and S+ to analyze and compare ROC curves. BMC Bioinformatics, 2011. 12: p. 77.
292. Obuchowski, N.A., M.L. Lieber, and F.H. Wians, Jr., ROC curves in clinical chemistry: uses, misuses, and possible solutions. Clin Chem, 2004. 50(7): p. 1118-25.
293. Cunningham, F., et al., Ensembl 2015. Nucleic Acids Res, 2015. 43(Database issue): p. D662-9.
294. Shattock, M.J., et al., Na+/Ca2+ exchange and Na+/K+-ATPase in the heart. J Physiol, 2015. 593(6): p. 1361-82.
295. Khananshvili, D., The SLC8 gene family of sodium-calcium exchangers (NCX) - structure, function, and regulation in health and disease. Mol Aspects Med, 2013. 34(2-3): p. 220-35.
296. Rajan, S., et al., Molecular and functional characterization of a novel cardiac-specific human tropomyosin isoform. Circulation, 2010. 121(3): p. 410-8.
297. Dube, D.K., et al., Recent Advances on the TPM4 Gene Expression in Humans. Journal of Clinical & Experimental Cardiology, 2016. 7(12).
298. Dewenter, M., et al., Calcium Signaling and Transcriptional Regulation in Cardiomyocytes. Circ Res, 2017. 121(8): p. 1000-1020.
299. Dolphin, A.C., Calcium channel diversity: multiple roles of calcium channel subunits. Curr Opin Neurobiol, 2009. 19(3): p. 237-44.
300. Buraei, Z. and J. Yang, The ss subunit of voltage-gated Ca2+ channels. Physiol Rev, 2010. 90(4): p. 1461-506.
301. Boularan, C. and C. Gales, Cardiac cAMP: production, hydrolysis, modulation and detection. Front Pharmacol, 2015. 6: p. 203.
302. Chen, J., L.R. Levin, and J. Buck, Role of soluble adenylyl cyclase in the heart. Am J Physiol Heart Circ Physiol, 2012. 302(3): p. H538-43.
303. Mattick, P., et al., Ca2+-stimulated adenylyl cyclase isoform AC1 is preferentially expressed in guinea-pig sino-atrial node cells and modulates the I(f) pacemaker current. J Physiol, 2007. 582(Pt 3): p. 1195-203.
304. Rukavina Mikusic, N.L., et al., Angiotensin Receptors Heterodimerization and Trafficking: How Much Do They Influence Their Biological Function? Front Pharmacol, 2020. 11: p. 1179.
305. Capote, L.A., R. Mendez Perez, and A. Lymperopoulos, GPCR signaling and cardiac function. Eur J Pharmacol, 2015. 763(Pt B): p. 143-8.
306. Forrester, S.J., et al., Angiotensin II Signal Transduction: An Update on Mechanisms of Physiology and Pathophysiology. Physiol Rev, 2018. 98(3): p. 1627-1738.
307. Stafford, N., et al., The Plasma Membrane Calcium ATPases and Their Role as Major New Players in Human Disease. Physiol Rev, 2017. 97(3): p. 1089-1125.
308. Sorensen, A.B., M.T. Sondergaard, and M.T. Overgaard, Calmodulin in a heartbeat. FEBS J, 2013. 280(21): p. 5511-32.

309. Saucerman, J.J. and D.M. Bers, Calmodulin binding proteins provide domains of local Ca2+ signaling in cardiac myocytes. J Mol Cell Cardiol, 2012. 52(2): p. 312-6.
310. Couchonnal, L.F. and M.E. Anderson, The role of calmodulin kinase II in myocardial physiology and disease. Physiology (Bethesda), 2008. 23: p. 151-9.
311. Hagemann, D., et al., Frequency-encoding Thr17 phospholamban phosphorylation is independent of Ser16 phosphorylation in cardiac myocytes. J Biol Chem, 2000. 275(29): p. 22532-6.
312. Kondo, S., et al., BBF2H7, a novel transmembrane bZIP transcription factor, is a new type of endoplasmic reticulum stress transducer. Mol Cell Biol, 2007. 27(5): p. 1716-29.
313. Wang, J., C. Gareri, and H.A. Rockman, G-Protein-Coupled Receptors in Heart Disease. Circ Res, 2018. 123(6): p. 716-735.
314. Communal, C., et al., Opposing effects of beta(1)- and beta(2)-adrenergic receptors on cardiac myocyte apoptosis : role of a pertussis toxin-sensitive G protein. Circulation, 1999. 100(22): p. 2210-2.
315. Oudit, G.Y. and J.M. Penninger, Cardiac regulation by phosphoinositide 3-kinases and PTEN. Cardiovasc Res, 2009. 82(2): p. 250-60.
316. Weber, S., et al., Counteracting Protein Kinase Activity in the Heart: The Multiple Roles of Protein Phosphatases. Front Pharmacol, 2015. 6: p. 270.
317. Lubbers, E.R. and P.J. Mohler, Roles and regulation of protein phosphatase 2A (PP2A) in the heart. J Mol Cell Cardiol, 2016. 101: p. 127-133.
318. Jideama, N.M., et al., Dephosphorylation specificities of protein phosphatase for cardiac troponin I, troponin T, and sites within troponin T. International Journal of Biological Sciences, 2006. 2(1): p. 1-9.
319. Bers, D.M., Cardiac excitation-contraction coupling. Nature, 2002. 415(6868): p. 198-205.
320. Pieples, K., et al., Tropomyosin 3 expression leads to hypercontractility and attenuates myofilament length-dependent Ca(2+) activation. Am J Physiol Heart Circ Physiol, 2002. 283(4): p. H1344-53.
321. Lohse, M.J., S. Engelhardt, and T. Eschenhagen, What is the role of beta-adrenergic signaling in heart failure? Circ Res, 2003. 93(10): p. 896-906.
322. Beuckelmann, D.J., M. Nabauer, and E. Erdmann, Intracellular calcium handling in isolated ventricular myocytes from patients with terminal heart failure. Circulation, 1992. 85(3): p. 1046-55.
323. Castaldi, A., et al., MicroRNA-133 modulates the beta1-adrenergic receptor transduction cascade. Circ Res, 2014. 115(2): p. 273-83.
324. Iwai-Kanai, E., et al., alpha- and beta-adrenergic pathways differentially regulate cell type-specific apoptosis in rat cardiac myocytes. Circulation, 1999. 100(3): p. 305-11.
325. Xu, C., et al., beta-Blocker carvedilol protects cardiomyocytes against oxidative stress-induced apoptosis by up-regulating miR-133 expression. J Mol Cell Cardiol, 2014. 75: p. 111-21.
326. He, B., et al., Role of miR-1 and miR-133a in myocardial ischemic postconditioning. J Biomed Sci, 2011. 18: p. 22.
327. Pan, Z., et al., miR-1 exacerbates cardiac ischemia-reperfusion injury in mouse models. PLoS One, 2012. 7(11): p. e50515.
328. Schulte, C., et al., Comparative Analysis of Circulating Noncoding RNAs Versus Protein Biomarkers in the Detection of Myocardial Injury. Circ Res, 2019. 125(3): p. 328-340.

329. Taganov, K.D., et al., NF-kappaB-dependent induction of microRNA miR-146, an inhibitor targeted to signaling proteins of innate immune responses. Proc Natl Acad Sci U S A, 2006. 103(33): p. 12481-6.
330. Frangogiannis, N.G., The inflammatory response in myocardial injury, repair, and remodelling. Nat Rev Cardiol, 2014. 11(5): p. 255-65.
331. Shubeita HE, M.P., Harris AN, Knowlton KU, Glembotski CC, Endothelin induction of inositol phospholipid hydrolysis, sarcomere assembly, and cardiac gene expression in ventricular myocytes. A paracrine mechanism for myocardial cell hypertrophy. J Biol Chem, 1990. 265: p. 20555–20562.
332. Ackland, G.L., et al., Preoperative systemic inflammation and perioperative myocardial injury: prospective observational multicentre cohort study of patients undergoing non-cardiac surgery. Br J Anaesth, 2019. 122(2): p. 180-187.
333. Widera, C., et al., Diagnostic and prognostic impact of six circulating microRNAs in acute coronary syndrome. J Mol Cell Cardiol, 2011. 51(5): p. 872-5.
334. Han, Z., et al., Change of plasma microRNA-208 level in acute myocardial infarction patients and its clinical significance. Ann Transl Med, 2015. 3(20): p. 307.
335. Pott, C., L. Eckardt, and J.I. Goldhaber, Triple threat: the Na+/Ca2+ exchanger in the pathophysiology of cardiac arrhythmia, ischemia and heart failure. Curr Drug Targets, 2011. 12(5): p. 737-47.
336. Mochizuki, S. and C. Jiang, Na+/Ca++ exchanger and myocardial ischemia/reperfusion. Jpn Heart J, 1998. 39(6): p. 707-14.
337. Mochizuki, S. and K.T. MacLeod, Effects of hypoxia and metabolic inhibition on increases in intracellular Ca2+ concentration induced by Na+/Ca2+ exchange in isolated guinea-pig cardiac myocytes. J Mol Cell Cardiol, 1997. 29(11): p. 2979-87.
338. Silverman, H.S. and M.D. Stern, Ionic basis of ischaemic cardiac injury: insights from cellular studies. Cardiovasc Res, 1994. 28(5): p. 581-97.
339. Hampton, T.G., et al., Enhanced gene expression of Na(+)/Ca(2+) exchanger attenuates ischemic and hypoxic contractile dysfunction. Am J Physiol Heart Circ Physiol, 2000. 279(6): p. H2846-54.
340. Little, S.C., et al., Protein phosphatase 2A regulatory subunit B56alpha limits phosphatase activity in the heart. Sci Signal, 2015. 8(386): p. ra72.
341. Puhl, S.L., et al., Role of type 2A phosphatase regulatory subunit B56alpha in regulating cardiac responses to beta-adrenergic stimulation in vivo. Cardiovasc Res, 2019. 115(3): p. 519-529.
342. Deshmukh, P.A., B.C. Blunt, and P.A. Hofmann, Acute modulation of PP2a and troponin I phosphorylation in ventricular myocytes: studies with a novel PP2a peptide inhibitor. Am J Physiol Heart Circ Physiol, 2007. 292(2): p. H792-9.
343. Adachi, T., et al., Plasma microRNA 499 as a biomarker of acute myocardial infarction. Clin Chem, 2010. 56(7): p. 1183-5.
344. May, S.M., et al., MicroRNA signatures of perioperative myocardial injury after elective noncardiac surgery: prospective observational mechanistic cohort study. British Journal of Anaesthesia, 2020.
345. Abbott, T.E., et al., Preoperative heart rate and myocardial injury after non-cardiac surgery: results of a predefined secondary analysis of the VISION study. Br J Anaesth, 2016. 117(2): p. 172-81.
346. Ladha, K.S., et al., Association between preoperative ambulatory heart rate and postoperative myocardial injury: a retrospective cohort study. Br J Anaesth, 2018. 121(4): p. 722-729.
347. Heusser, K., et al., Baroreflex failure. Hypertension, 2005. 45(5): p. 834-9.

348. Toner, A., et al., Baroreflex impairment and morbidity after major surgery. Br J Anaesth, 2016. 117(3): p. 324-31.
349. Tracey, K.J., Physiology and immunology of the cholinergic antiinflammatory pathway. J Clin Invest, 2007. 117(2): p. 289-96.
350. Zhang, Y., et al., Low-Level Vagus Nerve Stimulation Reverses Cardiac Dysfunction and Subcellular Calcium Handling in Rats With Post-Myocardial Infarction Heart Failure. Int Heart J, 2016. 57(3): p. 350-5.
351. Cobas, Troponin T Hs. 2015.
352. Bennett-Guerrero, E., et al., The use of a postoperative morbidity survey to evaluate patients with prolonged hospitalization after routine, moderate-risk, elective surgery. Anesth.Analg., 1999. 89(2): p. 514-519.
353. Backlund, M., et al., Changes in heart rate variability in elderly patients undergoing major noncardiac surgery under spinal or general anesthesia. Regional Anesthesia and Pain Medicine, 1999. 24(5): p. 386-392.
354. Licker, M., A. Spiliopoulos, and J.M. Tschopp, Influence of thoracic epidural analgesia on cardiovascular autonomic control after thoracic surgery. Br J Anaesth, 2003. 91(4): p. 525-31.
355. Tetzlaff, J.E., et al., Heart rate variability and the prone position under general versus spinal anesthesia. Journal of Clinical Anesthesia, 1998. 10(8): p. 656-659.
356. Casagrande, J.T., M.C. Pike, and P.G. Smith, An Improved Approximate Formula for Calculating Sample Sizes for Comparing Two Binomial Distributions. Biometrics, 1978. 34(3).
357. Devereaux, P.J., et al., Association of Postoperative High-Sensitivity Troponin Levels With Myocardial Injury and 30-Day Mortality Among Patients Undergoing Noncardiac Surgery. JAMA, 2017. 317(16): p. 1642-1642.
358. Wieske, L., et al., Autonomic dysfunction in ICU-acquired weakness: a prospective observational pilot study. Intensive Care Med, 2013. 39(9): p. 1610-7.
359. Group, K.D.I.G.O.K.C.W., KDIGO 2012 Clinical Practice Guideline for the Evaluation and Management of Chronic Kidney Disease. Kidney inter., Suppl. 2013; 3: 1–150., 2013. 3(1): p. 5-14.
360. Duma, A., et al., High-sensitivity cardiac troponin T in young, healthy adults undergoing non-cardiac surgery. Br J Anaesth, 2018. 120(2): p. 291-298.
361. Schwartz, P.J., et al., Autonomic mechanisms and sudden death. New insights from analysis of baroreceptor reflexes in conscious dogs with and without a myocardial infarction. Circulation, 1988. 78(4): p. 969-79.
362. Barber, M.J., et al., Interruption of sympathetic and vagal-mediated afferent responses by transmural myocardial infarction. Circulation, 1985. 72(3): p. 623-31.
363. Emch, G.S., G.E. Hermann, and R.C. Rogers, Tumor necrosis factor-α inhibits physiologically identified dorsal motor nucleus neurons in vivo. Brain Research, 2002. 951(2): p. 311-315.
364. Wang, X., et al., Propofol modulates gamma-aminobutyric acid-mediated inhibitory neurotransmission to cardiac vagal neurons in the nucleus ambiguus. Anesthesiology, 2004. 100(5): p. 1198-205.
365. Farias, M., 3rd, et al., Cardiac enkephalins interrupt vagal bradycardia via delta 2-opioid receptors in sinoatrial node. Am J Physiol Heart Circ Physiol, 2003. 284(5): p. H1693-701.
366. Browning, K.N., A.E. Kalyuzhny, and R.A. Travagli, Opioid Peptides Inhibit Excitatory But Not Inhibitory Synaptic Transmission in the Rat Dorsal Motor Nucleus of the Vagus. The Journal of Neuroscience, 2002. 22(8): p. 2998-3004.

367. Jooste, E., Y. Zhang, and C.W. Emala, Rapacuronium preferentially antagonizes the function of M2 versus M3 muscarinic receptors in guinea pig airway smooth muscle. Anesthesiology, 2005. 102(1): p. 117-24.
368. Roy, A., et al., Cardiomyocyte-secreted acetylcholine is required for maintenance of homeostasis in the heart. FASEB J, 2013. 27(12): p. 5072-82.
369. Mastitskaya, S., et al., Cardioprotection evoked by remote ischaemic preconditioning is critically dependent on the activity of vagal pre-ganglionic neurones. Cardiovasc Res, 2012. 95(4): p. 487-94.
370. Reimer, P., et al., Role of heart-rate variability in preoperative assessment of physiological reserves in patients undergoing major abdominal surgery. Ther Clin Risk Manag, 2017. 13: p. 1223-1231.
371. Mastitskaya, S., et al., Cardioprotection evoked by remote ischaemic preconditioning is critically dependent on the activity of vagal pre-ganglionic neurones. Cardiovascular Research, 2012. 95(4): p. 487-494.
372. van Waes, J.A., et al., Association between Intraoperative Hypotension and Myocardial Injury after Vascular Surgery. Anesthesiology, 2016. 124(1): p. 35-44.
373. Hallqvist, L., et al., Intraoperative hypotension is associated with myocardial damage in noncardiac surgery: An observational study. Eur J Anaesthesiol, 2016. 33(6): p. 450-6.
374. Meng, L., Heterogeneous impact of hypotension on organ perfusion and outcomes: a narrative review. Br J Anaesth, 2021. 127(6): p. 845-861.
375. Wijeysundera, D.N., et al., Assessment of functional capacity before major non-cardiac surgery: an international, prospective cohort study. The Lancet, 2018. 391(10140): p. 2631-2640.
376. Ackland, G.L. and T.E.F. Abbott, Hypotension as a marker or mediator of perioperative organ injury: a review. Br J Anaesth, 2022.
377. Goldstein, D.S., et al., Low-frequency power of heart rate variability is not a measure of cardiac sympathetic tone but may be a measure of modulation of cardiac autonomic outflows by baroreflexes. Exp Physiol, 2011. 96(12): p. 1255-61.
378. Aries, M.J., et al., Exaggerated postural blood pressure rise is related to a favorable outcome in patients with acute ischemic stroke. Stroke, 2012. 43(1): p. 92-6.
379. Schubert, A., et al., Heart rate, heart rate variability, and blood pressure during perioperative stressor events in abdominal surgery. Journal of Clinical Anesthesia, 1997. 9(1): p. 52-60.
380. Laitio, Timo T., M.D., et al., Correlation Properties and Complexity of Perioperative RR-Interval Dynamics in Coronary Artery Bypass Surgery Patients. Anesthesiology: The Journal of the American Society of Anesthesiologists, 2000. 93(1): p. 69-80.
381. Pousset, F., et al., Effects of bisoprolol on heart rate variability in heart failure. The American Journal of Cardiology, 1996. 77(8): p. 612-617.
382. Jepsen, P., et al., Interpretation of observational studies. Heart, 2004. 90(8): p. 956-60.
383. Keet, S.W., et al., Reproducibility of non-standardised autonomic function testing in the pre-operative assessment screening clinic*. Anaesthesia, 2011. 66(1): p. 10-4.
384. Pierpont, G.L. and E.J. Voth, Assessing autonomic function by analysis of heart rate recovery from exercise in healthy subjects. Am J Cardiol, 2004. 94(1): p. 64-8.
385. Software, N.S., Analysis of Covariance(ANCOVA) with Two Groups. 2021. Chapter 26: p. 1-34.
386. NCSS-Statistical-Software, Curve Fitting –General. 2021, NCSS.
387. Edgington, E.S., Randomization Tests, in *International Encyclopedia of Statistical Science*, M. Lovric, Editor. 2011, Springer Berlin Heidelberg: Berlin, Heidelberg. p. 1182-1183.

388. Imholz, B.P., et al., Non-invasive continuous finger blood pressure measurement during orthostatic stress compared to intra-arterial pressure. Cardiovasc Res, 1990. 24(3): p. 214-21.
389. Mazzarello, S., et al., Risk Factors for Failure to Rescue in Myocardial Infarction after Noncardiac Surgery: A Cohort Study. Anesthesiology, 2020. 133(1): p. 96-108.
390. Werfel, S., et al., Rapid and highly efficient inducible cardiac gene knockout in adult mice using AAV-mediated expression of Cre recombinase. Cardiovasc Res, 2014. 104(1): p. 15-23.
391. Machhada, A., et al., Optogenetic Stimulation of Vagal Efferent Activity Preserves Left Ventricular Function in Experimental Heart Failure. JACC Basic Transl Sci, 2020. 5(8): p. 799-810.
392. Krutzfeldt, J., et al., Silencing of microRNAs in vivo with 'antagomirs'. Nature, 2005. 438(7068): p. 685-9.
393. Stenvang, J., et al., Inhibition of microRNA function by antimiR oligonucleotides. Silence, 2012. 3(1): p. 1.
394. Montgomery, R.L., et al., Therapeutic inhibition of miR-208a improves cardiac function and survival during heart failure. Circulation, 2011. 124(14): p. 1537-47.
395. Huang, C.K., S. Kafert-Kasting, and T. Thum, Preclinical and Clinical Development of Noncoding RNA Therapeutics for Cardiovascular Disease. Circ Res, 2020. 126(5): p. 663-678.
396. Farmer, A.D., et al., International Consensus Based Review and Recommendations for Minimum Reporting Standards in Research on Transcutaneous Vagus Nerve Stimulation (Version 2020). Front Hum Neurosci, 2020. 14: p. 568051.
397. Patel, A.B.U., et al., The potential for autonomic neuromodulation to reduce perioperative complications and pain: a systematic review and meta-analysis. Br J Anaesth, 2022. 128(1): p. 135-149.

Appendix A

STROBE guidelines adherence for XMINS study

Table A.1 Adherence to The Strengthening and Reporting of Observational Studies in Epidemiology Statement,[245] XMINS study as reported in the publication:

May S.M et al. Acquired loss of cardiac vagal activity is associated with myocardial injury in patients undergoing non-cardiac surgery: prospective observational mechanistic cohort study. British Journal of Anaesthesia. 2019 Vol. 123 Issue 6 P758-767

	Item	Recommendation	Page
Title and abstract	1	(*a*) Indicate the study's design with a commonly used term in the title or the abstract (*b*) Provide in the abstract an informative and balanced summary of what was done and what was found	2
Introduction			
Background/rationale	2	Explain the scientific background and rationale for the investigation being reported	3
Objectives	3	State specific objectives, including any prespecified hypotheses	3
Methods			
Study design	4	Present key elements of study design early in the paper	4
Setting	5	Describe the setting, locations, and relevant dates, including periods of recruitment, exposure, follow-up, and data collection	4
Participants	6	(*a*) Give the eligibility criteria, and the sources and methods of selection of participants. Describe methods of follow-up (*b*) For matched studies, give matching criteria and number of exposed and unexposed	4

Variables	7	Clearly define all outcomes, exposures, predictors, potential confounders, and effect modifiers. Give diagnostic criteria, if applicable	4
Data sources/ measurement	8*	For each variable of interest, give sources of data and details of methods of assessment (measurement). Describe comparability of assessment methods if there is more than one group	5-8
Bias	9	Describe any efforts to address potential sources of bias	7
Study size	10	Explain how the study size was arrived at	8
Quantitative variables	11	Explain how quantitative variables were handled in the analyses. If applicable, describe which groupings were chosen and why	5-8
Statistical methods	12	(*a*) Describe all statistical methods, including those used to control for confounding (*b*) Describe any methods used to examine subgroups and interactions (*c*) Explain how missing data were addressed (*d*) If applicable, explain how loss to follow-up was addressed (*e*) Describe any sensitivity analyses	7-8
Results			
Participants	13*	(a) Report numbers of individuals at each stage of study—e.g., numbers potentially eligible, examined for eligibility, confirmed eligible, included in the study, completing follow-up, and analysed (b) Give reasons for non-participation at each stage (c) Consider use of a flow diagram	9
Descriptive data	14*	(a) Give characteristics of study participants (e.g., demographic, clinical, social) and information on exposures and potential confounders (b) Indicate number of participants with missing data for each variable of interest (c) Summarise follow-up time (e.g., average and total amount)	9
Outcome data	15*	Report numbers of outcome events or summary measures over time	9
Main results	16	(*a*) Give unadjusted estimates and, if applicable, confounder-adjusted estimates and their precision (e.g., 95% confidence interval). Make clear which confounders were adjusted for and why they were included	10

		(*b*) Report category boundaries when continuous variables were categorized (*c*) If relevant, consider translating estimates of relative risk into absolute risk for a meaningful time period	
Other analyses	17	Report other analyses done—e.g., analyses of subgroups and interactions, and sensitivity analyses	10
Discussion			
Key results	18	Summarise key results with reference to study objectives	12
Limitations	19	Discuss limitations of the study, taking into account sources of potential bias or imprecision. Discuss both direction and magnitude of any potential bias	14
Interpretation	20	Give a cautious overall interpretation of results considering objectives, limitations, multiplicity of analyses, results from similar studies, and other relevant evidence	12
Generalisability	21	Discuss the generalisability (external validity) of the study results	12
Other information			
Funding	22	Give the source of funding and the role of the funders for the present study and, if applicable, for the original study on which the present article is based	15

Appendix B
Statistical analysis plan for XMINS study

Working title for paper: Role of parasympathetic dysfunction in perioperative myocardial injury

Short Title: XMINS

December 2018 Version 2.0

UK Research Ethics committee Reference: 16/LO/0635

Investigators: Dr Shaun May, Dr Robert Stephens and Dr Gareth Ackland

Descriptive Statistics

Participants

All data in this study, missing data, and completeness of follow up will be illustrated using a CONSORT- style flow diagram. The inclusion criteria are all adult patients undergoing major elective noncardiac surgery with an expected surgical time of greater than 120 minutes and an American Society of Anaesthesiology Score of greater than 2. Patients with a known in-situ cardiac pacemaker and/or with pre-existing arrhythmia are excluded. All eligible patients' data should be recorded on a case record form. Patient data will then be transcribed onto a database file at the single centre site. A thorough data cleaning procedure will be implemented as follows:

Outliers and duplicates will be checked for using NCSS Version 12 (Kaysville, UT, USA) data screening tool.

Outliers will be checked for validity on CRF, and data source and duplicates will be removed.

Baseline characteristics

To give a broader understanding of the patients enrolled in the study, baseline characteristics of all thepatients will be presented as a table: numbers (%) or means (SD) and medians (IQR) will be given for each group (PMI status) as appropriate.

- Demographic: Age, gender, body mass index, ethnicity, smoking status and American Society(ASA) physical status grade, revised cardiac risk index score.
- Co-morbidities: Chronic obstructive pulmonary disease, asthma, interstitial lung disease, ischaemic heart disease, diabetes mellitus, heart failure, liver cirrhosis, active cancer (curativeor palliative), previous stroke, hypertension.
- Pre-operative medications: Beta-blockers, calcium channel blocker, doxazosin, diuretic,statin, ARB/ACE-I.
- Pre-operative blood tests. Haemoglobin, creatinine, and eGFR.
- Surgery related: Surgical procedure, severity and duration of surgery, cancer surgery, laparoscopic surgery.
- Intraoperative clinical management: duration, anaesthetic technique, intraoperative blood pressure (episode <90mmg), intravenous inotropes or vasopressors.

Primary Analysis

The primary outcome measure of this study is myocardial injury, as defined by raised plasma troponin >14ng/l following inpatient surgery, within 2 days after surgery.

A mixed model repeated measures approach will be used as opposed to a repeated measures analysis of variance to analyse continuous longitudinal data. Mixed model is a mathematical extension of the general linear repeated measure ANOVA model.[284] It can also be referred to as: multilevel models, hierarchical linear models, mixed models or random coefficient models. The different names reflect the scientific field in which they were first developed. The mixed model does not assume that repeated measures have the same variance, and all paired measurements have the same covariance, also referred to as compound symmetry. The mixed model can consider the different covariant patterns between individuals and groups. The mixed model analysis allows the flexibility to consider a wide variety of correlation patterns in repeated measures. The covariant modelling also helps overcome the limitation of missing data that is sometime unavoidable in clinical studies and reduces the bias created by this

limitation.[288] Longitudinal observations were analysed using a multi-level (mixed error-component) model. The levels examined will be: perioperative myocardial injury (HsTnT ≥15ng.L-1 and hsTnT ≤14ng.L-1); day relating to surgery (day of surgery, 24h after surgery and 48h after surgery); and body position (supine and 45 degrees sitting). Individual comparisons between groups will be calculated using post hoc Bonferroni tests.

Secondary Analysis

Individual domains of the POMS within the first 7 days of surgery.

The number and percentage of patients in each POMS defined type will be reported.

Length of stay: the median hospital length of stay (LOS) following the start of surgery. Postoperative LOS is the duration in days from the date of the end of surgery to the date of discharge from hospital.

Appendix C

UniSp3 Cq values used for calibration

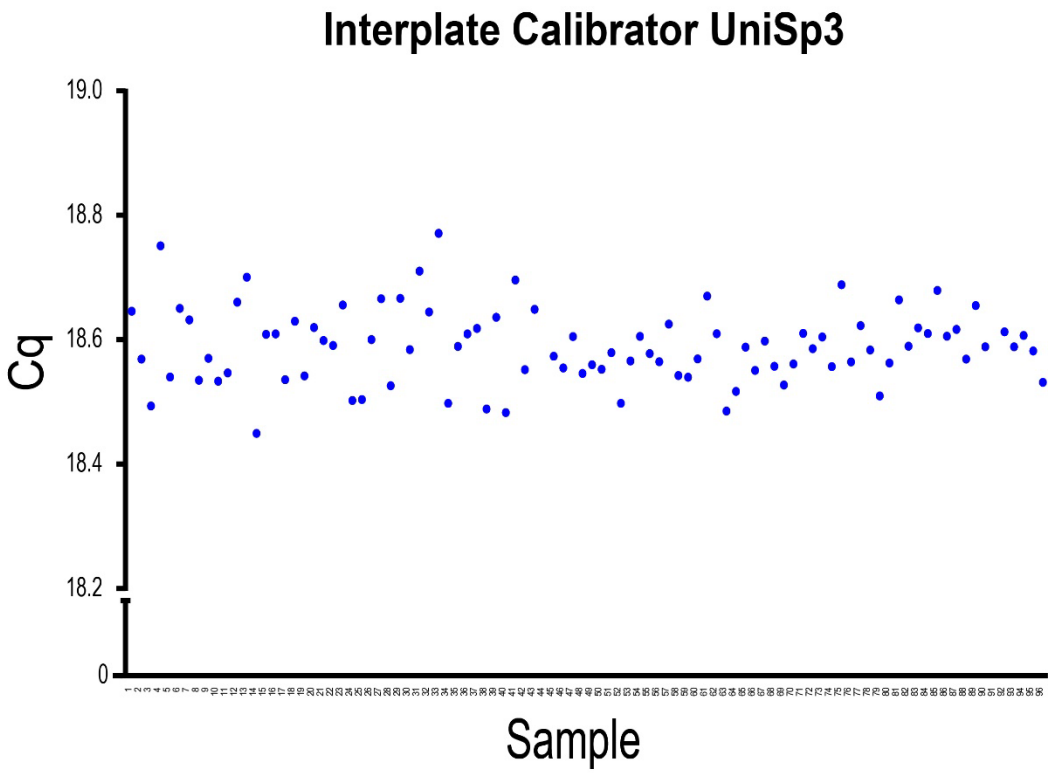

Figure C.3: Cq values of UniSp3 for each sample

UniSp3 was used as an interplate calibrator. The UniSP3 assay was pre-aliquoted by the manufacturer onto the plates, and therefore the variation of these assays is minimal from well to well and from plate to plate. The mean Cq value for UniSp3 was then calculated across all plates and then deducted from the mean for each individual plate to generate a calibration factor to be applied to raw Cq values before calibration.

Appendix D
Reference microRNA for Chapter 3

Isolation of microRNA:

The isolation of microRNA was carried out using the miReasy Serum/Plasma Advanced Kit (Qiagen, Denmark). Isolation protocols were carried out according to the manufacturer's instructions. 200µL of serum was thawed on melting ice and transferred to a 2ml RNase free microcentrifuge tube (Star Labs). Then 60µL of guanidine-based lysis Buffer RPL was added to the mixture, vortexed for 10s and incubated for 5 min at room temperature. For quality control, 1uL of spike in mixture (RNA Spike in kit, Qiagen) containing synthetic microRNA (UniSp3 (2 fmol.µl^{-1}), UniSp4 (0.02 fmol.µl^{-1}), and UniSp5 (0.00002 fmol.µl^{-1}) was added to each sample. 20uL of Buffer RPP was then added and the sample was vortexed for 30s and incubated at room temperature for 3 min. The sample were then centrifuged for 3 min at 11000rpm using the Prism Refrigerated microcentrifuge (Labnet International) to pellet the precipitate. The sample was inspected for a clear and colourless supernatant. 200µL of the supernatant was then transferred to a new 2ml RNAase-free microcentrifuge tube and 200µL of isopropanol was added before vortexing for 15s. The entire sample was then transferred to a RNeasy UCP MiniElute column. The sample was then centrifuged for 15s at 11000rpm and the flow-through was discarded. 700µL of buffer RWT was added onto the RNeasy UCP MiniElute column, samples vortexed at 11000rpm, and the flow-through was discarded. Then 500µL of buffer RPE was added onto the RNeasy UCP MiniElute column, samples vortexed at 11000rpm, and the flow-through was discarded. Then 500µL of 80% ethanol was added onto the RNeasy UCP MiniELute column, samples vortexed at 11000rpm, and the flow-

through was discarded. The RNeasy UCP MiniELute columns were then placed in new 2ml collection tubes, and with the spin columns' lids open, the samples were centrifuged at 13500rpm for 5min to dry the spin columns' membranes. Finally, the RNeasy UCP MiniELute columns were placed into new 1.5 ml collection tubes. 22µL of RNase free water was directly added to the centre of the spin column membrane and allowed to incubate for 1 min. The samples were then centrifuged for 1 minute at 13500 rpm to elute the RNA. 20µL Isolated RNA in the collection tube was then stored at -20˚C. MicroRNA was isolated in batches of 24 samples.

Quantitative RT-PCR

4µL of RNA was reversed transcribed in a 10µL final reaction volume using the miRCURY LNA RT kit (Qiagen Catalogue number 339340). Due to the low total RNA concentrations in serum samples, measuring RNA concentrations is challenging.[249] It is therefore recommended by the manufacturer that RNA amounts are based on starting sample volume, rather than RNA concentration. The master mix contained 4µL 5x miRCURY RT Reaction buffer, 9µL RNase-free water, 2µL 10x miRCURY RT Enzyme Mix, and 1µL UniSp6 Spike-in. The reactions were performed in a Primus 96 plus thermal cycler (MWG biotech) for 60 minutes at 42˚C, followed by incubation (inactivation of reaction) at 95˚C for 5 min, and then allowed to cool at 4˚C. The cDNA was then stored at -20˚C.

For qualitative PCR, undiluted cDNA was added to a 10µL reaction containing 5µL 2 x miRCURY SYBR Green Master Mix, 0.5µL ROX Reference Dye and 0.5µL RNAse free water. The Master Mix with cDNA was added to 2 x Qiagen miRCURY LNA miRNA Serum/Plasma Focus Panel plates containing 176 microRNA LNA PCR Primer assays (Table

D.1). Amplification was performed using the Applied Biosystem StepOneplus RT-PCR system (Applied Biosystems). The cycling parameters were: PCR initial heat activation at 95˚C for 2 minutes; 40 cycles of denaturation at 95˚C for 10s and annealing at 56˚C for 60s; followed by melting curve analysis from 60˚C to 95˚C. Cq values were determined using the second derivative method and melting curves obtained using the Applied Biosystem StepOneplus software. Cq values were calibrated using an interplate calibrator control assay, UniSp3, which had been pre-aliquoted onto each plate. Calibrated Cq values were used for statistical analysis.

Table D.1: 176 microRNA LNA PCR Primer assays and their sequence

MicroRNA	microRNA target sequence
hsa-miR-652-3p	AAUGGCGCCACUAGGGUUGUG
hsa-miR-221-3p	AGCUACAUUGUCUGCUGGGUUUC
hsa-let-7f-5p	UGAGGUAGUAGAUUGUAUAGUU
hsa-miR-27b-3p	UUCACAGUGGCUAAGUUCUGC
hsa-miR-374b-5p	AUAUAAUACAACCUGCUAAGUG
hsa-miR-93-5p	CAAAGUGCUGUUCGUGCAGGUAG
hsa-miR-200a-3p	UAACACUGUCUGGUAACGAUGU
hsa-miR-484	UCAGGCUCAGUCCCCUCCCGAU
hsa-miR-181a-5p	AACAUUCAACGCUGUCGGUGAGU
hsa-miR-106a-5p	AAAAGUGCUUACAGUGCAGGUAG
hsa-miR-145-5p	GUCCAGUUUUCCCAGGAAUCCCU
hsa-miR-486-5p	UCCUGUACUGAGCUGCCCCGAG
hsa-miR-26a-5p	UUCAAGUAAUCCAGGAUAGGCU
hsa-miR-143-3p	UGAGAUGAAGCACUGUAGCUC
hsa-miR-30a-5p	UGUAAACAUCCUCGACUGGAAG
hsa-miR-222-3p	AGCUACAUCUGGCUACUGGGU
hsa-miR-342-3p	UCUCACACAGAAAUCGCACCCGU
hsa-miR-324-5p	CGCAUCCCCUAGGGCAUUGGUGU
hsa-miR-185-5p	UGGAGAGAAAGGCAGUUCCUGA
hsa-let-7e-5p	UGAGGUAGGAGGUUGUAUAGUU
hsa-miR-139-5p	UCUACAGUGCACGUGUCUCCAGU
hsa-miR-451a	AAACCGUUACCAUUACUGAGUU
hsa-let-7a-5p	UGAGGUAGUAGGUUGUAUAGUU
hsa-miR-128-3p	UCACAGUGAACCGGUCUCUUU
hsa-miR-125a-5p	UCCCUGAGACCCUUUAACCUGUGA
hsa-miR-485-3p	GUCAUACACGGCUCUCCUCUCU
hsa-let-7b-3p	CUAUACAACCUACUGCCUUCCC

hsa-miR-25-3p	CAUUGCACUUGUCUCGGUCUGA
hsa-miR-375	UUUGUUCGUUCGGCUCGCGUGA
hsa-miR-33a-5p	GUGCAUUGUAGUUGCAUUGCA
hsa-miR-16-5p	UAGCAGCACGUAAAUAUUGGCG
hsa-let-7b-5p	UGAGGUAGUAGGUUGUGUGGUU
hsa-miR-152-3p	UCAGUGCAUGACAGAACUUGG
hsa-miR-30c-5p	UGUAAACAUCCUACACUCUCAGC
hsa-miR-197-3p	UUCACCACCUUCUCCACCCAGC
hsa-miR-99b-5p	CACCCGUAGAACCGACCUUGCG
hsa-miR-30e-5p	UGUAAACAUCCUUGACUGGAAG
hsa-miR-146a-5p	UGAGAACUGAAUUCCAUGGGUU
hsa-miR-424-5p	CAGCAGCAAUUCAUGUUUUGAA
hsa-miR-107	AGCAGCAUUGUACAGGGCUAUCA
hsa-miR-148b-3p	UCAGUGCAUCACAGAACUUUGU
hsa-miR-20a-5p	UAAAGUGCUUAUAGUGCAGGUAG
hsa-miR-17-5p	CAAAGUGCUUACAGUGCAGGUAG
hsa-miR-30d-5p	UGUAAACAUCCCCGACUGGAAG
hsa-miR-186-5p	CAAAGAAUUCUCCUUUUGGGCU
hsa-let-7i-5p	UGAGGUAGUAGUUUGUGCUGUU
hsa-miR-26b-5p	UUCAAGUAAUUCAGGAUAGGU
hsa-miR-34a-5p	UGGCAGUGUCUUAGCUGGUUGU
hsa-miR-320b	AAAAGCUGGGUUGAGAGGGCAA
hsa-miR-590-5p	GAGCUUAUUCAUAAAAGUGCAG
hsa-miR-191-5p	CAACGGAAUCCCAAAAGCAGCUG
hsa-miR-99a-5p	AACCCGUAGAUCCGAUCUUGUG
hsa-miR-301a-3p	CAGUGCAAUAGUAUUGUCAAAGC
hsa-miR-151a-5p	UCGAGGAGCUCACAGUCUAGU
hsa-miR-122-5p	UGGAGUGUGACAAUGGUGUUUG
hsa-miR-423-5p	UGAGGGGCAGAGAGCGAGACUUU
hsa-miR-101-3p	UACAGUACUGUGAUAACUGAA
hsa-miR-365a-3p	UAAUGCCCCUAAAAAUCCUUAU
hsa-miR-23a-3p	AUCACAUUGCCAGGGAUUUCC
hsa-miR-215-5p	AUGACCUAUGAAUUGACAGAC
hsa-miR-320a	AAAAGCUGGGUUGAGAGGGCGA
hsa-miR-338-3p	UCCAGCAUCAGUGAUUUUGUUG
hsa-miR-223-3p	UGUCAGUUUGUCAAAUACCCCA
hsa-miR-103a-3p	AGCAGCAUUGUACAGGGCUAUGA
hsa-miR-331-3p	GCCCCUGGGCCUAUCCUAGAA
hsa-miR-142-3p	UGUAGUGUUUCCUACUUUAUGGA
hsa-let-7d-3p	CUAUACGACCUGCUGCCUUUCU
hsa-miR-126-5p	CAUUAUUACUUUUGGUACGCG
hsa-miR-19a-3p	UGUGCAAAUCUAUGCAAAACUGA
hsa-miR-144-3p	UACAGUAUAGAUGAUGUACU
hsa-miR-126-3p	UCGUACCGUGAGUAAUAAUGCG
hsa-miR-148a-3p	UCAGUGCACUACAGAACUUUGU
hsa-miR-10b-5p	UACCCUGUAGAACCGAAUUUGUG

hsa-miR-195-5p	UAGCAGCACAGAAAUAUUGGC
hsa-miR-125b-5p	UCCCUGAGACCCUAACUUGUGA
hsa-miR-192-5p	CUGACCUAUGAAUUGACAGCC
hsa-miR-18b-5p	UAAGGUGCAUCUAGUGCAGUUAG
hsa-miR-335-5p	UCAAGAGCAAUAACGAAAAAUGU
hsa-miR-320d	AAAAGCUGGGUUGAGAGGA
hsa-let-7g-5p	UGAGGUAGUAGUUUGUACAGUU
hsa-miR-22-3p	AAGCUGCCAGUUGAAGAACUGU
hsa-miR-199a-3p	ACAGUAGUCUGCACAUUGGUUA
hsa-miR-19b-3p	UGUGCAAAUCCAUGCAAAACUGA
hsa-miR-29a-3p	UAGCACCAUCUGAAAUCGGUUA
hsa-miR-150-5p	UCUCCCAACCCUUGUACCAGUG
hsa-miR-30b-5p	UGUAAACAUCCUACACUCAGCU
hsa-miR-24-3p	UGGCUCAGUUCAGCAGGAACAG
hsa-miR-502-3p	AAUGCACCUGGGCAAGGAUUCA
hsa-miR-339-3p	UGAGCGCCUCGACGACAGAGCCG
hsa-miR-409-3p	GAAUGUUGCUCGGUGAACCCCU
hsa-miR-154-5p	UAGGUUAUCCGUGUUGCCUUCG
hsa-miR-155-5p	UUAAUGCUAAUCGUGAUAGGGGU
hsa-miR-140-3p	UACCACAGGGUAGAACCACGG
hsa-miR-92b-3p	UAUUGCACUCGUCCCGGCCUCC
hsa-miR-505-3p	CGUCAACACUUGCUGGUUUCCU
hsa-miR-23b-3p	AUCACAUUGCCAGGGAUUACC
hsa-miR-141-3p	UAACACUGUCUGGUAAAGAUGG
hsa-miR-361-5p	UUAUCAGAAUCUCCAGGGGUAC
hsa-miR-27a-3p	UUCACAGUGGCUAAGUUCCGC
hsa-miR-1	UGGAAUGUAAAGAAGUAUGUAU
hsa-miR-382-5p	GAAGUUGUUCGUGGUGGAUUCG
hsa-miR-32-5p	UAUUGCACAUUACUAAGUUGCA
hsa-miR-133b	UUUGGUCCCCUUCAACCAGCUA
hsa-let-7d-5p	AGAGGUAGUAGGUUGCAUAGUU
hsa-miR-133a-3p	UUUGGUCCCCUUCAACCAGCUG
hsa-miR-20b-5p	CAAAGUGCUCAUAGUGCAGGUAG
hsa-miR-106b-5p	UAAAGUGCUGACAGUGCAGAU
hsa-miR-328-3p	CUGGCCCUCUCUGCCCUUCCGU
hsa-miR-532-3p	CCUCCCACACCCAAGGCUUGCA
hsa-miR-15a-5p	UAGCAGCACAUAAUGGUUUGUG
hsa-miR-532-5p	CAUGCCUUGAGUGUAGGACCGU
hsa-miR-194-5p	UGUAACAGCAACUCCAUGUGGA
hsa-miR-660-5p	UACCCAUUGCAUAUCGGAGUUG
hsa-miR-574-3p	CACGCUCAUGCACACACCCACA
hsa-miR-320c	AAAAGCUGGGUUGAGAGGGU
hsa-miR-130a-3p	CAGUGCAAUGUUAAAAGGGCAU
hsa-miR-28-5p	AAGGAGCUCACAGUCUAUUGAG
hsa-miR-497-5p	CAGCAGCACACUGUGGUUUGU
hsa-miR-425-3p	AUCGGGAAUGUCGUGUCCGCCC

hsa-miR-132-3p	UAACAGUCUACAGCCAUGGUCG
hsa-let-7c-5p	UGAGGUAGUAGGUUGUAUGGUU
hsa-miR-18a-5p	UAAGGUGCAUCUAGUGCAGAUAG
hsa-miR-29b-3p	UAGCACCAUUUGAAAUCAGUGUU
hsa-miR-136-5p	ACUCCAUUUGUUUUGAUGAUGGA
hsa-miR-1260a	AUCCCACCUCUGCCACCA
hsa-miR-15b-3p	CGAAUCAUUAUUUGCUGCUCUA
hsa-miR-142-5p	CAUAAAGUAGAAAGCACUACU
hsa-miR-100-5p	AACCCGUAGAUCCGAACUUGUG
hsa-miR-326	CCUCUGGGCCCUUCCUCCAG
hsa-miR-362-3p	AACACACCUAUUCAAGGAUUCA
hsa-miR-421	AUCAACAGACAUUAAUUGGGCGC
hsa-miR-223-5p	CGUGUAUUUGACAAGCUGAGUU
hsa-miR-146b-5p	UGAGAACUGAAUUCCAUAGGCU
hsa-miR-205-5p	UCCUUCAUUCCACCGGAGUCUG
hsa-miR-339-5p	UCCCUGUCCUCCAGGAGCUCACG
hsa-miR-425-5p	AAUGACACGAUCACUCCCGUUGA
hsa-miR-454-3p	UAGUGCAAUAUUGCUUAUAGGGU
hsa-miR-874-3p	CUGCCCUGGCCCGAGGGACCGA
hsa-miR-193a-5p	UGGGUCUUUGCGGGCGAGAUGA
hsa-miR-885-5p	UCCAUUACACUACCCUGCCUCU
hsa-miR-127-3p	UCGGAUCCGUCUGAGCUUGGCU
hsa-miR-208a-3p	AUAAGACGAGCAAAAAGCUUGU
hsa-miR-16-2-3p	CCAAUAUUACUGUGCUGCUUUA
hsa-miR-140-5p	CAGUGGUUUUACCCUAUGGUAG
hsa-miR-130b-3p	CAGUGCAAUGAUGAAAGGGCAU
hsa-miR-629-5p	UGGGUUUACGUUGGGAGAACU
hsa-miR-200c-3p	UAAUACUGCCGGGUAAUGAUGGA
hsa-miR-501-3p	AAUGCACCCGGGCAAGGAUUCU
hsa-miR-423-3p	AGCUCGGUCUGAGGCCCCUCAGU
hsa-miR-376a-3p	AUCAUAGAGGAAAAUCCACGU
hsa-miR-22-5p	AGUUCUUCAGUGGCAAGCUUUA
hsa-miR-2110	UUGGGGAAACGGCCGCUGAGUG
hsa-miR-376c-3p	AACAUAGAGGAAAUUCCACGU
hsa-miR-93-3p	ACUGCUGAGCUAGCACUUCCCG
hsa-miR-144-5p	GGAUAUCAUCAUAUACUGUAAG
hsa-miR-210-3p	CUGUGCGUGUGACAGCGGCUGA
hsa-miR-199a-5p	CCCAGUGUUCAGACUACCUGUUC
hsa-miR-766-3p	ACUCCAGCCCCACAGCCUCAGC
hsa-miR-584-5p	UUAUGGUUUGCCUGGGACUGAG
hsa-miR-92a-3p	UAUUGCACUUGUCCCGGCCUGU
hsa-miR-363-3p	AAUUGCACGGUAUCCAUCUGUA
hsa-miR-374a-5p	UUAUAAUACAACCUGAUAAGUG
hsa-miR-483-5p	AAGACGGGAGGAAAGAAGGGAG
hsa-miR-7-1-3p	CAACAAAUCACAGUCUGCCAUA
hsa-miR-877-5p	GUAGAGGAGAUGGCGCAGGG

hsa-miR-151a-3p	CUAGACUGAAGCUCCUUGAGG
hsa-miR-28-3p	CACUAGAUUGUGAGCUCCUGGA
hsa-miR-324-3p	ACUGCCCCAGGUGCUGCUGG
hsa-miR-136-3p	CAUCAUCGUCUCAAAUGAGUCU
hsa-miR-15b-5p	UAGCAGCACAUCAUGGUUUACA
hsa-miR-106b-3p	CCGCACUGUGGGUACUUGCUGC
hsa-miR-29c-3p	UAGCACCAUUUGAAAUCGGUUA
hsa-miR-335-3p	UUUUUCAUUAUUGCUCCUGACC
hsa-miR-21-5p	UAGCUUAUCAGACUGAUGUUGA
hsa-miR-30e-3p	CUUUCAGUCGGAUGUUUACAGC
hsa-miR-543	AAACAUUCGCGGUGCACUUCUU
hsa-miR-7-5p	UGGAAGACUAGUGAUUUUGUUGU
hsa-miR-495-3p	AAACAAACAUGGUGCACUUCUU

Results: MicroRNA Normalisation genes

Using the Normfinder Algorithm,[264] the best combination of microRNA assays that showed the lowest stability, and therefore were most suitable for normalisation when comparing before and after surgery serum sample, were the microRNA hsa-miR-152-3p and hsa-miR-361-5p (Table B.2).

Table B.2: MicroRNA with lowest stability values and their respective Cq values

Stability value for the combination of the two microRNA is 0.077.

MicroRNA	Mean Cq Value (SD)
hsa-miR-152-3p	30.06 (1.14)
hsa-miR-361-5p	29.51 (1.24)

Appendix E

Peak heart rate calculation for Chapter 5

The peak heart rate was identified for each patient using the Excel spreadsheet function "=MAX (number1, [number2])", where number 1 and number 2 are the specified range in which the MAX value is identified. Using the spreadsheet below as an example, the function can identify the highest heart rate for each row (patient) for the range of time values 0s, 10s, 20s, 30s, 40s, 50s, where number 1 on the function would be 0s and number 2 be 50s. Peak HR were rounded up to nearest whole number for statistical analysis

Recruit	Time after completion of orthostatic manoeuvre						Peak HR
	0	10	20	30	40	50	
XMIN 005	66.7219	67.36557	76.69969	62.52335	64.58743	61.50093	76.69969
XMIN 006	57.02094	64.03287	76.49886	72.99821	86.88975	77.87728	86.88975
XMIN 007	72.00404	71.9017	70.88384	73.54483	66.77979	65.01755	73.54483
XMIN 013	81.15977	78.19335	78.13569	79.82546	78.43254	86.4897	86.48970
XMIN 015	72.78228	69.61124	71.07894	76.90611	66.15878	72.67292	76.90611
XMIN 017	60.97039	55.47207	58.48566	54.01532	54.90133	55.47352	60.97039
XMIN 018	58.56406	51.63637	51.00206	54.16649	52.9928	53.82112	58.56406
XMIN 020	94.74822	82.96347	97.94264	104.0541	92.80551	84.86472	104.05410
XMIN 021	81.41605	80.16743	84.25522	89.31565	77.38781	78.54374	89.31565
XMIN 024	116.2297	112.0531	114.5049	108.3134	105.148	104.2874	116.22970
XMIN 025	97.08958	87.81816	86.74896	85.96845	89.46867	94.44022	97.08958
XMIN 026	82.08026	83.91619	84.23126	86.32599	81.63397	82.87619	86.32599
XMIN 028	46.90229	46.18463	48.24673	51.61026	52.48118	49.05136	52.48118
XMIN 029	84.03394	78.56959	77.26056	82.19394	74.13951	74.03486	84.03394
XMIN 031	72.21575	59.82955	64.41517	59.2708	62.48037	61.86642	72.21575
XMIN 033	51.67554	50.40942	54.44586	71.6971	59.39559	59.36541	71.69710
XMIN 034	78.07407	70.7784	77.50039	91.4678	93.30547	93.36135	93.36135
XMIN 038	101.3554	87.12702	78.32701	73.09225	67.90129	75.43079	101.35540
XMIN 040	51.37176	51.85525	51.81734	51.61095	50.47057	50.59096	51.85525
XMIN 041	69.83424	97.44166	99.05758	93.13349	84.30467	92.03199	99.05758
XMIN 042	70.80184	73.92947	81.37872	92.94928	78.54006	86.0078	92.94928
XMIN 043	73.35103	86.24342	79.28824	99.20737	78.17892	66.79236	99.20737
XMIN 045	81.08177	77.89549	74.99138	89.78218	86.27663	79.72275	89.78218
XMIN 046	84.97682	82.98829	84.58706	85.22739	86.45689	81.26869	86.45689
XMIN 049	68.47126	68.2598	67.93295	66.39683	67.76249	65.55147	68.47126
XMIN 054	79.93468	118.1286	79.64922	80.07121	77.42039	74.41246	118.12860

XMIN 055	67.32295	71.09162	55.1529	52.34629	51.26418	48.03514	71.09162
XMIN 057	63.10286	57.00547	61.58702	76.7038	76.7334	71.59207	76.73340
XMIN 058	70.09583	75.9193	74.20414	73.11594	80.43938	79.23573	80.43938
XMIN 059	84.95675	85.02716	85.39007	86.30029	80.82645	80.73395	86.30029
XMIN 060	79.8974	82.57482	79.19528	80.53991	83.74207	90.14622	90.14622
XMIN 061	68.35306	71.77472	87.04256	82.6916	74.16873	69.71048	87.04256
XMIN 063	48.77608	55.74669	54.11607	69.85127	56.43938	58.14022	69.85127
XMIN 064	68.81713	74.49316	70.72578	78.31515	82.02937	78.51742	82.02937
XMIN 065	80.54285	79.695	85.77743	71.44481	73.2583	69.34293	85.77743
XMIN 066	96.11709	84.99867	95.80941	78.61276	94.10316	92.6992	96.11709
XMIN 069	50.8907	54.3058	70.3726	84.3115	61.1838	55.5575	84.31150
XMIN 072	62.13631	65.70852	61.64489	60.57133	62.77474	62.39949	65.70852
XMIN 074	49.45851	82.30267	87.7238	49.37356	50.39383	53.08971	87.72380
XMIN 075	80.0801	80.76026	83.48862	99.13362	82.04299	82.6105	99.13362
XMIN 079	80.36599	72.1265	76.63737	73.17732	74.59936	69.87611	80.36599
XMIN 081	64.19427	65.5151	79.65481	75.06454	74.13739	73.99265	79.65481
XMIN 082	78.09342	63.4941	66.34267	71.064	70.53359	64.42462	78.09342
XMIN 083	52.53116	54.24501	58.38521	50.96934	54.57237	68.06573	68.06573
XMIN 084	58.32998	58.95102	55.63587	78.3093	60.40032	59.58642	78.30930
XMIN 085	50.01614	53.48185	61.74976	55.59113	56.32907	53.55898	61.74976
XMIN 086	64.67912	79.98274	67.14173	63.94968	61.81381	63.3583	79.98274
XMIN 087	70.56399	71.49466	74.35406	75.63092	72.41272	71.92603	75.63092
XMIN 088	110.7709	90.32077	93.36225	92.12022	92.6653	89.76095	110.77090
XMIN 090	83.60539	85.67411	86.41578	87.46467	86.95664	86.58009	87.46467
XMIN 091	54.61049	55.64532	57.5719	61.3293	60.97077	55.62934	61.32930
XMIN 092	75.72928	77.95175	74.86338	79.15927	74.62756	75.43699	79.15927
XMIN 093	64.91388	69.48203	72.0922	72.72163	69.77582	72.8239	72.82390
XMIN 094	57.80501	57.93565	59.98732	74.38286	66.20734	70.1015	74.38286
XMIN 096	85.2197	90.58183	83.80877	89.64268	90.0669	83.02905	90.58183
XMIN 098	74.20245	103.182	76.05222	77.8495	75.49508	68.78422	103.18200
XMIN 099	64.87905	64.75963	68.52672	82.54044	87.04579	74.59974	87.04579
XMIN 100	75.37855	78.28034	73.48064	72.62441	72.88415	69.12854	78.28034
XMIN 104	87.13465	81.97991	78.91352	78.9283	82.0821	72.38311	87.13465
XMIN 106	49.00357	51.60573	53.77972	72.08561	54.28708	50.16291	72.08561
XMIN 108	74.137	71.97398	71.77286	73.00333	72.43533	72.4062	74.13700
XMIN 109	97.45778	98.47471	103.1523	104.1675	99.17409	98.58752	104.16750
XMIN 110	79.68165	80.86674	79.90038	90.14886	100.1295	90.77197	100.12950
XMIN 111	63.24301	79.26309	71.96222	69.83234	64.86735	60.07669	79.26309
XMIN 115	110.8383	80.72235	74.14218	72.64396	72.14888	71.6629	110.83830
XMIN 117	71.60522	71.52071	78.9193	82.30772	86.70665	86.17633	86.70665
XMIN 119	51.89422	56.03661	56.18224	58.76943	61.47078	64.01843	64.01843
XMIN 124	71.23086	68.08932	74.96988	66.01924	63.2966	61.02371	74.96988
XMIN 125	86.96125	84.8293	85.38903	84.35001	88.19223	87.68037	88.19223
XMIN 129	64.01198	63.73939	62.52506	68.7933	70.28331	70.83765	70.83765
XMIN 130	73.1788	71.06214	69.36607	75.75033	70.26257	64.17293	75.75033
XMIN 131	90.53231	90.17289	91.01511	89.74339	84.10961	87.95835	91.01511

XMIN 134	68.13027	70.70489	65.77184	58.8742	60.50044	59.59939	70.70489
XMIN 135	85.47043	80.70575	82.19219	84.5819	82.87407	73.45057	85.47043
XMIN 136	77.20437	89.50895	89.28901	86.70749	85.43372	86.70532	89.50895
XMIN 138	70.63373	70.76603	70.91916	70.9035	69.95829	70.33082	70.91916
XMIN 140	83.72118	81.97347	81.9344	83.58057	86.3536	88.25392	88.25392
XMIN 141	73.69319	92.96413	81.04348	77.66641	78.99671	84.06396	92.96413
XMIN 142	92.69591	98.23956	96.2696	91.93751	80.21591	81.34519	98.23956
XMIN 144	76.65821	84.79693	78.19441	80.58069	71.56574	79.43738	84.79693
XMIN 147	74.41323	76.40211	75.7924	81.09129	76.41601	74.01394	81.09129
XMIN 148	61.24661	60.06452	65.05476	63.86339	67.54956	58.03579	67.54956
XMIN 151	56.73532	53.77787	52.41825	53.32092	56.94129	57.66253	57.66253
XMIN 152	63.56738	64.30199	65.84472	63.36142	67.03081	71.81905	71.81905
XMIN 155	75.85343	76.59859	72.3321	71.45926	71.52004	74.07914	76.59859
XMIN 157	66.47645	65.67999	63.01914	65.31341	64.52453	65.48858	66.47645
XMIN 158	86.05392	92.42123	80.20613	80.11051	80.25216	79.36656	92.42123
XMIN 160	67.55557	63.89868	75.82385	82.70356	78.62924	77.38868	82.70356
XMIN 161	58.43451	60.95652	61.1929	60.12169	59.62374	61.45452	61.45452
XMIN 162	68.31299	67.51969	66.10379	66.34907	67.19796	70.36801	70.36801
XMIN 166	63.697	64.14856	64.05744	58.34847	59.60866	58.90208	64.14856
XMIN 169	53.90383	57.94911	59.01955	73.02668	64.00646	65.82052	73.02668
XMIN 170	44.97874	44.68861	50.96778	63.99573	65.1999	67.12659	67.12659
XMIN 171	69.09316	112.1921	79.96468	73.87598	76.53822	77.19778	112.19210
XMIN 172	69.12854	69.77425	69.10016	71.79992	68.82372	77.56299	77.56299
XMIN 173	58.08456	59.25013	60.06305	59.88696	63.67164	58.96953	63.67164
XMIN 174	78.27448	74.62694	74.02042	75.37885	72.81775	75.12815	78.27448
XMIN 175	96.06086	82.17181	83.41298	85.09262	77.7914	83.30564	96.06086
XMIN 177	96.8776	88.55575	94.97087	101.0286	82.34036	86.61364	101.02860
XMIN 178	88.42297	88.83326	84.03184	84.60967	83.449	83.25735	88.83326
XMIN 179	62.26461	62.87353	62.11675	69.34397	72.51102	62.7633	72.51102
XMIN 181	72.43674	73.78422	65.58725	70.78824	68.34958	65.84004	73.78422
XMIN 183	70.666	78.41574	75.6116	70.84966	55.11942	70.35241	78.41574
XMIN 184	53.33468	58.48013	60.68934	57.01913	59.67077	56.12284	60.68934
XMIN 185	46.74175	49.18168	56.4376	57.15823	52.62711	62.25561	62.25561
XMIN 187	61.92936	59.91184	68.57292	70.13663	70.26516	69.34279	70.26516
XMIN 188	69.2507	73.55854	69.66723	81.85701	81.55931	77.66401	81.85701
XMIN 189	93.56522	101.1452	97.08857	105.5767	110.6334	109.4238	110.63340
XMIN 190	78.50035	84.48239	83.85621	78.53573	82.27738	79.73459	84.48239
XMIN 191	80.11901	80.52744	79.04108	84.04249	88.76687	86.23199	88.76687
XMIN 193	76.8963	81.12261	87.51619	75.72702	92.996	80.00861	92.99600
XMIN 194	67.07404	66.54357	68.22113	89.14145	80.66193	88.71693	89.14145
XMIN 196	67.57253	65.12384	71.00671	80.21591	67.62098	71.62595	80.21591
XMIN 197	80.82079	84.87763	83.35576	84.91402	78.98213	94.74977	94.74977
XMIN 198	70.31252	71.60527	70.68336	71.34866	72.95099	74.86396	74.86396
XMIN 202	74.20245	74.5076	69.40446	99.98822	82.25641	78.43414	99.98822
XMIN 206	70.83832	74.05546	71.94438	75.37815	71.3526	82.12244	82.12244
XMIN 207	83.13741	88.64062	86.6641	83.182	86.84082	96.9378	96.93780

XMIN 208	82.68577	81.72633	86.50845	95.31839	90.2779	90.73575	95.31839
XMIN 210	88.38384	110.0167	108.5277	91.83907	109.0249	114.0687	114.06870
XMIN 004	65.60262	62.28662	59.56946	58.35454	60.27048	47.96046	65.60262
XMIN 023	103.9675	112.7915	95.95379	100.9199	97.56218	114.599	114.59900
XMIN 027	51.89437	52.25541	53.95739	52.02301	52.95851	52.60554	53.95739
XMIN 032	74.74357	81.01383	80.36046	85.04379	87.76929	85.55615	87.76929
XMIN 035	79.47381	86.49752	81.81842	80.10747	84.3997	87.50736	87.50736
XMIN 039	51.68511	59.19751	54.65583	59.89667	60.32238	61.5219	61.52190
XMIN 067	63.13715	63.06404	64.63317	63.30307	62.65193	62.12066	64.63317
XMIN 071	66.34488	64.2234	56.30114	68.42973	59.84946	60.89765	68.42973
XMIN 073	50.73825	52.13066	52.69517	54.67838	52.05602	51.54322	54.67838
XMIN 077	77.36085	87.99424	80.12955	77.4676	94.05139	83.19271	94.05139
XMIN 078	59.09862	65.94977	59.14496	55.37206	58.06938	59.8326	65.94977
XMIN 102	73.17487	67.52596	60.77974	61.01656	58.26618	62.39064	73.17487
XMIN 105	76.26132	79.29861	79.27185	74.96731	75.34703	75.13508	79.29861
XMIN 107	52.44339	46.23389	49.95895	51.29682	51.59355	51.71006	52.44339
XMIN 112	59.38007	57.99006	57.71699	59.70556	57.71246	58.56915	59.70556
XMIN 114	92.04364	88.98206	93.41161	90.64501	81.1909	84.45036	93.41161
XMIN 116	83.99718	85.75808	86.71728	88.5003	97.93294	93.95147	97.93294
XMIN 118	62.58434	61.71097	65.27885	57.79151	58.61689	57.40174	65.27885
XMIN 120	64.78373	67.74047	63.92124	79.53381	71.86815	73.45562	79.53381
XMIN 122	79.10336	79.25299	77.19381	77.42073	84.08449	88.12625	88.12625
XMIN 132	62.93717	72.46778	70.67242	68.38937	69.09828	68.49357	72.46778
XMIN 137	47.55841	50.43905	53.72735	57.73913	54.74053	61.3352	61.33520
XMIN 146	79.16679	74.97609	75.85359	74.93914	74.78693	76.71122	79.16679
XMIN 149	68.10728	73.23153	86.42082	82.77563	73.26954	74.43378	86.42082
XMIN 153	62.46389	63.47278	67.64341	62.35158	69.07625	62.07542	69.07625
XMIN 156	81.84398	83.95439	95.20438	95.37473	87.5614	78.455	95.37473
XMIN 159	57.4773	72.68775	78.09845	57.86508	57.97558	63.84714	78.09845
XMIN 163	74.51673	71.59952	65.58552	71.96412	71.80178	70.62278	74.51673
XMIN 164	87.78183	89.52758	97.30026	97.93608	122.2241	135.5985	135.59850
XMIN 165	61.29325	60.81567	84.06805	69.66557	66.96394	63.96114	84.06805
XMIN 168	70.90682	70.57124	70.68583	72.24268	71.40203	74.51142	74.51142
XMIN 176	80.70471	69.42851	74.35236	78.45582	75.63108	77.09038	80.70471
XMIN 195	67.26531	66.62088	67.69764	67.34353	68.10776	85.18766	85.18766
XMIN 199	55.17934	54.31976	56.9609	57.8194	63.81508	67.09161	67.09161
XMIN 200	53.45123	65.92532	68.03011	67.78947	60.8059	63.72628	68.03011
XMIN 201	71.66004	70.06875	70.45077	72.73713	77.29234	72.44301	77.29234
XMIN 204	75.9501	97.5246	86.6028	78.49176	80.80288	65.08881	97.52460
						Mean	81.60332
						95% LCI	79.2577
						95% UCI	83.94.89

Appendix F

Fold change values for microRNA hsa-miR-208b-3p and hsa-miR-499a-5p

Figure F.1 Bar graph showing relative expression levels (fold change) of detectable serum microRNA before and after noncardiac surgery, in relation to the development of myocardial injury. Red = PMI. Blue = No PMI.

Data are presented as mean microRNA expression values with 95% confidence interval. MicroRNA expression calculated using relative Cq method and normalised to reference microRNA. There was no significant difference between the groups (mixed model analysis).

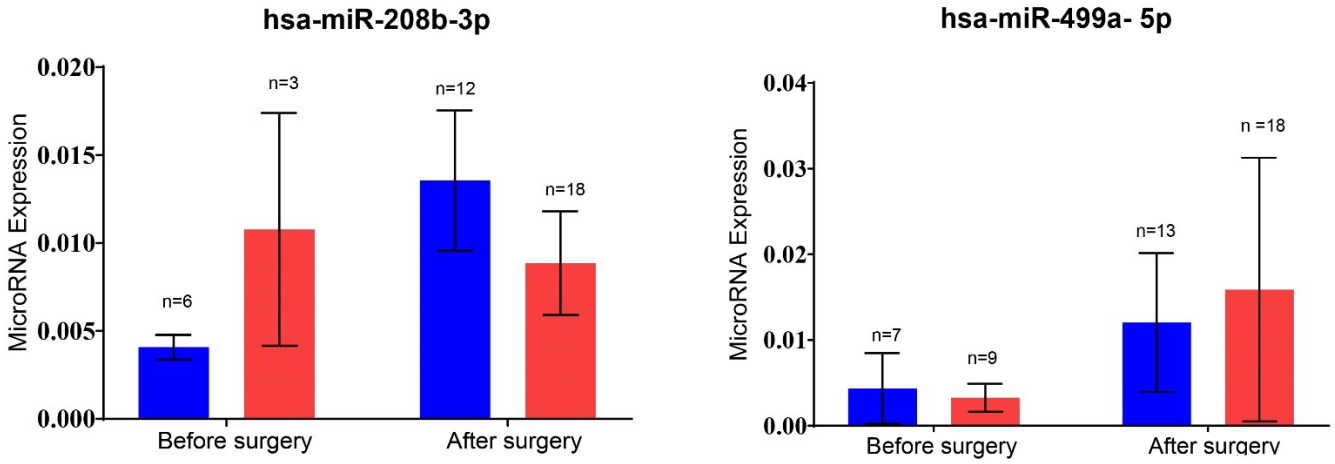

Appendix G

Mixed model comparison terms for Chapter 3

Below are the statistical tests for the mixed model levels and individual comparisons of terms for each microRNA

hsa-miR-1-3p

Table G.1: Test of mixed model terms

DAY: before; after surgery. PMI: perioperative myocardial injury (TnI $\geq$0.04ng.mL^{-1} and TnI <0.04ng.mL^{-1}). Model Term: the name of the term in the model. F-Value: the test statistic value corresponding to the L matrix used for testing the model term. Numerator degrees of freedom (DF): the numerator degrees of freedom for the F test. Denominator degrees of freedom (DF): the denominator degrees of freedom for the F test.

Model Term	F-Value	Numerator DF	Denominator DF	Probability
DAY	35.4164	1	46.0	<0.001
PMI	0.1157	1	47.0	0.735237
PMI * DAY	1.5118	1	46.0	0.225128

Table G.2: Individual comparisons of mixed model terms

F-Value: the test statistic value corresponding to the L matrix used for testing the model term. Numerator degrees of freedom (DF): the numerator degrees of freedom for the F test. Denominator degrees of freedom (DF): the denominator degrees of freedom for the F test. Bonferroni Probability Level: gives the p-value adjusted to multiple testing

Comparison	F-Value	Numerator DF	Denominator DF	Bonferroni Probability
DAY				
Before vs after surgery	48.2494	1	42.0	<0.001

hsa-miR-146a-5p

Table G.3: Test of mixed model terms

DAY: before; after surgery. PMI: perioperative myocardial injury (TnI $\geq$0.04ng.mL^{-1} and TnI <0.04ng.mL^{-1}). Model Term: the name of the term in the model. F-Value: the test statistic value corresponding to the L matrix used for testing the model term. Numerator degrees of freedom (DF): the numerator degrees of freedom for the F test. Denominator degrees of freedom (DF): the denominator degrees of freedom for the F test.

Model Term	F-Value	Numerator DF	Denominator DF	Probability
DAY	5.7084	1	33.4	0.023
PMI	0.2842	1	35.9	0.597
PMI * DAY	1.7891	1	33.4	0.190

Table G.4: Individual comparisons of mixed model terms

F-Value: the test statistic value corresponding to the L matrix used for testing the model term. Numerator degrees of freedom (DF): the numerator degrees of freedom for the F test. Denominator degrees of freedom (DF): the denominator degrees of freedom for the F test. Bonferroni Probability Level: gives the p-value adjusted to multiple testing.

Comparison	F-Value	Numerator DF	Denominator DF	Bonferroni Probability
DAY				
Before vs after surgery	5.7084	1	33.4	0.023

hsa-miR-133-3p

Table G.5: Test of mixed model terms

DAY: before; after surgery. PMI: perioperative myocardial injury (TnI $\geq$0.04ng.mL^{-1} and TnI <0.04ng.mL^{-1}). Model Term: the name of the term in the model. F-Value: the test statistic value corresponding to the L matrix used for testing the model term. Numerator degrees of freedom (DF): the numerator degrees of freedom for the F test. Denominator degrees of freedom (DF): the denominator degrees of freedom for the F test.

Model Term	F-Value	Numerator DF	Denominator DF	Probability
DAY	48.2494	1	42	<0.001
PMI	0.7045	1	42	0.406
PMI * DAY	1.7208	1	42	0.197

Table G.6: Individual comparisons of mixed model terms

F-Value: the test statistic value corresponding to the L matrix used for testing the model term. Numerator degrees of freedom (DF): the numerator degrees of freedom for the F test. Denominator degrees of freedom (DF): the denominator degrees of freedom for the F test. Bonferroni Probability Level: gives the p-value adjusted to multiple testing.

Comparison	F-Value	Numerator DF	Denominator DF	Bonferroni Probability
DAY				
Before vs after surgery	48.2494	1	42	<0.001

hsa-miR-21-5p

Table G.7: Test of mixed model terms

DAY: before; after surgery. PMI: perioperative myocardial injury (TnI ≥0.04ng.mL^{-1} and TnI <0.04ng.mL^{-1}). Model Term: the name of the term in the model. F-Value: the test statistic value corresponding to the L matrix used for testing the model term. Numerator degrees of freedom (DF): the numerator degrees of freedom for the F test. Denominator degrees of freedom (DF): the denominator degrees of freedom for the F test.

Model Term	F-Value	Numerator DF	Denominator DF	Probability
DAY	0.6283	1	44.7	0.432
PMI	0.0048	1	45.6	0.945
PMI * DAY	0.0976	1	44.7	0.756

Table G.8: Individual comparisons of mixed model terms

F-Value: the test statistic value corresponding to the L matrix used for testing the model term. Numerator degrees of freedom (DF): the numerator degrees of freedom for the F test. Denominator degrees of freedom (DF): the denominator degrees of freedom for the F test. Bonferroni Probability Level: gives the p-value adjusted to multiple testing.

Comparison of Levels	F-Value	Numerator DF	Denominator DF	Bonferroni Probability
DAY				
Before vs after surgery	0.6283	1	44.7	0.432

Appendix H RMSSD values before surgery

Table H.1 Raw RMSSD values from available Holter ECGs

Proportion of patients with RMSSD values <19ms in the resting sitting position on the day of surgery. Comparisons are made for patients who developed PMI (HsTnT ≥15n.gL^{-1}) and those who remained free of PMI (HsTnT ≤14 ng.L^{-1}). Data are presented as n (%). All comparisons made by two-tailed Fisher's exact test. OR, odds ratio; CI, confidence interval. RMSSD; root of the mean of the sum of the squares of the successive differences between adjacent beat-to beat intervals.

	HsTnT ≤14ng L^{-1} *n* = 116	HsTnT ≥15ng L^{-1} *n* = 27	OR (95% CI)	P-value
RMSSD <19	51 (44)	11 (41)	0.89 (0.24-2.22)	0.831

Appendix I

Mixed model comparison terms for Chapter 4

Table I.1: Test of mixed model terms for heart rate

PMI: perioperative myocardial injury (hsTnT $\geq$15ng.L^{-1} and hsTnT $\leq$14ng.L^{-1}). DAY: day relating to surgery (day of surgery, 24h after surgery and 48h after surgery). Position: body position (supine and 45-degrees sitting). Model Term: the name of the term in the model. F-Value: the test statistic value corresponding to the L matrix used for testing the model term. Numerator degrees of freedom (DF): the numerator degrees of freedom for the F test. Denominator degrees of freedom (DF): the denominator degrees of freedom for the F test.

Model Term HR	F-Value	Numerator Degree of freedom	Denominator Degrees of freedom	Probability
PMI	0.45	1	183.6	0.506
DAY	52.45	2	669.3	<0.001
POSITION	1.91	1	638.5	0.168
PMI * DAY	2.37	2	669.3	0.095
PMI * POSITION	1.68	1	638.5	0.196
DAY*POSITION	0.59	2	637.8	0.556
PMI*DAY*POSITION	0.16	2	637.8	0.851

Table I.2: Individual comparisons of mixed model terms for heart rate

F-Value: the test statistic value corresponding to the L matrix used for testing the model term. Numerator degrees of freedom (DF): the numerator degrees of freedom for the F test. Denominator degrees of freedom (DF): the denominator degrees of freedom for the F test. Bonferroni Probability Level: gives the p-value adjusted to multiple testing.

Comparison of levels HR	F-Value	Numerator DF	Denominator DF	Bonferroni Probability
DAY				
Before surgery vs 24h after surgery	6.1693	1	668.2	0.039728
Before surgery vs 48h after surgery	95.7475	1	677	<0.001
24h vs 48h after surgery	58.0292	1	663.2	<0.001
PMI * DAY				
NO PMI*Before surgery vs 24h after surgery	2.5489	1	648.1	0.665165
NO PMI* Before surgery vs 48h after surgery	71.9749	1	650.2	<0.001
NO PMI*24h vs 48h after surgery	45.3666	1	650	<0.001
PMI*Before surgery vs 24h after surgery	3.9026	1	673.4	0.291713
PMI* Before surgery vs 48h after surgery	44.7561	1	683.6	<0.001
PMI*24h vs 48h after surgery	25.1473	1	667.1	<0.001
Before surgery*PMI vs NO PMI	2.174	1	295.7	0.424286
24h after surgery*PMI vs NO PMI	0.4012	1	287.4	1.000
48h after surgery*PMI vs NO PMI	0.1184	1	298.2	1.000

Table I.3: Test of mixed model terms for LnRMSSD

PMI: perioperative myocardial injury (hsTnT ≥15ng.L^{-1} and hsTnT ≤14ng.L^{-1}). DAY: day relating to surgery (day of surgery, 24h after surgery and 48h after surgery). Position: body position (supine and 45-degrees sitting). Model Term: the name of the term in the model. F-Value: the test statistic value corresponding to the L matrix used for testing the model term. Numerator degrees of freedom (DF): the numerator degrees of freedom for the F test. Denominator degrees of freedom (DF): the denominator degrees of freedom for the F test.

Model Term RMSD	F-Value	Numerator DF	Denominator DF	Probability
PMI	0.03	1	189.7	0.869
DAY	11.82	2	681.2	<0.001
POSITION	0.88	1	647.6	0.348
PMI * DAY	4.56	2	681.2	0.011
PMI * POSITION	0.63	1	647.6	0.426
DAY*POSITION	0.41	2	646.8	0.664
PMI*DAY*POSITION	0.07	2	646.8	0.931

Table I.4: Individual comparisons of mixed model terms for LnRMSSD

F-Value: the test statistic value corresponding to the L matrix used for testing the model term. Numerator degrees of freedom (DF): the numerator degrees of freedom for the F test. Denominator degrees of freedom (DF): the denominator degrees of freedom for the F test. Bonferroni Probability Level: gives the p-value adjusted to multiple testing.

Comparison RMSSD	F-Value	Numerator DF	Denominator DF	Bonferroni Probability
DAY				
Before surgery vs 24h after surgery	15.45	1	679.9	<0.001
Before surgery vs 48h after surgery	20.08	1	689.8	<0.001
24h vs 48h after surgery	0.47	1	674.6	1.000
PMI * DAY				
NO PMI*Before surgery vs 24h after surgery	1.95	1	656.7	0.976
NO PMI* Before surgery vs 48h after surgery	4.43	1	661.2	0.214
NO PMI*24h vs 48h after surgery	0.52	1	659.9	1.000
PMI*Before surgery vs 24h after surgery	13.67	1	685.8	0.001
PMI* Before surgery vs 48h after surgery	15.66	1	696.8	<0.001
PMI*24h vs 48h after surgery	0.15	1	678.9	1.000
Before surgery*PMI vs NO PMI	1.92	1	320.8	0.501
24h after surgery*PMI vs NO PMI	0.84	1	311.7	1.000
48h after surgery*PMI vs NO PMI	0.82	1	324.2	1.000

Table I.5: Test of mixed model terms for LnSDNN

PMI: perioperative myocardial injury (hsTnT $\geq$15ng.L^{-1} and hsTnT $\leq$14ng.L^{-1}). DAY: day relating to surgery (day of surgery, 24h after surgery and 48h after surgery). Position: body position (supine and 45-degrees sitting). Model Term: the name of the term in the model. F-Value: the test statistic value corresponding to the L matrix used for testing the model term. Numerator degrees of freedom (DF): the numerator degrees of freedom for the F test. Denominator degrees of freedom (DF): the denominator degrees of freedom for the F test.

Model Term SD	F-Value	Numerator DF	Denominator DF	Probability
PMI	0.59	1	186.3	0.443
DAY	16.45	2	687	<0.001
POSITION	0.17	1	646.8	0.684
PMI * DAY	4.21	2	687	0.015
PMI * POSITION	0.40	1	646.8	0.526
DAY*POSITION	0.51	2	645.8	0.598
PMI*DAY*POSITION	0.08	2	645.8	0.923

Table I.6: Individual comparisons of mixed model terms LnSDNN

F-Value: the test statistic value corresponding to the L matrix used for testing the model term. Numerator degrees of freedom (DF): the numerator degrees of freedom for the F test. Denominator degrees of freedom (DF): the denominator degrees of freedom for the F test. Bonferroni Probability Level: gives the p-value adjusted to multiple testing.

Comparison SD	F-Value	Numerator DF	Denominator DF	Bonferroni Probability
DAY				
Before surgery vs 24h after surgery	20.29	1	685.5	<0.001
Before surgery vs 48h after surgery	28.81	1	697.1	<0.001
24h vs 48h after surgery	1.04	1	679.3	0.928
PMI * DAY				
NO PMI*Before surgery vs 24h after surgery	4.00	1	658.3	0.276
NO PMI* Before surgery vs 48h after surgery	11.53	1	663.7	0.004
NO PMI*24h vs 48h after surgery	1.97	1	662.8	0.965
PMI*Before surgery vs 24h after surgery	16.30	1	692.3	<0.001
PMI* Before surgery vs 48h after surgery	18.48	1	705.3	<0.001
PMI*24h vs 48h after surgery	0.16	1	684.1	1.000
Before surgery*PMI vs NO PMI	0.86	1	346.9	1.000
24h after surgery*PMI vs NO PMI	2.55	1	335.9	0.334
48h after surgery*PMI vs NO PMI	1.63	1	350.9	0.608

Table I.7: Test of mixed model terms for Ln High frequency

PMI: perioperative myocardial injury (hsTnT ≥15ng.L^{-1} and hsTnT ≤14ng.L^{-1}). DAY: day relating to surgery (day of surgery, 24h after surgery and 48h after surgery). Position: body position (supine and 45 degrees sitting). Model Term: the name of the term in the model. F-Value: the test statistic value corresponding to the L matrix used for testing the model term. Numerator degrees of freedom (DF): the numerator degrees of freedom for the F test. Denominator degrees of freedom (DF): the denominator degrees of freedom for the F test.

Model Term HF	F-Value	Numerator DF	Denominator DF	Probability
PMI	0.55	1	188	0.461
DAY	13.00	2	680.5	<0.001
POSITION	2.80	1	644.9	0.095
PMI * DAY	5.96	2	680.5	0.003
PMI * POSITION	0.39	1	644.9	0.534
DAY*POSITION	0.45	2	644.1	0.638
PMI*DAY*POSITION	0.16	2	644.1	0.856

Table I.8: Individual comparisons of mixed model terms for Ln High frequency

F-Value: the test statistic value corresponding to the L matrix used for testing the model term. Numerator degrees of freedom (DF): the numerator degrees of freedom for the F test. Denominator degrees of freedom (DF): the denominator degrees of freedom for the F test. Bonferroni Probability Level: gives the p-value adjusted to multiple testing.

Comparison HF	F-Value	Numerator DF	Denominator DF	Bonferroni Probability
DAY				
Before surgery vs 24h after surgery	15.56	1	679.3	<0.001
Before surgery vs 48h after surgery	23.09	1	689.2	<0.001
24h vs 48h after surgery	1.00	1	673.6	0.951
PMI * DAY				
NO PMI*Before surgery vs 24h after surgery	0.51	1	656.5	1.000
NO PMI* Before surgery vs 48h after surgery	6.11	1	659	0.082
NO PMI*24h vs 48h after surgery	2.96	1	659.2	0.513
PMI*Before surgery vs 24h after surgery	16.49	1	685.1	<0.001
PMI* Before surgery vs 48h after surgery	17.11	1	696.7	<0.001
PMI*24h vs 48h after surgery	0.04	1	677.8	1.000
Before surgery*PMI vs NO PMI	1.24	1	327.1	0.800
24h after surgery*PMI vs NO PMI	3.25	1	317	0.217
48h after surgery*PMI vs NO PMI	1.49	1	330.2	0.669

Table I.9: Test of mixed model terms for Ln Low frequency

PMI: perioperative myocardial injury (hsTnT ≥15ng.L^{-1} and hsTnT ≤14ng.L^{-1}). DAY: day relating to surgery (day of surgery, 24h after surgery and 48h after surgery). Position: body position (supine and 45 degrees sitting). Model Term: the name of the term in the model. F-Value: the test statistic value corresponding to the L matrix used for testing the model term. Numerator degrees of freedom (DF): the numerator degrees of freedom for the F test. Denominator degrees of freedom (DF): the denominator degrees of freedom for the F test.

Model Term LF	F-Value	Numerator DF	Denominator DF	Probability
PMI	1.90	1	176.5	0.170
DAY	22.21	2	693.2	<0.001
POSITION	0.26	1	640.5	0.612
PMI * DAY	2.14	2	693.2	0.118
PMI * POSITION	0.22	1	640.5	0.641
DAY*POSITION	0.37	2	639	0.694
PMI*DAY*POSITION	0.22	2	639	0.799

Table I.10: Individual comparisons of mixed model terms for Ln High frequency

F-Value: the test statistic value corresponding to the L matrix used for testing the model term. Numerator degrees of freedom (DF): the numerator degrees of freedom for the F test. Denominator degrees of freedom (DF): the denominator degrees of freedom for the F test. Bonferroni Probability Level: gives the p-value adjusted to multiple testing.

Comparison LF	F-Value	Numerator DF	Denominator DF	Bonferroni Probability
DAY				
Before surgery vs 24h after surgery	20.76	1	691.2	<0.001
Before surgery vs 48h after surgery	42.45	1	705.8	<0.001
24h vs 48h after surgery	4.55	1	683.6	0.100
PMI * DAY				
NO PMI*Before surgery vs 24h after surgery	7.69	1	659.5	0.034
NO PMI* Before surgery vs 48h after surgery	32.04	1	663.5	<0.001
NO PMI*24h vs 48h after surgery	8.21	1	665.4	0.026
PMI*Before surgery vs 24h after surgery	13.69	1	699.3	0.001
PMI* Before surgery vs 48h after surgery	19.64	1	716.2	<0.001
PMI*24h vs 48h after surgery	0.75	1	688.9	1.000
Before surgery*PMI vs NO PMI	0.01	1	391.5	1.000
24h after surgery*PMI vs NO PMI	4.14	1	377.1	0.128
48h after surgery*PMI vs NO PMI	1.87	1	395.7	0.515